DISS. ETH NO. 30221

Engineering chimeric antigen receptor signaling architectures for T cell immunotherapies

A thesis submitted to attain the degree of

DOCTOR OF SCIENCES

(Dr. sc. ETH Zurich)

presented by

Rocío Castellanos Rueda

MRes. Imperial College London

born on 12.12.1994

Prof. Dr. Sai Reddy

Prof. Dr. Georg Höllander

Prof. Dr. Bruno Correia

2024

To my parents

Abstract

Chimeric Antigen Receptors (CARs) are rationally designed synthetic receptors that are engineered to redirect the specificity and effector function of T lymphocytes toward a target surface antigen. Particularly in the realm of cancer therapeutics, CAR T cells designed to target tumor-associated antigens have emerged as a groundbreaking approach within cellular immunotherapy, showcasing remarkable clinical efficacy in the treatment of B cell malignancies. The field of CAR T cell therapy offers a promising avenue for cancer treatment, yet significant hurdles remain in optimizing efficacy and applicability across diverse clinical contexts. This emphasizes the need for innovative tools to identify the factors impeding the success of current CAR T cell therapies and to drive the development of enhanced CAR designs. Through the combination of directed evolution approaches and single-cell sequencing techniques, we contribute to this effort by establishing a tool for efficient high-throughput diversification and screening of CAR signaling architectures, thereby accelerating the engineering of more effective CAR constructs and advancing our comprehension of CAR-induced T cell phenotypes.

Chapter 1 serves as an introduction to CAR T cell therapy, emphasizing the emerging role of single-cell RNA sequencing (scRNAseq) in characterizing T cell heterogeneity and CAR-induced phenotypes. Whether in preclinical settings or during clinical trials, scRNAseq is rapidly becoming an essential tool for studying CAR-T cell behavior. This proves particularly valuable to assess the therapeutic potential of new engineering strategies or receptor candidates, as well as providing insights into the molecular profiles associated with disease outcomes. Furthermore, this chapter delves into the principles of traditional and high-throughput CAR T cell engineering, representing the current frontier in addressing challenges within CAR T cell therapies and laying the groundwork for subsequent Chapters.

In Chapter 2, we introduce speedingCARs, a method for effective CAR T cell engineering that integrates CRISPR Cas9 genome editing, pooled functional assays and single-cell sequencing to perform high-throughput screening of CAR signaling domain libraries. Despite the critical role of CAR signaling domains in T cell activation, only a limited number of immune signaling architectures have been explored. By leveraging the modularity of signaling proteins and the extensive existing diversity of immune receptor domains involved in the T cell signaling network, we generate a library of 180 unique CAR variants through domain recombination, driving diversification of CAR signaling. After targeted genomic integration of the CAR library into primary human T cells, in vitro tumor cell co-culture, followed by scRNAseq, enables high-throughput functional screening of CAR-induced phenotypes. This multidimensional readout provides valuable insights into the phenotypic diversity triggered by different CAR architectures and allows the identification of CAR variants driving enhanced antitumor effector properties. This comprehensive approach can be used to expand the CAR signaling domain combination space and guide the selection of new variants better suited to tackle current immunotherapeutic challenges.

In Chapter 3 the speedingCARs workflow is adapted to systematically investigate the impact of varying the choice, number and order of 5 costimulatory domains on T cell phenotype. Additionally, we introduce an in vitro model of CAR T cell dysfunction, simulating chronic tumor stimulation, a recurring limitation during clinical treatment. Using a mid-sized library of 32 candidates, we use single-cell sequencing to dissect the intricate relationship between CAR design and T cell phenotype during activation and long-term persistence. Parallel comparisons of CAR variants at early, middle and late time points during chronic stimulation reveal the predominant influence of membrane-proximal domains in driving T cell phenotype, with CD40 costimulation emerging as crucial for promoting potent and persistent T cell responses. These findings not only deepen our understanding of CAR T cell biology but also offer actionable insights for refining CAR design strategies to enhance therapeutic efficacy.

The culmination of these chapters underscores the effectiveness of integrating high-throughput CAR engineering strategies with single-cell transcriptomics to unravel the complex relationship between CAR signaling and T cell phenotype. Moreover, they emphasize the value of employing domain recombination, harnessing naturally optimized immune receptor domains, to expand CAR signaling architectures that rewire T cell signaling. By providing a highly efficient means of screening libraries of synthetic receptors, this thesis lays the foundation for the advancement of more effective CAR T cell therapies. Furthermore, this integrated approach holds great promise for unlocking the full therapeutic potential of CAR T cell therapy and enhancing outcomes for cancer patients.

Zusammenfassung

Chimäre Antigenrezeptoren (CARs) sind rational entwickelte synthetische Rezeptoren, die so konstruiert sind, dass sie die Spezifität und Effektorfunktion von T-Lymphozyten gegen ein Zieloberflächenantigen umlenken. Insbesondere im Bereich der Krebstherapeutika haben sich CAR-T-Zellen, die gegen tumorassoziierte Antigene reagieren, als bahnbrechender Ansatz in der zellulären Immuntherapie herausgestellt und zeigen eine bemerkenswerte klinische Wirksamkeit bei der Behandlung von B-Zell-Erkrankungen. Der Bereich der CAR-T-Zelltherapie bietet einen vielversprechenden Weg zur Krebsbehandlung, doch bestehen nach wie vor erhebliche Hürden bei der Optimierung der Wirksamkeit und Anwendbarkeit in verschiedenen klinischen Kontexten. Dies unterstreicht den Bedarf an innovativen Methoden, um die Faktoren zu identifizieren, die den Erfolg aktueller CAR-T-Zelltherapien zurückhalten, und um die Entwicklung verbesserter CAR-Designs voranzutreiben. Durch die Kombination von gezielten Evolutionsansätzen und Einzelzellsequenzierungstechniken tragen wir zu diesen Bemühungen bei, indem wir eine Methode für die effiziente Hochdurchsatz-Diversifizierung und das Screening von CAR-Signalarchitekturen etablieren, wodurch wir die Entwicklung effektiverer CAR-Konstrukte beschleunigen und unser Verständnis von CAR-induzierte T-Zell-Phänotypen verbessern.

Kapitel 1 dient als Einführung in die CAR-T-Zelltherapie und betont die neue Rolle der Einzelzell-RNA-Sequenzierung (scRNAseq) bei der Charakterisierung der T-Zell-Heterogenität und CAR-induzierten Phänotypen. Ob in präklinischen Umgebungen oder während klinischer Studien, scRNAseq entwickelt sich schnell zu einer unverzichtbaren Methode für die Untersuchung des Verhaltens von CAR-T-Zellen. Dies erweist sich als besonders wertvoll, um das therapeutische Potenzial neuer technischer Strategien oder Rezeptorkandidaten zu bewerten und Einblicke in die molekularen Profile zu erhalten, die mit therapeutischen Ergebnissen verbunden sind. Darüber hinaus befasst sich dieses Kapitel mit den Prinzipien des traditionellen CAR-T-Zell-Engineerings und des Hochdurchsatz-CAR-T-Zell-Engineerings, die die aktuelle Grenze bei der Bewältigung von Herausforderungen bei CAR-T-Zelltherapien darstellen und den Grundstein für nachfolgende Kapitel legen.

In Kapitel 2 stellen wir speedingCARs vor, eine Methode für effektives CAR-T-Zell-Engineering, die CRISPR Cas9-Genombearbeitung, gepoolte Funktionstests und Einzelzellsequenzierung integriert, um ein Hochdurchsatz-Screening von CAR-Signaldomänenbibliotheken durchzuführen. Trotz der entscheidenden Rolle von CAR-Signaldomänen bei der T-Zell-Aktivierung wurde nur eine begrenzte Anzahl von Immunsignalarchitekturen erforscht. Durch die Nutzung der Modularität von Signalproteinen und der umfangreichen existierenden Vielfalt an Immunrezeptordomänen, die am T-Zell-Signalnetzwerk beteiligt sind, generieren wir durch Domänenrekombination eine Bibliothek von 180 einzigartigen CAR-Varianten und treiben so die Diversifizierung der CAR-Signalisierung voran. Nach der gezielten genomischen Integration der CAR-Bibliothek in primäre menschliche T-Zellen, ermöglicht die In-vitro-Kokultur von Tumorzellen, gefolgt von scRNAseq, ein funktionelles Hochdurchsatz-Screening von CAR-induzierten Phänotypen. Diese mehrdimensionale Auswertung liefert wertvolle

Einblicke in die phänotypische Vielfalt, die durch verschiedene CAR-Architekturen ausgelöst wird, und ermöglicht die Identifizierung von CAR-Varianten, die zu verbesserten Antitumor-Effektoreigenschaften führen. Dieser umfassende Ansatz kann verwendet werden, um den Kombinationsraum der CAR-Signaldomänen zu erweitern und die Auswahl neuer Varianten zu steuern, die besser für die Bewältigung aktueller immuntherapeutischer Herausforderungen geeignet sind.

In Kapitel 3 wird der Arbeitsablauf von speedingCARs angepasst, um systematisch die Auswirkungen der unterschiedlichen Auswahl, Anzahl und Reihenfolge von 5 kostimulatorischen Domänen auf den T-Zell-Phänotyp zu untersuchen. Darüber hinaus stellen wir ein In-vitro-Modell der CAR-T-Zell-Dysfunktion vor, das eine chronische Tumorstimulation simuliert, eine wiederkehrende Einschränkung während der klinischen Behandlung. Anhand einer mittelgroßen Bibliothek von 32 Kandidaten verwenden wir Einzelzellsequenzierung, um die komplexe Beziehung zwischen CAR-Design und T-Zell-Phänotyp während der Aktivierung und Langzeitpersistenz zu analysieren. Parallele Vergleiche von CAR-Varianten zu frühen, mittleren und späten Zeitpunkten während der chronischen Stimulation zeigen den vorherrschenden Einfluss membrannaher Domänen auf die Steuerung des T-Zell-Phänotyps, wobei sich die CD40-Kostimulation als entscheidend für die Förderung starker und anhaltender T-Zell-Reaktionen herausstellt. Diese Erkenntnisse vertiefen nicht nur unser Verständnis der CAR-T-Zellbiologie, sondern bieten auch umsetzbare Erkenntnisse für die Verfeinerung von CAR-Designstrategien zur Verbesserung der therapeutischen Wirksamkeit.

Der Abschluss dieser Kapitel unterstreicht die Wirksamkeit der Integration von Hochdurchsatz-CAR-Engineering-Strategien mit Einzelzell-Transkriptomik, um die komplexe Beziehung zwischen CAR-Signalen und T-Zell-Phänotyp zu entschlüsseln. Darüber hinaus betonen sie den Wert des Einsatzes der Domänenrekombination und der Nutzung natürlich optimierter Immunrezeptordomänen, um CAR-Signalarchitekturen zu erweitern, die die T-Zell-Signalisierung neu verkabeln. Durch die Entwicklung einer hocheffizienten Methode zum Screening von Bibliotheken synthetischer Rezeptoren legt diese Arbeit den Grundstein für die Weiterentwicklung wirksamerer CAR-T-Zelltherapien. Darüber hinaus ist dieser integrierte Ansatz vielversprechend, um das volle therapeutische Potenzial der CAR-T-Zelltherapie auszuschöpfen und die therapeutischen Ergebnisse für Krebspatienten zu verbessern.

Acknowledgements

First and foremost, I would like to thank Prof. Sai Reddy for granting me the opportunity to embark on this journey and work in such an exciting research topic. His guidance and support have been instrumental throughout this process, and I am truly grateful for the trust and freedom he has provided me to explore and shape my own research path. Working in the Reddy Lab has been a profoundly enriching experience, contributing significantly to my personal and academic growth.

I would also like to extend my sincere appreciation to my committee members, Prof. Georg Höllander and Prof. Bruno Correia, for their insightful feedback and constructive critiques. Additionally, thank you to Prof. Barbara Treutlein for chairing the defense.

A special acknowledgment goes to my mentor and co-author, Raphaël B. Di Roberto, whose collaboration and discussions have been very valuable and enriching. His dedication and passion for science and research have been a constant source of motivation and inspiration.

I am grateful to have collaborated with great scientists Florian Bieberich, Darya Palianina, Oanh T. P. Nguyen and Alice Driessen. Your expertise, support and willingness to share your knowledge have been invaluable to our projects' success. In addition, I would like to thank my students, Fabrice S. Schlatter, Juliette L. Forster, Jessica A. Frank and Kai-Ling K. Wang, whom I had the pleasure of supervising. I am grateful for your hard work, enthusiasm and fresh perspectives that have contributed significantly to our research endeavors, but also given me the opportunity to learn from you along the way.

The Reddy Lab has been my academic home, and I would like to express my gratitude to all its members. A special mention to our lab manager, Ulrike Haessler, and fellow friends and colleagues Florian Bieberich, Rita Pertseva, Lena Erlach and Mason Minot. Your company during project discussions, coffee breaks, and non-science related adventures has significantly enriched my time at the lab. I would also like to thank the members of the CAR subgroup for fostering such an enjoyable and collaborative workspace.

A special thank you to the single cell and genomics facility teams at BSSE for their indispensable support and expertise, which have been crucial to my research.

To my Basel family, Jaime, Bego, Isa, Pau, Ivan, Jojo, Sthefan, Luca, Giacomo and Meghan, your warmth and friendship have made Basel feel like home. Thank you for your constant support, for sharing crazy adventures and for always transmitting positive energy. To my confidants and amazing travel buddies Danay and Vitto, thank you for being such inspiring women, for always knowing how to cheer me up and for believing in me more than I do. To

my beloved friends back home, Irene, Bea, Jiang, Carmen and Fernando, your support, despite the distance, has been a source of strength. I am truly honored to have had all of you over the last years.

I would like to take this opportunity to acknowledge my high school science teacher, Javier González Entonado, and my genetics professor, Juan Orellana Saavedra, for igniting my passion for science and guiding me in the career choices that have led me to this point.

Lastly, to my family, Mercedes and Juan Carlos, my pillars of strength, and my brother Miguel, for your constant love and encouragement. Your example of determination and perseverance always pushes me to do better. Thank you for your patience and constant support which has truly been invaluable in this journey. To my cousin Paula, you're like a little sister to me and always a source of warmth and emotional support. And to Ma Jose, Javier, Luis and Antonio, my second family, who have consistently shown care and encouragement, supporting me every step of the way.

Abbreviations

ACT: Adoptive cell transfer

ALL: acute lymphoblastic leukemia

APC: antigen-presenting cell

ATAC: Assay for Transposase-Accessible Chromatin

BCMA: B-cell maturation antigen

BCR: B cell receptor

DMS: deep mutational scanning

CAR: Chimeric antigen receptor

CDR: Complementarity determining region

CITE: cellular indexing of transcriptomes and epitopes

CLL: chronic lymphocytic leukemia

FACS: Fluorescence-activated cell sorting

ICB: immune-checkpoint blockade

ITAM: Immunoreceptor-tyrosine-based-activation-motif

ITSM: Immunoreceptor-tyrosine-based switch motifs

MM: Multiple myeloma

HDR: Homology-directed repair

HER2: Human epidermal growth factor receptor 2

NHEJ: non-homologous end joining

NHL: non-Hodgkin lymphoma

NGS: Next generation sequencing

NSCLC: non-small-cell lung cancer

LBCL: large B-cell lymphoma

PCA: Principal component analysis

RAS: Repeated antigen stimulation

scFv: single-chain variable fragment

scRNAseq: Single-cell RNA sequencing

TAA: Tumor-associated antigen

TCR: T cell receptor

TIL: Tumor infiltrating lymphocyte

TNFR: Tumor Necrosis Factor Receptor

TMD: transmembrane domain

TME: Tumor microenvironment

TRAC: TCR alpha chain

UMAP: Uniform manifold approximation and projection

Chapter 1: General Introduction

Section 1.2 of this chapter is an author-produced adaptation and expansion of a peer-reviewed review article “Leveraging Single-Cell Sequencing for Chimeric Antigen Receptor T Cell Therapies”, accepted for publication in Trends in Biotechnology, 2021 (https://doi.org/10.1016/j.tibtech.2021.03.005).

Authors: Rocío Castellanos-Rueda, Raphaël B. Di Roberto, Fabrice S. Schlatter and Sai T. Reddy

Author contributions: R.C.R. conceptualized the review, R.C.R., R.B.D.R., S.T.R. wrote the manuscript (R.C.R. prepared sections focusing on the use of scRNAseq in CAR T cell research and concluding remarks, R.B.D.R. prepared introductory sections and concluding remarks and S.T.R. revised and edited the final manuscript). F.S.S. compiled the tables.

1.1 Introduction to CAR T cell therapy

Chimeric Antigen Receptors (CARs) are rationally designed synthetic receptors engineered to redirect the specificity and effector function of T lymphocytes toward a target surface antigen. They are highly modular proteins built by combining naturally existing protein domains. The CAR architecture comprises an extracellular antigen-binding domain, a transmembrane domain (TMD) and a signaling intracellular region (Figure 1). The extracellular antigen-binding portion is typically a single-chain variable fragment (scFv) derived from a monoclonal antibody, granting the CAR the ability to bind to an antigen of interest. Following the scFv, a flexible hinge region links the antigen-binding module to the TMD, which anchors the CAR to the cell membrane and facilitates signal transduction through the intracellular signaling region. The CAR intracellular region combines signaling domains from the T cell receptor (TCR) or its co-receptors contributing to the T cell activation process.

CARs can be divided into different generations based on the usage of signaling domains (Figure 1). While first-generation CARs use only a single signaling domain from CD3ζ (*1*), part of the TCR complex, second- and third-generation CARs have been developed to incorporate one or more additional domains, respectively. By doing this, CARs are designed to integrate CD3ζ-mediated activation with additional costimulatory signaling, which is typically provided by the T cell synapse and is known to be crucial to drive successful and sustained T cell responses. Currently, most CARs use domains from CD28 (*2*) or 4-1BB (*3*) (herein termed 28z and BBz) due to their established co-stimulatory properties; however, the

diversity of CAR designs is growing by exploring a range of different costimulatory molecules or domain modifications, thereby endowing the CAR with distinct functional properties (see section 1.3).

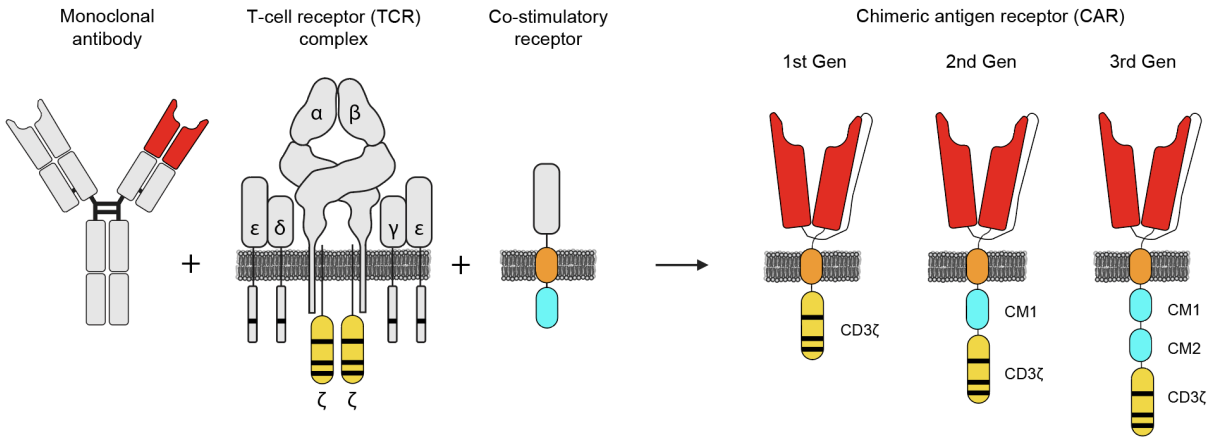

Figure 1. Structural design of chimeric antigen receptors

Upon expression of a CAR by T cells and their interaction with cells expressing the targeted antigen, CAR binding initiates signaling cascades that trigger genetic cues, leading to T cell activation. This activation induces proliferation, differentiation, cytokine secretion and cytotoxicity, ultimately resulting in the elimination of target cells, as well as the development of persistent immunity through the generation of long-lived memory T cells. The specificity of this response, coupled with the clinical demand for new therapies to treat cancer patients who are refractory to current standard-of-care treatments, has made CAR-T cell therapy highly attractive for cancer treatment. First described in 1989 (*4*), CAR T cells designed to target tumor-associated antigens (TAAs) have since become a major breakthrough in the field of cellular immunotherapies and have shown impressive clinical results in treating patients with relapsed or refractory B-cell malignancies such as acute lymphoblastic leukemia (ALL), large B-cell lymphoma (LBCL), chronic lymphocytic leukemia (CLL), non-Hodgkin lymphoma (NHL) and multiple myeloma (MM) (*5–10*). Presently, the U.S. Food and Drug Administration (FDA) has approved six CAR T cell therapies (four targeting CD19 and two targeting B-cell maturation antigen (BCMA)) and over a thousand clinical trials are assessing safety and efficacy of different CAR T cell products (*11*). These treatments rely on the isolation, genetic engineering and re-infusion of autologous T cells into patients, where they target and destroy TAA expressing cancer cells (Figure 2), a process termed adoptive cell transfer (ACT).

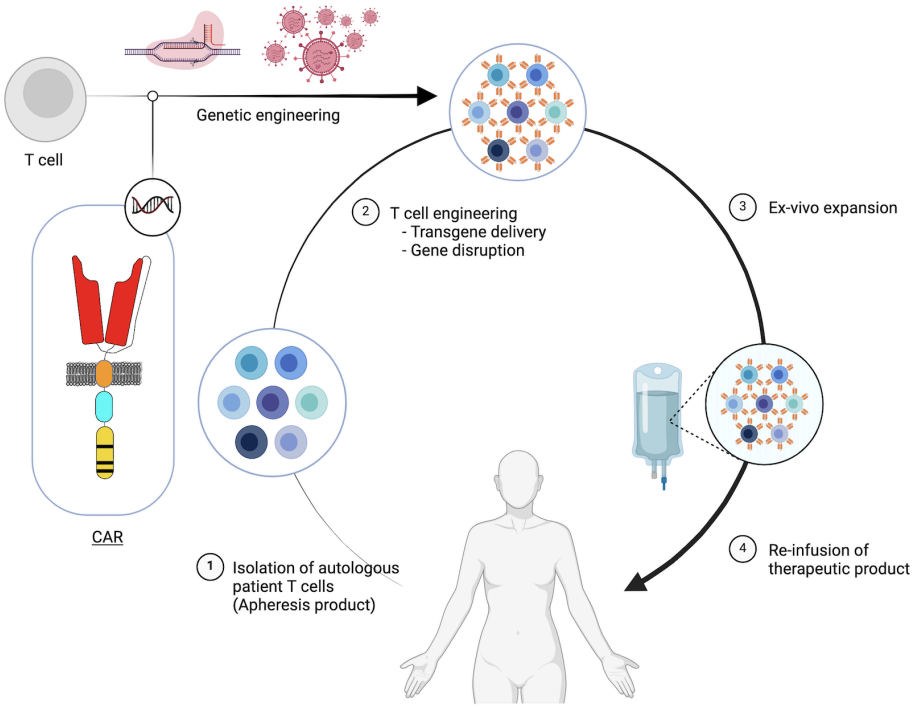

Figure 2. Adoptive cell transfer (ACT) of CAR engineered T cell therapies

Despite their established clinical efficacy in treating hematological malignancies, a significant portion of patients still relapse following CAR T cell treatment (*12*). In addition, as the field has continued to expand to address other cancers, many clinical trials have found frequent and varied adverse events, as well as low response rates, exposing the limitations of current CAR-T cells (*13*). Major challenges include the lack of persistence of T cells due to prolonged tumor stimulation or the development of antigen escape mechanisms by tumor cells, both of which compromise the long-term efficacy of CAR T cell therapies. Furthermore, CAR T cell therapies are associated with toxicities, including cytokine release syndrome and neurotoxicity, which can limit their tolerability and require management strategies. In the context of solid tumors, the hostile tumor microenvironment (TME) fosters immunosuppression and T cell exhaustion, while impeding effective tumor infiltration. Lastly, the heterogeneous expression of TAA complicates target selection, raising concerns of on-target off-tumor toxicities. These disappointing outcomes do not always have clear explanations, since a full characterization of T cell behavior in vivo is challenging. Thus there is now a growing focus on understanding what drives successful CAR-T cell immune responses and the use of that knowledge to engineer CAR T cells products with enhanced therapeutic power.

1.2 Leveraging single-cell sequencing for CAR T cell therapies

The deep sequencing of cellular mRNA (RNA-seq) provides an effective strategy for the high-throughput and quantitative profiling of gene expression and transcriptome signatures. When performed on a bulk population of isolated cells, the major transcription programs can be highlighted and compared across distinct cell populations. However, this requires subsetting cells by the expression of established surface markers, potentially introducing bias. Recently, the emergence of single-cell RNA sequencing (scRNAseq) has become a powerful approach to augment bulk RNA-seq by providing a greater resolution of transcriptome and gene expression patterns and further deciphering cellular phenotypes (*14*, *15*). First demonstrated by Tang et al. on a single mouse blastomere (*16*), scRNAseq has progressed rapidly and become a major tool to study cells of the immune system, including in the context of immunotherapy (*17–20*). In this section, we review the use of scRNAseq and its constituent technologies in the study of CAR-T cell therapies. Specifically, we provide an overview of scRNAseq concepts and methods adapted for immune cell profiling. We then outline work in immunotherapy research focusing on T cell states before genetic modification, after CAR transgene integration and following preclinical and clinical use (effector cells extracted from patients). Finally, we discuss how scRNAseq can be used to guide the design and engineering of the next generation of CAR-T cells to enhance therapeutic and safety outcomes.

1.2.1 Single-cell sequencing of T lymphocytes: An overview

scRNAseq stands at the juncture of two technological feats: the ability to add unique molecular barcodes to mRNA transcripts in isolated cells and the ability to sequence these transcripts from the minute amounts of material present in a single cell (*16*). Improvements in the reliability of microfluidics and encapsulation have been key, enabling the compartmentalization of individual cells before lysis and barcoding. Likewise, polymerase enzymes with improved fidelity and yield, together with molecular barcodes, enable the amplification of the genetic material of a single cell into usable amounts without suffering from extensive bias. These steps have been streamlined into several adaptable protocols, such as SMART-seq2 (*21*), REAP-seq (*22*), SPLiT-seq (*23*) and DART-seq (*24*), or simplified by commercial systems, including the 10X Genomics Chromium, Takara Bio ICELL8 and Fluidigm C1 platforms (*25*). Similarly, the analysis and visualization of the resulting data previously required extensive bioinformatics expertise, but open-access software packages, such as Monocle (*26*) and Seurat (*27*), have simplified this

process and widened its accessibility. Thus, scRNAseq is rapidly becoming a standard assay to investigate cell biology questions thoroughly, including those pertaining to immunology and immunotherapy.

scRNAseq is a valuable tool for studying T lymphocytes and their ability to coordinate, shape and carry out an adaptive immune response through paracrine signaling and direct cell–cell contact. These processes involve an array of distinct molecular actors, but classical methods, such as flow cytometry and ELISA, are limited in their ability to characterize the expression of more than a dozen proteins. In fact, one of the most striking insights from scRNAseq has been the extensive heterogeneity discovered in cell populations (i.e., effector and memory phenotypes) that were previously assumed to be homogeneous based on a set of commonly assayed surface markers or cytokines. In some cases, this has led to the discovery of new T cell subsets, which may be key for certain disease outcomes (*28–30*), while in other cases, it is unclear whether subsets can be defined at all, featuring instead a continuous distribution of expression levels (*31*).

In addition, scRNAseq has been especially valuable for profiling of lymphocyte adaptive immune receptor repertoires. Both TCRs and B cell receptors (BCR) comprise pairs of polypeptide chains encoded by separate genes. This polygenic structure complicates the identification of functional receptors from a pool of diverse transcripts. However, since each lymphocyte typically expresses a single receptor, knowing the originating cell of a given chain can reveal its pairing partner, thereby revealing receptors that are potentially antigen specific. In addition, protocols combining whole-transcriptome sequencing as well as targeted gene enrichment to capture TCR and BCR repertoires can be devised (*32*, *33*). In this way, scRNAseq has been used to gain insight into the development of a specific immune response throughout the course of an illness (*17–19*) or to identify TCRs and BCRs of possible therapeutic interest (*34–37*). In addition to their biological role in antigen recognition, TCR and BCR repertoires have been exploited as a cellular barcode for cell lineage tracing using scRNAseq. By sequencing TCR or BCR RNA transcripts, populations of cells derived from a single cell (clonotype) can be traced to study clonal dynamics and a direct comparison between clonotype and phenotype can be addressed. In this way, scRNAseq has made itself indispensable for T cell research by revealing features that only this technology can capture.

To date, scRNAseq of T cells has been performed in a variety of contexts. Of particular interest are tumor-infiltrating lymphocytes (TILs), which have pivotal roles in antitumor responses and are key for several cancer immunotherapy strategies. When extracting TILs from tumors, scRNAseq can be performed on them alongside malignant cells to characterize gene expression profiles and the interplay of

this complex microenvironment (*28*, *38–41*). This can help relate specific TIL profiles to a given prognosis, especially when treatment-naïve and treated subjects are compared (*29*, *42–44*). Additionally, it is also possible to identify the specific T cell receptor (TCR) sequences of expanded clones and their associated transcriptomes, which may correlate with tumor reactivity and specificity (*18*, *45*). Furthermore, T cell clones exhibiting gene expression patterns that correlate with other desirable features, such as high persistence and low exhaustion, may be valuable candidates for adoptive cell transfer (ACT) (*46–49*) or immune checkpoint blockade therapy (*20*). As we describe next, transcriptome analysis, most notably scRNAseq, is becoming a valuable tool for also characterizing CAR-T cell therapies, shedding light on the genotypic profiles that are correlated with clinical success.

1.2.2 The transcriptional landscape of CAR-T cells: Design and readiness

CAR-T cell development relies on different preclinical models to reproduce the interactions between tumor and immune cells and to assess the therapeutic potential of new engineering strategies or receptor candidates. Conventional CAR-T cell discovery uses in vitro co-culture assays and in vivo xenograft mouse models, where cell surface marker expression, cytokine secretion and tumor cell killing are evidence of functionality (Figure 3). Despite their well-established value, these assays cannot capture the full spectrum of T cell immunosurveillance effectors. ScRNAseq technologies are more comprehensive and fast becoming an essential tool to study CAR-T cell behavior before, as well as during, clinical trials (Table 1). In the following section, we review how transcriptomics has been used to interrogate CAR-T cell biology with in vitro and in vivo preclinical studies.

1.2.2.1 The components and architecture of CARs

As expected, CAR-T cell effectiveness is heavily influenced by the architecture of the CAR transgene. Small changes within not only the binding and signaling domains, but also structural elements, such as the transmembrane helix and the linkers, can have a strong impact on downstream signaling and the extent of T cell activation (*50–53*). Therefore, assessing CAR designs before and after antigen encounter is of primary importance.

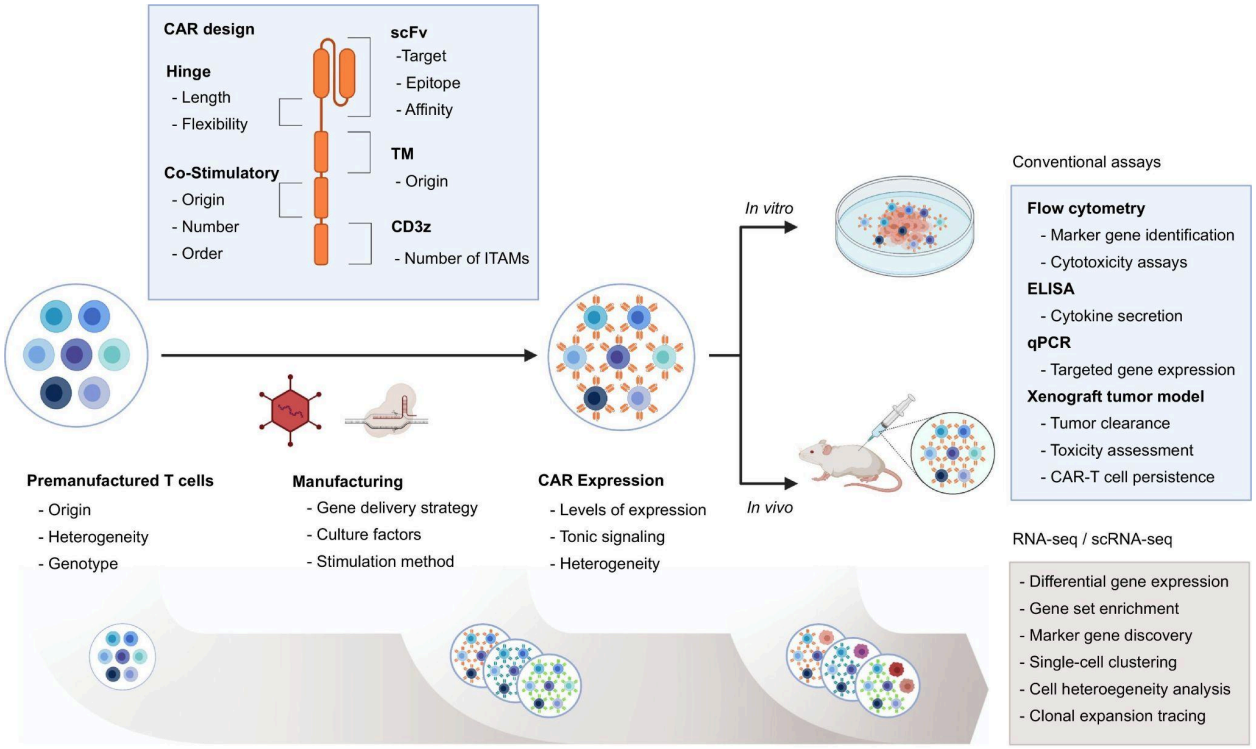

Figure 3. Outline of the Chimeric Antigen Receptor (CAR)-T Cell Therapy Development Workflow and the Main Factors Contributing to Therapy Performance.

CARs have a highly modular architecture integrated by an antigen-binding domain (generally a single-chain variable fragment; scFv), a hinge, a transmembrane domain (TM), a varying number of co-stimulatory signaling domains, and a CD3ζ signaling domain containing three immunoreceptor tyrosine-based activation motifs (ITAMs). Modifications of any of its endo-and ectodomains can modify the CAR specificity and T cell activation potential. Therefore, the engineering of CAR-T cell therapies starts with the design of new receptor candidates. Subsequently, CARs are engineered into T cells to generate CAR-T cells that can be characterized before and throughout different in vitro and in vivo assays. Variations in the premanufactured T cell product used to generate CAR-T cells as well as differences in the manufacturing protocol may influence the fitness of the newly engineered cells and combine with differences in CAR expression levels to shape the nature of the final CAR-T cell product. Characterization of these CAR-T cells conventionally makes use of standard molecular biology techniques to measure surface marker expression, cytokine secretion and cell killing. However, with the development of sequencing technologies, RNA-sequencing (RNA-seq) and single-cell (sc)RNA-seq are now able to capture a high degree of molecular complexity and are becoming an engaging option to interrogate CAR-T cell biology. Figure created with BioRender

One of the first examples of using transcriptomics to resolve the phenotypic landscape of old and new CAR designs was described by Kagoya et al., who constructed a CD19 CD28-ΔIL2RB-z CAR and, using microarrays, compared its associated transcriptional signature to that of the prototype 28z and BBz CARs (*54*). In another study, Prinzing et al. performed RNA-seq to determine the impact of incorporating MyD88 and CD40 (MCz) signaling domains in a EphA2-specific CAR, showing that MCz induced a

proliferation signature and a less differentiated phenotype compared with 28z and BBz (*55*). Other examples investigated specific motifs within CAR domains and their modularity. For instance, Guedan and et al. replaced the SH2-binding motif in CD28 with that of the co-signaling receptor ICOS in CARs targeting mesothelin antigen, demonstrating that this replacement was sufficient to promote a less differentiated phenotype and a Th17 polarization, both hallmarks of ICOSz signaling (*56*). Together, these reports show how RNA-seq confirmed that changes in CAR designs led to functional differences at the whole-transcriptome level and could aid in providing molecular insight into the functional properties observed from in vitro and in vivo assays.

When analyzing gene expression from bulk RNA-seq, meaningful differences within defined immune cell subpopulations can be masked. As with natural, unmodified T cells (*57*), CAR-T cells display significant heterogeneity and a range of cell fates. This heterogeneity is intrinsic, but it can also be influenced by the CAR design and impact treatment efficacy and safety. To study cell heterogeneity and fully characterize the interplay of T cell subtypes in CAR-T cell therapies, single-cell resolution is essential. By providing an unbiased transcriptomic profile for every individual cell, scRNAseq ensures that subpopulations are represented and that their contributions to an overall response can be identified; moreover, scRNASeq obviates the need to perform phenotypic labeling and sorting based on cellular surface markers. The use of scRNAseq to study the impact of CARs on T cell heterogeneity was first reported by Xhangolli et al., who investigated the third-generation CD19-28/BBz CAR with a particular focus on T cell CD4+/CD8+ subsets, Th polarization and T cell differentiation status (*58*). scRNAseq data revealed similar expression levels of effector molecules and cytokines for both CD4+ and CD8+ CAR-T cells, suggesting that both subsets of CAR-T cells are equally capable of exerting cell-mediated cytotoxicity regardless of their differentiation state. Additionally, a mixed Th1/Th2 polarization state based on cytokine and transcription factor gene expression was identified, a property seemingly distinct to CAR-induced T cell activation.

In a more recent study, Wang et al., explored the T cell phenotypes associated with different stages in the production of a dual BCMA- and TACI-targeting CD28/OX40z third-generation CAR (*59*). Single-cell transcriptomic analysis showed evidence of tonic signaling occurring in a small fraction of unactivated CAR-T cells. In addition, it allowed for identification of a consistent and distinct CAR-induced molecular signature of T cell activation, characterized by a strong MYC transcription factor-induced gene expression signature, limited exhaustion and a combined CD4+/CD8+ effector response. Finally, Boroughs et al. combined bulk RNA-seq and scRNAseq to create a high-resolution atlas of the underlying differences between a CD19 first-generation CAR with that of 28z and BBz (*60*). scRNAseq more accurately captured the degree of similarity found between samples, and the independent cell clustering of BBz

CAR-T cells confirmed their distinct transcriptional signature compared with the first-generation and 28z CARs. The gene expression pattern of BBz included the enrichment of genes and gene sets related to fatty acid metabolism, the IL21 cytokine axis and central memory and Th1 polarization. In addition, it was found that CAR tonic signaling from 28z and BBz CARs can skew the predominance of particular T cell subpopulations within resting CAR-T cells. By assigning subset markers to scRNAseq clusters, BBz CARs were found to be enriched in CD8+ central memory cells as opposed to CD8+ effector and CD4+ central memory cells in 28z CARs. This showed how the co-stimulatory domain in second-generation CARs can shape the heterogeneity of unique transcriptional T cell activation profiles.

1.2.2.2 Engineering T cells for CAR therapy

CAR-T cell engineering is not limited to the receptor itself, but can include additional gene knock-ins or knock-outs. Understanding the coordinated activity of genes involved in T cell signaling is essential for this strategy. Transcriptomics has been used to study the impact of additional gene mutations in CAR-T cells (*61–63*). In addition, RNA-seq can be used as a forward genetic approach to identify key players linked to a particular phenotype. This approach was used by Lynn et al. to study an exhaustion-prone GD2 CAR-T cell model compared with non-exhausted CD19 CAR-T cells (*64*). Bulk RNA-seq and scRNAseq data showed that, while known T cell exhaustion markers were differentially expressed, other genes, such as the AP-1 binding bZIP/IRF family of transcription factors, were also observed, offering new targets to mitigate exhaustion. In a similar way, Chen et al. investigated exhaustion in murine CD19 CAR-T cells (*65*). After injection into tumor-bearing mice, tumor-infiltrating CAR-T cells were recovered and sorted based on markers of exhaustion; bulk RNA-seq identified the overexpression of the NRA4 family of genes in exhausted CAR-T cells. Both strategies were validated by the characterization of JUN-overexpressing and NRA4 triple-knockout CAR-T cells, respectively, which confirmed unexhausted transcriptional signatures with downregulation of exhaustion marker and inhibitory surface receptors genes in addition to enhanced antitumor properties.

In another study, Wang et al. implemented a genome-wide CRISPR screen approach on IL13Rα2 CAR-T cells to discover gene targets with the potential to modulate exhaustion (*66*). Following tumor stimulation, single guide (sg)RNA enrichment in PD1– cells identified previously unexplored candidate genes. Characterization of single knockout CAR-T cells revealed improved antitumor activity and cell fitness, which was accompanied by differential expression of various T cell regulators and upregulation of proinflammatory and T cell activation signaling pathways. scRNAseq of top knockout candidates (TLE4 and IKZF2) showed that cell clustering was minimally impacted by gene knockouts. However, following

tumor stimulation, specific T cell subsets with distinct transcriptomic signatures appeared to be preserved or expanded compared with the wild-type. Following this example, scRNAseq has continued to be used in later studies to characterize the change in phenotype induced by specific gene knock-outs such as ID3, SOX4 (*67*) and EGR2 (*68*). Altogether, these studies demonstrate how the transcriptome analysis of CAR-T cells can identify novel ways to reduce T cell exhaustion.

1.2.2.3 Extrinsic modulatory conditions of CAR-T cells

In addition to the genetic modification of T cells, other elements, such as manufacturing conditions or combination therapies with immunomodulatory drugs, can influence the performance of CAR-T cells. For instance, the method used to deliver the CAR transgene can influence receptor expression and signaling and, consequently, T cell behavior (*69*). Aiming to elucidate mechanistic explanations for these functional differences, scRNAseq has been employed to study the phenotypes of CAR T cell products engineered using viral gene delivery or virus-free CRISPR-based targeted genomic integration into immunologically relevant loci such as *TRAC* (*70*) or *PD1* (*71*). RNA-seq has also been leveraged to study the impact of different ex-vivo culture conditions in CAR T cell therapeutic potential. CAR-T cells in the presence of IL-15 had a less differentiated central memory phenotype as well as reduced expression of exhaustion markers and glycolytic metabolism genes (*72*). Additionally, supplementing cell media during CAR-T cell expansion with the S enantiomer of 2-hydroxyglutarate increased central memory CD8+ phenotype and downregulated STAT5 signature genes (*73*). In both cases, these results correlated with an enhanced antitumor response in experimental assays. To further resolve the impact of manufacturing conditions during treatment, Lu et al. designed a multiplexed technology using a scRNAseq. This technology traces the single-cell phenotypes of CAR T cells manufactured ex-vivo in combination with different cytokines and small-molecule inhibitors following infusion into an in vivo mouse model (*74*).

Lastly combination therapies can also modulate T cell function and impact the effectiveness of CAR T cell therapies. The combination of an anti-BCMA CAR therapy with the immunomodulatory drug lenalidomide led to the upregulation of genes associated with T cell chemotaxis, cytoskeleton remodeling and a Th1 response (*75*). In addition, scRNAseq demonstrates that combination treatment with long-acting form of recombinant human interleukin-7 (rhIL-7-hyFc) preferentially expands IL7R+ effector memory CAR T cells in an in vivo xenograft model leading to improved antitumor properties (*76*).

Table 1. Overview of scRNAseq studies on CAR-T cells*

CAR Design	Study type	Cell Source	CAR T Cell Sample	Technology	Ref.
antiCD19–4-1BB–CD28–CD3z	Pre-clinical	hT cells	6 hours co-culture with Raji	scRNAseq	(*58*)
antiGD2–CD28–CD3z	Pre-clinical	hT cells	Naïve T cell subset	scRNAseq	(*64*)
antiCD19–CD28–CD3z					
antiHER2–4-1BB–CD3z			14 days post-infusion into 143B osteosarcoma mouse xenograft model		
antiCD19–CD28–CD3z	Pre-clinical	hT cells	24 hours co-culture with NALM6	scRNAseq	(*60*)
antiCD19–4-1BB–CD3z					
APRIL–CD28–OX40–CD3z	Pre-clinical	hT cells	Product sample and 20 hours co-culture with MM1.S	scRNAseq	(*59*)
antiIL13Rα2–4-1BB–CD3z	Pre-clinical	hT cells	48 hours co-culture with glioblastoma stem cells, KO (TLE and IKZF2) and control CAR T cells with or without stimulation by tumor cells	scRNAseq	(*66*)
anti-MSLN–4-1BB–CD3z	Pre-clinical	hT cells	0, 20 or 28 days following repeated stimulation with AsPC1 cell line	scRNAseq	(*67*)
antiCD19–CD28–4-1BB–CD3z	Pre-clinical	hT cells	14 and 28 days post-infusion into CD19+ mouse xenograft model	scRNAseq	(*76*)
antiCD19–4-1BB–CD3z	Pre-clinical	hT cells	0, 6 and 48h hours co-culture with Nalm6	scRNAseq + scATACseq	(*68*)
antiCD19–4-1BB–CD3z	Pre-clinical	hT cells	LV or virus free manufacturing with or without PD-1 KO	scRNAseq	(*71*)
antiGD2–CD28–OX40–CD3z	Pre-clinical	hT cells	Retroviral or virus free manufacturing before and after 24h co-culture with CHLA20 cells	scRNAseq	(*70*)
antiHER2 CAR library	Pre-clinical	hT cells	36 hours co-culture with SKBR3 cells	scRNAseq + scCARseq	(*99*)
antiCD19–4-1BB–CD3z	Pre-clinical	hT cells	48 hours co-culture with K562 cells	scRNAseq + scCITEseq	(*100*)
antiCD19–CD28–CD3z					
antiCD19–BAFF-R–CD3z					
antiCD19–TACI–CD3z					
antiCD19–CD40–CD3z					
antiCD19–CD3z					
antiPSMA–4-1BB–CD3z	Pre-clinical	hT cells	Several rounds of repeated stimulation with PC3-PSMA cells	scRNAseq + scATACseq	(*101*)
antiCD19–CD28–CD3z	Pre-clinical	hT cells	42 days post-infusion into a NALM6 leukaemia mouse xenograft model	scRNAseq + scTCRseq + scSSNseq	(*74*)
antiCD19–4-1BB–CD3z	Clinical	ALL, CLL, NHL patients	Infusion product and peripheral blood 7-14 days, 26-30 days and 83-112 days post-infusion	scRNAseq + scTCRseq	(*78*)
antiCD19–4-1BB–CD3z (tisa-cel)	Clinical	ALL patients	Infusion product and peripheral blood 10 days post-infusion	scRNAseq + scTCRseq	(*98*)
antiCD19–CD28–CD3z (axi-cel)	Clinical	LBCL patients	Infusion product	scRNAseq + scTCRseq	(*89*)

antiBCMA–4-1BB–CD3z	Clinical	PCL patient	Infusion product and peripheral blood 8 days and 15 days post-infusion	scRNAseq	(*79*)
antiCD19–4-1BB–CD3z	Clinical	CLL patient	9.3 years after treatment	scRNAseq + scTCRseq + scCITEseq	(*80*)
antiGD2–4-1BB–CD3z	Clinical	Glioma patients	Baseline, Infusion product and cells isolated from cerebrospinal fluid at different timepoints post-infusion	scRNAseq	(*84*)
antiCD19–4-1BB–CD3z	Clinical	ALL patients	Infusion product stimulated in vitro with CD19-3T3 or MSLN-3T3 cells or with CD3/CD28 beads	scRNAseq + scCITEseq	(*90*)
antiBCMA–4-1BB– CD3z	Clinical	MM patients	Cells isolated from peripheral blood at 10-13 days and 29-33 days post-infusion	scRNAseq + scATACseq	(*68*)
antiCD19–4-1BB–CD3z	Clinical	NHL patients	Infusion product, peripheral blood 7-10 days and 28-29 days post-infusion	scRNAseq	(*71*)
antiCD19–4-1BB–CD3z	Clinical	B-ALL patients	Infusion product and sorted cells from peripheral blood or BM samples: weeks 1–4, week 8 and months 3 and 6 post-infusion.	scRNAseq + scTCRseq	(*81*)
antiCD19–4-1BB–CD3z	Clinical	NHL patients	Infusion product and sorted cells from peripheral blood 14 and 30 days post-infusion.	scRNAseq + scCITEseq	(*93*)
antiCD19–CD28–CD3z (axi-cel) antiCD19–4-1BB–CD3z (tisa-cel)	Clinical	LBCL patients	Baseline, Infusion product and sorted CAR+ or CAR- fractions of peripheral blood 7 days post-infusion	scRNAseq + scTCRseq	(*91*)
antiBCMA–4-1BB– CD3z	Clinical	MM patients	BM mononuclear cells before and after therapy (28 days or 3 to 6 months following infusion)	scRNAseq + scTCRseq + scCITEseq	(*94*)
antiCD19(CAT)–4-1BB–CD3z	Clinical	B-ALL patients	Infusion product and peripheral blood or BM samples from early (months 1–3), mid (months 4–6) and late (month 7 onwards) timepoints post-infusion.	scRNAseq + scTCRseq	(*82*)
antiCD19/CD20–4-1BB–CD3z	Clinical	LBCL patients	Infusion product	scRNAseq	(*95*)
antiCD19–CD28–4-1BB–CD3z	Clinical	BCL patients	Infusion product	scRNAseq	(*96*)
antiCD19–CD28–CD3z (axi-cel)	Clinical	LBCL patients	Infusion product	scRNAseq	(*97*)
antiCD19–4-1BB–CD3z	Clinical (allogenic)	B-ALL or LBCL patients	Infusion product and PBMC before and up to 1 month after infusion	scRNAseq + scTCRseq + scCITEseq	(*83*)

*Abbreviations: B-ALL, B cell acute lymphoblastic leukemia; APRIL, 'a proliferation-inducing ligand', a high-affinity ligand for the receptors BCMA and TACI; BM, Bone Marrow; CLL, chronic lymphocytic leukemia; hT cells, human T cells; LBCL, large B cell lymphoma; NHL, non-Hodgkin lymphoma; MM, Multiple myeloma; PCL, plasma cell leukemia; scSSNseq shielded-small-nucleotide-based scRNAseq.

1.2.3 Monitoring CAR-T cell performance in the clinic

Following encouraging preclinical results obtained from emerging CAR designs, several ongoing clinical trials aim to demonstrate their efficacy and safety profile (*77*). During or in the follow-up of ACT, the therapeutic CAR-T cell product can be recovered for characterization. To maximize the value of these samples, scRNAseq can be used to study the underlying molecular profiles linked to clinical outcomes through high-resolution views of gene expression, cell heterogeneity, trajectory analysis and cell lineage tracing (Figure 4).

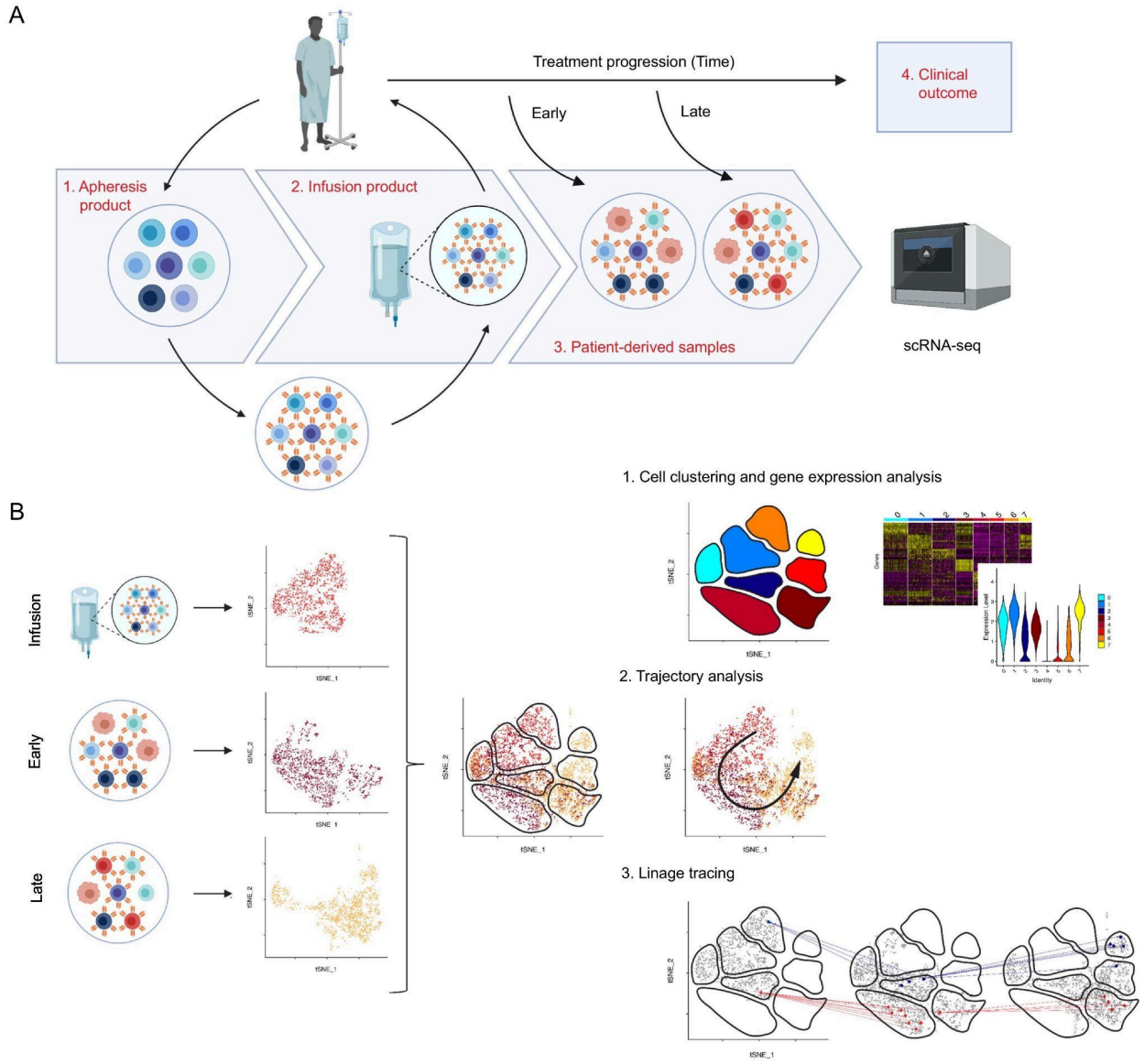

Figure 4. Application of Single-Cell RNA Sequencing (scRNAseq) Analysis to Chimeric Antigen Receptor (CAR) T Cell Clinical Studies.

A) CAR-T cell therapy begins with the retrieval of a patient's own T cells through leukapheresis (apheresis product), T cells are engineered, and, following quality assessment, the CAR-T cell product is reinfused into the patient. Thereafter, treatment progression is monitored over time and clinical information is recorded. In addition, patient samples, which contain the therapeutic product, can be recovered, obtaining snapshots of CAR-T cells at different stages of the treatment regime. To fully characterize such samples, scRNAseq can be used to assess CAR-T cells states at high resolution. **B)** scRNAseq data record the transcriptional signature of each individual cell in a given sample. Following normalization, feature selection and dimensionality reduction methods, the transcriptional differences between cells can be identified and analyzed. Furthermore, multiple scRNAseq datasets can be integrated and cells from different samples can be directly compared with each other. To this end, the scRNAseq analysis toolbox comprises a diverse range of computational resources, including unsupervised cell clustering and differential gene expression analysis, trajectory analysis and lineage tracing. Figure created with BioRender

1.2.3.1 Transcriptomic profiling of CAR-T cells throughout treatment progression

Following infusion into a patient, CAR-T cells are exposed to a dynamic tumor microenvironment and repeatedly triggered by antigen-expressing cancer cells, prompting tumor regression with the potential to confer long-lasting antitumor immunity. However, how the tumor microenvironment and the changing tumor burden affects the state of CAR-T cells through time is not well described. Sheih et al. were the first to utilize scRNAseq combined with TCR repertoire sequencing to study the behavior of CD19-BBz CAR-T cells following their infusion into patients (*78*). The single-cell transcriptional signature of the infusion product and CAR-T cells recovered from patients at different time points after infusion were compared. Increased expression of aerobic metabolism and cell cytotoxicity marker genes were found during early and mid-stages of treatment, but decreased at later stages, along with a drop in the presence of the targeted antigen following tumor clearance. Moreover, by tracing the TCR clonal composition of infusion products and in patient-retrieved CAR-T cells, it was possible to follow how the transcriptional signature of individual CAR-T cells can affect the fate of these cells after infusion (lineage tracing). Mapping of the lineages onto scRNAseq data showed which infusion product cell clusters were enriched in more proliferative and persistent clones in vivo.

In a similar way, Li et al. examined the dynamics of BCMA-BBz CAR-T cells before, at peak, or during remission phases post infusion (*79*). ScRNAseq data identified changes in population subsets, with a CD4+-rich infusion product, a heterogeneous population of CD8+ cytotoxic cells at peak stage and a CD8+ memory-like signature following remission. Mapping of cell states onto a constructed developmental trajectory resolved the dispersed clustering found at peak phase by identifying a transition from highly proliferative to cytotoxic T cells. This state transition was confirmed by differences in the expression of immunomodulatory genes and enriched gene signatures across cell clusters. Interestingly, this same study reanalyzed the data produced by Sheih et al. (*78*) and identified consistent dynamics between CD19 and BCMA CAR-T cells following cell infusion.

Following Sheih and Li, a growing number of studies have employed scRNAseq to investigate the dynamics of different CAR T cell products across diverse clinical contexts. These include different types of leukemias or lymphomas (*80–83*), multiple myeloma (*68*) and even solid tumors. Notably Majzner et al. sequenced for the first time CAR T cells retrieved from glioblastoma patients (*84*). Among these studies, noteworthy findings include Wilson et al.'s utilization of lineage tracing to identify a distinct gene expression profile within a subset of cells in the infused product, which subsequently led to the development of highly effective CAR T-cell phenotypes post-infusion (*81*). Jiang et al. combined scRNAseq with scATAC-seq to investigate dynamic changes in chromatin accessibility of CAR T cells

following infusion, identifying transcription factors involved in driving exhaustion programs (*68*). Moreover, Anderson et al. and Melenhorst et al. conducted long-term studies, observing CAR+ T cells persisting in patients for up to 5 and even 10 years following treatment (*80*, *82*). Altogether, these reports exemplify how scRNAseq data of a few thousand CAR-T cells at different stages of treatment can be sufficient to monitor state transitions and identify previously unknown cell subtypes with distinct transcriptional programs.

1.2.3.2 Correlation of CAR-T cell transcriptome profiles with disease response

An important goal for advancing new CAR-T cell therapies is identifying predictive indicators of clinical outcome. Currently, CAR-T cells are produced using the patient's own T cells, and their quality and variability can have an outsized impact. Several studies have linked T cell properties in leukapheresis material or pre-infusion CAR-T cell products to patient response (*85–87*). In a similar way, by leveraging transcriptomics, Fraietta et al. found predictive hallmarks for patients with chronic lymphocytic leukemia and their likelihood of response to treatment based on pre-manufactured or pre-infusion CAR-T cell products (*88*). In a more recent study, scRNAseq was used to analyze infusion products from a cohort of patients with large B cell lymphoma (LBCL) receiving CD19 CAR-T cell therapy (*89*). A CD8+ central memory signature was observed in complete responders as opposed to a CD8+ dysfunction signature in partial responders, with the latter enriched in exhaustion and activation markers and genes encoding MHC class II proteins. In addition, the single-cell resolution revealed specific T cell subsets linked to different clinical outcomes. The enrichment of CD8+ cells expressing CCR7 and CD27 marker genes was correlated with complete-response samples, and a small population with a monocyte-skewed transcriptional signature was linked to the occurrence of treatment-associated neurotoxicities, a recurrent adverse effect.

In a different study, Bai et al. examined the relationship between the phenotypes of in vitro stimulated infusion products and the clinical performance of a CD19-BBz CAR in patients with ALL. They identified Th2 function and early memory potential as predictive factors for a positive clinical response (*90*). Similarly, Haradhvala et al. conducted a comparative analysis of the phenotypes of pre- and post-infusion CAR T cells, correlating them with clinical outcomes in patients with LBCL. Notably, they compared FDA-approved CD19-CARs bearing CD28 or 4-1BB costimulatory domains (axicabtagene ciloleucel [axi-cel] or tisagenlecleucel [tisa-cel]). Proliferative memory-like CD8 clones were predictive of positive responses to tisa-cel, whereas axi-cel recipients exhibited greater CD8+ heterogeneity amongst responders and an enrichment of CAR-T regulatory cells among non-responders (*91*). These studies

highlight the emerging significance of integrating single-cell transcriptomic analyses with clinical data to better understand the intricacies of CAR T cell therapy and uncover predictors of treatment outcomes as reviewed by Haradhvala & Maus (*92*). Additional studies (*93–97*) are detailed in Table 1.

Lastly, Markers on tumor biopsies can also predict CAR-T cell dysfunction in response to the tumor microenvironment. Singh et al. correlated the absence of a death receptor signaling signature in leukemia cells to the development of resistance to CAR-T cells (*98*). This was validated using RNA-seq data from bone marrow samples of responding and non-responding patients. In addition, resistance to treatment was linked to the increased expression of exhaustion markers by performing scRNAseq on infusion product and CAR-T cells retrieved from a responding and a non-responding patient. Altogether, these findings show how transcriptional signatures from tumor biopsy samples, T cell aphaeresis products and infusion products, can be combined to identify predictive hallmarks of clinical response before treatment, which can then be used to adapt personalized therapies.

1.2.3 Concluding remarks and Future perspectives

Future successes in CAR-T cell immunotherapy will hinge on our growing understanding of the behavior of engineered cells. The application of scRNAseq to this challenge seeks to provide a comprehensive and high-resolution view of the genes and population subsets involved in an effective (or ineffective) therapeutic response. By accounting for cell heterogeneity, enabling robust comparisons of transcriptomic signatures and tracking cell lineages, scRNAseq is providing novel insight at all stages of CAR-T cell development. As future research helps address the current challenges, it may eventually become a standard and essential tool for the field.

The increasing use of scRNAseq to study CAR T cells in both pre-clinical and clinical studies has contributed to gaining a mechanistic understanding and further resolve CAR-T cell biology. Furthermore, the growing amount of available scRNAseq datasets, some of which include annotations on clinical performance, presents the opportunity to compile a comprehensive atlas of CAR T cell phenotypes, thereby integrating recorded information as a tool to help advance clinical treatments. In the future, the field would benefit from a more systematic analysis of scRNAseq data sets and a consensus in data interpretation. Similar to ProjecTILs (*102*) and PanglaoDB (*103*), a CAR-T cell atlas linking transcriptome data with functional preclinical or clinical responses would facilitate the interpretation of

results. In addition, the accumulation of single-cell CAR-T cell data sets may soon enable the use of predictive algorithms, helping determine precisely why a therapy regimen succeeded or failed.

Despite its well-established value, the interpretation of scRNAseq data must take into account some caveats. First, significant cell–cell variability means that a substantial sample size is needed to discern real population subsets from stochastic noise (*104*) or confounding factors, such as the cell cycle (*105*). In addition, the direct comparison of data between and within different studies relies on the choice of integration algorithms, which can regress out the batch effect generated by differences in sample processing or sequencing protocols (*106*). Finally, the relationship between transcription, translation and function is not always strong (*107–109*). Thus, scRNAseq data should be used to guide further experiments if mechanistic conclusions are sought. Combining this method with high-throughput assays of protein expression, such as CITE-seq (*110*), single-cell mass cytometry (*111*), or multiplexed cytokine profiling (*21*), can help to validate such conclusions.

Lastly, scRNAseq tools have so far been used to analyze the molecular complexity and diversity of cell populations bearing a single CAR design. However, because scRNAseq can be used to resolve complex cell populations, simultaneously screening of diverse CAR constructs is an exciting prospect. Pioneering work from Marson and colleagues used scRNAseq coupled to CRISPR/Cas9 genome editing to screen gene knockout phenotypes from sgRNA libraries (*112*), or to screen pooled knock-in libraries of synthetic constructs in primary T cells (*113*). Similar strategies could be used to link specific CAR transcriptomic profiles to the most suitable situation or, inversely, to guide CAR-T cell development as will be the subject of study in the following chapters of this thesis. This opens the door to the potential use of scRNAseq as a tool to identify customized CAR designs for specific patient needs, enhancing the prospects of immunotherapy as personalized medicine.

1.3: CAR T cell engineering

The field of CAR therapies has witnessed remarkable progress in recent years, significant challenges still remain, which has hindered its widespread application across various clinical indications (*13*). The inherent modularity of CARs presents an opportunity for extensive optimization and refinement. Through precise modifications to the different components of the CAR, many researchers aim to engineer the CAR molecule to enhance its specificity, potency, and safety. As the field of CAR engineering advances, new

and more diverse CAR architectures are being described, prompting consideration of CARs as a family of synthetic receptors.

1.3.1 Engineering CAR modules

Engineering efforts have highlighted that even subtle changes in any of the CAR domains or spacer peptides can significantly impact T cell function (*13*, *114*). One primary strategy to engineer CAR functionality involves reprogramming the antigen specificity of CAR T cells to target different TAAs. While FDA-approved CAR T cell therapies have primarily targeted CD19 and BCMA, a growing body of literature describes CARs targeting a diverse array of TAA. These efforts aim to broaden the application of CAR T cell therapies to a wider spectrum of cancers, including solid tumors (*115*) and reflect on ongoing advances in TAA discovery. In addition to the choice of target antigen, properties of the antigen-binding CAR module, such as affinity (*116*, *117*), charge density (*118*), or epitope selection, also influence CAR signaling function. Consequently, selecting an appropriate scFv clone or performing affinity maturation (*117*) has become common practice to engineer CARs with improved safety profiles and enhanced effector function.

Following the antigen-binding domain, a flexible linker region regulates the distance of the scFv from the cell surface, while a TMD anchors the CAR into the cell membrane, ensuring proper surface expression. Both the hinge and TMD play pivotal roles in stabilizing the CAR structure, facilitating receptor complexing and recruiting additional signaling molecules. By leveraging naturally occurring domains (i.e., IgG4, CD8a, CD28) or designing de novo sequences (*119*), modifications in the choice, length, or flexibility of the hinge and TMD are strategies that have been employed to fine-tune CAR receptor functions (*50*, *120*, *121*), highlighting the significance of appropriate domain combinations in driving effective immune responses.

Finally considering the intracellular portion of the CAR, it is well understood that signaling domains play a crucial role in signal transduction, activating the pathways necessary for T cell activation. Alongside the pivotal role of ITAM-containing domains (i.e. CD3ζ) in T cell activation, a variety of co-stimulatory receptors steer T cell signaling, with the potential to tune distinct T cell responses. Given the complexity of the T cell signaling network and the intricate nature of the system governing T cell activation, engineering the CAR signaling architecture has immense potential to shape T cell responses. Following the design of 28z and BBz CARs, which triggered distinct effects on T cells in terms of proliferation, cytokine secretion, differentiation and persistence owing to variations in signaling domain utilization

(*122*, *123*), researchers have investigated the effects of integrating additional immunologically relevant signaling domains into second or third generation CAR architectures. For example Guedan et al., incorporated an ICOS signaling domain in a second-generation CAR, which significantly improved T cell persistence. Subsequent combination of ICOS with 4-1BB in a third-generation CAR demonstrated enhanced antitumor effects and prolonged persistence in a mouse model (*124*). In another study, researchers replaced the CD3ζ domain with that of other CD3 chains from the TCR complex, each containing one ITAM, identifying 4-1BB-based CARs with enhanced functionality, especially when combined with CD3δ (*125*). Other examples have explored the incorporation of signaling domains from OX40, CD27, CD40, HVEM, GITR (*126*), CTLA4 (*68*), IL2Rβ (*54*), Dectin-1 (*127*) or TLR2 (*128*), highlighting how the choice, number and order of signaling domains can influence the therapeutic potential of CARs.

In addition to the use of domain rearrangements for CAR engineering, some studies have focused on studying the effect of modifying specific signaling motifs involved in signal transduction. For instance, Feucht et al. evaluated the impact of mutating the ITAM motifs of the CD3ζ chain in a CD28-based CAR to assess and calibrate its T cell activation potential (*51*). In parallel, other studies investigated the effects of single mutations in motifs found in the CD28 signaling domain. By replacing the CD28 SH2 binding motif with that of ICOS receptor Guedan et al. describe a 28z CAR with reduced exhaustion (*56*). Similarly, Boucher et al., incorporated null mutations in the YNMN and PRRP motifs (28z-FMNM/ARRA) showing a reduced expression of exhaustion-related genes and an NFAT transcription factor (*129*).

Moving away from conventional CAR designs, the field of CAR engineering continues to expand as researchers seek novel solutions to address challenges such as cell trafficking, tumor microenvironment resistance and CAR therapy-associated toxicities. Next-generation CAR designs incorporate synthetic biology approaches such as logic-gating, molecular switches or additional synthetic constructs to provide better control over T cell effector potential (*130*). Logic-gate CARs are capable of responding to multiple input signals by recognizing different target antigens in a programmable and conditional manner. Examples include syn-Notch CAR (*131*), where the recognition of a first TAA leads to the expression of a CAR with specificity towards a second antigen (AND gate), or tandem CARs with specificity towards two target antigens (OR gate) (*132*). Various types of CAR switches now enable inducible or reversible activation of T cell effector functions in response to the administration of a drug (i.e. iCasp9 CAR (*133*) or STOP CAR (*134*)) or an adaptor molecule (i.e. SUPRA CAR (*135*)). Lastly, armored CAR T cells are

engineered to secrete additional factors such as cytokines or antibodies, enhancing their therapeutic properties (*136*, *137*).

1.3.2 High throughput CAR T cell engineering

Through the combination of single mutations, segment rearrangement and domain recombination with natural selection, evolution has granted us with optimized biological systems capable of regulating immune responses with the utmost precision. CARs leverage these systems by combining existing protein domains to redirect the specificity and function of T cells. However, transplanting a particular domain into a different protein architecture or cellular context may alter its overall function (*138*), suggesting that rational protein design may not always yield the most optimal solution for addressing newly defined challenges. For this reason, some research groups have implemented directed evolution-like strategies as a high-throughput method for exploring the design space of CARs. In such approaches, genetic diversity is introduced into a specific module of the CAR gene, creating a CAR library. This library is then incorporated into a relevant biological system (such as cell lines or primary T cells) through gene editing of viral gene transduction, enabling the assessment of the CAR phenotype. A selection criteria (i.e. tumor cell killing, cytokine production or resistance to T cell exhaustion) is subsequently applied to screen for candidates with desired functional characteristics (see Figure 5).

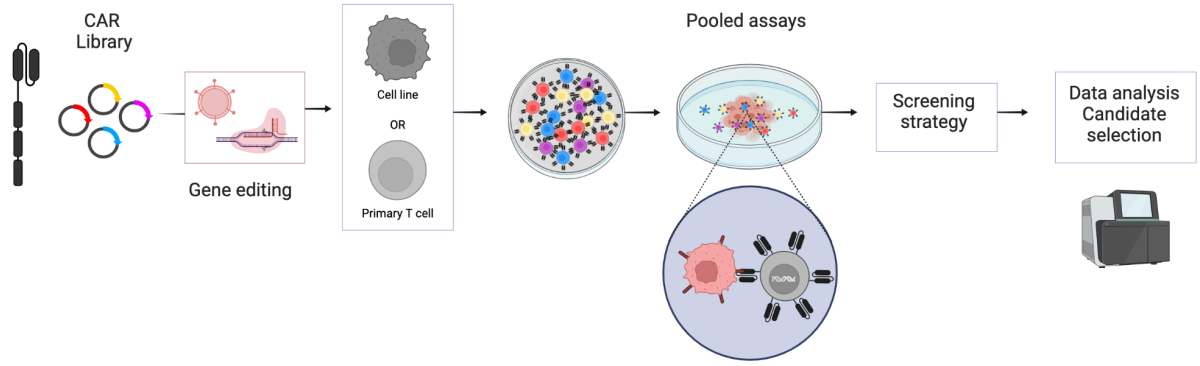

Figure 5. Overview of the CAR high-throughput engineering pipeline

In an attempt to bridge scFv binding affinity with CAR function, different cell-based reporter systems have been developed to perform high-throughput engineering of the CAR antigen-binding module. For example, Rydzek et al. established a Jurkat cell line with dual NFAT and NFkB reporter systems and used

it to screen a CAR library generated by targeted mutagenesis of the complementarity determining region 3 (CDR3) of an antiROR1 scFv (*139*). Similarly, Di Roberto et al. (including my contribution as a co-author of this study), developed a CAR T cell display platform containing an IL2-linked GFP reporter, facilitating high-throughput functional screening of displayed CARs using antigen binding and/or signaling-based screening. Using CRISPR-Cas9 genome editing and deep mutational scanning (DMS), we performed affinity maturation of a high-affinity anti-HER2 CAR and identified CARs capable of effectively discriminating between cells with different antigen expression levels, thereby mitigating on-target/off-tumor toxicities (*140*).

As previously discussed, the choice, number and order of signaling domains integrated into the CAR intracellular region can significantly impact T cell activation programs and, consequently, the anti-tumor properties of CAR T cells. With the extensive array of immune signaling proteins available, rewiring the signaling network of T cell activation holds great potential for engineering CARs with enhanced therapeutic characteristics (*141*). In order to explore the vast CAR signaling domain combination space, recent studies, including the work presented in this thesis, have developed high-throughput approaches to explore and engineer new CAR signaling architectures (summarized in Table 2).

Pioneered by Gordon et al., the utilization of the Jurkat cell line was demonstrated as a convenient setup for screening CAR libraries comprising up to $7x10^5$ candidates. Through pooled screens, fluorescence-activated cell sorting (FACS)-based selection and deep sequencing, distinct functional features of signaling domain combinations were identified (*142*). Similarly, Si et al. utilized Jurkat cells to conduct arrayed screens of 60 CAR variants, which incorporated modules from four different co-stimulatory signaling domains. Leveraging a reporter system-based readout, they identified novel CAR architectures capable of modulating T cell signaling toward distinct transcriptional programs (*143*).

CAR signal transduction relies on its interaction with the intricate T cell signaling network, which is composed of a complex array of proteins and signaling molecules. The cell's ability to respond to genetic triggers (i.e. gene expression, protein production or cytokine secretion) serves as a qualitative and quantitative phenotypic readout. Maintaining the integrity of these cellular components is crucial for accurately studying the relationship between genotype and phenotype in receptor library screening. However, cell lines often lack this physiological integrity. To enhance the translatability of results, the use of engineered primary T cells has been more popular to screen libraries of signaling architectures, even if this means compromising the size of the CAR library (*99*, *100*, *144–146*). Amongst such studies, sort-based screening was often the screening method of choice (*100*, *145*, *146*), focusing on T cell

phenotypic features such as cytokine secretion, proliferation or the use of T cell marker genes of activation or cytotoxicity. Alternatively, Daniels et al. presented an innovative approach by performing arrayed screening of a fraction of their library using flow cytometry, and then employing machine learning algorithms to predict the phenotype from the rest of their library. By doing this they aimed to decode a motif recombination CAR library of 2379 variants (*144*). Furthermore, the research outlined in this thesis describes the utilization of scRNAseq as a screening technique that can profile the multidimensional transcriptomic readout of single CAR T cells beyond the scope of conventional flow cytometry panels (Chapters 2 and 3 (*99*, *146*)). By combining CRISPR Cas9 targeted genomic integration with pooled screens, we leveraged scRNAseq to identify CAR architectures exhibiting unique functional attributes from a library comprising 180 variants (*99*). Additionally, we systematically investigated the impact of co-stimulation during prolonged antigen exposure using a library containing 32 variants (*146*).

Table 2. Overview of high throughput approaches for the engineering of CAR signaling architectures

	Cell type	CAR design	Library size	Gene editing	CAR stimulation	Screening	Pooled	Ref.
Gordon & Kyun et al., 2022	Jurkat cell line	Domain recombination	700,000	Lentivirus (random)	Soluble CD19 protein	Sort based on: - CD69 - PD1	Pooled	(*142*)
Goodman & Azimi et al., 2022	Primary T cells	2nd gen. CAR	40	Lentivirus (random)	Irradiated CD19+ cell line	Sort based on - IFNg (18h) - IL-2 (18h) - CD69 (18h) - Proliferation (RAS) - Relative expansion (RAS)	Pooled	(*100*)
Castellanos-Rueda & Di Roberto et al., 2022	Primary T cells	Domain recombination	180	CRISPR-Cas9 (*TRAC* locus)	HER2+ cell line	scRNAseq: profiling of multi-dimensional cellular phenotypes	Pooled	(*99*)
Daniels et al., 2023	Primary T cells	Motif recombination	- 246 tested - 2379 predicted	Lentivirus (random)	CD19+ cell line	Sort based on: -Stemness (IL7Ra+/KLRG-) -Cytotoxicity (E:T ratio post killing) Machine learning	Arrayed	(*144*)
Si et al., 2023	Jurkat cell line	Modules recombination	60	Lentivirus (random)	K562 cells (CD19)	Jurkat reporter: NFAT + NF-kB	Arrayed	(*143*)
Rios et al., 2023	Jurkat cells and Primary T cells	Full length CAR domain recombination	2x180 (two scFv; CD19 and GD2)	Lentivirus (random)	Raji cells for CD19 CHLA-255 cells for GD2	Sort based on: - Jurkat cells: CD69 - Primary T cells: expansion and proliferation after RAS	Pooled	(*145*)
Castellanos-Rueda et al., 2024 (Preprint)	Primary T cells	Domain recombination	32	CRISPR-Cas9 (TRAC locus)	HER2+ cell line	Sort based on: - CD107a (RAS) - IFNg (RAS) scRNAseq profiling (RAS)	Pooled	(*146*)

Abbreviations: RAS, Repeated antigen stimulation.

Lastly, other high-throughput approaches to engineer CAR T cells through the incorporation of additional gene modifications have been described. For instance, inspired by previous CRISPR screens conducted in various T cell contexts (*112*, *147*, *148*), researchers have engineered sgRNA libraries alongside the CAR transgene identifying gene knock-outs that enhance the functional capabilities of CAR T cells, including PRDM1 (*149*), MED12 and CCNC (*150*). In another approach, Blaeschke et al., simultaneously knocked in a CAR transgene and libraries containing either 100 transcription factors or 129 natural and synthetic surface receptors in primary T cells. In vitro screens revealed that the knock-in of the AP4 transcription factor improved the fitness of CAR-T cells during chronic stimulation (*151*). This study thus contributes to the diversification of high-throughput strategies for CAR T cell engineering, integrating complex gene constructs to modulate cellular functions.

References for Chapter 1

1. Z. Eshhar, T. Waks, G. Gross, D. G. Schindler, Specific activation and targeting of cytotoxic lymphocytes through chimeric single chains consisting of antibody-binding domains and the gamma or zeta subunits of the immunoglobulin and T-cell receptors. *Proc. Natl. Acad. Sci. U. S. A.* **90**, 720–724 (1993).

2. H. M. Finney, A. D. Lawson, C. R. Bebbington, A. N. Weir, Chimeric receptors providing both primary and costimulatory signaling in T cells from a single gene product. *J. Immunol.* **161**, 2791–2797 (1998).

3. C. Imai, K. Mihara, M. Andreansky, I. C. Nicholson, C.-H. Pui, T. L. Geiger, D. Campana, Chimeric receptors with 4-1BB signaling capacity provoke potent cytotoxicity against acute lymphoblastic leukemia. *Leukemia* **18**, 676–684 (2004).

4. G. Gross, T. Waks, Z. Eshhar, Expression of immunoglobulin-T-cell receptor chimeric molecules as functional receptors with antibody-type specificity. *Proc. Natl. Acad. Sci. U. S. A.* **86**, 10024–10028 (1989).

5. J. N. Kochenderfer, W. H. Wilson, J. E. Janik, M. E. Dudley, M. Stetler-Stevenson, S. A. Feldman, I. Maric, M. Raffeld, D.-A. N. Nathan, B. J. Lanier, R. A. Morgan, S. A. Rosenberg, Eradication of B-lineage cells and regression of lymphoma in a patient treated with autologous T cells genetically engineered to recognize CD19. *Blood* **116**, 4099–4102 (2010).

6. D. L. Porter, B. L. Levine, M. Kalos, A. Bagg, C. H. June, Chimeric antigen receptor-modified T cells in chronic lymphoid leukemia. *N. Engl. J. Med.* **365**, 725–733 (2011).

7. S. J. Schuster, J. Svoboda, E. A. Chong, S. D. Nasta, A. R. Mato, Ö. Anak, J. L. Brogdon, I. Pruteanu-Malinici, V. Bhoj, D. Landsburg, M. Wasik, B. L. Levine, S. F. Lacey, J. J. Melenhorst, D. L. Porter, C. H. June, Chimeric Antigen Receptor T Cells in Refractory B-Cell Lymphomas. *N. Engl. J. Med.* **377**, 2545–2554 (2017).

8. J. H. Park, I. Rivière, M. Gonen, X. Wang, B. Sénéchal, K. J. Curran, C. Sauter, Y. Wang, B. Santomasso, E. Mead, M. Roshal, P. Maslak, M. Davila, R. J. Brentjens, M. Sadelain, Long-Term Follow-up of CD19 CAR Therapy in Acute Lymphoblastic Leukemia. *N. Engl. J. Med.* **378**, 449–459 (2018).

9. C. J. Turtle, L.-A. Hanafi, C. Berger, M. Hudecek, B. Pender, E. Robinson, R. Hawkins, C. Chaney, S. Cherian, X. Chen, L. Soma, B. Wood, D. Li, S. Heimfeld, S. R. Riddell, D. G. Maloney, Immunotherapy of non-Hodgkin's lymphoma with a defined ratio of CD8+ and CD4+ CD19-specific chimeric antigen receptor-modified T cells. *Sci. Transl. Med.* **8**, 355ra116 (2016).

10. N. C. Munshi, L. D. Anderson Jr, N. Shah, D. Madduri, J. Berdeja, S. Lonial, N. Raje, Y. Lin, D. Siegel, A. Oriol, P. Moreau, I. Yakoub-Agha, M. Delforge, M. Cavo, H. Einsele, H. Goldschmidt, K. Weisel, A. Rambaldi, D. Reece, F. Petrocca, M. Massaro, J. N. Connarn, S. Kaiser, P. Patel, L. Huang, T. B. Campbell, K. Hege, J. San-Miguel, Idecabtagene Vicleucel in Relapsed and Refractory Multiple Myeloma. *N. Engl. J. Med.* **384**, 705–716 (2021).

11. V. Wang, M. Gauthier, V. Decot, L. Reppel, D. Bensoussan, Systematic Review on CAR-T Cell Clinical Trials Up to 2022: Academic Center Input. *Cancers* **15** (2023).

12. K. M. Cappell, J. N. Kochenderfer, Long-term outcomes following CAR T cell therapy: what we know so far. *Nat. Rev. Clin. Oncol.* **20**, 359–371 (2023).

13. R. C. Sterner, R. M. Sterner, CAR-T cell therapy: current limitations and potential strategies. *Blood Cancer J.* **11**, 69 (2021).

14. V. Svensson, R. Vento-Tormo, S. A. Teichmann, Exponential scaling of single-cell RNA-seq in the past decade. *Nat. Protoc.* **13**, 599–604 (2018).

15. M. J. T. Stubbington, O. Rozenblatt-Rosen, A. Regev, S. A. Teichmann, Single-cell transcriptomics to explore the immune system in health and disease. *Science* **358**, 58–63 (2017).

16. F. Tang, C. Barbacioru, Y. Wang, E. Nordman, C. Lee, N. Xu, X. Wang, J. Bodeau, B. B. Tuch, A. Siddiqui, K. Lao, M. A. Surani, mRNA-Seq whole-transcriptome analysis of a single cell. *Nat. Methods* **6**, 377–382 (2009).

17. F. Horns, C. L. Dekker, S. R. Quake, Memory B Cell Activation, Broad Anti-influenza Antibodies, and Bystander Activation Revealed by Single-Cell Transcriptomics. *Cell Rep.* **30**, 905–913.e6 (2020).

18. K. Joshi, M. R. de Massy, M. Ismail, J. L. Reading, I. Uddin, A. Woolston, E. Hatipoglu, T. Oakes, R. Rosenthal, T. Peacock, T. Ronel, M. Noursadeghi, V. Turati, A. J. S. Furness, A. Georgiou, Y. N. S. Wong, A. Ben Aissa, M. W. Sunderland, M. Jamal-Hanjani, S. Veeriah, N. J. Birkbak, G. A. Wilson, C. T. Hiley, E. Ghorani, J. A. Guerra-Assunção, J. Herrero, T. Enver, S. R. Hadrup, A. Hackshaw, K. S. Peggs, N. McGranahan, C. Swanton, TRACERx consortium, S. A. Quezada, B. Chain, Spatial heterogeneity of the T cell receptor repertoire reflects the mutational landscape in lung cancer. *Nat. Med.* **25**, 1549–1559 (2019).

19. J.-Y. Zhang, X.-M. Wang, X. Xing, Z. Xu, C. Zhang, J.-W. Song, X. Fan, P. Xia, J.-L. Fu, S.-Y. Wang, R.-N. Xu, X.-P. Dai, L. Shi, L. Huang, T.-J. Jiang, M. Shi, Y. Zhang, A. Zumla, M. Maeurer, F. Bai, F.-S. Wang, Single-cell landscape of immunological responses in patients with COVID-19. *Nat. Immunol.* **21**, 1107–1118 (2020).

20. M. Sade-Feldman, K. Yizhak, S. L. Bjorgaard, J. P. Ray, C. G. de Boer, R. W. Jenkins, D. J. Lieb, J. H. Chen, D. T. Frederick, M. Barzily-Rokni, S. S. Freeman, A. Reuben, P. J. Hoover, A.-C. Villani, E. Ivanova, A. Portell, P. H. Lizotte, A. R. Aref, J.-P. Eliane, M. R. Hammond, H. Vitzthum, S. M. Blackmon, B. Li, V. Gopalakrishnan, S. M. Reddy, Z. A. Cooper, C. P. Paweletz, D. A. Barbie, A. Stemmer-Rachamimov, K. T. Flaherty, J. A. Wargo, G. M. Boland, R. J. Sullivan, G. Getz, N. Hacohen, Defining T Cell States Associated with Response to Checkpoint Immunotherapy in Melanoma. *Cell* **175**, 998–1013.e20 (2018).

21. D. Ramsköld, S. Luo, Y.-C. Wang, R. Li, Q. Deng, O. R. Faridani, G. A. Daniels, I. Khrebtukova, J. F. Loring, L. C. Laurent, G. P. Schroth, R. Sandberg, Full-length mRNA-Seq from single-cell levels of RNA and individual circulating tumor cells. *Nat. Biotechnol.* **30**, 777–782 (2012).

22. V. M. Peterson, K. X. Zhang, N. Kumar, J. Wong, L. Li, D. C. Wilson, R. Moore, T. K. McClanahan, S. Sadekova, J. A. Klappenbach, Multiplexed quantification of proteins and transcripts in single cells. *Nat. Biotechnol.* **35**, 936–939 (2017).

23. A. B. Rosenberg, C. M. Roco, R. A. Muscat, A. Kuchina, P. Sample, Z. Yao, L. T. Graybuck, D. J. Peeler, S. Mukherjee, W. Chen, S. H. Pun, D. L. Sellers, B. Tasic, G. Seelig, Single-cell profiling of the developing mouse brain and spinal cord with split-pool barcoding. *Science* **360**, 176–182 (2018).

24. M. Saikia, P. Burnham, S. H. Keshavjee, M. F. Z. Wang, M. Heyang, P. Moral-Lopez, M. M. Hinchman, C. G. Danko, J. S. L. Parker, I. De Vlaminck, Simultaneous multiplexed amplicon sequencing and transcriptome profiling in single cells. *Nat. Methods* **16**, 59–62 (2019).

25. W. Chen, Y. Zhao, X. Chen, Z. Yang, X. Xu, Y. Bi, V. Chen, J. Li, H. Choi, B. Ernest, B. Tran, M. Mehta, P. Kumar, A. Farmer, A. Mir, U. A. Mehra, J.-L. Li, M. Moos Jr, W. Xiao, C. Wang, A multicenter study benchmarking single-cell RNA sequencing technologies using reference samples. *Nat. Biotechnol.* **39**, 1103–1114 (2021).

26. J. Cao, M. Spielmann, X. Qiu, X. Huang, D. M. Ibrahim, A. J. Hill, F. Zhang, S. Mundlos, L. Christiansen, F. J. Steemers, C. Trapnell, J. Shendure, The single-cell transcriptional landscape of mammalian organogenesis. *Nature* **566**, 496–502 (2019).

27. A. Butler, P. Hoffman, P. Smibert, E. Papalexi, R. Satija, Integrating single-cell transcriptomic data across different conditions, technologies, and species. *Nat. Biotechnol.* **36**, 411–420 (2018).

28. T. Aoki, L. C. Chong, K. Takata, K. Milne, M. Hav, A. Colombo, E. A. Chavez, M. Nissen, X. Wang, T. Miyata-Takata, V.

Lam, E. Viganò, B. W. Woolcock, A. Telenius, M. Y. Li, S. Healy, C. Ghesquiere, D. Kos, T. Goodyear, J. Veldman, A. W. Zhang, J. Kim, S. Saberi, J. Ding, P. Farinha, A. P. Weng, K. J. Savage, D. W. Scott, G. Krystal, B. H. Nelson, A. Mottok, A. Merchant, S. P. Shah, C. Steidl, Single-Cell Transcriptome Analysis Reveals Disease-Defining T-cell Subsets in the Tumor Microenvironment of Classic Hodgkin Lymphoma. *Cancer Discov.* **10**, 406–421 (2020).

29. P. Savas, B. Virassamy, C. Ye, A. Salim, C. P. Mintoff, F. Caramia, R. Salgado, D. J. Byrne, Z. L. Teo, S. Dushyanthen, A. Byrne, L. Wein, S. J. Luen, C. Poliness, S. S. Nightingale, A. S. Skandarajah, D. E. Gyorki, C. M. Thornton, P. A. Beavis, S. B. Fox, Kathleen Cuningham Foundation Consortium for Research into Familial Breast Cancer (kConFab), P. K. Darcy, T. P. Speed, L. K. Mackay, P. J. Neeson, S. Loi, Single-cell profiling of breast cancer T cells reveals a tissue-resident memory subset associated with improved prognosis. *Nat. Med.* **24**, 986–993 (2018).

30. Å. K. Björklund, M. Forkel, S. Picelli, V. Konya, J. Theorell, D. Friberg, R. Sandberg, J. Mjösberg, The heterogeneity of human CD127(+) innate lymphoid cells revealed by single-cell RNA sequencing. *Nat. Immunol.* **17**, 451–460 (2016).

31. J. T. Gaublomme, N. Yosef, Y. Lee, R. S. Gertner, L. V. Yang, C. Wu, P. P. Pandolfi, T. Mak, R. Satija, A. K. Shalek, V. K. Kuchroo, H. Park, A. Regev, Single-Cell Genomics Unveils Critical Regulators of Th17 Cell Pathogenicity. *Cell* **163**, 1400–1412 (2015).

32. A. A. Eltahla, S. Rizzetto, M. R. Pirozyan, B. D. Betz-Stablein, V. Venturi, K. Kedzierska, A. R. Lloyd, R. A. Bull, F. Luciani, Linking the T cell receptor to the single cell transcriptome in antigen-specific human T cells. *Immunol. Cell Biol.* **94**, 604–611 (2016).

33. A. Yermanos, A. Agrafiotis, R. Kuhn, D. Robbiani, J. Yates, C. Papadopoulou, J. Han, I. Sandu, C. Weber, F. Bieberich, R. Vazquez-Lombardi, A. Dounas, D. Neumeier, A. Oxenius, S. T. Reddy, Platypus: an open-access software for integrating lymphocyte single-cell immune repertoires with transcriptomes. *NAR Genom Bioinform* **3**, lqab023 (2021).

34. S.-M. Kim, L. Bhonsle, P. Besgen, J. Nickel, A. Backes, K. Held, S. Vollmer, K. Dornmair, J. C. Prinz, Analysis of the paired TCR α- and β-chains of single human T cells. *PLoS One* **7**, e37338 (2012).

35. M. J. Spindler, A. L. Nelson, J. M. Heather, E. K. Wagner, A. S. Adler, D. S. Johnson, High-throughput screening for rare antigen-reactive TCRs using natively-paired TCRαβ expression libraries generated from millions diverse primary T cells. *J. Immunol.* **204**, 243.23–243.23 (2020).

36. B. J. DeKosky, T. Kojima, A. Rodin, W. Charab, G. C. Ippolito, A. D. Ellington, G. Georgiou, In-depth determination and analysis of the human paired heavy- and light-chain antibody repertoire. *Nat. Med.* **21**, 86–91 (2015).

37. A. Han, J. Glanville, L. Hansmann, M. M. Davis, Linking T-cell receptor sequence to functional phenotype at the single-cell level. *Nat. Biotechnol.* **32**, 684–692 (2014).

38. S. V. Puram, I. Tirosh, A. S. Parikh, A. P. Patel, K. Yizhak, S. Gillespie, C. Rodman, C. L. Luo, E. A. Mroz, K. S. Emerick, D. G. Deschler, M. A. Varvares, R. Mylvaganam, O. Rozenblatt-Rosen, J. W. Rocco, W. C. Faquin, D. T. Lin, A. Regev, B. E. Bernstein, Single-Cell Transcriptomic Analysis of Primary and Metastatic Tumor Ecosystems in Head and Neck Cancer. *Cell* **171**, 1611–1624.e24 (2017).

39. Y. Zhang, J. Song, Z. Zhao, M. Yang, M. Chen, C. Liu, J. Ji, D. Zhu, Single-cell transcriptome analysis reveals tumor immune microenvironment heterogenicity and granulocytes enrichment in colorectal cancer liver metastases. *Cancer Lett.* **470**, 84–94 (2020).

40. I. Tirosh, B. Izar, S. M. Prakadan, M. H. Wadsworth 2nd, D. Treacy, J. J. Trombetta, A. Rotem, C. Rodman, C. Lian, G. Murphy, M. Fallahi-Sichani, K. Dutton-Regester, J.-R. Lin, O. Cohen, P. Shah, D. Lu, A. S. Genshaft, T. K. Hughes, C. G. K. Ziegler, S. W. Kazer, A. Gaillard, K. E. Kolb, A.-C. Villani, C. M. Johannessen, A. Y. Andreev, E. M. Van Allen, M. Bertagnolli, P. K. Sorger, R. J. Sullivan, K. T. Flaherty, D. T. Frederick, J. Jané-Valbuena, C. H. Yoon, O. Rozenblatt-Rosen, A. K. Shalek, A. Regev, L. A. Garraway, Dissecting the multicellular ecosystem of metastatic melanoma by single-cell RNA-seq. *Science* **352**, 189–196 (2016).

41. W. Chung, H. H. Eum, H.-O. Lee, K.-M. Lee, H.-B. Lee, K.-T. Kim, H. S. Ryu, S. Kim, J. E. Lee, Y. H. Park, Z. Kan, W. Han, W.-Y. Park, Single-cell RNA-seq enables comprehensive tumour and immune cell profiling in primary breast cancer. *Nat. Commun.* **8**, 15081 (2017).

42. X. Guo, Y. Zhang, L. Zheng, C. Zheng, J. Song, Q. Zhang, B. Kang, Z. Liu, L. Jin, R. Xing, R. Gao, L. Zhang, M. Dong, X. Hu, X. Ren, D. Kirchhoff, H. G. Roider, T. Yan, Z. Zhang, Global characterization of T cells in non-small-cell lung cancer by single-cell sequencing. *Nat. Med.* **24**, 978–985 (2018).

43. C. Zheng, L. Zheng, J.-K. Yoo, H. Guo, Y. Zhang, X. Guo, B. Kang, R. Hu, J. Y. Huang, Q. Zhang, Z. Liu, M. Dong, X. Hu,

W. Ouyang, J. Peng, Z. Zhang, Landscape of Infiltrating T Cells in Liver Cancer Revealed by Single-Cell Sequencing. *Cell* **169**, 1342–1356.e16 (2017).

44. T. B. Buus, A. Willerslev-Olsen, S. Fredholm, E. Blümel, C. Nastasi, M. Gluud, T. Hu, L. M. Lindahl, L. Iversen, H. Fogh, R. Gniadecki, I. V. Litvinov, J. L. Persson, C. M. Bonefeld, C. Geisler, J. P. Christensen, T. Krejsgaard, T. Litman, A. Woetmann, N. Ødum, Single-cell heterogeneity in Sézary syndrome. *Blood Adv* **2**, 2115–2126 (2018).

45. W. Scheper, S. Kelderman, L. F. Fanchi, C. Linnemann, G. Bendle, M. A. J. de Rooij, C. Hirt, R. Mezzadra, M. Slagter, K. Dijkstra, R. J. C. Kluin, P. Snaebjornsson, K. Milne, B. H. Nelson, H. Zijlmans, G. Kenter, E. E. Voest, J. B. A. G. Haanen, T. N. Schumacher, Low and variable tumor reactivity of the intratumoral TCR repertoire in human cancers. *Nat. Med.* **25**, 89–94 (2019).

46. Y.-C. Lu, L. Jia, Z. Zheng, E. Tran, P. F. Robbins, S. A. Rosenberg, Single-Cell Transcriptome Analysis Reveals Gene Signatures Associated with T-cell Persistence Following Adoptive Cell Therapy. *Cancer Immunol Res* **7**, 1824–1836 (2019).

47. Z.-C. Ding, H. Shi, N. S. Aboelella, K. Fesenkova, E.-J. Park, Z. Liu, L. Pei, J. Li, R. A. McIndoe, H. Xu, G. A. Piazza, B. R. Blazar, D. H. Munn, G. Zhou, Persistent STAT5 activation reprograms the epigenetic landscape in CD4+ T cells to drive polyfunctionality and antitumor immunity. *Sci Immunol* **5** (2020).

48. J. Wei, L. Long, W. Zheng, Y. Dhungana, S. A. Lim, C. Guy, Y. Wang, Y.-D. Wang, C. Qian, B. Xu, A. Kc, J. Saravia, H. Huang, J. Yu, J. G. Doench, T. L. Geiger, H. Chi, Targeting REGNASE-1 programs long-lived effector T cells for cancer therapy. *Nature* **576**, 471–476 (2019).

49. L. Ye, J. J. Park, M. B. Dong, Q. Yang, R. D. Chow, L. Peng, Y. Du, J. Guo, X. Dai, G. Wang, Y. Errami, S. Chen, In vivo CRISPR screening in CD8 T cells with AAV-Sleeping Beauty hybrid vectors identifies membrane targets for improving immunotherapy for glioblastoma. *Nat. Biotechnol.* **37**, 1302–1313 (2019).

50. Z. Ying, X. F. Huang, X. Xiang, Y. Liu, X. Kang, Y. Song, X. Guo, H. Liu, N. Ding, T. Zhang, P. Duan, Y. Lin, W. Zheng, X. Wang, N. Lin, M. Tu, Y. Xie, C. Zhang, W. Liu, L. Deng, S. Gao, L. Ping, X. Wang, N. Zhou, J. Zhang, Y. Wang, S. Lin, M. Mamuti, X. Yu, L. Fang, S. Wang, H. Song, G. Wang, L. Jones, J. Zhu, S.-Y. Chen, A safe and potent anti-CD19 CAR T cell therapy. *Nat. Med.* **25**, 947–953 (2019).

51. J. Feucht, J. Sun, J. Eyquem, Y.-J. Ho, Z. Zhao, J. Leibold, A. Dobrin, A. Cabriolu, M. Hamieh, M. Sadelain, Calibration of CAR activation potential directs alternative T cell fates and therapeutic potency. *Nat. Med.* **25**, 82–88 (2019).

52. F. A. Hartl, E. Beck-Garcìa, N. M. Woessner, L. J. Flachsmann, R. M.-H. V. Cárdenas, S. M. Brandl, S. Taromi, G. J. Fiala, A. Morath, P. Mishra, O. S. Yousefi, J. Zimmermann, N. Hoefflin, M. Köhn, B. M. Wöhrl, R. Zeiser, K. Schweimer, S. Günther, W. W. Schamel, S. Minguet, Noncanonical binding of Lck to CD3ε promotes TCR signaling and CAR function. *Nat. Immunol.* **21**, 902–913 (2020).

53. M. Hudecek, D. Sommermeyer, P. L. Kosasih, A. Silva-Benedict, L. Liu, C. Rader, M. C. Jensen, S. R. Riddell, The nonsignaling extracellular spacer domain of chimeric antigen receptors is decisive for in vivo antitumor activity. *Cancer Immunol Res* **3**, 125–135 (2015).

54. Y. Kagoya, S. Tanaka, T. Guo, M. Anczurowski, C.-H. Wang, K. Saso, M. O. Butler, M. D. Minden, N. Hirano, A novel chimeric antigen receptor containing a JAK-STAT signaling domain mediates superior antitumor effects. *Nat. Med.* **24**, 352–359 (2018).

55. B. Prinzing, P. Schreiner, M. Bell, Y. Fan, G. Krenciute, S. Gottschalk, MyD88/CD40 signaling retains CAR T cells in a less differentiated state. *JCI Insight* **5** (2020).

56. S. Guedan, A. Madar, V. Casado-Medrano, C. Shaw, A. Wing, F. Liu, R. M. Young, C. H. June, A. D. Posey Jr, Single residue in CD28-costimulated CAR-T cells limits long-term persistence and antitumor durability. *J. Clin. Invest.* **130**, 3087–3097 (2020).

57. P. A. Szabo, H. M. Levitin, M. Miron, M. E. Snyder, T. Senda, J. Yuan, Y. L. Cheng, E. C. Bush, P. Dogra, P. Thapa, D. L. Farber, P. A. Sims, Single-cell transcriptomics of human T cells reveals tissue and activation signatures in health and disease. *Nat. Commun.* **10**, 4706 (2019).

58. I. Xhangolli, B. Dura, G. Lee, D. Kim, Y. Xiao, R. Fan, Single-cell Analysis of CAR-T Cell Activation Reveals A Mixed TH1/TH2 Response Independent of Differentiation. *Genomics Proteomics Bioinformatics* **17**, 129–139 (2019).

59. X. Wang, C. Peticone, E. Kotsopoulou, B. Göttgens, F. J. Calero-Nieto, Single-cell transcriptome analysis of CAR T-cell products reveals subpopulations, stimulation, and exhaustion signatures. *Oncoimmunology* **10**, 1866287 (2021).

60. A. C. Boroughs, R. C. Larson, N. D. Marjanovic, K. Gosik, A. P. Castano, C. B. M. Porter, S. J. Lorrey, O. Ashenberg, L. Jerby, M. Hofree, G. Smith-Rosario, R. Morris, J. Gould, L. S. Riley, T. R. Berger, S. J. Riesenfeld, O. Rozenblatt-Rosen, B. D. Choi, A. Regev, M. V. Maus, A Distinct Transcriptional Program in Human CAR T Cells Bearing the 4-1BB Signaling Domain Revealed by scRNA-Seq. *Mol. Ther.* **28**, 2577–2592 (2020).

61. K. Ishii, M. Pouzolles, C. D. Chien, R. A. Erwin-Cohen, M. E. Kohler, H. Qin, H. Lei, S. Kuhn, A. K. Ombrello, A. Dulau-Florea, M. A. Eckhaus, H. Shalabi, B. Yates, D. A. Lichtenstein, V. S. Zimmermann, T. Kondo, J. F. Shern, H. A. Young, N. Taylor, N. N. Shah, T. J. Fry, Perforin-deficient CAR T cells recapitulate late-onset inflammatory toxicities observed in patients. *J. Clin. Invest.* **130**, 5425–5443 (2020).

62. X. Ma, P. Shou, C. Smith, Y. Chen, H. Du, C. Sun, N. Porterfield Kren, D. Michaud, S. Ahn, B. Vincent, B. Savoldo, Y. Pylayeva-Gupta, S. Zhang, G. Dotti, Y. Xu, Interleukin-23 engineering improves CAR T cell function in solid tumors. *Nat. Biotechnol.* **38**, 448–459 (2020).

63. N. Tang, C. Cheng, X. Zhang, M. Qiao, N. Li, W. Mu, X.-F. Wei, W. Han, H. Wang, TGF-β inhibition via CRISPR promotes the long-term efficacy of CAR T cells against solid tumors. *JCI Insight* **5** (2020).

64. R. C. Lynn, E. W. Weber, E. Sotillo, D. Gennert, P. Xu, Z. Good, H. Anbunathan, J. Lattin, R. Jones, V. Tieu, S. Nagaraja, J. Granja, C. F. A. de Bourcy, R. Majzner, A. T. Satpathy, S. R. Quake, M. Monje, H. Y. Chang, C. L. Mackall, c-Jun overexpression in CAR T cells induces exhaustion resistance. *Nature* **576**, 293–300 (2019).

65. J. Chen, I. F. López-Moyado, H. Seo, C.-W. J. Lio, L. J. Hempleman, T. Sekiya, A. Yoshimura, J. P. Scott-Browne, A. Rao, NR4A transcription factors limit CAR T cell function in solid tumours. *Nature* **567**, 530–534 (2019).

66. D. Wang, B. C. Prager, R. C. Gimple, B. Aguilar, D. Alizadeh, H. Tang, D. Lv, R. Starr, A. Brito, Q. Wu, L. J. Y. Kim, Z. Qiu, P. Lin, M. H. Lorenzini, B. Badie, S. J. Forman, Q. Xie, C. E. Brown, J. N. Rich, CRISPR Screening of CAR T Cells and Cancer Stem Cells Reveals Critical Dependencies for Cell-Based Therapies. *Cancer Discov.* **11**, 1192–1211 (2021).

67. C. R. Good, M. A. Aznar, S. Kuramitsu, P. Samareh, S. Agarwal, G. Donahue, K. Ishiyama, N. Wellhausen, A. K. Rennels, Y. Ma, L. Tian, S. Guedan, K. A. Alexander, Z. Zhang, P. C. Rommel, N. Singh, K. M. Glastad, M. W. Richardson, K. Watanabe, J. L. Tanyi, M. H. O'Hara, M. Ruella, S. F. Lacey, E. K. Moon, S. J. Schuster, S. M. Albelda, L. L. Lanier, R. M. Young, S. L. Berger, C. H. June, An NK-like CAR T cell transition in CAR T cell dysfunction. *Cell* **184**, 6081–6100.e26 (2021).

68. P. Jiang, Z. Zhang, Y. Hu, Z. Liang, Y. Han, X. Li, X. Zeng, H. Zhang, M. Zhu, J. Dong, H. Huang, P. Qian, Single-cell ATAC-seq maps the comprehensive and dynamic chromatin accessibility landscape of CAR-T cell dysfunction. *Leukemia* **36**, 2656–2668 (2022).

69. J. Eyquem, J. Mansilla-Soto, T. Giavridis, S. J. C. van der Stegen, M. Hamieh, K. M. Cunanan, A. Odak, M. Gönen, M. Sadelain, Targeting a CAR to the TRAC locus with CRISPR/Cas9 enhances tumour rejection. *Nature* **543**, 113–117 (2017).

70. K. P. Mueller, N. J. Piscopo, M. H. Forsberg, L. A. Saraspe, A. Das, B. Russell, M. Smerchansky, D. Cappabianca, L. Shi, K. Shankar, L. Sarko, N. Khajanchi, N. La Vonne Denne, A. Ramamurthy, A. Ali, C. R. Lazzarotto, S. Q. Tsai, C. M. Capitini, K. Saha, Production and characterization of virus-free, CRISPR-CAR T cells capable of inducing solid tumor regression. *J Immunother Cancer* **10** (2022).

71. J. Zhang, Y. Hu, J. Yang, W. Li, M. Zhang, Q. Wang, L. Zhang, G. Wei, Y. Tian, K. Zhao, A. Chen, B. Tan, J. Cui, D. Li, Y. Li, Y. Qi, D. Wang, Y. Wu, D. Li, B. Du, M. Liu, H. Huang, Non-viral, specifically targeted CAR-T cells achieve high safety and efficacy in B-NHL. *Nature* **609**, 369–374 (2022).

72. D. Alizadeh, R. A. Wong, X. Yang, D. Wang, J. R. Pecoraro, C.-F. Kuo, B. Aguilar, Y. Qi, D. K. Ann, R. Starr, R. Urak, X. Wang, S. J. Forman, C. E. Brown, IL15 Enhances CAR-T Cell Antitumor Activity by Reducing mTORC1 Activity and Preserving Their Stem Cell Memory Phenotype. *Cancer Immunol Res* **7**, 759–772 (2019).

73. I. P. Foskolou, L. Barbieri, A. Vernet, D. Bargiela, P. P. Cunha, P. Velica, E. Suh, S. Pietsch, R. Matuleviciute, H. Rundqvist, D. McIntyre, K. G. C. Smith, R. S. Johnson, The S enantiomer of 2-hydroxyglutarate increases central memory CD8 populations and improves CAR-T therapy outcome. *Blood Adv* **4**, 4483–4493 (2020).

74. X. Lu, S. M. Lofgren, Y. Zhao, P. K. Mazur, Multiplexed transcriptomic profiling of the fate of human CAR T cells in vivo via genetic barcoding with shielded small nucleotides. *Nat Biomed Eng* **7**, 1170–1187 (2023).

75. M. Works, N. Soni, C. Hauskins, C. Sierra, A. Baturevych, J. C. Jones, W. Curtis, P. Carlson, T. G. Johnstone, D. Kugler, R. J. Hause, Y. Jiang, L. Wimberly, C. R. Clouser, H. K. Jessup, B. Sather, R. A. Salmon, M. O. Ports, Anti-B-cell Maturation Antigen Chimeric Antigen Receptor T cell Function against Multiple Myeloma Is Enhanced in the Presence of

Lenalidomide. *Mol. Cancer Ther.* **18**, 2246–2257 (2019).

76. M. Y. Kim, R. Jayasinghe, J. M. Devenport, J. K. Ritchey, M. P. Rettig, J. O'Neal, K. W. Staser, K. M. Kennerly, A. J. Carter, F. Gao, B. H. Lee, M. L. Cooper, J. F. DiPersio, A long-acting interleukin-7, rhIL-7-hyFc, enhances CAR T cell expansion, persistence, and anti-tumor activity. *Nat. Commun.* **13**, 3296 (2022).

77. E. Moreno-Cortes, J. V. Forero-Forero, P. A. Lengerke-Diaz, J. E. Castro, Chimeric antigen receptor T cell therapy in oncology - Pipeline at a glance: Analysis of the ClinicalTrials.gov database. *Crit. Rev. Oncol. Hematol.* **159**, 103239 (2021).

78. A. Sheih, V. Voillet, L.-A. Hanafi, H. A. DeBerg, M. Yajima, R. Hawkins, V. Gersuk, S. R. Riddell, D. G. Maloney, M. E. Wohlfahrt, D. Pande, M. R. Enstrom, H.-P. Kiem, J. E. Adair, R. Gottardo, P. S. Linsley, C. J. Turtle, Clonal kinetics and single-cell transcriptional profiling of CAR-T cells in patients undergoing CD19 CAR-T immunotherapy. *Nat. Commun.* **11**, 219 (2020).

79. X. Li, X. Guo, Y. Zhu, G. Wei, Y. Zhang, X. Li, H. Xu, J. Cui, W. Wu, J. He, M. E. Ritchie, T. M. Weiskittel, H. Li, H. Yu, L. Ding, M. Shao, Q. Luo, X. Xu, X. Teng, A. H. Chang, J. Zhang, H. Huang, Y. Hu, Single-Cell Transcriptomic Analysis Reveals BCMA CAR-T Cell Dynamics in a Patient with Refractory Primary Plasma Cell Leukemia. *Mol. Ther.* **29**, 645–657 (2021).

80. J. J. Melenhorst, G. M. Chen, M. Wang, D. L. Porter, C. Chen, M. A. Collins, P. Gao, S. Bandyopadhyay, H. Sun, Z. Zhao, S. Lundh, I. Pruteanu-Malinici, C. L. Nobles, S. Maji, N. V. Frey, S. I. Gill, A. W. Loren, L. Tian, I. Kulikovskaya, M. Gupta, D. E. Ambrose, M. M. Davis, J. A. Fraietta, J. L. Brogdon, R. M. Young, A. Chew, B. L. Levine, D. L. Siegel, C. Alanio, E. J. Wherry, F. D. Bushman, S. F. Lacey, K. Tan, C. H. June, Decade-long leukaemia remissions with persistence of CD4+ CAR T cells. *Nature* **602**, 503–509 (2022).

81. T. L. Wilson, H. Kim, C.-H. Chou, D. Langfitt, R. C. Mettelman, A. A. Minervina, E. K. Allen, J.-Y. Métais, M. V. Pogorelyy, J. M. Riberdy, M. P. Velasquez, P. Kottapalli, S. Trivedi, S. R. Olsen, T. Lockey, C. Willis, M. M. Meagher, B. M. Triplett, A. C. Talleur, S. Gottschalk, J. C. Crawford, P. G. Thomas, Common Trajectories of Highly Effective CD19-Specific CAR T Cells Identified by Endogenous T-cell Receptor Lineages. *Cancer Discov.* **12**, 2098–2119 (2022).

82. N. D. Anderson, J. Birch, T. Accogli, I. Criado, E. Khabirova, C. Parks, Y. Wood, M. D. Young, T. Porter, R. Richardson, S. J. Albon, B. Popova, A. Lopes, R. Wynn, R. Hough, S. H. Gohil, M. Pule, P. J. Amrolia, S. Behjati, S. Ghorashian, Transcriptional signatures associated with persisting CD19 CAR-T cells in children with leukemia. *Nat. Med.* **29**, 1700–1709 (2023).

83. R. H. Y. Louie, C. Cai, J. Samir, M. Singh, I. W. Deveson, J. M. Ferguson, T. G. Amos, H. M. McGuire, K. Gowrishankar, T. Adikari, R. Balderas, M. Bonomi, M. Ruella, D. Bishop, D. Gottlieb, E. Blyth, K. Micklethwaite, F. Luciani, CAR+ and CAR- T cells share a differentiation trajectory into an NK-like subset after CD19 CAR T cell infusion in patients with B cell malignancies. *Nat. Commun.* **14**, 7767 (2023).

84. R. G. Majzner, S. Ramakrishna, K. W. Yeom, S. Patel, H. Chinnasamy, L. M. Schultz, R. M. Richards, L. Jiang, V. Barsan, R. Mancusi, A. C. Geraghty, Z. Good, A. Y. Mochizuki, S. M. Gillespie, A. M. S. Toland, J. Mahdi, A. Reschke, E. H. Nie, I. J. Chau, M. C. Rotiroti, C. W. Mount, C. Baggott, S. Mavroukakis, E. Egeler, J. Moon, C. Erickson, S. Green, M. Kunicki, M. Fujimoto, Z. Ehlinger, W. Reynolds, S. Kurra, K. E. Warren, S. Prabhu, H. Vogel, L. Rasmussen, T. T. Cornell, S. Partap, P. G. Fisher, C. J. Campen, M. G. Filbin, G. Grant, B. Sahaf, K. L. Davis, S. A. Feldman, C. L. Mackall, M. Monje, GD2-CAR T cell therapy for H3K27M-mutated diffuse midline gliomas. *Nature* **603**, 934–941 (2022).

85. J. Rossi, P. Paczkowski, Y.-W. Shen, K. Morse, B. Flynn, A. Kaiser, C. Ng, K. Gallatin, T. Cain, R. Fan, S. Mackay, J. R. Heath, S. A. Rosenberg, J. N. Kochenderfer, J. Zhou, A. Bot, Preinfusion polyfunctional anti-CD19 chimeric antigen receptor T cells are associated with clinical outcomes in NHL. *Blood* **132**, 804–814 (2018).

86. A. D. Cohen, J. J. Melenhorst, A. L. Garfall, S. F. Lacey, M. Davis, D. T. Vogl, L. Tian, V. Gonzalez, I. Pruteanu, A. M. Nelson, G. Plesa, A. Waxman, R. M. Young, B. L. Levine, C. H. June, E. A. Stadtmauer, M. C. Milone, Predictors of T Cell Expansion and Clinical Responses Following B-Cell Maturation Antigen-Specific Chimeric Antigen Receptor T Cell Therapy (CART-BCMA) for Relapsed/Refractory Multiple Myeloma (MM). *Blood* **132**, 1974 (2018).

87. O. C. Finney, H. M. Brakke, S. Rawlings-Rhea, R. Hicks, D. Doolittle, M. Lopez, R. B. Futrell, R. J. Orentas, D. Li, R. A. Gardner, M. C. Jensen, CD19 CAR T cell product and disease attributes predict leukemia remission durability. *J. Clin. Invest.* **129**, 2123–2132 (2019).

88. J. A. Fraietta, S. F. Lacey, E. J. Orlando, I. Pruteanu-Malinici, M. Gohil, S. Lundh, A. C. Boesteanu, Y. Wang, R. S. O'Connor, W.-T. Hwang, E. Pequignot, D. E. Ambrose, C. Zhang, N. Wilcox, F. Bedoya, C. Dorfmeier, F. Chen, L. Tian, H. Parakandi, M. Gupta, R. M. Young, F. B. Johnson, I. Kulikovskaya, L. Liu, J. Xu, S. H. Kassim, M. M. Davis, B. L. Levine, N. V. Frey, D. L. Siegel, A. C. Huang, E. J. Wherry, H. Bitter, J. L. Brogdon, D. L. Porter, C. H. June, J. J. Melenhorst,

Determinants of response and resistance to CD19 chimeric antigen receptor (CAR) T cell therapy of chronic lymphocytic leukemia. *Nat. Med.* **24**, 563–571 (2018).

89. Q. Deng, G. Han, N. Puebla-Osorio, M. C. J. Ma, P. Strati, B. Chasen, E. Dai, M. Dang, N. Jain, H. Yang, Y. Wang, S. Zhang, R. Wang, R. Chen, J. Showell, S. Ghosh, S. Patchva, Q. Zhang, R. Sun, F. Hagemeister, L. Fayad, F. Samaniego, H. C. Lee, L. J. Nastoupil, N. Fowler, R. Eric Davis, J. Westin, S. S. Neelapu, L. Wang, M. R. Green, Characteristics of anti-CD19 CAR T cell infusion products associated with efficacy and toxicity in patients with large B cell lymphomas. *Nat. Med.* **26**, 1878–1887 (2020).

90. Z. Bai, S. Woodhouse, Z. Zhao, R. Arya, K. Govek, D. Kim, S. Lundh, A. Baysoy, H. Sun, Y. Deng, Y. Xiao, D. M. Barrett, R. M. Myers, S. A. Grupp, C. H. June, R. Fan, P. G. Camara, J. J. Melenhorst, Single-cell antigen-specific landscape of CAR T infusion product identifies determinants of CD19-positive relapse in patients with ALL. *Sci Adv* **8**, eabj2820 (2022).

91. N. J. Haradhvala, M. B. Leick, K. Maurer, S. H. Gohil, R. C. Larson, N. Yao, K. M. E. Gallagher, K. Katsis, M. J. Frigault, J. Southard, S. Li, M. C. Kann, H. Silva, M. Jan, K. Rhrissorrakrai, F. Utro, C. Levovitz, R. A. Jacobs, K. Slowik, B. P. Danysh, K. J. Livak, L. Parida, J. Ferry, C. Jacobson, C. J. Wu, G. Getz, M. V. Maus, Distinct cellular dynamics associated with response to CAR-T therapy for refractory B cell lymphoma. *Nat. Med.* **28**, 1848–1859 (2022).

92. N. J. Haradhvala, M. V. Maus, Understanding Mechanisms of Response to CAR T-cell Therapy through Single-Cell Sequencing: Insights and Challenges. *Blood Cancer Discov*, OF1–OF4 (2024).

93. Z. Jackson, C. Hong, R. Schauner, B. Dropulic, P. F. Caimi, M. de Lima, M. F. Giraudo, K. Gupta, J. S. Reese, T. H. Hwang, D. N. Wald, Sequential Single-Cell Transcriptional and Protein Marker Profiling Reveals TIGIT as a Marker of CD19 CAR-T Cell Dysfunction in Patients with Non-Hodgkin Lymphoma. *Cancer Discov.* **12**, 1886–1903 (2022).

94. K. M. Dhodapkar, A. D. Cohen, A. Kaushal, A. L. Garfall, R. J. Manalo, A. R. Carr, S. S. McCachren, E. A. Stadtmauer, S. F. Lacey, J. J. Melenhorst, C. H. June, M. C. Milone, M. V. Dhodapkar, Changes in Bone Marrow Tumor and Immune Cells Correlate with Durability of Remissions Following BCMA CAR T Therapy in Myeloma, *Blood cancer discovery*. **3** (2022)pp. 490–501.

95. Y. Wang, C. Tong, Y. Lu, Z. Wu, Y. Guo, Y. Liu, J. Wei, C. Wang, Q. Yang, W. Han, Characteristics of premanufacture CD8+T cells determine CAR-T efficacy in patients with diffuse large B-cell lymphoma. *Signal Transduct Target Ther* **8**, 409 (2023).

96. T. Sarén, M. Ramachandran, G. Gammelgård, T. Lövgren, C. Mirabello, Å. K. Björklund, K. Wikström, J. Hashemi, E. Freyhult, H. Ahlström, R.-M. Amini, H. Hagberg, A. Loskog, G. Enblad, M. Essand, Single-Cell RNA Analysis Reveals Cell-Intrinsic Functions of CAR T Cells Correlating with Response in a Phase II Study of Lymphoma Patients. *Clin. Cancer Res.* **29**, 4139–4152 (2023).

97. X. Li, J. Henderson, M. J. Gordon, I. Sheikh, L. J. Nastoupil, J. Westin, C. Flowers, S. Ahmed, L. Wang, S. S. Neelapu, P. Strati, Q. Deng, M. R. Green, A single-cell atlas of CD19 chimeric antigen receptor T cells. *Cancer Cell* **41**, 1835–1837 (2023).

98. N. Singh, Y. G. Lee, O. Shestova, P. Ravikumar, K. E. Hayer, S. J. Hong, X. M. Lu, R. Pajarillo, S. Agarwal, S. Kuramitsu, E. J. Orlando, K. T. Mueller, C. R. Good, S. L. Berger, O. Shalem, M. D. Weitzman, N. V. Frey, S. L. Maude, S. A. Grupp, C. H. June, S. Gill, M. Ruella, Impaired Death Receptor Signaling in Leukemia Causes Antigen-Independent Resistance by Inducing CAR T-cell Dysfunction. *Cancer Discov.* **10**, 552–567 (2020).

99. R. Castellanos-Rueda, R. B. Di Roberto, F. Bieberich, F. S. Schlatter, D. Palianina, O. T. P. Nguyen, E. Kapetanovic, H. Läubli, A. Hierlemann, N. Khanna, S. T. Reddy, speedingCARs: accelerating the engineering of CAR T cells by signaling domain shuffling and single-cell sequencing. *Nat. Commun.* **13**, 6555 (2022).

100. D. B. Goodman, C. S. Azimi, K. Kearns, A. Talbot, K. Garakani, J. Garcia, N. Patel, B. Hwang, D. Lee, E. Park, V. S. Vykunta, B. R. Shy, C. J. Ye, J. Eyquem, A. Marson, J. A. Bluestone, K. T. Roybal, Pooled screening of CAR T cells identifies diverse immune signaling domains for next-generation immunotherapies. *Sci. Transl. Med.* **14**, eabm1463 (2022).

101. I.-Y. Jung, R. L. Bartoszek, A. J. Rech, S. M. Collins, S.-K. Ooi, E. F. Williams, C. R. Hopkins, V. Narayan, N. B. Haas, N. V. Frey, E. O. Hexner, D. L. Siegel, G. Plesa, D. L. Porter, A. Cantu, J. K. Everett, S. Guedan, S. L. Berger, F. D. Bushman, F. Herbst, J. A. Fraietta, Type I Interferon Signaling via the EGR2 Transcriptional Regulator Potentiates CAR T Cell-Intrinsic Dysfunction. *Cancer Discov.* **13**, 1636–1655 (2023).

102. M. Andreatta, J. Corria-Osorio, S. Müller, R. Cubas, G. Coukos, S. J. Carmona, Interpretation of T cell states from single-cell transcriptomics data using reference atlases. *Nat. Commun.* **12**, 2965 (2021).

103. O. Franzén, L.-M. Gan, J. L. M. Björkegren, PanglaoDB: a web server for exploration of mouse and human single-cell RNA sequencing data. *Database* **2019** (2019).

104. M. B. Elowitz, A. J. Levine, E. D. Siggia, P. S. Swain, Stochastic gene expression in a single cell. *Science* **297**, 1183–1186 (2002).

105. F. Buettner, K. N. Natarajan, F. P. Casale, V. Proserpio, A. Scialdone, F. J. Theis, S. A. Teichmann, J. C. Marioni, O. Stegle, Computational analysis of cell-to-cell heterogeneity in single-cell RNA-sequencing data reveals hidden subpopulations of cells. *Nat. Biotechnol.* **33**, 155–160 (2015).

106. H. T. N. Tran, K. S. Ang, M. Chevrier, X. Zhang, N. Y. S. Lee, M. Goh, J. Chen, A benchmark of batch-effect correction methods for single-cell RNA sequencing data. *Genome Biol.* **21**, 12 (2020).

107. F. Edfors, F. Danielsson, B. M. Hallström, L. Käll, E. Lundberg, F. Pontén, B. Forsström, M. Uhlén, Gene-specific correlation of RNA and protein levels in human cells and tissues. *Mol. Syst. Biol.* **12**, 883 (2016).

108. C. Vogel, R. de S. Abreu, D. Ko, S.-Y. Le, B. A. Shapiro, S. C. Burns, D. Sandhu, D. R. Boutz, E. M. Marcotte, L. O. Penalva, Sequence signatures and mRNA concentration can explain two-thirds of protein abundance variation in a human cell line. *Mol. Syst. Biol.* **6**, 400 (2010).

109. A. Ghazalpour, B. Bennett, V. A. Petyuk, L. Orozco, R. Hagopian, I. N. Mungrue, C. R. Farber, J. Sinsheimer, H. M. Kang, N. Furlotte, C. C. Park, P.-Z. Wen, H. Brewer, K. Weitz, D. G. Camp 2nd, C. Pan, R. Yordanova, I. Neuhaus, C. Tilford, N. Siemers, P. Gargalovic, E. Eskin, T. Kirchgessner, D. J. Smith, R. D. Smith, A. J. Lusis, Comparative analysis of proteome and transcriptome variation in mouse. *PLoS Genet.* **7**, e1001393 (2011).

110. M. Stoeckius, C. Hafemeister, W. Stephenson, B. Houck-Loomis, P. K. Chattopadhyay, H. Swerdlow, R. Satija, P. Smibert, Simultaneous epitope and transcriptome measurement in single cells. *Nat. Methods* **14**, 865–868 (2017).

111. M. Orecchioni, D. Bedognetti, L. Newman, C. Fuoco, F. Spada, W. Hendrickx, F. M. Marincola, F. Sgarrella, A. F. Rodrigues, C. Ménard-Moyon, G. Cesareni, K. Kostarelos, A. Bianco, L. G. Delogu, Single-cell mass cytometry and transcriptome profiling reveal the impact of graphene on human immune cells. *Nat. Commun.* **8**, 1109 (2017).

112. E. Shifrut, J. Carnevale, V. Tobin, T. L. Roth, J. M. Woo, C. T. Bui, P. J. Li, M. E. Diolaiti, A. Ashworth, A. Marson, Genome-wide CRISPR Screens in Primary Human T Cells Reveal Key Regulators of Immune Function. *Cell* **175**, 1958–1971.e15 (2018).

113. T. L. Roth, P. J. Li, F. Blaeschke, J. F. Nies, R. Apathy, C. Mowery, R. Yu, M. L. T. Nguyen, Y. Lee, A. Truong, J. Hiatt, D. Wu, D. N. Nguyen, D. Goodman, J. A. Bluestone, C. J. Ye, K. Roybal, E. Shifrut, A. Marson, Pooled Knockin Targeting for Genome Engineering of Cellular Immunotherapies. *Cell* **181**, 728–744.e21 (2020).

114. N. Singh, M. V. Maus, Synthetic manipulation of the cancer-immunity cycle: CAR-T cell therapy. *Immunity* **56**, 2296–2310 (2023).

115. T. Yan, L. Zhu, J. Chen, Current advances and challenges in CAR T-Cell therapy for solid tumors: tumor-associated antigens and the tumor microenvironment. *Exp. Hematol. Oncol.* **12**, 14 (2023).

116. M. L. Olson, E. R. V. Mause, S. V. Radhakrishnan, J. D. Brody, A. P. Rapoport, A. L. Welm, D. Atanackovic, T. Luetkens, Low-affinity CAR T cells exhibit reduced trogocytosis, preventing rapid antigen loss, and increasing CAR T cell expansion. *Leukemia* **36**, 1943–1946 (2022).

117. X. Liu, S. Jiang, C. Fang, S. Yang, D. Olalere, E. C. Pequignot, A. P. Cogdill, N. Li, M. Ramones, B. Granda, L. Zhou, A. Loew, R. M. Young, C. H. June, Y. Zhao, Affinity-Tuned ErbB2 or EGFR Chimeric Antigen Receptor T Cells Exhibit an Increased Therapeutic Index against Tumors in Mice. *Cancer Res.* **75**, 3596–3607 (2015).

118. J. Chen, S. Qiu, W. Li, K. Wang, Y. Zhang, H. Yang, B. Liu, G. Li, L. Li, M. Chen, J. Lan, J. Niu, P. He, L. Cheng, G. Fan, X. Liu, X. Song, C. Xu, H. Wu, H. Wang, Tuning charge density of chimeric antigen receptor optimizes tonic signaling and CAR-T cell fitness. *Cell Res.* **33**, 341–354 (2023).

119. A. Elazar, N. J. Chandler, A. S. Davey, J. Y. Weinstein, J. V. Nguyen, R. Trenker, R. S. Cross, M. R. Jenkins, M. J. Call, M. E. Call, S. J. Fleishman, De novo-designed transmembrane domains tune engineered receptor functions. *Elife* **11** (2022).

120. K. Fujiwara, A. Tsunei, H. Kusabuka, E. Ogaki, M. Tachibana, N. Okada, Hinge and Transmembrane Domains of Chimeric Antigen Receptor Regulate Receptor Expression and Signaling Threshold. *Cells* **9** (2020).

121. Y. D. Muller, D. P. Nguyen, L. M. R. Ferreira, P. Ho, C. Raffin, R. V. B. Valencia, Z. Congrave-Wilson, T. L. Roth, J. Eyquem, F. Van Gool, A. Marson, L. Perez, J. A. Wells, J. A. Bluestone, Q. Tang, The CD28-Transmembrane Domain Mediates Chimeric Antigen Receptor Heterodimerization With CD28. *Front. Immunol.* **12**, 639818 (2021).

122. O. U. Kawalekar, R. S. O'Connor, J. A. Fraietta, L. Guo, S. E. McGettigan, A. D. Posey Jr, P. R. Patel, S. Guedan, J. Scholler, B. Keith, N. W. Snyder, I. A. Blair, M. C. Milone, C. H. June, Distinct Signaling of Coreceptors Regulates Specific Metabolism Pathways and Impacts Memory Development in CAR T Cells. *Immunity* **44**, 380–390 (2016).

123. S. J. Priceman, E. A. Gerdts, D. Tilakawardane, K. T. Kennewick, J. P. Murad, A. K. Park, B. Jeang, Y. Yamaguchi, X. Yang, R. Urak, L. Weng, W.-C. Chang, S. Wright, S. Pal, R. E. Reiter, A. M. Wu, C. E. Brown, S. J. Forman, Co-stimulatory signaling determines tumor antigen sensitivity and persistence of CAR T cells targeting PSCA+ metastatic prostate cancer. *Oncoimmunology* **7**, e1380764 (2018).

124. S. Guedan, A. D. Posey Jr, C. Shaw, A. Wing, T. Da, P. R. Patel, S. E. McGettigan, V. Casado-Medrano, O. U. Kawalekar, M. Uribe-Herranz, D. Song, J. J. Melenhorst, S. F. Lacey, J. Scholler, B. Keith, R. M. Young, C. H. June, Enhancing CAR T cell persistence through ICOS and 4-1BB costimulation. *JCI Insight* **3** (2018).

125. R. M.-H. Velasco Cárdenas, S. M. Brandl, A. V. Meléndez, A. E. Schlaak, A. Buschky, T. Peters, F. Beier, B. Serrels, S. Taromi, K. Raute, S. Hauri, M. Gstaiger, S. Lassmann, J. B. Huppa, M. Boerries, G. Andrieux, B. Bengsch, W. W. Schamel, S. Minguet, Harnessing CD3 diversity to optimize CAR T cells. *Nat. Immunol.* **24**, 2135–2149 (2023).

126. Y. He, M. Vlaming, T. van Meerten, E. Bremer, The Implementation of TNFRSF Co-Stimulatory Domains in CAR-T Cells for Optimal Functional Activity. *Cancers* **14** (2022).

127. X. Liang, Y. Huang, D. Li, X. Yang, L. Jiang, W. Zhou, J. Su, N. Chen, W. Wang, Distinct functions of CAR-T cells possessing a dectin-1 intracellular signaling domain. *Gene Ther.* **30**, 411–420 (2021).

128. P. George, N. Dasyam, G. Giunti, B. Mester, E. Bauer, B. Andrews, T. Perera, T. Ostapowicz, C. Frampton, P. Li, D. Ritchie, C. M. Bollard, I. F. Hermans, R. Weinkove, Third-generation anti-CD19 chimeric antigen receptor T-cells incorporating a TLR2 domain for relapsed or refractory B-cell lymphoma: a phase I clinical trial protocol (ENABLE). *BMJ Open* **10**, e034629 (2020).

129. J. C. Boucher, G. Li, H. Kotani, M. L. Cabral, D. Morrissey, S. B. Lee, K. Spitler, N. J. Beatty, E. V. Cervantes, B. Shrestha, B. Yu, A. Kazi, X. Wang, S. M. Sebti, M. L. Davila, CD28 Costimulatory Domain-Targeted Mutations Enhance Chimeric Antigen Receptor T-cell Function. *Cancer Immunol Res* **9**, 62–74 (2021).

130. P. Zhang, G. Zhang, X. Wan, Challenges and new technologies in adoptive cell therapy. *J. Hematol. Oncol.* **16**, 97 (2023).

131. K. T. Roybal, L. J. Rupp, L. Morsut, W. J. Walker, K. A. McNally, J. S. Park, W. A. Lim, Precision Tumor Recognition by T Cells With Combinatorial Antigen-Sensing Circuits. *Cell* **164**, 770–779 (2016).

132. N. N. Shah, B. D. Johnson, D. Schneider, F. Zhu, A. Szabo, C. A. Keever-Taylor, W. Krueger, A. A. Worden, M. J. Kadan, S. Yim, A. Cunningham, M. Hamadani, T. S. Fenske, B. Dropulić, R. Orentas, P. Hari, Bispecific anti-CD20, anti-CD19 CAR T cells for relapsed B cell malignancies: a phase 1 dose escalation and expansion trial. *Nat. Med.* **26**, 1569–1575 (2020).

133. A. Di Stasi, S.-K. Tey, G. Dotti, Y. Fujita, A. Kennedy-Nasser, C. Martinez, K. Straathof, E. Liu, A. G. Durett, B. Grilley, H. Liu, C. R. Cruz, B. Savoldo, A. P. Gee, J. Schindler, R. A. Krance, H. E. Heslop, D. M. Spencer, C. M. Rooney, M. K. Brenner, Inducible apoptosis as a safety switch for adoptive cell therapy. *N. Engl. J. Med.* **365**, 1673–1683 (2011).

134. G. Giordano-Attianese, P. Gainza, E. Gray-Gaillard, E. Cribioli, S. Shui, S. Kim, M.-J. Kwak, S. Vollers, A. D. J. Corria Osorio, P. Reichenbach, J. Bonet, B.-H. Oh, M. Irving, G. Coukos, B. E. Correia, A computationally designed chimeric antigen receptor provides a small-molecule safety switch for T-cell therapy. *Nat. Biotechnol.* **38**, 426–432 (2020).

135. J. H. Cho, J. J. Collins, W. W. Wong, Universal Chimeric Antigen Receptors for Multiplexed and Logical Control of T Cell Responses. *Cell* **173**, 1426–1438.e11 (2018).

136. M. Koneru, T. J. Purdon, D. Spriggs, S. Koneru, R. J. Brentjens, IL-12 secreting tumor-targeted chimeric antigen receptor T cells eradicate ovarian tumors in vivo. *Oncoimmunology* **4**, e994446 (2015).

137. E. R. Suarez, D. K. Chang, J. Sun, J. Sui, G. J. Freeman, S. Signoretti, Q. Zhu, W. A. Marasco, Chimeric antigen receptor T cells secreting anti-PD-L1 antibodies more effectively regress renal cell carcinoma in a humanized mouse model. *Oncotarget* **7**, 34341–34355 (2016).

138. S. G. Peisajovich, J. E. Garbarino, P. Wei, W. A. Lim, Rapid diversification of cell signaling phenotypes by modular domain recombination. *Science* **328**, 368–372 (2010).

139. J. Rydzek, T. Nerreter, H. Peng, S. Jutz, J. Leitner, P. Steinberger, H. Einsele, C. Rader, M. Hudecek, Chimeric Antigen Receptor Library Screening Using a Novel NF-κB/NFAT Reporter Cell Platform. *Mol. Ther.* **27**, 287–299 (2019).

140. R. B. Di Roberto, R. Castellanos-Rueda, S. Frey, D. Egli, R. Vazquez-Lombardi, E. Kapetanovic, J. Kucharczyk, S. T. Reddy, A Functional Screening Strategy for Engineering Chimeric Antigen Receptors with Reduced On-Target, Off-Tumor Activation. *Mol. Ther.* **28**, 2564–2576 (2020).

141. R. B. Di Roberto, B. M. Scott, S. G. Peisajovich, Directed Evolution Methods to Rewire Signaling Networks. *Methods Mol. Biol.* **1596**, 321–337 (2017).

142. K. S. Gordon, T. Kyung, C. R. Perez, P. V. Holec, A. Ramos, A. Q. Zhang, Y. Agarwal, Y. Liu, C. E. Koch, A. Starchenko, B. A. Joughin, D. A. Lauffenburger, D. J. Irvine, M. T. Hemann, M. E. Birnbaum, Screening for CD19-specific chimaeric antigen receptors with enhanced signalling via a barcoded library of intracellular domains. *Nat Biomed Eng* **6**, 855–866 (2022).

143. W. Si, Y.-Y. Fan, S.-Z. Qiu, X. Li, E.-Y. Wu, J.-Q. Ju, W. Huang, H.-P. Wang, P. Wei, Design of diversified chimeric antigen receptors through rational module recombination. *iScience* **26**, 106529 (2023).

144. K. G. Daniels, S. Wang, M. S. Simic, H. K. Bhargava, S. Capponi, Y. Tonai, W. Yu, S. Bianco, W. A. Lim, Decoding CAR T cell phenotype using combinatorial signaling motif libraries and machine learning. *Science* **378**, 1194–1200 (2022).

145. X. Rios, O. Pardias, M. A. Morales, P. Bhattacharya, Y. Chen, L. Guo, C. Zhang, E. J. Di Pierro, G. Tian, G. A. Barragan, P. Sumazin, L. S. Metelitsa, Refining chimeric antigen receptors via barcoded protein domain combination pooled screening. *Mol. Ther.* **31**, 3210–3224 (2023).

146. R. Castellanos-Rueda, K.-L. K. Wang, J. L. Forster, A. Driessen, J. A. Frank, M. R. Martinez, S. T. Reddy, Dissecting the role of CAR signaling architectures on T cell activation and persistence using pooled screening and single-cell sequencing, *bioRxiv* (2024)p. 2024.02.26.582129.

147. M. P. Trefny, N. Kirchhammer, P. Auf der Maur, M. Natoli, D. Schmid, M. Germann, L. Fernandez Rodriguez, P. Herzig, J. Lötscher, M. Akrami, J. C. Stinchcombe, M. A. Stanczak, A. Zingg, M. Buchi, J. Roux, R. Marone, L. Don, D. Lardinois, M. Wiese, L. T. Jeker, M. Bentires-Alj, J. Rossy, D. S. Thommen, G. M. Griffiths, H. Läubli, C. Hess, A. Zippelius, Deletion of SNX9 alleviates CD8 T cell exhaustion for effective cellular cancer immunotherapy. *Nat. Commun.* **14**, 86 (2023).

148. J. A. Belk, W. Yao, N. Ly, K. A. Freitas, Y.-T. Chen, Q. Shi, A. M. Valencia, E. Shifrut, N. Kale, K. E. Yost, C. V. Duffy, B. Daniel, M. A. Hwee, Z. Miao, A. Ashworth, C. L. Mackall, A. Marson, J. Carnevale, S. A. Vardhana, A. T. Satpathy, Genome-wide CRISPR screens of T cell exhaustion identify chromatin remodeling factors that limit T cell persistence. *Cancer Cell* **40**, 768–786.e7 (2022).

149. X. Dai, J. J. Park, Y. Du, Z. Na, S. Z. Lam, R. D. Chow, P. A. Renauer, J. Gu, S. Xin, Z. Chu, C. Liao, P. Clark, H. Zhao, S. Slavoff, S. Chen, Massively parallel knock-in engineering of human T cells. *Nat. Biotechnol.* **41**, 1239–1255 (2023).

150. K. A. Freitas, J. A. Belk, E. Sotillo, P. J. Quinn, M. C. Ramello, M. Malipatlolla, B. Daniel, K. Sandor, D. Klysz, J. Bjelajac, P. Xu, K. A. Burdsall, V. Tieu, V. T. Duong, M. G. Donovan, E. W. Weber, H. Y. Chang, R. G. Majzner, J. M. Espinosa, A. T. Satpathy, C. L. Mackall, Enhanced T cell effector activity by targeting the Mediator kinase module. *Science* **378**, eabn5647 (2022).

151. F. Blaeschke, Y. Y. Chen, R. Apathy, B. Daniel, A. Y. Chen, P. A. Chen, K. Sandor, W. Zhang, Z. Li, C. T. Mowery, T. N. Yamamoto, W. A. Nyberg, A. To, R. Yu, R. Bueno, M. C. Kim, R. Schmidt, D. B. Goodman, T. Feuchtinger, J. Eyquem, C. Jimmie Ye, J. Carnevale, A. T. Satpathy, E. Shifrut, T. L. Roth, A. Marson, Modular pooled discovery of synthetic knockin sequences to program durable cell therapies. *Cell* **186**, 4216–4234.e33 (2023).

Chapter 2: speedingCARs: accelerating the engineering of CAR T cells by signaling domain shuffling and single-cell sequencing

This chapter is an author-produced adaptation of a peer-reviewed research article “speedingCARs: accelerating the engineering of CAR T cells by signaling domain shuffling and single-cell sequencing”, accepted for publication in Nature Communications, 2022 (https://doi.org/10.1038/s41467-022-34141-8).

Authors: Rocío Castellanos-Rueda*, Raphaël B. Di Roberto*, Florian Bieberich, Fabrice S. Schlatter, Darya Palianina, Oanh T. P. Nguyen, Edo Kapetanovic, Heinz Läubli, Andreas Hierlemann, Nina Khanna and Sai T. Reddy. *These authors contributed equally to this work.

Author's contribution: R.C.R., R.B.D.R and S.T.R. designed the study; R.C.R., R.B.D.R., F.S.S. and D.P. performed experiments; R.C.R. and F.B. performed and interpreted bioinformatic analyses; O.T.P.N. and E.K. assisted with obtaining biological material. R.C.R. , R.B.D.R. and S.T.R. discussed results. R.C.R. and R.B.D.R. wrote the manuscript with input and commentaries from all authors.

Note on shared first authorship: Both R.C.R. and R.B.D.R. were involved in the research project conceptualization, design and execution, discussed results and wrote the manuscript. R.C.R. carried out the CAR library construction and performed the CRISPR-Cas9 based T cell engineering work, designed the scCARseq methodology, performed the scRNAseq experiments and generated and analyzed the sequencing data. R.B.D.R. carried out cell line engineering and designed T cell functional characterization assays which were later performed and analyzed by R.C.R. and R.B.D.R.. Peer-review revisions were performed by R.C.R..

Abstract

Chimeric antigen receptors (CARs) consist of an antigen-binding region fused to intracellular signaling domains, enabling customized T cell responses against targets. Despite their major role in T cell activation, effector function and persistence, only a small set of immune signaling domains have been explored. Here we present speedingCARs, an integrated method for engineering CAR T cells via signaling domain shuffling and pooled functional screening. Leveraging the inherent modularity of

natural signaling domains, we generate a library of 180 unique CAR variants genomically integrated into primary human T cells by CRISPR-Cas9. In vitro tumor cell co-culture, followed by single-cell RNA sequencing (scRNAseq) and single-cell CAR sequencing (scCARseq), enables high-throughput screening for identifying several variants with tumor killing properties and T cell phenotypes markedly different from standard CARs. Mapping of the CAR scRNAseq data onto that of tumor infiltrating lymphocytes further helps guide the selection of variants. These results thus help expand the CAR signaling domain combination space, and support speedingCARs as a tool for the engineering of CARs for potential therapeutic development.

2.1 Introduction

Cellular immunotherapies against cancer have made substantial progress in recent years, with six FDA-approved chimeric antigen receptor (CAR) T cell treatments against hematological malignancies. These treatments rely on synthetic protein receptors that have been engineered for precise molecular recognition of a cell surface antigen (e.g., CD19 on the surface of B cell lymphomas). The infusion of autologous CAR T cells results in a cytotoxic response against tumor cells and, as in a classical immune reaction, this treatment can potentially result in persistent immunity, with CAR T cells recently observed in patients several years post-treatment (*1*). However, success in this field has been difficult to replicate outside of hematological B cell malignancies. For example, solid tumor cancers, such as in the breast or lung, are more resistant to CAR T cell-mediated killing and have struggled to make progress clinically. Instances of relapse, sometimes through antigen escape (*2*) have also highlighted the limitations of CAR T cell persistence and of the monoclonality of the infusion product. Furthermore, strong adverse events, such as cytokine release syndrome (CRS) and transient neurotoxicity (*3*) are frequently associated with treatment and thus represent considerable safety concerns. Together, these pitfalls of CAR T cell therapies form substantial obstacles to their broader use against a wider range of cancer types.

In order to enhance CAR T cell responses against tumors, recent work has leveraged immunological mechanisms to counter the immunosuppressive microenvironment. For example, co-administration with immune-checkpoint blockade inhibitors (ICB; e.g., monoclonal antibodies targeting PD-1/PD-L1) can activate tumor-infiltrating T cells (*4*); or alternatively, armoring CAR T cells with additional genetic modifications to make them overexpress certain cytokines (e.g., IL-12, IL-23, etc.) can potentially sensitize tumors to cell-mediated cytotoxicity (*5*). Furthermore, synthetic biology approaches that incorporate controllable domains (*6–8*) are being utilized to design CARs responsive to drugs or antigenic

cues in order to tune the strength, duration and specificity of the inflammatory response. While promising, all of these strategies require additional drug compounds or genetic modifications, introducing further complexity to a therapeutic regimen that is already laborious and sensitive.

Recent advances in molecular immune profiling, such as single-cell sequencing and transcriptome analysis, are contributing important quantitative insights on CAR T cell-mediated responses and patient outcomes (*9*). By going beyond methods for standard cell phenotyping (e.g., detection of surface markers by flow cytometry), transcriptional phenotyping can uncover gene expression patterns and metabolic pathways, or when used to track therapy progression and outcomes, can help to identify predictors of therapeutic efficacy. A key observation from such studies is that the molecular components and design of a CAR have a major influence on the features of the transcriptional response (*10*). A conventional CAR is rationally designed based on the fusion of modular gene elements: an extracellular antigen-recognition domain (frequently an antibody single chain variable fragment (scFv)), structural elements (a hinge, a transmembrane helix and peptide linkers), as well as one or more intracellular signal-transducing domains. The signaling domains are essential for linking the antigen-cell binding event to a cascade of intracellular molecular events, culminating in the expression of pro-inflammatory and cytotoxic genes. As would be expected, the signaling domains used can impact the type of response induced. However, almost all CARs in clinical trials to date combine the signaling domain CD3ζ of the T cell receptor (TCR) complex and the signaling domains of the co-receptors CD28 and 4-1BB (*11*). Only a small panel of alternative signaling domains has been individually investigated preclinically, and even fewer in parallel (*10*, *12*, *13*). This lack of diversity is partly due to the low-throughput aspect of rational CAR design as well as the laboriousness of performing in vitro functional assays. Recently, two studies from Gordon et al. and Goodman et al. developed approaches to generate pooled CAR signaling domain libraries, which were screened by combining fluorescence-activated cell sorting (FACS) using standard T cell markers and amplicon sequencing to identify novel functional variants (*14*, *15*).

Here, we describe speedingCARs: single-cell sequencing of pooled engineered signaling domain libraries of CARs. Natural immune signaling domains are combinatorially shuffled to generate a highly diverse library of CAR variants. This library is expressed in primary human T cells by genome editing and co-cultured with tumor targets to screen variant's functional capabilities, comparing their induced single-cell transcriptional profiles. The resulting high-quality and high-resolution data is mapped onto the transcriptional landscape of tumour-infiltrating lymphocytes (TILs) derived from lung tumors of treatment-responsive patients. The combination of single-cell RNA sequencing (scRNA-seq), single-cell CAR sequencing (scCARseq), together with clinical data mapping serves to guide the selection of

promising variants which are then functionally validated based on cytokine secretion, differentiation and cell-mediated cytotoxicity. Thus, speedingCARs can be used to rapidly expand the diversity of the CAR synthetic protein family, offering a range of flexible immune phenotypes to tackle immunotherapeutic challenges.

2.2 Results

2.2.1 Design, generation and expression of a CAR signaling domain library in primary human T cells

In order to generate a library of CAR variants that could induce diverse T cell transcriptional phenotypes, we designed a modular cloning and assembly strategy for shuffling intracellular signaling elements (Fig. 1a). In a standard CAR, the intracellular region is composed of a CD3ζ signaling domain on the C-terminal end and co-receptor domains CD28 and/or 4-1BB on the N-terminal end (proximal to the transmembrane domain). CD3ζ is notable among other immune signaling proteins by the presence of three immunoreceptor tyrosine activation motifs (ITAMs), which play an important role in triggering downstream signaling events in response to receptor clustering. Although co-receptor domains such as CD28 and 4-1BB do not have ITAMs, their presence mimics the co-stimulation that accompanies TCR engagement with an activated antigen-presenting cell (APC), resulting in a more durable response.

Although recent work has highlighted some degree of plasticity in the number and configuration of ITAMs (*16*), our library design retained a total sum of three ITAMs to maximize functionality. To ensure this, we segmented the CD3ζ gene between the first and second ITAM and retained the two-ITAM segment for the CAR library. We then selected intracellular domains from a variety of immune co-receptors for inclusion into two pools of gene segments: domains A and B (Fig. 1b). The pool of domain A was generated from 15 receptors that have been described as providing co-stimulation in immune cell-cell interactions, ranging from the major contributors CD28 and 4-1BB to potentially more minor receptors, such as CD30 or CD150 and CD84 of the signaling lymphocytic activation molecule (SLAM) family. We also included lesser-known or inhibitory receptors such as FCRL6, CD244 and LAG3 to investigate their synergistic effects (*17*). The pool of domain B consisted of 12 genes that each possessed a single ITAM. This included receptors such as FcγRIIA, DAP12 and CD79B, which are expressed in diverse immune cells from both myeloid and lymphoid lineages, as well as T cell-specific genes involved in the TCR complex such as CD3G. In addition, we included three viral receptors, LMP2

(Epstein-Barr virus), K1 (Kaposi's sarcoma-associated herpesvirus) and GP (New York virus), to investigate whether their non-human origin could lead to unique functional response profiles. Lastly, we also used the first segment of CD3ζ, which would reconstitute the full intracellular domain upon assembly.

To shuffle and assemble the domain gene segments within the CAR genetic chassis, we used a Type IIS restriction cloning strategy (*18*) (Fig. 1c). In this method, customized restriction sites within a cloning cassette ensure that domains assemble in an orderly fashion: assembly of domain A on the N-terminal side and domain B on the C-terminal side results in the three ITAMs being proximal to each other. The two variable signaling domains are joined by a minimal linker. The remainder of the CAR chassis consisted of the following constant elements: (i) a secretion signal peptide from CD8α; (ii) an extracellular scFv based on the monoclonal antibody trastuzumab (scFv clone: 4D5); (iii) a CD28-derived hinge and transmembrane domain; (iv) the partial segment of CD3ζ bearing two-ITAMs. Through the scFv, all CAR variants in the library have binding specificity for the oncogenic human epidermal growth factor receptor 2 (HER2), a clinically relevant target for CAR T cell therapy due to its prominence in many cancers (*19*). Following cloning in a plasmid vector, the diversity of the resulting signaling domain library was assessed by deep sequencing, showing that the library possessed 179/180 possible combinations, with balanced representation (Fig. 1d).

To express the library of CAR variants in a physiologically relevant context, we performed genome editing with CRISPR-Cas9 on primary human T cells from healthy donors. Homology-directed repair (HDR) was used to target the CAR library for genomic integration at the TCR alpha chain (*TRAC*) locus (Fig. 1e). The precise integration of CARs at the *TRAC* locus has previously been shown to enhance tumor cell killing while conferring notable advantages over viral gene delivery (e.g., retrovirus, lentivirus): it ensures most T cells are monoclonal (only a single and unique CAR); it leads to transgene expression that is more consistent across cells and physiologically regulated, and it knocks out the endogenous TCR to avoid confounding effects (*20*). Following genome editing, CAR T cells were isolated from non-edited cells by FACS based on surface expression of a Strep tag and deletion of the TCR (Fig. 1f). The post-sort purity of the CAR T cell population and its ability to bind to soluble HER2 antigen was confirmed by flow cytometry (Fig. 1g), while genotyping validated targeted integration into the *TRAC* locus (Supplementary Fig. 1).

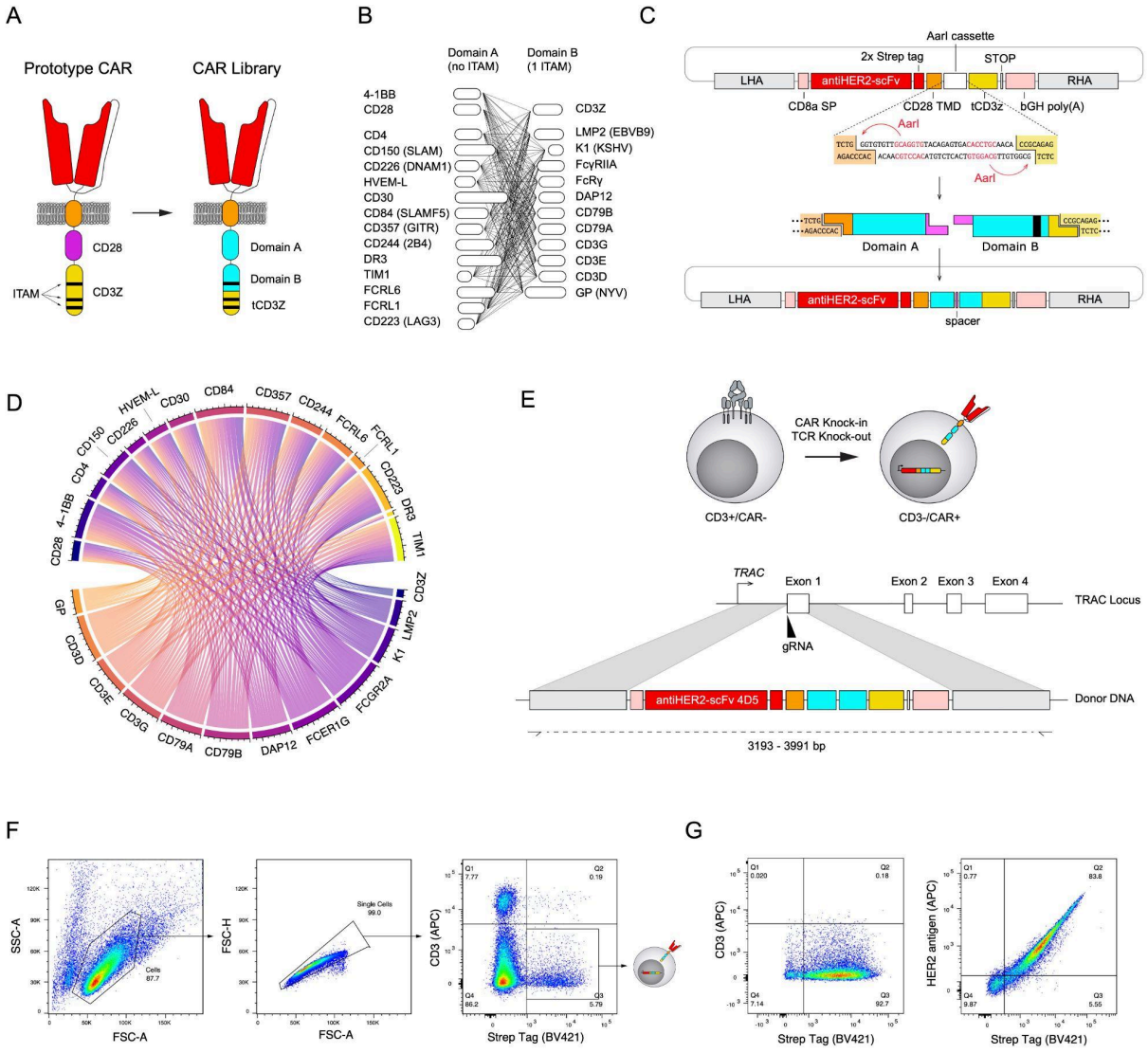

Figure 1: Combining modular domain shuffling and genome editing to express a library of CAR variants in primary human T cells.

A) Schematic representation of CAR architecture for the shuffling of signaling domains. The CAR variant library is derived from an initial second-generation CAR featuring the intracellular signaling domains of CD28 and CD3ζ; the scFv (4D5) is based on the variable domains of the clinical antibody trastuzumab (specificity to the antigen HER2). The entire CD28 signaling domain and a segment of the CD3ζ domain are exchanged with signaling domains from two pools: Domain A and B, which possess either zero or one ITAM, respectively. A truncated CD3ζ (tCD3Z) possessing two ITAMs is retained. **B**) Combinatorial shuffling of Domain A and Domain B intracellular signaling domains yields a library of 180 possible CAR variants. **C)** Schematic representation of the cloning strategy for domain shuffling. A backbone vector was designed to encode a CAR chassis composed of the following conserved elements: the CD8α secretion peptide, the scFv 4D5, two Strep tags separated by G4S linkers, the CD28 hinge and transmembrane domains and a partial region of CD3ζ. A cloning cassette between the transmembrane domain and CD3ζ domain has outward-facing recognition sequences of the Type IIS restriction enzyme AarI. A restriction digest yields unique overhangs that are compatible with the ligation of one domain from pool A and one domain from pool B, in that order (5' to 3'). The construct is completed by a polyadenylation signal and flanked by homology arms for the targeted genomic integration of the transgene in the human *TRAC* locus. **D)** Long-read deep sequencing was performed following cloning and assembly of the signaling domain shuffling library. Circos plot shows that 179/180 possible combinations are present in balanced

proportions. **E)** Schematic of the strategy for targeted genomic integration of a CAR library into the *TRAC* locus of primary human T cells by CRISPR-Cas9 HDR. **F and G)** Flow cytometry sequential gating of human primary T cells after transfection (F) and after selection for CAR expression (G).

2.2.2 Functional and pooled screening of CAR T cell library by single-cell sequencing

In order to achieve functional and pooled screening of the CAR T cell library, we performed co-cultures with tumor cells followed by scRNAseq. This enabled us to trigger the activation of the CAR signaling domain variants and to profile the associated transcriptional phenotypes and key gene expression signatures. This approach provides sufficient coverage of a CAR library of 180 unique variants by taking advantage of the current capacity of 10^3–10^4 cells for scRNAseq (e.g., 10X Genomics, as used here). In addition, we designed scCARseq, a strategy to de-multiplex the CAR library from the resulting scRNAseq data. For this, CAR single-cell barcoded transcripts found in the scRNAseq cDNA product are selectively amplified and long-read deep sequencing (Pacbio) is used to capture the barcode identifiers that link the CAR signaling domain variant to a given cell (Supplementary Fig. 2).

Primary human T cells expressing the CAR library were co-cultured with the HER2-expressing breast cancer cell line SKBR3. To serve as a benchmark in subsequent analyses, we also spiked-in T cells bearing clinically used standard CARs with the CD28-CD3ζ and 4-1BB-CD3ζ domain combinations (abbreviated to 28z and BBz) into the pooled co-cultures. Negative controls consisted of co-cultured TCR-negative T cells (generated by Cas9-induced non-homologous end joining (NHEJ) in the *TRAC* locus; TCR-) and unstimulated (no tumor co-culture) 28z CAR T cells. Following co-culture (36 h), CAR T cells were isolated by FACS (Supplementary Fig. 3) and processed for scRNAseq through the 10X Genomics pipeline. RNA transcripts were barcoded and amplified as cDNA to generate a gene expression (GEX) library suitable for deep sequencing. In parallel, scCARseq was performed and the resulting amplified transcripts were used for long-read deep sequencing.

2.2.3 Identification of CAR-specific induced transcriptional phenotypes

Following pre-processing and quality filtering, a total of 19,321 stimulated CAR T cells across three donors were sequenced by scRNAseq. Among these, 55% could be annotated with a single specific CAR variant, while 4% had to be discarded due to the identification of more than one different CAR construct in the same cell. This resulted in a total of 10,692 annotated cellular transcriptomes (averaging ~2.5×10^4

reads/cell) covering 156 unique CAR variants from our library. Although we selected a relatively short co-culture time of 36 h in order to minimize more proliferative variants from becoming over-represented, we saw evidence of clonal variant expansion (Supplementary Fig. 4a). In order to do a clustering and gene expression analysis encompassing both over- and under-represented variants, we randomly subsampled up to 250 cells per variant and 500 cells for each negative control sample. To confirm that this did not significantly affect clustering, 50 independent iterations of the subsampling and clustering algorithms were performed and the adjusted Rand index (ARI) was computed for each pair of partitions. This measure of data clustering similarity was consistently high, confirming that no specific subsample would likely change our results (Supplementary Fig. 4b–d). The reduced dataset was used to do cell clustering and CAR variant enrichment analysis thereafter.

To determine whether CAR variants could trigger different functional T cell states upon encounter with tumor cells, we assessed the enrichment of each variant across T cell phenotypes. Unsupervised clustering identified thirteen clusters which were annotated based on CD4 and CD8 expression, predicted cell cycle phase and the differential gene expression of T cell marker genes (Fig. 2a, b, and Supplementary Fig. 5a–c); CD8+ cells were divided into a memory cluster characterized by having a low number of cycling cells and high expression of CCR7, IL7R, CD27, CD7, LEF1 and TCF7 genes; a proliferative BATF3 + cluster with low expression of cytotoxicity and T cell activation markers and enrichment in stress response and HLA genes; and 4 clusters presenting effector-like features: Effector A (KLRD, GNLY, and PRF), Effector B (NKG7,GZMK,GZMH, and EOMES), Cytotoxic (GZMB, IFNG, TNFRSF9, CCL3, CCL4, CSF2, XCL1, and CRTAM) and Terminal effector (TIGIT, ENTPD1, NPW, SOX4, LAIR2). CD4+ clusters were annotated as resting and cycling memory (expressing STAT1 and the previously described memory markers), activated memory (CCR7, IL2RA, LIF, ZBED2), KLF2 + resting, activated (IL26, IL17A, IL4I1, TNFRSF4, and TNFRSF18) and effector (DUSP4, ID3, TIGIT, and NPW). Finally, we observed a metabolically active mix of CD4/CD8 cells.

After defining the main cell clusters, the enrichment of CAR variants across clusters was evaluated to assess their effect on T cell activation. With few exceptions, most CAR variants were found to be distributed across multiple clusters (Fig. 2c and Supplementary Fig. 6). This was also the case for positive (28z and BBz) and negative control groups (TCR-negative and unstimulated 28z). However, five clusters were strongly enriched in the former and depleted in the latter (Fig. 2d, e). The low presence of TCR-negative and unstimulated 28z cells in these clusters suggests that they are associated with CAR induced stimulation (CAR Induced Clusters; CICs). The other eight clusters could result from either CAR stimulation and/or residual signaling received during standard in vitro T cell manipulation (CD3ζ/CD28

bead activation and IL-2 treatment). Pathway enrichment analysis of differentially-expressed genes between CICs and non-CICs support this: non-CICs were enriched in pathways associated with CD3ζ/CD28 stimulation, such as TCR binding and downstream signaling, antigen presentation, MHC protein interaction and CD28 costimulation, as opposed to CICs, which upregulated genes enriched in a broader set of pathways including cytokine, chemokine and receptor signaling (Supplementary Fig. 7). The enrichment of CAR variants in CICs was therefore used as a measure of CAR activity and to further investigate their profiles (Fig. 2f). Several CAR candidates appeared enriched in the CD8 Terminal Effector cluster (e.g. CD30-CD79B and CD4-K1). The CD8 Cytotoxic cluster was preferentially enriched by 28z compared to BBz cells, consistent with the enhanced cytotoxic potency of the former, and accounted for a large fraction of cells in variants such as CD28-FCGR2A and FCRL6-CD3G. Regarding CD4+ clusters, CD4 Activated Memory was more enriched in 28z and BBz cells compared to CD4 Cycling Memory, which seemed to be more expanded in variants such as 4-1BB-FCER1G and TIM1-CD3D. The CD4 effector cluster was exclusively enriched in 4-1BB-CD79A. In addition, a few CAR variants showed close to no enrichment in any of the CICs (e.g. TIM1-CD79B, CD357-CD79B and CD30-CD3D). The similarity of these cells to CAR unstimulated cells might indicate reduced potency of these CARs. Overall, the complex distribution of CAR variants across clusters (Supplementary Fig. 8) and in particular within CICs illustrates the diverse range of phenotypes that can be triggered by alternative CAR architectures.

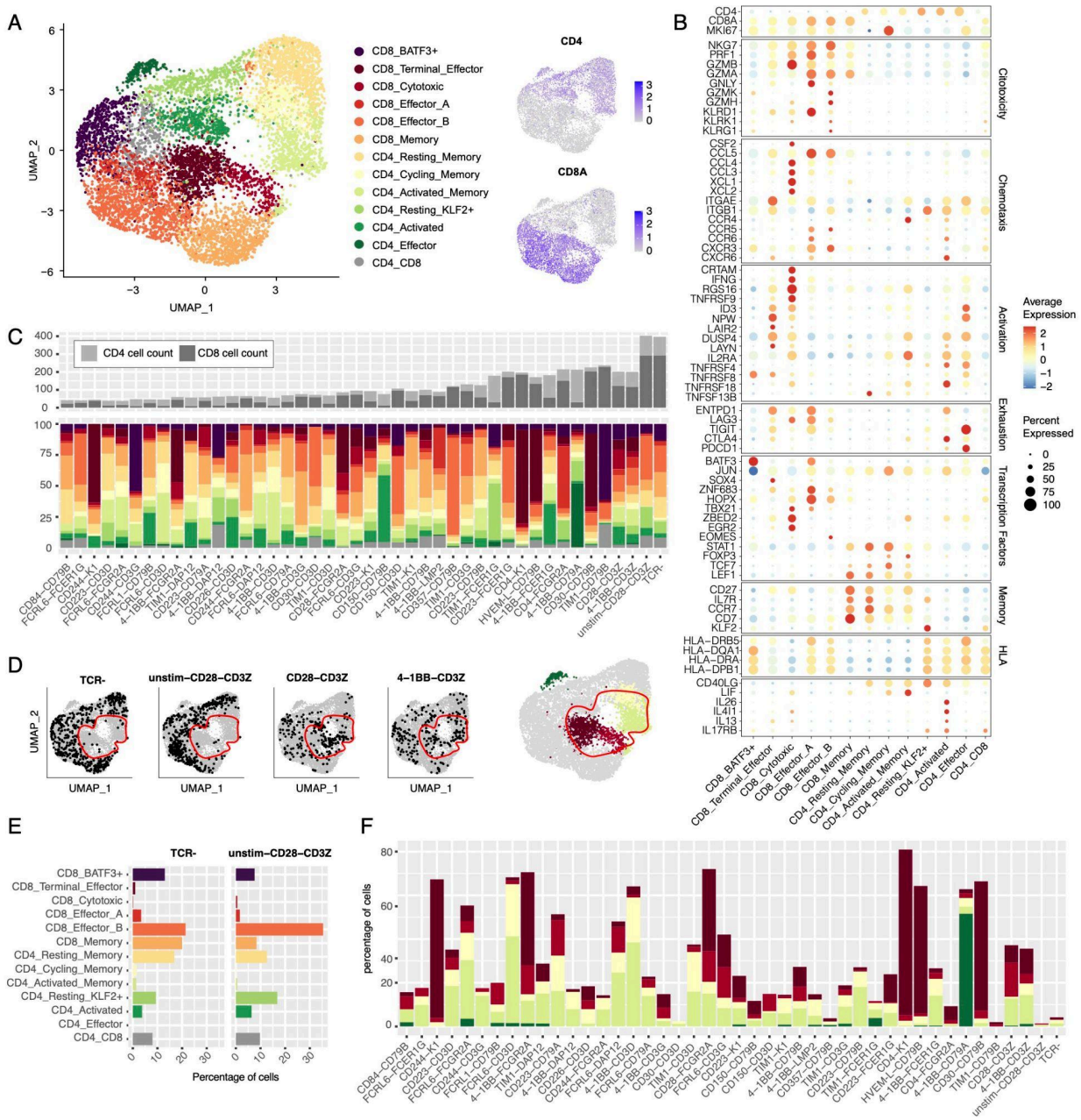

Figure 2: Unsupervised cell clustering classifies CAR variants based on distinct transcriptional phenotypes.

A) UMAP embedding and unsupervised cell clustering based on scRNA-seq data of the pooled CAR T cell library following functional activation (co-culture with cognate antigen-expressing SKBR3 tumor cells). Shown are data from 7,244 variant-assigned CAR T cells with random subsampling restricting it to a maximum of 250 cells per CAR construct. In addition, 500 cells for TCR-negative (TCR-) and unstim-CD28-CD3Z negative control samples were included. On the right, UMAP feature plots show the distribution of CD4- and CD8-expressing cells. **B)** Dot plot showing the expression of a selection of T cell marker genes across clusters found in A. Color and size indicate differences in expression levels between groups. **C)** Cluster enrichment observed for the top 40 most represented CAR variants (variants with at least 50 cells assigned), benchmark controls (CD28-CD3Z and 4-1BB-CD3Z) and negative controls (TCR- and unstim-CD28-CD3Z). Variants are ordered by a confidence score based on the number of available cells. The top panel displays the CD4 and CD8 counts for each group and the bottom panel the fraction of cells found in each of the clusters from A. **D)** Distribution of the unstimulated controls and the benchmark controls within the UMAP embedding of a. On the right a UMAP embedding plot highlights the CICs. In all UMAP plots, a red line depicts the region where there was no enrichment of unstimulated control samples. **E)** Bar plot showing the distribution of

CAR unstimulated control cells between the different clusters. f Bar plot depicting the percentage of cells per CAR variant that belong to the 5 different CICs.

2.2.4 Examining CAR variant-specific transcriptional signatures

The classification of cells into clusters can identify general patterns in the data. However, computational algorithms delineate clusters in an unsupervised manner, which may not capture intra-cluster differences found in such a heterogeneous population of T cells. For this reason, we next examined the gene expression signature of each CAR variant individually using the full dataset of sequenced cells. A pseudo-bulking strategy was used to compare CAR variants with the standard 28z and BBz CARs and TCR-negative cells. Principal component analysis (PCA) revealed that different signaling domain combinations induce different T cell signatures; individual variants were found to be spread across the T cell phenotypic space (Fig. 3a). As expected, PC1 and PC2 clearly separate positive controls 28Z and BBz from the negative control TCR-negative. In addition, we observed a trend in the distribution of variants across the two main principal components and their enrichment in CICs. While PC1 drives the separation of samples based on memory vs effector features, PC2 separates samples based on their enrichment in CICs. It is reasonable to infer that proximity to 28z and BBz controls could be an indicator of CAR activity, while candidates that remain close to TCR-negative probably have limited antitumor potential.

In a similar way, comparing CD8+ pseudo-bulked samples of a selection of variants against the clinically standard CARs and negative control groups revealed differences across key genetic markers (Fig. 3b). Hierarchical clustering based on the gene expression levels of 42 T cell marker genes indicated a clear separation of samples based on their enrichment in CD8 CICs; CICs-low samples were enriched in memory and resting related genes versus cytotoxic and effector genes for CICs-high samples. Moreover, clustering on this basis further separated CIC-high samples based on their similarity to 28z or BBz CARs while highlighting underlying transcriptional differences. Notably, despite having a CD8+ phenotype close to that of 28z, FCRL6-CD3G and CD28-FCGR2A variants showed reduced expression levels of proinflammatory factors such as IFNG, CCL3, CCL4, and CSF2. In addition CD223-CD79A and FCRL6-FCGR2A presented higher expression of memory markers, including TCF7 and CD27 while still presenting high levels of effector genes, two potentially interesting hybrid phenotypes.

A different approach used to analyze individual CAR variants employs gene-set scoring, which allows us to systematically screen variants for specific T cell signatures and compares them to the clinically used CARs. By defining gene sets based on the expression of T cell marker genes as well as previously

reported associations to phenotype (*21–23*), such as our own CAR-induced signature obtained from the most differentially expressed genes in the CICs, one can identify CAR variants predicted to have specific transcriptional states that can guide candidate selection (Fig. 3c, Supplementary Fig. 9 and Supplementary Data 1).

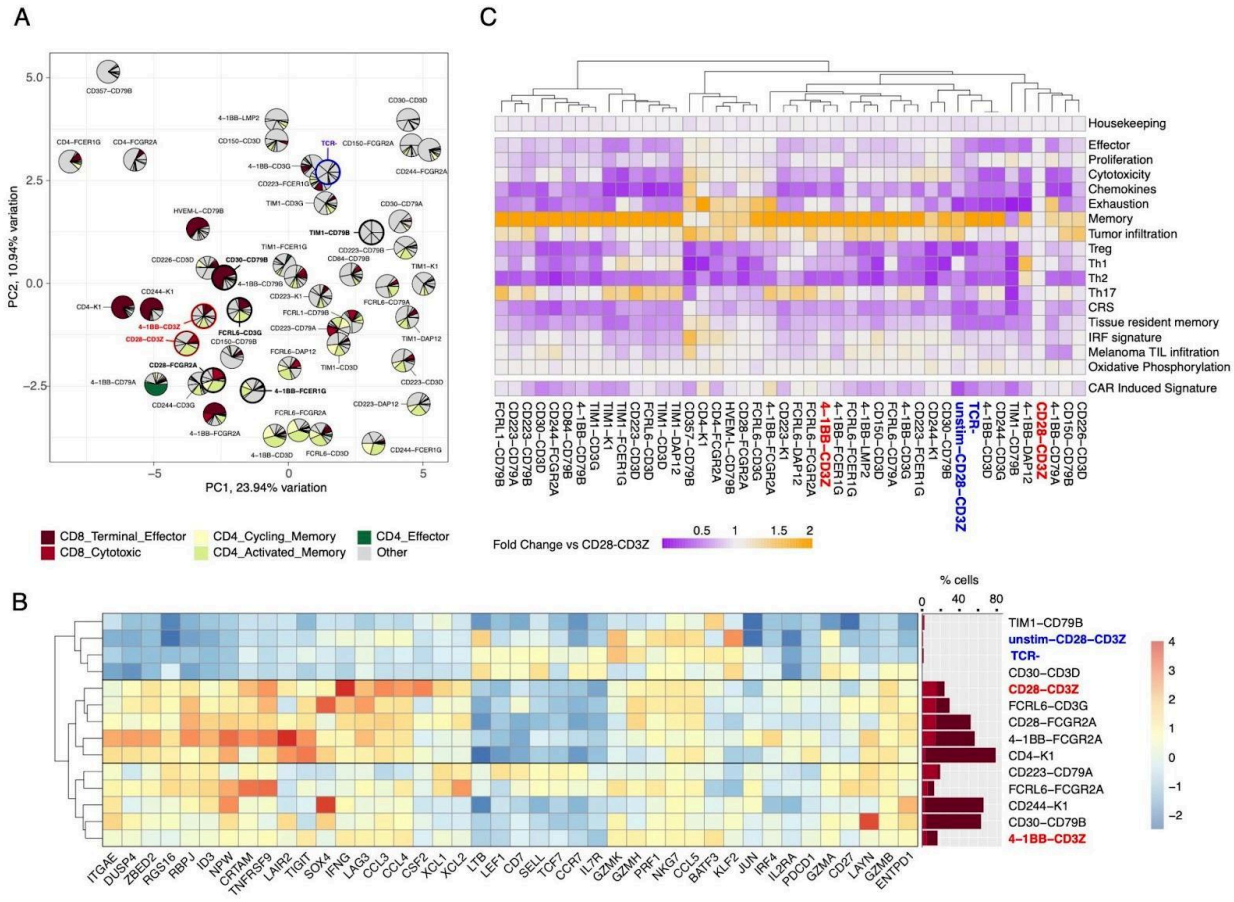

Figure 3: Specific gene transcriptional signatures are used to assess CAR T cell functionality.

A) Principal component analysis (PCA) of pseudo-bulked scRNAseq data from the top 40 most represented CAR variants studied in Fig. 2. Also included are cells expressing 28z (CD28-CD3Z) and BBz (4-1BB-CD3Z) colored in red and CAR negative T cells (TCR-) colored in blue. To avoid batch effect variation, only data from Donor 3 is used. Overlayed over each data point, pie charts represent the enrichment of cells in CICs from Fig. 2F. **B)** Expression levels of a set of 42 T cell marker genes across CD8+ pseudo-bulked scRNAseq samples of a small panel of 10 different CAR T cell variants, 28z and BBz benchmark CAR T cells, TCR- T cells and unstimulated 28z CAR T cells. CAR variants were selected based on their distinct enrichment in CD8 CICs. Marker genes describe phenotypes such as memory, activation, cytotoxicity and exhaustion. Color indicates normalized gene expression deviation from average. Genes and samples are ordered by hierarchical clustering. On the top, a bar plot indicates the percentage of cells identified to be part of the two main CD8+ CICs. **C)** Heatmap showing the difference in gene-set scores (score based on the simultaneous expression of different gene sets computed for each single cell) between the 40 most represented CAR variants, 28z and BBz CARs, unstimulated 28z CAR and CAR negative T cells, for 18 different gene sets. The mean score per variant is given as a fold change measurement when compared to 28z WT CAR.

2.2.5 Mapping of CAR T cell scRNAseq data onto a patient-derived TIL dataset

In order to evaluate our CAR variants in a more translational context, we compared our in vitro generated CAR transcriptional phenotypes to clinically relevant T cell phenotypes, such as TILs. The presence of CD8+ TILs in solid tumors is associated with a better prognosis (*24*, *25*). The complexity of the tumor microenvironment, consisting not only of malignant cells but by a constantly evolving aggregate of tumor, immune and stromal cells, their secreted factors and extracellular matrix, cannot currently be reproduced adequately by in vitro and in vivo mouse models. T cells that manage to infiltrate, survive the solid tumor microenvironment and exert cytotoxicity (tumor-reactive TILs) likely present desired properties that drive a successful antitumor response. This makes the diverse transcriptomic landscape of TILs that are found to be associated with tumor regression a valuable and suitable reference to compare CAR T cell phenotypes.

As a reference, we used the recent work of Liu et al., which consisted of scRNA-seq data of CD8+ TILs recovered from patients with non-small-cell lung cancer (NSCLC) subjected to ICB therapy (anti-PD-1 antibody treatment) (*26*). In this study, ICB promoted the accumulation of reactivated and newly infiltrated T cells which presented precursor exhausted (Texp) and terminally exhausted (Tex) phenotypes and correlated with a beneficial antitumor response. Mapping of our CD8+ CAR T cells onto TILs showed a high degree of overlap of the two datasets and, consistent with our previous results, CAR T cells annotated as CICs segregated from negative control cells (TCR-negative and unstimulated 28z CAR T cells) as opposed to non-CICs cells which shared a similar distribution (Fig. 4a). Unsupervised cell clustering identified two clusters (C8 and C12) that were selectively enriched in CICs cells and also harbored a large number of TILs (Fig. 4b, c). To understand what clinically-related phenotypes can be induced by our CAR variants, we examined the underlying characteristics associated with C8 and C12 TILs. We found that CXCL13, described by Liu et al. (*26*), to be exclusively and highly expressed in Tex cells and Texp cells following ICB treatment, to be amongst the most differentially expressed genes for both clusters (Fig. 4d, e). In addition C8 and C12 TILs presented different expression levels of co-stimulatory receptors and genes associated with T cell activation and tissue cell retention (Fig. 4e). This suggests that C8 and C12 both represent distinct phenotypes with a role in tumor infiltration and a positive antitumor response in lung cancer following ICB.

We next examined the enrichment of our library in the tumor-reactive TIL associated clusters C8 and C12 (Fig. 4f). Several CARs, including 28z, had high enrichment within them. Variants such as 4-1BB-FCGR2A, CD244-K1, and CD28-FCGR2A displayed even higher overall enrichment than 28z. In

addition, different C8 to C12 ratios to 28z, found in variants like CD150-CD79B and CD30-CD79B, present phenotypes that are worthy of further study. Overall, our mapping approach reveals additional CAR variants of interest possessing transcriptional phenotypes similar to ICB-treatment responsive TILs and thus may thus hold potential for the treatment of solid tumors, in particular NSCLC.

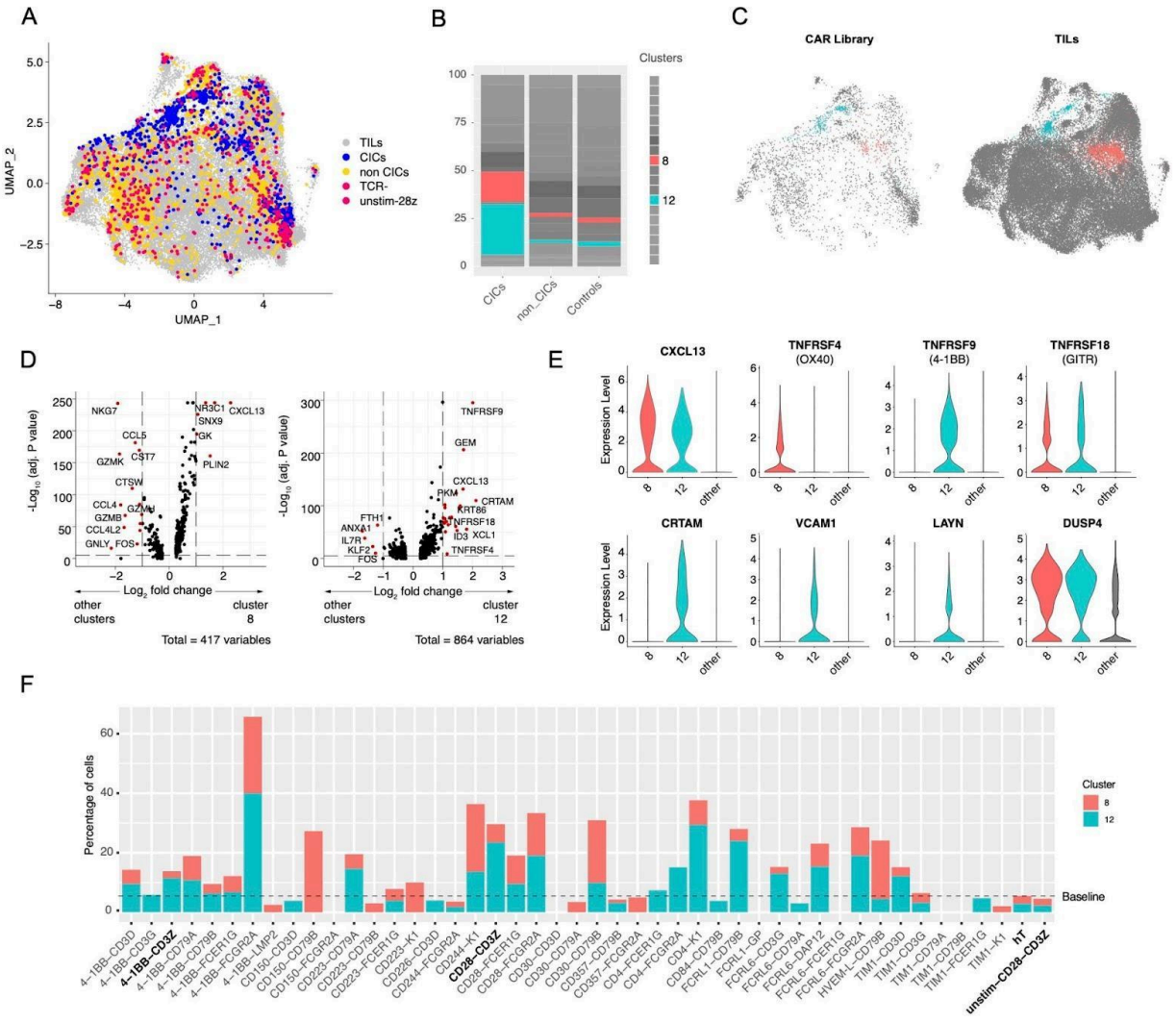

Figure 4: Guiding the selection of CAR variants through transcriptional mapping on TILs.

A) UMAP embedding resulting from the integration of CD8+ CAR library T cells with CD8+ TILs recovered from patients with non-small-cell lung cancer pre- and post-anti-PD-1 ICB treatment (*26*). CAR T cells are highlighted and colored based on the cluster annotations from Fig. 2. CICs = CAR-induced clusters. **B)** Enrichment of CAR library T cells across the 19 different clusters generated from unsupervised cell clustering. **C)** UMAP plots highlighting cells from clusters 8 and 12. CAR library T cells and TILs are separated in two individual plots. **D)** Volcano plots showing differentially expressed genes for TILs between clusters 8 or 12 and all the rest of clusters. Statistical significance was determined through the adjusted p-values generated using the FindMarker() function of Seurat package (two-sided Wilcoxon Rank Sum test). **E)** Violin plots showing the expression levels of a selection of marker genes (only TILs). **F)** Enrichment of cells in clusters 8 and 12 across different CAR variants. Only variants with at least 20 CD8 T cells are shown. In all panels, TCR- refers to T cells without a TCR.

2.2.6 In-depth functional characterization of selected CAR variants

Guided by scRNAseq data and transcriptional mapping to TIL data, we selected ten CAR variants and the clinical benchmarks 28z and BBz for characterization with functional assays. The variants were rationally selected on the basis of their notable transcriptional and signaling-associated phenotypes (Fig. 5a, Supplementary Fig. 10): variants A (FCRL6-CD3G) and B (CD28-FCGR2A) were enriched in cytotoxic and terminal effector CD8 CICs and display an overall CD8+ transcriptional phenotype similar to 28z, though they showed reduced expression of CRS-associated factors with variant A displaying a potentially less terminally differentiated phenotype; variant C (4-1BB-FCER1G) presented a CD8+ phenotype closer to BBz CAR; D (FCRL6-FCER2A) and E (FCRL1-CD79B) showed increased expression of memory associated markers while still presenting enrichment in key CICs and tumor-reactive TIL associated clusters; variants F (4-1BB-FCER2A), G (CD150-CD79B), H (CD30-CD79B) and I (CD244-K1) all presented a high enrichment in tumor-reactive TIL associated cluster 8 and a different range of enrichments in cluster 12; variant J (TIM1-CD79B) showed no enrichment in CICs or tumor-reactive TIL associated clusters and maintained a closer phenotype to the unstimulated controls. As an additional control, we also sorted TCR-negative T cells. Flow cytometry analysis of CAR surface expression showed significantly different CAR expression levels across variants. With the exception of CAR E, variants were expressed at lower levels compared to the standard 28z CAR (Supplementary Fig. 11). Since all CARs are expressed from the same genomic locus, this may be the result of combining different cytoplasmic architectures with the CD28 transmembrane domain.

In order to determine the extent to which CAR variants influence T cell differentiation programs, we performed multi-parameter flow cytometry on 18 surface markers, including that characteristic of memory, activated and exhausted T cell phenotypes (Supplementary Fig. 12). Following 4-day co-cultures with SKBR3 (HER2-positive) tumor cells, surface expression profiles revealed moderate differences across variants and TCR-negative control cells. CD62L and CD45RA markers were used to determine different T cell differentiation states (Fig. 5b). Whilst CD4+ cells maintained a central memory phenotype in a high percentage of the cells for all samples, the CD8+ cell compartment showed more notable differences. CARs E, I and J showed a more effector memory and terminally differentiated phenotype closer to that of 28z CAR. BBz CAR on the other hand had a larger central memory compartment more similar to CARs A, G and H. Interestingly CAR F had a more expanded Tscm, comparable to that of TCR-negative cells. Regarding activation, the expression of early (CD69), middle (CD25) and late

(HLA-DR) T cell activation markers indicate comparable levels of activation across CAR variants with moderate expression of early and very high expression of middle and late marker genes (Supplementary Fig. 13a). The TCR-negative control group had as expected reduced expression of both CD69 and CD25 but high expression of HLA-DR, which is probably a result of initial CD3/CD28 bead activation. CD39 and CD137 were expressed at low levels and only moderate differences were observed in the CD8+ cells. In order to assess T cell exhaustion, we measured the number of exhaustion markers (CTLA4, LAG3, TIGIT, TIM3, and PD1) simultaneously expressed per cell (Fig. 5c and Supplementary Fig. 13b). This number was considerably higher in all CAR variants compared to TCR-negative cells reflecting CAR induced T cell activation, however, no meaningful differences were found across variants except for those in the expression of single markers (Supplementary Fig. 9b), such as LAG3. Longer stimulation times would be needed in order to assess differences in exhaustion.

Next, we measured the cytotoxic capacity of the selected CAR variants for tumor cell control and elimination through live-cell imaging. As target cell lines, we used SKBR3 and MCF-7, the latter of which is another breast cancer cell line expressing HER2, albeit at lower level (*27*). To track the cytotoxic activity via cancer cell death, we engineered GFP-expressing target lines using CRISPR-Cas9 HDR (Supplementary Fig. 14a). After three rounds of iterative sorting, the resulting populations showed stable expression of GFP in over 90% of cells (Supplementary Fig. 14b–e). For SKBR3, we tracked the total fluorescence of standard (sparse) co-cultures with the selected CAR T cell variants at various ratios (Fig. 5d, f and Supplementary Fig. 15a). At the lowest ratio of CAR-T to tumor cells (1:1) only most potent CAR variants (28z, BBz and CARs A-D) were able to control tumor growth. Nevertheless, CAR variants E-J still showed evidence of tumor killing as tumor growth was delayed. At the intermediate and high ratios (3:1 and 8:1) all CARs were able to control or eliminate SKBR3 expansion, however different killing dynamics could be observed: CARs A and D showed the fastest killing, followed by CARs B, C, 28z, and BBz, all of which had similar killing rates, CARs E and F which had only a slight delay over the benchmarks, CARs G-I and finally CAR J which was considerably the slowest. As an alternative cytotoxicity model, we sought to challenge the CAR variants against three-dimensional cancer microtissues (spheroid structures). We established conditions under which the GFP+ MCF-7 cell line forms spheroids (Supplementary Fig. 14f, g), which were then cultured with CAR T cell variants at various ratios (Fig. 5e, g and Supplementary Fig. 15b). Within this spheroid setting, we observed faster-killing dynamics probably due to the co-localization and high density of tumor and T cells in a reduced compartment. Despite this, we were able to observe consistent results with SKBR3 killing. Again, CAR A showed the most potent killing followed by CARs B, C, 28z, BBz, D and E. As before and across different E:T ratios, CAR J was the slowest.

Next, following 4-day co-cultures with SKBR3 target cells, we profiled the secretion of a panel of eight cytokines across variants. The cytokines assayed were pro-inflammatory and/or Th1-associated (GM-CSF, IFNγ, TNFα, and IL-12p70), Th2-associated (IL-4, Il-5, and IL-13) and IL-10, which despite being considered an anti-inflammatory Th2-associated cytokine, it has a pleiotropic function in tumor biology and has been closely related to CRS in the context of CAR T cell therapy (Fig. 5h). As previously reported in literature, 28z CAR consistently secreted the highest levels of nearly every cytokine compared to BBz (*28*), this was particularly clear for the pro-inflammatory cytokines GM-CSF, IFNγ and TNFα. Notably, with few exceptions, this was also the case when comparing 28z to the panel of ten candidate CAR variants. Amongst CARs A-D, which displayed similar or faster killing dynamics than the benchmark CARs, CARs B, and D showed strong similarity with BBz, occupying the middle range of cytokine secretion levels, whereas A and C showed even lower levels of secretion than BBz. CARs E, F, G, and I presented different patterns of intermediate secretion levels characterized by high expression of IL-12 and IL-10 and significantly high levels of IL13 in variant G. CARs H and J consistently presented the lowest cytokine secretion resembling that of the unstimulated controls (TCR-negative and SKBR3 cells alone).

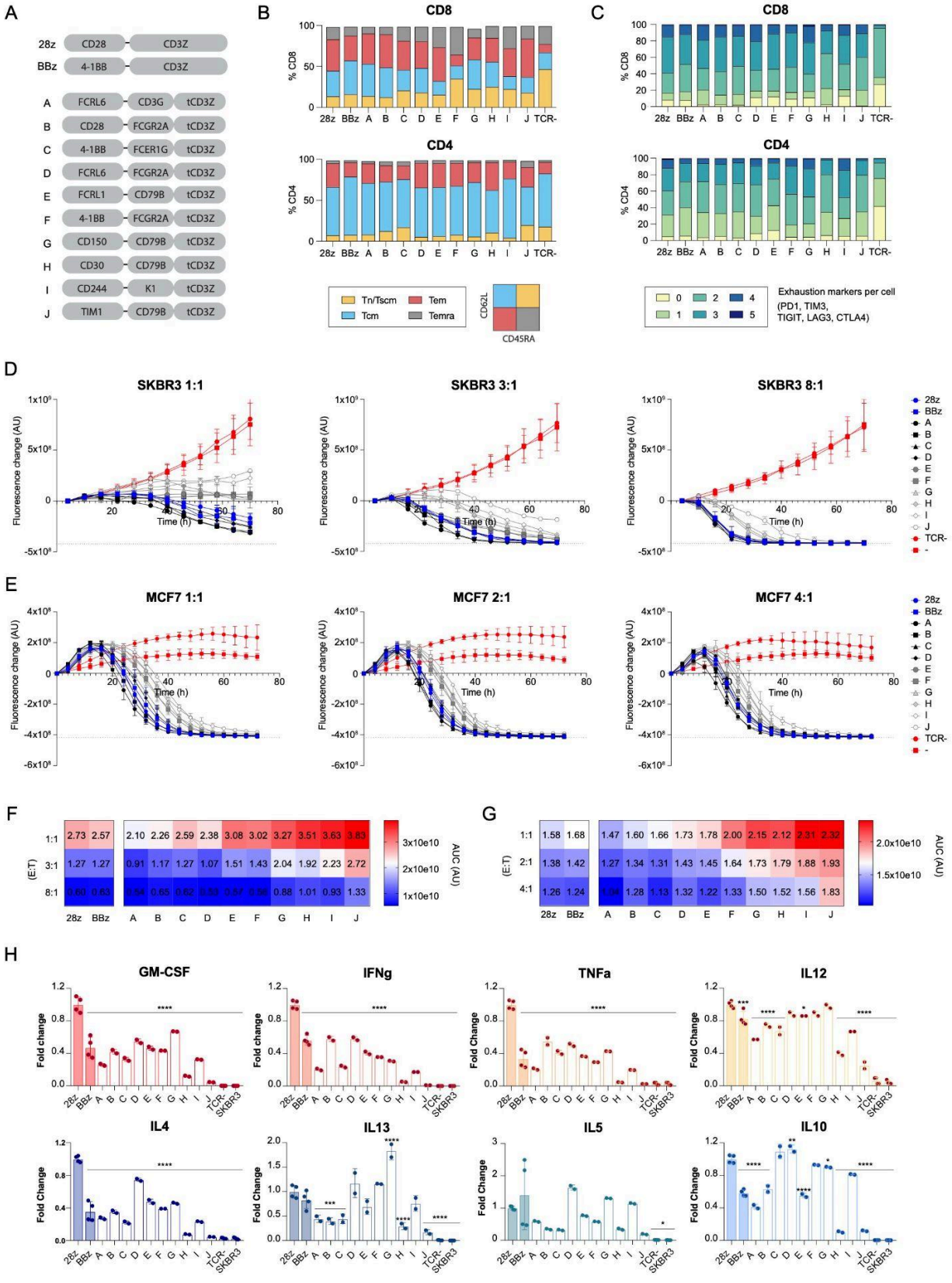
A
28z CD28 CD3Z
BBz 4-1BB CD3Z
A FCRL6 CD3G tCD3Z
B CD28 FCGR2A tCD3Z
C 4-1BB FCER1G tCD3Z
D FCRL6 FCGR2A tCD3Z
E FCRL1 CD79B tCD3Z
F 4-1BB FCGR2A tCD3Z
G CD150 CD79B tCD3Z
H CD30 CD79B tCD3Z
I CD244 K1 tCD3Z
J TIM1 CD79B tCD3Z
B
CD8
% CD8
CD4
% CD4
28z BBz A B C D E F G H I J TCR-
Tn/Tscm
Tcm
Tem
Temra
CD62L
CD45RA
C
CD8
CD4
% CD8
% CD4
0 1 2 3 4 5
Exhaustion markers per cell
(PD1, TIM3,
TIGIT, LAG3, CTLA4)
D
SKBR3 1:1
SKBR3 3:1
SKBR3 8:1
Fluorescence change (AU)
Time (h)
28z BBz A B C D E F G H I J TCR- -
E
MCF7 1:1
MCF7 2:1
MCF7 4:1
Fluorescence change (AU)
Time (h)
28z BBz A B C D E F G H I J TCR- -
F
(E:T)
1:1 2.73 2.57 2.10 2.26 2.59 2.38 3.08 3.02 3.27 3.51 3.63 3.83
3:1 1.27 1.27 0.91 1.17 1.27 1.07 1.51 1.43 2.04 1.92 2.23 2.72
8:1 0.60 0.63 0.64 0.65 0.62 0.53 0.57 0.56 0.88 1.01 0.93 1.33
28z BBz A B C D E F G H I J
AUC (AU)
3x10e10
2x10e10
1x10e10
G
(E:T)
1:1 1.58 1.68 1.47 1.60 1.66 1.73 1.78 2.00 2.15 2.12 2.31 2.32
2:1 1.38 1.42 1.27 1.34 1.31 1.43 1.45 1.64 1.73 1.79 1.88 1.93
4:1 1.26 1.24 1.04 1.28 1.13 1.32 1.22 1.33 1.50 1.52 1.56 1.83
28z BBz A B C D E F G H I J
AUC (AU)
2.0x10e10
1.5x10e10
H
GM-CSF
IFNg
TNFa
IL12
IL4
IL13
IL5
IL10
Fold Change
28z BBz A B C D E F G H I J TCR- SKBR3

Fig. 5: Functional characterization of selected CAR variants confirms their diverse phenotypes and potential enhanced properties.

A) Ten CAR signaling domain variants were selected for individual characterization along with the clinically used 28z and BBz CARs. **B)** Proportion of T cell differentiation subsets observed in CAR or TCR-negative (TCR-) T cells following a 4 day co-culture with SKBR3 cells (4:1 E:T ratio) as measured by CD62L and CD45RA surface expression (naive T cells (Tn), stem central memory T cells (Tscm), central memory T cells (Tcm), Effector Memory T cells (TEM), Effector Memory RA-positive T cells (TEMRA)). **C)** Proportion of CAR or TCR- T cells simultaneously expressing different number of exhaustion markers (PD1, TIM3, TIGIT, LAG3, and CTLA4) following the co-culture conditions described in B. **D and E)** CAR T cell-mediated cytotoxicity of HER2+ /GFP+ tumor cells quantified over time by fluorescence microscopy. The fluorescence change values represent the difference in GFP intensity compared to time point 0, and a dashed line represents the baseline where no GFP+ cells are left. CAR T cells were co-cultured at different E: T ratios with either SKBR3 adherent cells in a sparse 2D culture in D or with a single tumor spheroid of MCF-7 cells in E. **F and G)** Heat maps comparing the area under the curve (AUC) of the killing curves in d, e across different CAR variants. **H)** Cytokine secretion profile of a selection of 8 cytokines following a 4 day co-culture of CAR T cells and SKBR3 cells at a 4:1 E: T ratio. The levels of cytokines in the co-culture medium were quantified by fluorescence-encoded multiplex bead assays and are shown as fold change compared to the benchmark 28z CAR. To assess significant differences between each variant and 28z, a one-way ANOVA and Dunnett's multiple comparisons test was used with the following significance indicators: *p-value <0.05, **p-value <0.01, ***p-value <0.001 and ****p-value <0.0001. In all panels, TCR- refers to T cells without a TCR and error bars represent the S.D. (n = 2 independent technical replicates for variants A-J and n = 2 technical replicates from two independent experiments for control groups).

2.3 Discussion

Here, we developed speedingCARs, an integrated method that combines signaling domain shuffling and single-cell sequencing to expand the range and functional profiles of CAR T cells (Fig. 6), which may eventually enable enhanced and personalized cell therapies. Our approach is designed for rapid and productive CAR engineering and utilizes two important concepts. First, CARs were conceived with modularity in mind, making them especially suitable for the combinatorial shuffling of signaling domains derived from a wide range of receptor types. Second, scRNA-seq is currently feasible at an appropriate scale for screening a pooled library of CAR variants in order to identify transcriptional phenotypes with unique T cell activation profiles. To maximize translatability, we introduced the signaling domain-shuffled library into primary human T cells and triggered CAR activation through a co-culture with tumor cells expressing cognate antigen (HER2). This unique strategy allowed us to identify functional CARs with previously unused intracellular signaling domain combinations. These candidates exhibit properties that are uncommon in current standard designs and, thus may lead to new applications for CAR T cells. In addition, the depth and resolution of the output data allowed us to compare CAR T cell-induced phenotypes to the transcriptional landscape found in clinically relevant settings, comprising the first steps towards customized CAR T cell therapies.

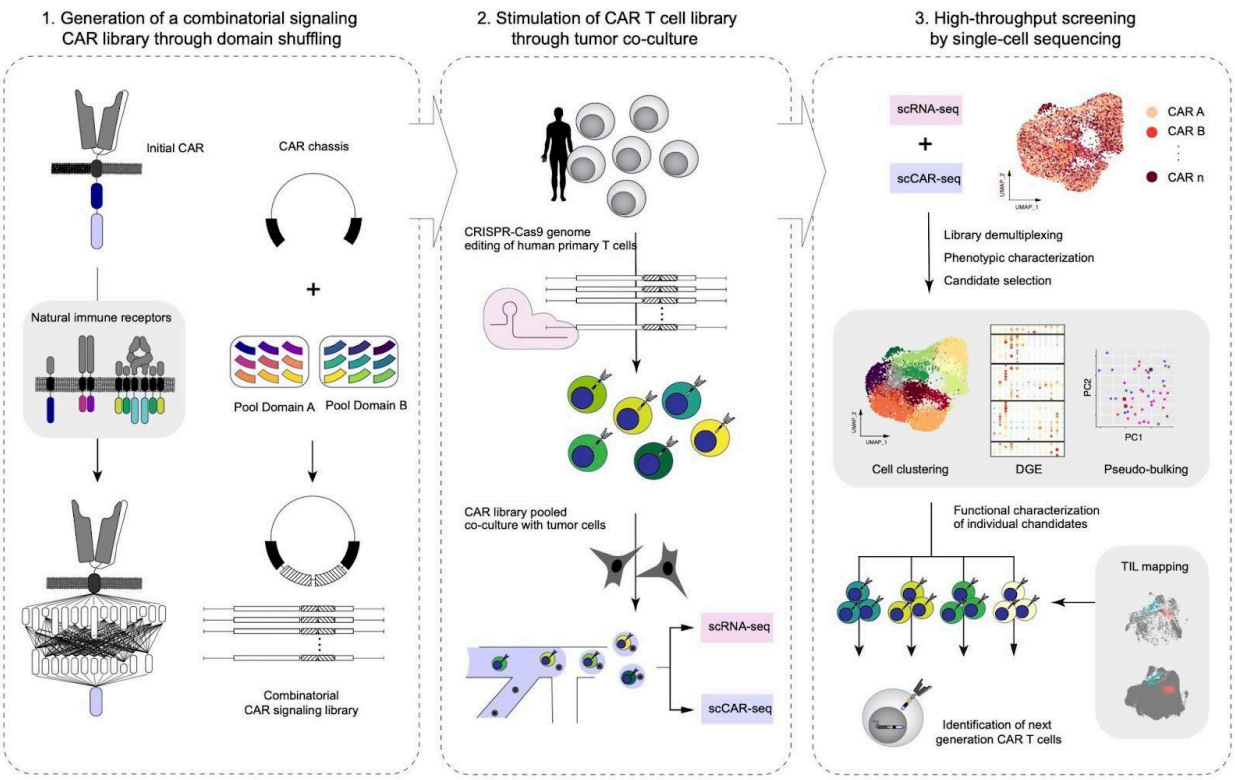

Fig. 6: Schematic overview of speedingCARs: an integrated approach for the rapid engineering of CARs.

(1) First, an initial CAR architecture is chosen based on functionality and encoded in a DNA plasmid. Next, one or more modular domains of the CAR are swapped for alternative natural immune intracellular signaling domain in a semi-random combinatorial fashion, resulting in a plasmid library of CAR variants with diverse combinations. (2) The plasmid library of CAR variants is genomically integrated at the *TRAC* locus of primary human T cells via CRISPR-Cas9 genome editing. This ensures that each cell expresses a single CAR variant, and simultaneously deletes the endogenous TCR. A pooled library of CAR T cells is co-cultured in the presence of tumor cells expressing cognate antigens. (3) The functional screening of the pooled CAR T cell library is performed by scRNAseq and scCARseq, revealing the transcriptional phenotype. This dataset is used to select promising variants for in-depth characterization with functional assays.

Among natural proteins, domain shuffling is thought to be a major evolutionary driver (*29*). By definition, a domain's structure is modular and its function is portable. DNA translocation events that carry a domain-coding sequence into another gene can thus be well-tolerated from a functional standpoint. A domain might synergize with its neighboring domains, e.g. a kinase domain joining a binding domain, potentially creating a new pathway branch (*30*, *31*). Signaling proteins are especially likely to be modular, leading to their embedding in complex networks of protein-protein interactions. With their signaling domains typically taken from T cell immune receptors, CARs are no exception. While the understanding of natural T cell signaling has benefited from decades of research, there is little knowledge on the effects of mixing and matching signaling domains in synthetic receptors such as CARs. Efforts to date have selected domain combinations largely by trial and error and from a small pool of known effectors (*10*, *12*,

13). Inspired by natural evolution, the speedingCARs method relies on random domain shuffling to generate a library of all possible combinations from which functional pairings can be identified.

While domain shuffling constitutes a powerful method for rapidly engineering new diversity in a protein, this can make the choice of screening strategy a challenging ordeal. Previous work for CAR engineering relied on functional screening based on the expression of single reporter genes or proteins (e.g., IL-2, NFAT, CD69) in immortalized cell lines (*14*, *27*, *32–34*). While these approaches enable high-throughput screening of CAR libraries, they are limited by their uni-dimensionality: they generally reveal only a single aspect of the effector response and do not capture the full complexity of the deeply interconnected signaling network of T cell activation. Furthermore, immortalized cell lines do not fully recapitulate primary T cells, reducing the translatability of the screening results. Rather, to obtain multi-dimensional and translatable CAR functional profiles, primary T cells and RNA-seq offer a powerful alternative. The use of scRNAseq, in particular, is fast becoming an important tool in the characterization of CAR T cells before and during their clinical evaluation (*9*), and is especially suited for the screening of a pooled library of engineered cells. Recent work by Roth et al. demonstrated how scRNAseq can be used to capture the transcriptome and the corresponding identity of a library member in engineered cells (*35*). In their approach, a pooled library of 36 knock-in genes was screened in combination with a NY-ESO-1-specific TCR to find transcriptional phenotypes that could enhance the induced T cell response. As the capacity of scRNAseq continues to grow, larger libraries can be screened in this way. Here, we harnessed current scRNAseq capabilities to screen a library of 180 possible CAR signaling variants and directly identify unique transcriptional phenotypes of T cell activation. Our method circumvents the need for engineered cell lines and reporter genes, as it retains a robust throughput while greatly enhancing the translatability of the screening results.

Many of the pitfalls of CAR T cells are being addressed with complementary solutions such as additional gene editing to enhance the T cell immune response or the co-administration of immunomodulating compounds (*4–8*). These solutions risk adding layers of complexity to what remains a challenging treatment to administer. Ideally, a single genome-integrated CAR would suffice, as in currently approved regimens, but different tumors may require slightly different approaches, making it challenging to find an optimal construct for a given situation. By shuffling signaling domains from diverse origins, we aimed to identify CARs that promote unique transcriptional phenotypes, as well as domains that may be associated with novel immunological profiles and functions. Indeed, we found significant phenotypic diversity in our CAR library, especially with genes related to effector and cytotoxic function, memory differentiation, Th1/Th2 classification and tumor infiltration. These unique profiles may prove valuable in specific

contexts where maximal cytotoxicity is not the only sought-after property. For instance, in clinical settings, BBz CARs have sometimes proven to be superior to the 28z combination with respect to T cell exhaustion and persistence in vivo (*36*, *37*), or showing a reduced incidence of adverse events (*37*). Despite the limited translatability of in vitro assays to therapeutic efficiency and the lack of clinical validation of our tested candidates, the cytokine and cytotoxicity functional assays we performed suggest that all of our selected CAR variants have some ability to trigger a response compared to the controls. scRNAseq guided the rational selection of four CAR variants (A-D) that perform equally well or better than clinical benchmarks based on different in vitro killing assays and trigger distinct T cell activation phenotypes. Such phenotypes include in some cases the reduced secretion of proinflammatory molecules such as GM-CSF, IFNγ, and TNFα, where reduced expression has been positively correlated with safer and more effective CAR T cell products in different therapeutic settings (*38–40*).

Furthermore, we observed interesting patterns and synergies regarding the choice of CAR signaling domains; some signaling domains appear more productive than others. For instance, in terms of representation in the transcriptomics screen, the prominence of combinations featuring CD79B may reflect an ability to induce proliferation. In addition, Fc or Fc-like receptor domains were often present in variants with high enrichment in CICs. Following selection, we indeed found that variants A-F, all featuring these domains, induce the most potent tumor-killing dynamics. FcεRIγ, present in variant C, was one of the two original signaling domains used in early CARs, the other being CD3ζ (*41*). Our results suggest that other Fc domains and combinations may be worth testing further. Likewise, CD30, a member of the Tumor Necrosis Factor Receptor (TNFR) superfamily and CD150, a member of the SLAM family may be responsible for the enhanced response of variants G and H over J. Little is known on the exact function of these receptors, however, the interaction of CD30 with TNFR-associated factors (TRAF) (*42*) or the signaling of CD150 through its immunoreceptor tyrosine-based switch motifs (ITSM) (*43*) may have a superior synergy with CD79B and CD3z signaling. In their flow cytometry-based CAR screening method, Goodman et al. also identified TNFR superfamily members as conferring functional enhancements (*15*), on the other hand SLAM receptor domains have not been studied in the context of a CAR. Lastly, we note that the presence of the CD28 and 4-1BB signaling domains among selected variants confirm their important co-stimulatory properties. However, other CAR constructs incorporating these domains (e.g. 4-1BB-LMP2 and 4-1BB-DAP12) showed poor T cell effector potential in the transcriptomics data and CAR F performed less effectively than BBz in functional assays, affirming that the contribution of all signaling domains in a CAR matters.

What constitutes the optimal T cell phenotype for adoptive cell therapies is an elusive question. The killing of tumor cells with in vitro assays and in vivo mouse models does not always translate to clinical efficacy in patients. This may be due to a limited understanding of other dimensions of the T cell response, such as differentiation-linked phenotypes and the interplay with the patient's immune system and tumor microenvironment. Furthermore, each clinical context might benefit from a therapeutic T cell product more precisely tailored for the given situation (*44*). Due to the multi-dimensionality of scRNAseq data, in the present study and as a proof-of-concept analysis, we attempted to bridge the gap between phenotypic characterization and clinically relevant T cell states by mapping our new CAR induced T cell phenotypes to the transcriptional landscape found in TILs isolated from lung cancer patients following successful ICB treatment. Similarity between CAR-induced phenotypes and TILs from responding patients uncovered CAR variants worthy of further development since they may have the potential to drive superior T cell responses for the treatment of solid tumors, a major challenge in the field. Indeed, our functional characterization showed that enrichment in tumor-reactive TIL associated clusters generally correlated with the selection of functional CARs. As the scRNAseq data analysis toolbox keeps evolving and the available datasets become more diverse in contexts (*45*), mapping of in vitro generated transcriptomes of CAR libraries to clinical reference atlases may guide the selection of variants with beneficial properties for precisely defined clinical indications.

Altogether the speedingCARs method offers a path towards the next step in personalized and precision medicine. This can be expanded to the now growing interest in using CARs against other indications, such as viral infections (*46*, *47*), autoimmune disease (*48*, *49*) or organ transplants (*50*). In addition, the expression of CARs in other cells of the immune system, such as natural killer cells, macrophages or neutrophils, is also being considered (*46*, *51–53*). The use of a CAR to direct a targeted antitumor response while also exploiting characteristics of these other cell types such as their natural tropism towards tumor sites, distinct cytokine secretion signature, antigen-independent tumor killing abilities as well as their lack of alloreactivity could help break through current CAR T cell therapy limitations (*54*).

2.4 Materials and methods

Library cloning

The CAR signaling domain library was constructed in a DNA plasmid vector using a Type IIS restriction enzyme cloning strategy, as previously described (*18*). Briefly, the vector was designed with a cloning cassette within a CAR chassis, as illustrated in Fig. 1c. In this chassis, the CD3ζ signaling domain was

segmented, retaining amino acids 100 to 164 (amino acids 52 to 99 were used in the pool of domain B). The vector was digested with the Type IIS restriction enzyme AarI (Thermo Fisher) for 4 h at 37 °C and treated with Antarctic phosphatase (NEB) for 30 min at 37 °C. The signaling domains were amplified from synthetic DNA gene templates (Twist Bioscience) with primer pairs F1/R1 or F2/R2 (Supplementary Table 2) and digested with AarI. An equimolar mix of all domain fragments was prepared for ligation into the digested CAR chassis vector with T4 ligase (NEB). The ligated plasmids were transformed and amplified in chemically-competent E. coli DH5α cells (NEB).

Primary human T cell isolation and culture

Buffy coats from healthy donors were obtained from the Blutspendezentrum (University of Basel) following the general consent guidelines approved by swissethics (Swiss Association of Research Ethics Committees). All recruited volunteers provided written informed consent. Peripheral blood mononuclear cells (PBMCs) were extracted from buffy coats using a Ficoll gradient. T cells were then isolated using the EasySep human T cell isolation kit (Stemcell) and activated with human T-activator CD3/CD28 Dynabeads (Gibco) at a bead:cell ratio of 1:1. Activated T cells were cultured in X-VIVO 15 (Lonza) supplemented with 5% fetal bovine serum (FBS), 50 µM β-mercaptoethanol, 100 µg/mL Normocin (Invivogen) and 200 U/mL IL-2 (Peprotech), thereafter referred to as T cell growth medium. After 2-3 days, the beads were magnetically removed.

Primary human T cell genome editing

We adapted our previous CRISPR-Cas9 genome editing protocol (*27*) to introduce CAR genes at the *TRAC* genomic locus. Double-stranded HDR DNA repair template was produced through PCR amplification. The primers F3 and R3 (Supplementary Table 2) were used to amplify the CAR gene and homology arms whilst incorporating truncated Cas9 target sequences (tCTS) as described in (*55*). The product was purified using a QIAquick PCR Purification Kit (Qiagen). The ribonucleoprotein (RNP) particles were assembled by first duplexing the CRISPR RNA (crRNA; Supplementary Table 1) and trans-activating CRISPR RNA (tracrRNA) (IDT) through co-incubation at a 1:1 ratio (95 °C for 5 min). After cooling, 4 µL of duplexed RNA (100 µM) were complexed with 2 µL of Cas9 protein (62 µM; IDT) at room temperature for 20 min.

To generate CAR library T cells, 2 µg of DNA repair template was added to 6 µL of RNP and diluted in 100 µL P3 nucleofection buffer (Lonza). This mixture was nucleofected with 2×10^6 stimulated human primary T cells 72 h after bead stimulation, using the 4D-Nucleofector (Lonza) with the program EO-115. The cells were then immediately diluted in 600 µL of T cell growth medium. To generate individual CAR

T cell variants, 0.4 μg of DNA repair template was added to 1.2 μL of RNP and diluted in 20 μL P3 nucleofection buffer (Lonza). This mixture was nucleofected with 1×106 stimulated human primary T cells 48 h after bead stimulation, using the program EH-115. The cells were then immediately diluted in 150 μL of T cell growth medium.

Cancer cell line culture and genome editing

HER2 expressing cell lines SKBR3 and MCF-7 (*27*) were cultured in Dulbecco's Modified Eagle Medium (DMEM) (Gibco) supplemented with 10% FBS, 1% penicillin-streptomycin (Gibco) and 100 μg/mL Normocin (Invivogen), thereafter referred to as cell line growth medium. CRISPR-Cas9 genome editing in these cell lines was performed with RNP particles as described above with the following differences: the crRNA was specific for CCR5 (*56*) (Supplementary Table 1); the nucleofection buffer was Dulbecco's phosphate-buffered saline (DPBS) (Gibco); the nucleofector protocol was EO-117 for SKBR3 and EN-130 for MCF-7; and the cells were diluted in cell line growth medium.

Library sequencing

We used next-generation sequencing to characterize the diversity of the CAR signaling domain library. To examine the library at a plasmid level, we amplified the shuffled signaling domains using a PCR reaction with primers annealing to flanking sequences (F4 and R4; Supplementary Table 2) and purified the resulting product ranging between 304 and 1096 bp. To assess the library diversity following genome editing, we performed a two-step PCR. First, genomic DNA was extracted from 10^4 to 10^5 CAR-expressing T cells using QuickExtract buffer (Lucigen). The resulting product was used as a DNA template for a first PCR amplification reaction using F5 and R5 primers (Supplementary Table 2) to produce a long amplicon which confirmed *TRAC* locus genomic integration. This product was then used as DNA template for a second PCR amplification using primers F4 and R4. The final amplimers were purified and sequenced by long amplicon sequencing (PacBio) or Illumina paired-end sequencing (GENEWIZ).

FACS of CAR expression and binding

Analytical and sorting flow cytometry protocols to confirm genomic integration of CAR constructs were described before and adapted here to primary human T cells (*27*) (Fig. 1f). The knock-out of the T cell receptor (TCR) was assessed with the absence of signal after staining 1:200 with CD3ε-APC (UCHT1,Biolegend). Each CAR construct contained a Strep tag which allowed for a two-step staining to validate successful knock-in; a 1:200 biotinylated anti-Strep tag antibody (GenScript) treatment was followed by a 1:400 Streptavidin-BrilliantViolet 421 conjugate (Biolegend). Similarly, HER2 binding was

confirmed with 2.5 µg/mL soluble HER2 antigen (Merck) and subsequent 1:200 APC-labeled anti-HER2 antibody (Biolegend) incubation. Cells were washed in cold DPBS and kept on ice until analysis. CAR T cells were sorted into room temperature T cell growth medium and maintained for 5 days to recover before co-culture assays.

Single cell sequencing and data analysis

Previously sorted library CAR T cells (rested for 8–10 days following bead removal) were co-cultured for 36 h with the high HER2-expressing tumor cell line SKBR3. An E:T ratio of 1:2 was used to maximize the contact of CAR T cells with their target antigen. Immediately after co-culture, CAR-T cells were sorted by FACS (Supplementary Fig. 3) and single-cell RNA sequencing was performed using the 10X Genomics Chromium system (Chromium Single Cell 3' Reagent Kit, v3 chemistry; PN-1000075) following manufacturer's instructions. In short 4,000–20,000 cells were resuspended in PBS and loaded into a chromium microfluidics chip. Following GEM formation, reverse transcription and cDNA amplification, 25% of the sample was used for 3' gene expression library preparation, including the incorporation of Chromium i7 multiplex indices (PN-120262). The resulting transcriptome libraries were sequenced using the Illumina NovaSeq platform. scRNAseq data were generated from three individual donors.

Single cell CAR sequencing (scCARseq)

In order to de-multiplex the CAR T cell library within the scRNAseq data, a scCARseq strategy was developed (adapted from (*35*); Supplementary Fig. 2). Using 40 µg of 10X cDNA, the cytoplasmic region of the 10X pooled barcoded CAR cDNA molecules was amplified using KAPA-HIFI, a Read1-p5 primer (F6) and a customized Strep-Tag specific Read2 primer (R6, Supplementary Table 2). Following a 10 cycle PCR (95 C for 3', [98 C for 20", 67 C for 30", 72 C for 60"] x10, 72 C for 2') and a X0.65 SPRI bead DNA clean up (AMPure XP, Beckman Coulter) a second PCR using a p5 primer (F7, Supplementary Table 2) and a i7-Read2 primer (Chromium i7 Multiplex Kit, 10X Genomics, PN-120262) were used to further amplify the genetic material for 15 cycles (95 C for 3', [98 C for 20", 54 C for 30", 72 C for 60"] x15, 72 C for 2'). CAR amplicons were then sequenced using PacBio SMRT sequencing platform and Biostrings R package was used to assign a CAR variant to each 10X single-cell barcode.

Analysis of scRNAseq data

The raw scRNAseq data was aligned to the human genome (GRCh38) using Cell Ranger (10x Genomics, version 3.1.0) and downstream analysis was carried out using the Seurat R package (version 4.0.1) (*57*). Low quality cells were removed based on the detection of low and high number of UMIs (500

<nFeature_RNA < 10,000) and high percentage of mitochondrial genes (Percentage_MT < 15% of total reads). scCARseq results were then used to assign CAR variants to each sequenced cell, obtaining an assignment rate of 59% of cells, and only cells assigned to a single CAR variant (55%) were used for downstream analysis.

After QC and CAR T cell assignment a total number of 9,193 stimulated library CAR T cells, 1,093 stimulated 28z CAR T cells, 406 stimulated BBz CAR T cells, 3,755 unstimulated 28z CAR T cells and 8828 stimulated TCR-negative T cells were obtained. Each dataset was log normalized with a scale factor of 10,000 and sample integration was performed applying the reciprocal PCA seurat pipeline using 2,000 variable integration features. Integrated data were then scaled regressing out cell cycle genes and dimensionality reduction was done using the RunPCA function. FindNeighbors and FindClusters functions were used to do unsupervised cell clustering and differential gene expression (FindAllMarkers) was used to find marker genes used for cluster annotation. The results were then visualized using UMAP dimensionality reduction. Gene set enrichment analysis was carried out using gProfiler2 R package (*58*). Pseudo-bulk samples were generated using the AverageExpression Seurat function on cells grouped by CAR variant metadata annotation. The normalized counts data was used to do PCA analysis (PCAtools) and the scaled data was used to look at the expression of marker genes. Gene set scores were computed using Ucell R package (*59*).

Integration and analysis of TIL and CAR scRNAseq data

The count scRNAseq data from Liu et al. (*26*), accessible under GSE179994 (GSE179994_all.Tcell.rawCounts.rds.gz) was downloaded and the following samples were selected s for downstream analysis: P1.tr.1, P1.tr.2, P1.tr.3, P1.ut, P13.tr.1, P13.tr.2, P13.ut, P19.tr, P19.ut, P30.tr, P30.ut, P36.tr.1, P38.tr.1. Data analysis and QC was performed as previously described using the Seurat R package (version 4.1.0) (*57*). In addition, CD8+ cells were selected based on the lack of CD4 expression. Next, CAR and TIL seurat objects were joined and split by patient identity using the SplitObject function. To remove bias from cell cycle stages, a cell cycle score was assigned to every cell using CellCycleScoring. Before integration, SCTransform was used on each list object while regressing out Percentage_MT and cell cycle scores. Following the Seurat integration pipeline, 3000 integration features were selected using SelectIntegrationFeatures, and all seurat objects (CAR and TIL datasets) were combined using the merge function (using the previously selected 3000 integration features as variable features). Consecutively, RunPCA and RunHarmony from the Harmony R package (version 1.0) (*60*) were used to remove batch effects. Finally, we used RunUMAP, FindNeighbors, and FindClusters to generate a UMAP visualization and to perform unsupervised clustering of the integrated data.

Cytokine secretion

The cytokine secretion of CAR T cells was measured following co-culture with SKBR3 target cells. For each replicate, 40,000 CAR T cells and 10,000 target cells were incubated in a volume of 200 µL of T cell growth medium supplemented with 50 U/mL IL-2 for 4 days. The culture supernatant was obtained by centrifugation and cytokine levels was analyzed using a Bio-Plex Pro Human Cytokine Th1/Th2 Assay (Bio-rad) according to manufacturer's instructions. Briefly, supernatants were co-incubated with washed magnetic fluorescent beads coated with capture antibodies for the analytes GM-CSF, IFN-γ, TNF-α, IL-2, IL-4, IL-5, IL-10, IL-12 (p70), and IL-13. Following washes, beads were co-incubated with PE-labeled antibodies specific to the analytes. After final washes, beads were analyzed using a Bio-Plex MAGPIX (Bio-rad). IL-2 data were excluded from the analysis due to the supplementation of this cytokine in the medium.

Formation of MCF-7/GFP spheroids

Individual MCF-7/GFP spheroids were formed in ultra-low adherent, Nunclon™ Sphera™ U-shaped-bottom, 96-well plate (Thermo Fisher Scientific). In brief, cells were detached from the cell culture flask using 1X TrypLE™ Express enzyme (Gibco) and re-suspended at a density of 10^4 cells/mL in pre-warmed complete minimum essential media (MEM) that contains 5 µg/mL human recombinant insulin (Gibco), 1X MEM non-essential amino acids (NEAA) (Gibco), 1 mM sodium pyruvate (Merck), and 50 µg/mL Kanamycin (BioConcept). 100 µL of cell suspension was loaded into each U-shaped-bottom well, resulting in an initial seeding of 1000 cells/spheroid. Cells were spun down at 250 g for 2 min and then kept in a humidified incubator at 37 °C and 5% CO2 (Binder GmbH) without medium exchange for 3 days. Before each experiment, MCF-7 spheroids were imaged with a Cell3iMager Neo plate scanning system (SCREEN Group) for quality check. Compact MCF-7/GFP spheroids with a diameter of approximately 350 µm were qualified for further experiment.

Live imaging of cytotoxicity

CAR T cells and GFP-expressing cancer cells were co-cultured in an incubated chamber equipped with a wide-field Nikon Ti2 microscope to visualize target cell death. For 2D SKBR3 killing, cells were mixed at designated ratios in a glass bottom 96-well plate in phenol red-free MEM supplemented with 1X NEAA (Gibco), 1X Glutamax (Gibco), 1 mM sodium pyruvate (Merck), 10% FBS (Gibco) and 50 U/mL IL-2 (Peprotech). For 3D MCF-7 killing, microtissues of 10^3 cells were co-cultured at designated ratios in MT medium supplemented with 50 U/mL IL-2. Images were captured every 4 or 6 h for 72 h. For image analysis, a pipeline combining Ilastik (only for 2D SKBR3 killing) and Fiji was used to do background

subtraction, segmentation and finally extract the total fluorescence of detected cell objects. The resulting values were analyzed with R and plotted with Graphpad (Prism).

Multi-parameter flow cytometry for immunological markers

Following 4-day co-cultures of CAR T cells and SKBR3 cells at a ratio of 4:1, cells were extracted by centrifugation and prepared for flow cytometry analysis of immunological markers. First, cells were stained for viability (Zombie Aqua, Biolegend) in PBS, washed and stained in FACS buffer (2% FBS, 0.1% NaN3 in PBS) for the following markers: HLA-DR-Alexa Fluor 647 (L243), CD69-Pacific Blue (FN50), CD25-PE/Cy7 (M-A251), CD137/4-1BB-PE/Dazzle 594 (4B4-1), CD45RA- PE/Dazzle 594 (HI100), CCR7-APC/Cy7 (3D12), CD27-BV570 (O323), CD39-FITC (A1), CD127-PE (A019D5), CTLA-4-BV785 (L3D10), LAG-3-BV711 (11C3C65), TIGIT-BV421 (A15153G) from Biolegend; and CD3-BUV395 (UCHT1), CD4-BUV496 (SK3), CD8-BUV805 (SK1), CD62L-BV650 (SK11), PD-1-BB700 (EH12.1), TIM3-BV480 (7D3) from BD Biosciences (Supplementary Table 3). After washing, cells were analyzed using the Cytek Aurora full-spectrum flow cytometry technology. Data were further processed with FlowJo 10 software (BD Biosciences; Supplementary Fig. 12).

Statistics & reproducibility

Statistical analysis was performed using Prism 9 software (GradPad) with the exception of sc-RNAseq data which was analyzed with R Studio using the packages mentioned above. No statistical method was used to predetermine sample size. When required, outliers resulting from technical problems were excluded from the analysis. Blinding was not relevant as data was quantified by software and not subject to investigators input. Except for scRNAseq data, where randomization was used to obtain a balanced representation of CAR variants, experiments were not randomized. When micrographs are shown, at least three independent experiments were run, presenting similar results.

Data availability

All data are included in the Figures, Supplemental Information or available from the authors upon reasonable requests, as are unique reagents used in this Article. The raw and processed sequencing data generated in this study have been deposited in the Gene Expression Omnibus under accession number GSE214231 (https://www.ncbi.nlm.nih.gov/geo/query/acc.cgi?acc=GSE214231).

Code availability

The custom R scripts used for data analysis are publicly available at the GitHub repository: https://github.com/LSSI-ETH/SpeedingCARs_2022.

References for Chapter 2

1. J. J. Melenhorst, G. M. Chen, M. Wang, D. L. Porter, C. Chen, M. A. Collins, P. Gao, S. Bandyopadhyay, H. Sun, Z. Zhao, S. Lundh, I. Pruteanu-Malinici, C. L. Nobles, S. Maji, N. V. Frey, S. I. Gill, A. W. Loren, L. Tian, I. Kulikovskaya, M. Gupta, D. E. Ambrose, M. M. Davis, J. A. Fraietta, J. L. Brogdon, R. M. Young, A. Chew, B. L. Levine, D. L. Siegel, C. Alanio, E. J. Wherry, F. D. Bushman, S. F. Lacey, K. Tan, C. H. June, Decade-long leukaemia remissions with persistence of CD4+ CAR T cells. *Nature*. **602**, 503–509 (2022).

2. M. Ruella, M. V. Maus, Catch me if you can: Leukemia Escape after CD19-Directed T Cell Immunotherapies. *Comput. Struct. Biotechnol. J.* **14**, 357–362 (2016).

3. A. V. Hirayama, C. J. Turtle, Toxicities of CD19 CAR-T cell immunotherapy. *Am. J. Hematol.* **94**, S42–S49 (2019).

4. R. Grosser, L. Cherkassky, N. Chintala, P. S. Adusumilli, Combination Immunotherapy with CAR T Cells and Checkpoint Blockade for the Treatment of Solid Tumors. *Cancer Cell*. **36**, 471–482 (2019).

5. M. Chmielewski, H. Abken, TRUCKs: the fourth generation of CARs. *Expert Opin. Biol. Ther.* **15**, 1145–1154 (2015).

6. W.-H. Leung, J. Gay, U. Martin, T. E. Garrett, H. M. Horton, M. T. Certo, B. R. Blazar, R. A. Morgan, P. D. Gregory, J. Jarjour, A. Astrakhan, Sensitive and adaptable pharmacological control of CAR T cells through extracellular receptor dimerization. *JCI Insight*. **5** (2019), doi:10.1172/jci.insight.124430.

7. J. H. Cho, A. Okuma, K. Sofjan, S. Lee, J. J. Collins, W. W. Wong, Engineering advanced logic and distributed computing in human CAR immune cells. *Nat. Commun.* **12**, 792 (2021).

8. J. H. Choe, P. B. Watchmaker, M. S. Simic, R. D. Gilbert, A. W. Li, N. A. Krasnow, K. M. Downey, W. Yu, D. A. Carrera, A. Celli, J. Cho, J. D. Briones, J. M. Duecker, Y. E. Goretsky, R. Dannenfelser, L. Cardarelli, O. Troyanskaya, S. S. Sidhu, K. T. Roybal, H. Okada, W. A. Lim, SynNotch-CAR T cells overcome challenges of specificity, heterogeneity, and persistence in treating glioblastoma. *Sci. Transl. Med.* **13** (2021), doi:10.1126/scitranslmed.abe7378.

9. R. Castellanos-Rueda, R. B. Di Roberto, F. S. Schlatter, S. T. Reddy, Leveraging Single-Cell Sequencing for Chimeric Antigen Receptor T Cell Therapies. *Trends Biotechnol.* **39**, 1308–1320 (2021).

10. B. Prinzing, P. Schreiner, M. Bell, Y. Fan, G. Krenciute, S. Gottschalk, MyD88/CD40 signaling retains CAR T cells in a less differentiated state. *JCI Insight*. **5** (2020), doi:10.1172/jci.insight.136093.

11. E. Moreno-Cortes, J. V. Forero-Forero, P. A. Lengerke-Diaz, J. E. Castro, Chimeric antigen receptor T cell therapy in oncology - Pipeline at a glance: Analysis of the ClinicalTrials.gov database. *Crit. Rev. Oncol. Hematol.* **159**, 103239 (2021).

12. H. Kintz, E. Nylen, A. Barber, Inclusion of Dap10 or 4-1BB costimulation domains in the chPD1 receptor enhances anti-tumor efficacy of T cells in murine models of lymphoma and melanoma. *Cell. Immunol.* **351**, 104069 (2020).

13. J. Julamanee, S. Terakura, K. Umemura, Y. Adachi, K. Miyao, S. Okuno, E. Takagi, T. Sakai, D. Koyama, T. Goto, R. Hanajiri, M. Hudecek, P. Steinberger, J. Leitner, T. Nishida, M. Murata, H. Kiyoi, Composite CD79A/CD40 co-stimulatory endodomain enhances CD19CAR-T cell proliferation and survival. *Mol. Ther.* **29**, 2677–2690 (2021).

14. K. S. Gordon, T. Kyung, C. R. Perez, P. V. Holec, A. Ramos, A. Q. Zhang, Y. Agarwal, Y. Liu, C. E. Koch, A. Starchenko, B. A. Joughin, D. A. Lauffenburger, D. J. Irvine, M. T. Hemann, M. E. Birnbaum, Screening for CD19-specific chimaeric antigen receptors with enhanced signalling via a barcoded library of intracellular domains. *Nat Biomed Eng*. **6**, 855–866 (2022).

15. D. B. Goodman, C. S. Azimi, K. Kearns, A. Talbot, K. Garakani, J. Garcia, N. Patel, B. Hwang, D. Lee, E. Park, V. S. Vykunta, B. R. Shy, C. J. Ye, J. Eyquem, A. Marson, J. A. Bluestone, K. T. Roybal, Pooled screening of CAR T cells identifies diverse immune signaling domains for next-generation immunotherapies. *Sci. Transl. Med.* **14**, eabm1463

(2022).

16. J. R. James, Tuning ITAM multiplicity on T cell receptors can control potency and selectivity to ligand density. *Sci. Signal.* **11** (2018), doi:10.1126/scisignal.aan1088.

17. L. Chen, D. B. Flies, Molecular mechanisms of T cell co-stimulation and co-inhibition. *Nat. Rev. Immunol.* **13**, 227–242 (2013).

18. R. B. Di Roberto, B. M. Scott, S. G. Peisajovich, Directed Evolution Methods to Rewire Signaling Networks. *Methods Mol. Biol.* **1596**, 321–337 (2017).

19. D. Yu, M. C. Hung, Overexpression of ErbB2 in cancer and ErbB2-targeting strategies. *Oncogene*. **19**, 6115–6121 (2000).

20. J. Eyquem, J. Mansilla-Soto, T. Giavridis, S. J. C. van der Stegen, M. Hamieh, K. M. Cunanan, A. Odak, M. Gönen, M. Sadelain, Targeting a CAR to the TRAC locus with CRISPR/Cas9 enhances tumour rejection. *Nature*. **543**, 113–117 (2017).

21. B. V. Kumar, W. Ma, M. Miron, T. Granot, R. S. Guyer, D. J. Carpenter, T. Senda, X. Sun, S.-H. Ho, H. Lerner, A. L. Friedman, Y. Shen, D. L. Farber, Human Tissue-Resident Memory T Cells Are Defined by Core Transcriptional and Functional Signatures in Lymphoid and Mucosal Sites. *Cell Rep.* **20**, 2921–2934 (2017).

22. A. Sheih, V. Voillet, L.-A. Hanafi, H. A. DeBerg, M. Yajima, R. Hawkins, V. Gersuk, S. R. Riddell, D. G. Maloney, M. E. Wohlfahrt, D. Pande, M. R. Enstrom, H.-P. Kiem, J. E. Adair, R. Gottardo, P. S. Linsley, C. J. Turtle, Clonal kinetics and single-cell transcriptional profiling of CAR-T cells in patients undergoing CD19 CAR-T immunotherapy. *Nat. Commun.* **11**, 219 (2020).

23. K. Yan, Y. Lu, Z. Yan, Y. Wang, 9-Gene Signature Correlated With CD8+ T Cell Infiltration Activated by IFN-γ: A Biomarker of Immune Checkpoint Therapy Response in Melanoma. *Front. Immunol.* **12**, 622563 (2021).

24. J. Galon, A. Costes, F. Sanchez-Cabo, A. Kirilovsky, B. Mlecnik, C. Lagorce-Pagès, M. Tosolini, M. Camus, A. Berger, P. Wind, F. Zinzindohoué, P. Bruneval, P.-H. Cugnenc, Z. Trajanoski, W.-H. Fridman, F. Pagès, Type, density, and location of immune cells within human colorectal tumors predict clinical outcome. *Science*. **313**, 1960–1964 (2006).

25. C. G. Clemente, M. C. Mihm Jr, R. Bufalino, S. Zurrida, P. Collini, N. Cascinelli, Prognostic value of tumor infiltrating lymphocytes in the vertical growth phase of primary cutaneous melanoma. *Cancer*. **77**, 1303–1310 (1996).

26. B. Liu, X. Hu, K. Feng, R. Gao, Z. Xue, S. Zhang, Y. Zhang, E. Corse, Y. Hu, W. Han, Z. Zhang, Temporal single-cell tracing reveals clonal revival and expansion of precursor exhausted T cells during anti-PD-1 therapy in lung cancer. *Nat Cancer*. **3**, 108–121 (2022).

27. R. B. Di Roberto, R. Castellanos-Rueda, S. Frey, D. Egli, R. Vazquez-Lombardi, E. Kapetanovic, J. Kucharczyk, S. T. Reddy, A Functional Screening Strategy for Engineering Chimeric Antigen Receptors with Reduced On-Target, Off-Tumor Activation. *Mol. Ther.* **28**, 2564–2576 (2020).

28. K. M. Cappell, J. N. Kochenderfer, A comparison of chimeric antigen receptors containing CD28 versus 4-1BB costimulatory domains. *Nat. Rev. Clin. Oncol.* **18**, 715–727 (2021).

29. R. B. Di Roberto, S. G. Peisajovich, The role of domain shuffling in the evolution of signaling networks. *J. Exp. Zool. B Mol. Dev. Evol.* **322**, 65–72 (2014).

30. P. M. Sato, K. Yoganathan, J. H. Jung, S. G. Peisajovich, The robustness of a signaling complex to domain rearrangements facilitates network evolution. *PLoS Biol.* **12**, e1002012 (2014).

31. S. G. Peisajovich, J. E. Garbarino, P. Wei, W. A. Lim, Rapid diversification of cell signaling phenotypes by modular domain recombination. *Science*. **328**, 368–372 (2010).

32. J. Rydzek, T. Nerreter, H. Peng, S. Jutz, J. Leitner, P. Steinberger, H. Einsele, C. Rader, M. Hudecek, Chimeric Antigen Receptor Library Screening Using a Novel NF-κB/NFAT Reporter Cell Platform. *Mol. Ther.* **27**, 287–299 (2019).

33. R. Uchibori, T. Teruya, H. Ido, K. Ohmine, Y. Sehara, M. Urabe, H. Mizukami, J. Mineno, K. Ozawa, Functional Analysis of an Inducible Promoter Driven by Activation Signals from a Chimeric Antigen Receptor. *Mol Ther Oncolytics*. **12**, 16–25 (2019).

34. C. P. M. Duong, J. A. Westwood, C. S. M. Yong, A. Murphy, C. Devaud, L. B. John, P. K. Darcy, M. H. Kershaw, Engineering T cell function using chimeric antigen receptors identified using a DNA library approach. *PLoS One*. **8**, e63037 (2013).

35. T. L. Roth, P. J. Li, F. Blaeschke, J. F. Nies, R. Apathy, C. Mowery, R. Yu, M. L. T. Nguyen, Y. Lee, A. Truong, J. Hiatt, D. Wu, D. N. Nguyen, D. Goodman, J. A. Bluestone, C. J. Ye, K. Roybal, E. Shifrut, A. Marson, Pooled Knockin Targeting for Genome Engineering of Cellular Immunotherapies. *Cell*. **181**, 728–744.e21 (2020).

36. A. H. Long, W. M. Haso, J. F. Shern, K. M. Wanhainen, M. Murgai, M. Ingaramo, J. P. Smith, A. J. Walker, M. E. Kohler, V. R. Venkateshwara, R. N. Kaplan, G. H. Patterson, T. J. Fry, R. J. Orentas, C. L. Mackall, 4-1BB costimulation ameliorates T cell exhaustion induced by tonic signaling of chimeric antigen receptors. *Nat. Med.* **21**, 581–590 (2015).

37. S. Guedan, A. D. Posey Jr, C. Shaw, A. Wing, T. Da, P. R. Patel, S. E. McGettigan, V. Casado-Medrano, O. U. Kawalekar, M. Uribe-Herranz, D. Song, J. J. Melenhorst, S. F. Lacey, J. Scholler, B. Keith, R. M. Young, C. H. June, Enhancing CAR T cell persistence through ICOS and 4-1BB costimulation. *JCI Insight*. **3** (2018), doi:10.1172/jci.insight.96976.

38. Z. Ying, X. F. Huang, X. Xiang, Y. Liu, X. Kang, Y. Song, X. Guo, H. Liu, N. Ding, T. Zhang, P. Duan, Y. Lin, W. Zheng, X. Wang, N. Lin, M. Tu, Y. Xie, C. Zhang, W. Liu, L. Deng, S. Gao, L. Ping, X. Wang, N. Zhou, J. Zhang, Y. Wang, S. Lin, M. Mamuti, X. Yu, L. Fang, S. Wang, H. Song, G. Wang, L. Jones, J. Zhu, S.-Y. Chen, A safe and potent anti-CD19 CAR T cell therapy. *Nat. Med.* **25**, 947–953 (2019).

39. M. J. Cox, C. Manriquez Roman, E. E. Tapper, E. L. Siegler, D. Chappell, C. Durrant, O. Ahmed, S. Sinha, R. Mwangi, N. S. Scott, M. Hefazi, K. J. Schick, P. Horvei, M. W. Ruff, I. Can, M. Adada, E. Bezerra, L. A. Kankeu Fonkoua, S. A. Parikh, N. E. Kay, R. Sakemura, S. S. Kenderian, GM-CSF disruption in CART cells modulates T cell activation and enhances CART cell anti-tumor activity. *Leukemia*. **36**, 1635–1645 (2022).

40. R. M. Sterner, R. Sakemura, M. J. Cox, N. Yang, R. H. Khadka, C. L. Forsman, M. J. Hansen, F. Jin, K. Ayasoufi, M. Hefazi, K. J. Schick, D. K. Walters, O. Ahmed, D. Chappell, T. Sahmoud, C. Durrant, W. K. Nevala, M. M. Patnaik, L. R. Pease, K. E. Hedin, N. E. Kay, A. J. Johnson, S. S. Kenderian, GM-CSF inhibition reduces cytokine release syndrome and neuroinflammation but enhances CAR-T cell function in xenografts. *Blood*. **133**, 697–709 (2019).

41. C. Romeo, B. Seed, Cellular immunity to HIV activated by CD4 fused to T cell or Fc receptor polypeptides. *Cell*. **64**, 1037–1046 (1991).

42. C. A. van der Weyden, S. A. Pileri, A. L. Feldman, J. Whisstock, H. M. Prince, Understanding CD30 biology and therapeutic targeting: a historical perspective providing insight into future directions. *Blood Cancer J.* **7**, e603 (2017).

43. D. Howie, M. Simarro, J. Sayos, M. Guirado, J. Sancho, C. Terhorst, Molecular dissection of the signaling and costimulatory functions of CD150 (SLAM): CD150/SAP binding and CD150-mediated costimulation. *Blood*. **99**, 957–965 (2002).

44. D. S. Chen, I. Mellman, Elements of cancer immunity and the cancer-immune set point. *Nature*. **541**, 321–330 (2017).

45. R. G. Majzner, S. Ramakrishna, K. W. Yeom, S. Patel, H. Chinnasamy, L. M. Schultz, R. M. Richards, L. Jiang, V. Barsan, R. Mancusi, A. C. Geraghty, Z. Good, A. Y. Mochizuki, S. M. Gillespie, A. M. S. Toland, J. Mahdi, A. Reschke, E. H. Nie, I. J. Chau, M. C. Rotiroti, C. W. Mount, C. Baggott, S. Mavroukakis, E. Egeler, J. Moon, C. Erickson, S. Green, M. Kunicki, M. Fujimoto, Z. Ehlinger, W. Reynolds, S. Kurra, K. E. Warren, S. Prabhu, H. Vogel, L. Rasmussen, T. T. Cornell, S. Partap, P. G. Fisher, C. J. Campen, M. G. Filbin, G. Grant, B. Sahaf, K. L. Davis, S. A. Feldman, C. L. Mackall, M. Monje, GD2-CAR T cell therapy for H3K27M-mutated diffuse midline gliomas. *Nature*. **603**, 934–941 (2022).

46. M. T. Ma, S. Badeti, C.-H. Chen, J. Kim, A. Choudhary, B. Honnen, C. Reichman, D. Calianese, A. Pinter, Q. Jiang, L. Shi, R. Zhou, H. Xu, Q. Li, W. Gause, D. Liu, CAR-NK Cells Effectively Target SARS-CoV-2-Spike-Expressing Cell Lines In Vitro. *Front. Immunol.* **12**, 652223 (2021).

47. M. Hale, T. Mesojednik, G. S. Romano Ibarra, J. Sahni, A. Bernard, K. Sommer, A. M. Scharenberg, D. J. Rawlings, T. A. Wagner, Engineering HIV-Resistant, Anti-HIV Chimeric Antigen Receptor T Cells. *Mol. Ther.* **25**, 570–579 (2017).

48. M. Fransson, E. Piras, J. Burman, B. Nilsson, M. Essand, B. Lu, R. A. Harris, P. U. Magnusson, E. Brittebo, A. S. I. Loskog, CAR/FoxP3-engineered T regulatory cells target the CNS and suppress EAE upon intranasal delivery. *J. Neuroinflammation*. **9**, 112 (2012).

49. M. Tenspolde, K. Zimmermann, L. C. Weber, M. Hapke, M. Lieber, J. Dywicki, A. Frenzel, M. Hust, M. Galla, L. E. Buitrago-Molina, M. P. Manns, E. Jaeckel, M. Hardtke-Wolenski, Regulatory T cells engineered with a novel insulin-specific chimeric antigen receptor as a candidate immunotherapy for type 1 diabetes. *J. Autoimmun.* **103**, 102289 (2019).

50. A. Sicard, C. Lamarche, M. Speck, M. Wong, I. Rosado-Sánchez, M. Blois, N. Glaichenhaus, M. Mojibian, M. K. Levings, Donor-specific chimeric antigen receptor Tregs limit rejection in naive but not sensitized allograft recipients. *Am. J. Transplant*. **20**, 1562–1573 (2020).

51. X. Tang, L. Yang, Z. Li, A. P. Nalin, H. Dai, T. Xu, J. Yin, F. You, M. Zhu, W. Shen, G. Chen, X. Zhu, D. Wu, J. Yu, First-in-man clinical trial of CAR NK-92 cells: safety test of CD33-CAR NK-92 cells in patients with relapsed and refractory acute myeloid leukemia. *Am. J. Cancer Res.* **8**, 1083–1089 (2018).

52. M. Klichinsky, M. Ruella, O. Shestova, X. M. Lu, A. Best, M. Zeeman, M. Schmierer, K. Gabrusiewicz, N. R. Anderson, N. E. Petty, K. D. Cummins, F. Shen, X. Shan, K. Veliz, K. Blouch, Y. Yashiro-Ohtani, S. S. Kenderian, M. Y. Kim, R. S. O'Connor, S. R. Wallace, M. S. Kozlowski, D. M. Marchione, M. Shestov, B. A. Garcia, C. H. June, S. Gill, Human chimeric antigen receptor macrophages for cancer immunotherapy. *Nat. Biotechnol.* **38**, 947–953 (2020).

53. Y. Chang, R. Syahirah, X. Wang, G. Jin, S. Torregrosa-Allen, B. D. Elzey, S. N. Hummel, T. Wang, C. Li, X. Lian, Q. Deng, H. E. Broxmeyer, X. Bao, Engineering chimeric antigen receptor neutrophils from human pluripotent stem cells for targeted cancer immunotherapy. *Cell Rep.* **40**, 111128 (2022).

54. D. Cortés-Selva, B. Dasgupta, S. Singh, I. S. Grewal, Innate and Innate-Like Cells: The Future of Chimeric Antigen Receptor (CAR) Cell Therapy. *Trends Pharmacol. Sci.* **42**, 45–59 (2021).

55. D. N. Nguyen, T. L. Roth, P. J. Li, P. A. Chen, R. Apathy, M. R. Mamedov, L. T. Vo, V. R. Tobin, D. Goodman, E. Shifrut, J. A. Bluestone, J. M. Puck, F. C. Szoka, A. Marson, Polymer-stabilized Cas9 nanoparticles and modified repair templates increase genome editing efficiency. *Nat. Biotechnol.* **38**, 44–49 (2020).

56. E. Aznauryan, A. Yermanos, E. Kinzina, A. Devaux, E. Kapetanovic, D. Milanova, G. M. Church, S. T. Reddy, Discovery and validation of human genomic safe harbor sites for gene and cell therapies. *Cell Rep Methods*. **2**, 100154 (2022).

57. A. Butler, P. Hoffman, P. Smibert, E. Papalexi, R. Satija, Integrating single-cell transcriptomic data across different conditions, technologies, and species. *Nat. Biotechnol.* **36**, 411–420 (2018).

58. U. Raudvere, L. Kolberg, I. Kuzmin, T. Arak, P. Adler, H. Peterson, J. Vilo, g:Profiler: a web server for functional enrichment analysis and conversions of gene lists (2019 update). *Nucleic Acids Res.* **47**, W191–W198 (2019).

59. M. Andreatta, S. J. Carmona, UCell: Robust and scalable single-cell gene signature scoring. *Comput. Struct. Biotechnol. J.* **19**, 3796–3798 (2021).

60. I. Korsunsky, N. Millard, J. Fan, K. Slowikowski, F. Zhang, K. Wei, Y. Baglaenko, M. Brenner, P.-R. Loh, S. Raychaudhuri, Fast, sensitive and accurate integration of single-cell data with Harmony. *Nat. Methods*. **16**, 1289–1296 (2019).

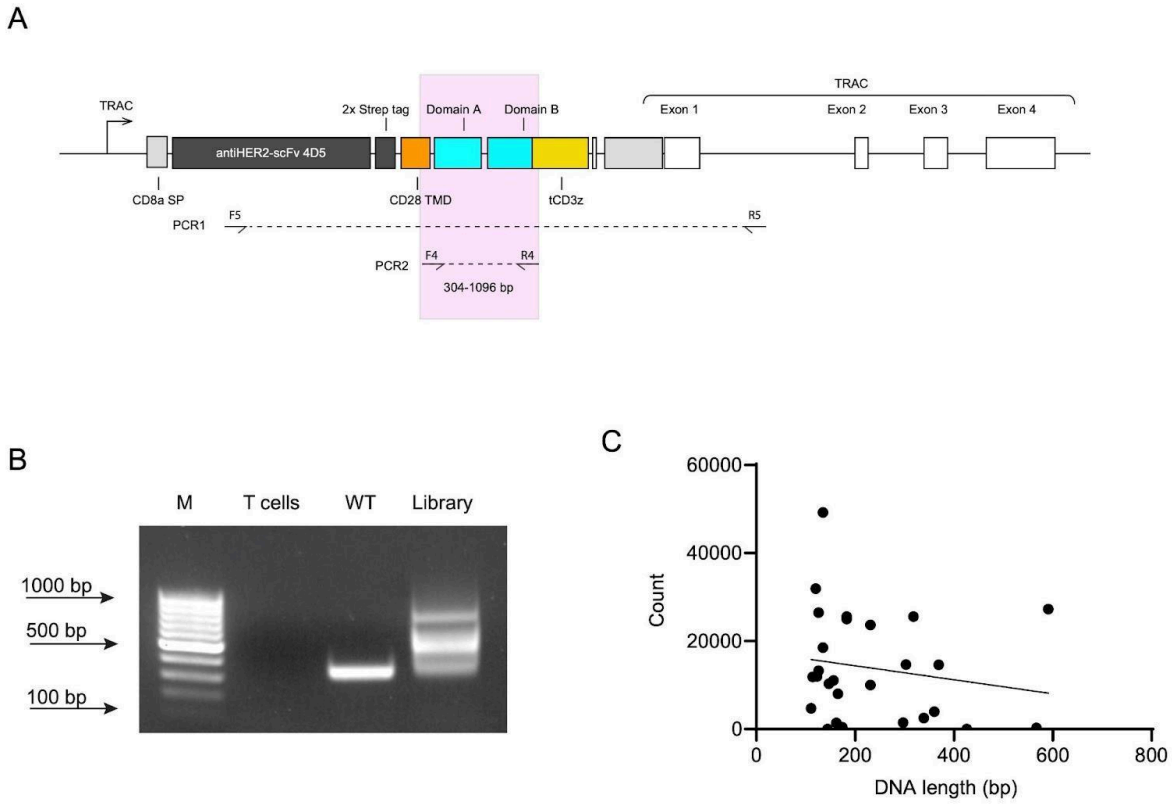

Supplementary Figure 1: PCR amplification confirms the integration of the CAR library

A) Schematic representation of the PCR amplification strategy to obtain amplicons of the integrated CAR gene. **B)** Agarose gel electrophoresis of the genomic amplicons from primary T cells (T cell), 28z CAR (WT) and sorted CAR T cells expressing the library of signaling domain variants (Library), all run alongside a DNA molecular weight marker (M). The library lane shows the range of expected amplicons owing to different signaling domain sizes. **C)** Scatter plot of the signaling domain's DNA length against their abundance in the CAR T cell library (post transfection, post sort). There is no significant correlation between the two variables.

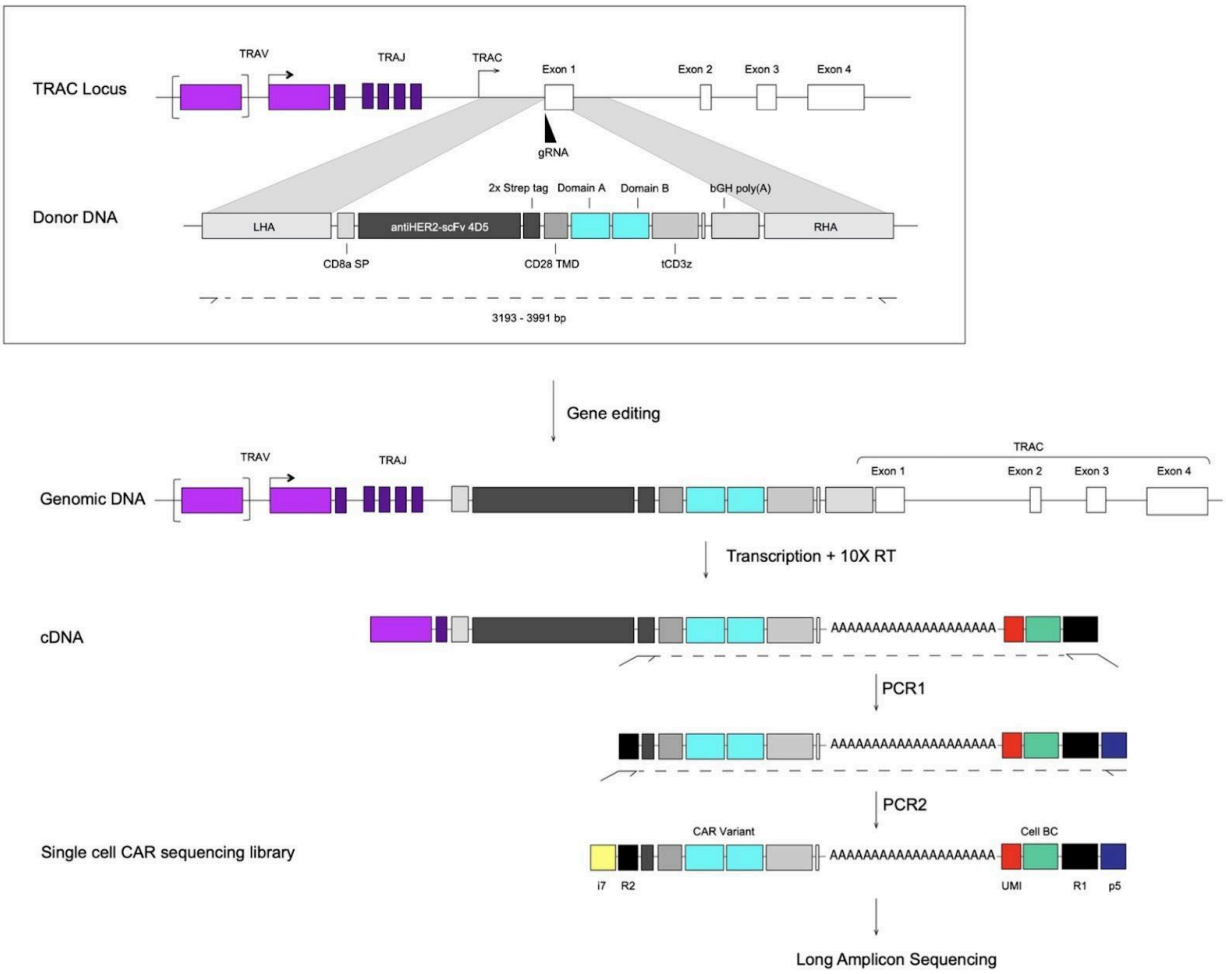

Supplementary Figure 2: scCARseq PCR amplification strategy for library de-multiplexing

Following CRISPR-Cas9 based gene editing CAR T cells incorporate a single copy of a CAR gene into the *TRAC* locus. Guided by *TRAC* specific gene expression regulation the CAR gene is transcribed into mRNA and translated into a CAR. During 10X droplet encapsulation, reverse transcription and cDNA synthesis each CAR transcript incorporates a barcode specific to its cell of origin (cell-BC). A two-step PCR amplification strategy that makes use of the synthetic Strep tag sequence found in the CAR gene, allows to selectively amplify cell-BC linked CAR transcripts from the 10X cDNA mix. This scCARseq library can then be sequenced using long amplicon technologies (PacBio) to trace the origin of CAR transcripts to each individual cell identified in the 10X gene expression pipeline.

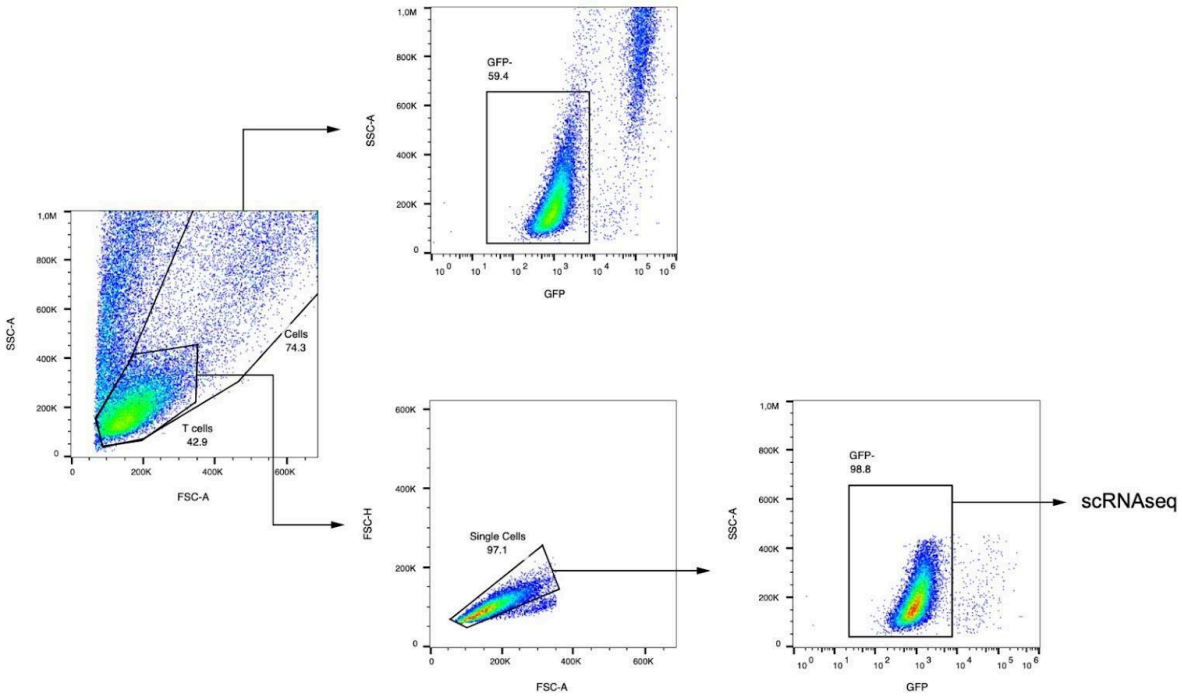

Supplementary Figure 3: FACs gating strategy used to isolate T cells following tumor co-culture

Following 36h of co-culture between CAR T cells and SKBR3-GFP tumor cell lines T cells were sorted based on size, density and lack of expression of GFP.

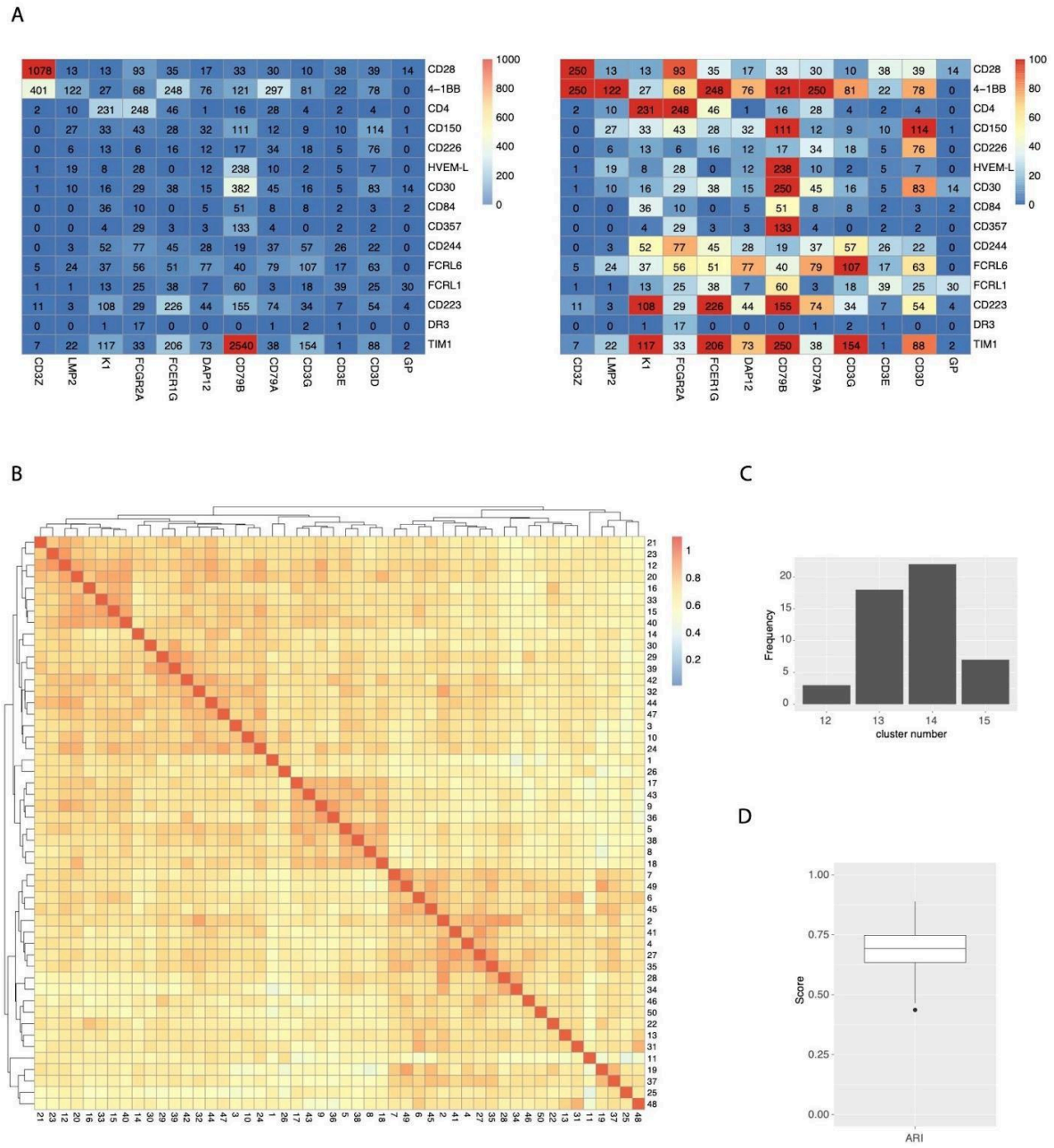

Supplementary Figure 4: scRNA-seq clustering analysis is robust to cell subsampling

A) Heatmaps showing the numbers of cells assigned to each CAR variant before (left) and after (right) subsampling a maximum number of 250 cells from each CAR variant. Of note; CD28-CD3ζ and 4-1BB-CD3ζ T cells were spiked-into the pooled library of CAR T cells prior to co-culture. **B)** Matrix of the adjusted Rand index (ARI) of the first 50 seed outputs for the clustering analysis featured in Figure 3 of the main text. This analysis relies on the random subsampling of 250 cells from each CAR variant with larger cell numbers and 500 cells from each negative control sample to balance the dataset. We tested how likely the subsampling can result in aberrant clustering by simulating 50 clustering procedures and measuring the similarity of the top differentially expressed genes using the ARI in a pairwise fashion. **c)** The number of clusters identified by the procedure throughout the 50 seeds can vary from 12 to 14. **D)** The distribution of ARIs is centered around 0.69 (lower and higher quartile 0.63 and 0.75 respectively, maxima 0.89 and minima 0.43). n=225 independent comparisons.

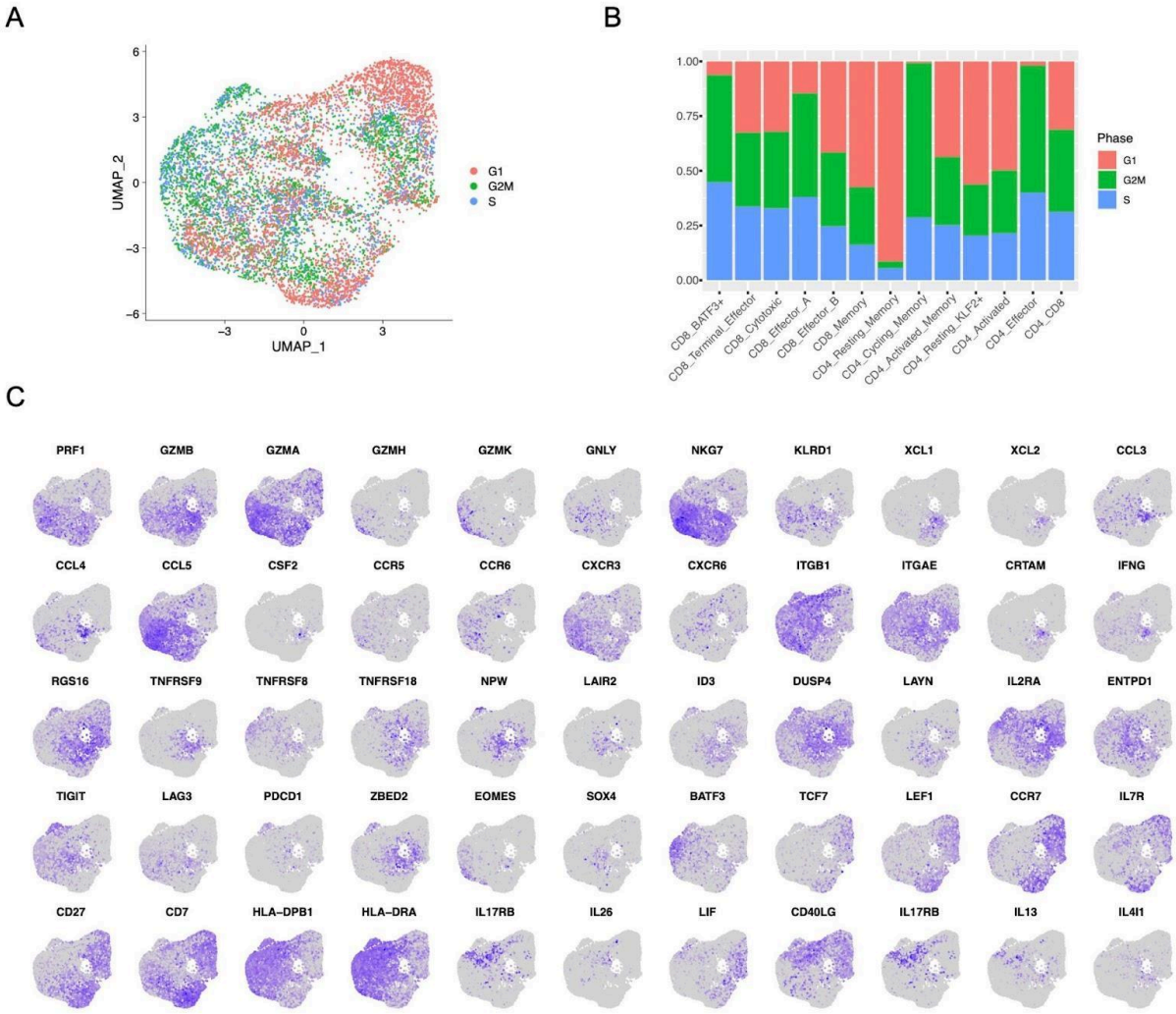

Supplementary Figure 5: Single cell sequencing analysis of pooled library CAR T cells following tumor cell co-culture

A) Cell cycle phase prediction overlaid on its UMAP embedding. **B)** Cell cycle phase enrichment across the different clusters annotated in Figure 3. **C)** Feature plots showing the distribution of expression of a selection of genes across the UMAP embedding.

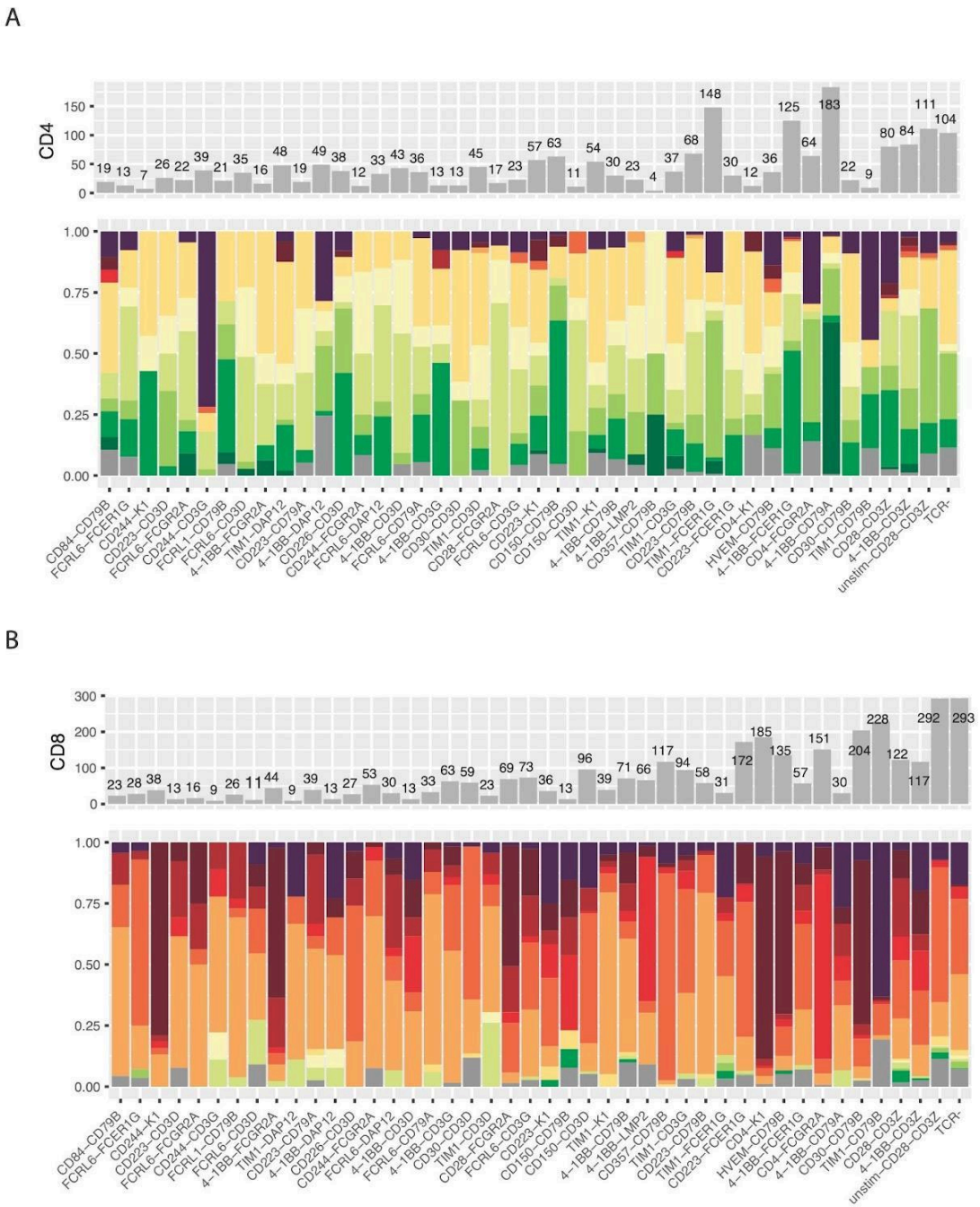

Supplementary Figure 6: CD4 and CD8 cluster enrichment

Cluster enrichment of CD4 (**A**) or CD8 cells (**B**) observed for the top 40 most represented CAR variants, benchmark controls (CD28-CD3Z and 4-1BB-CD3Z) and negative controls (hT and unstim-CD28-CD3Z). The top panel displays the total counts of CD4 or CD8 cells for each sample group and the bottom panel the fraction of cells found in each of the clusters in Figure 3.

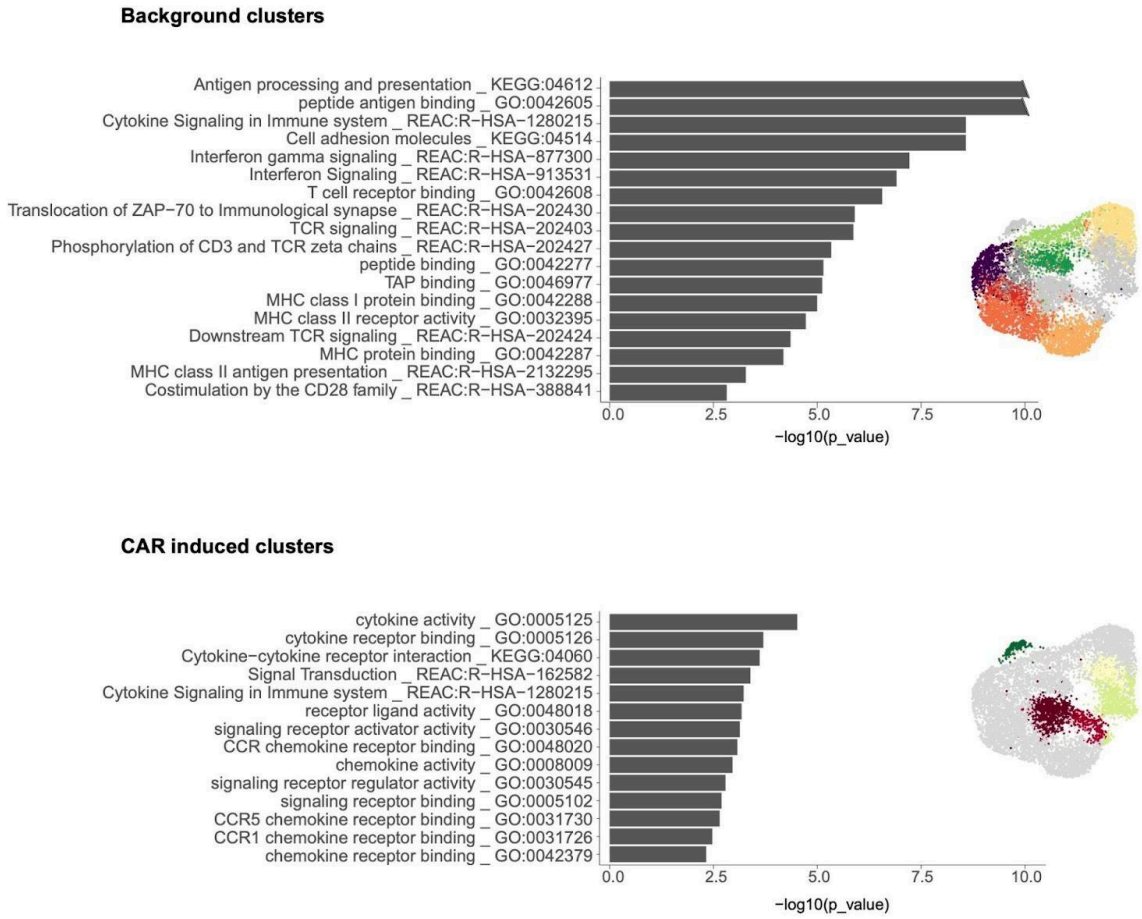

Supplementary Figure 7: Pathway enrichment analysis of CICs and nonCICs

Pathway enrichment analysis on the differentially expressed genes between CAR induced clusters and background clusters defined in Figure 3. For each group, a selection of the most immunologically relevant gene sets is shown. On the right UMAP plots are shown highlighting the clusters that integrate each group. Statistical significance was determined using the adjusted p-values generated using g:SCS method from g:Profiler for multiple comparison testing.

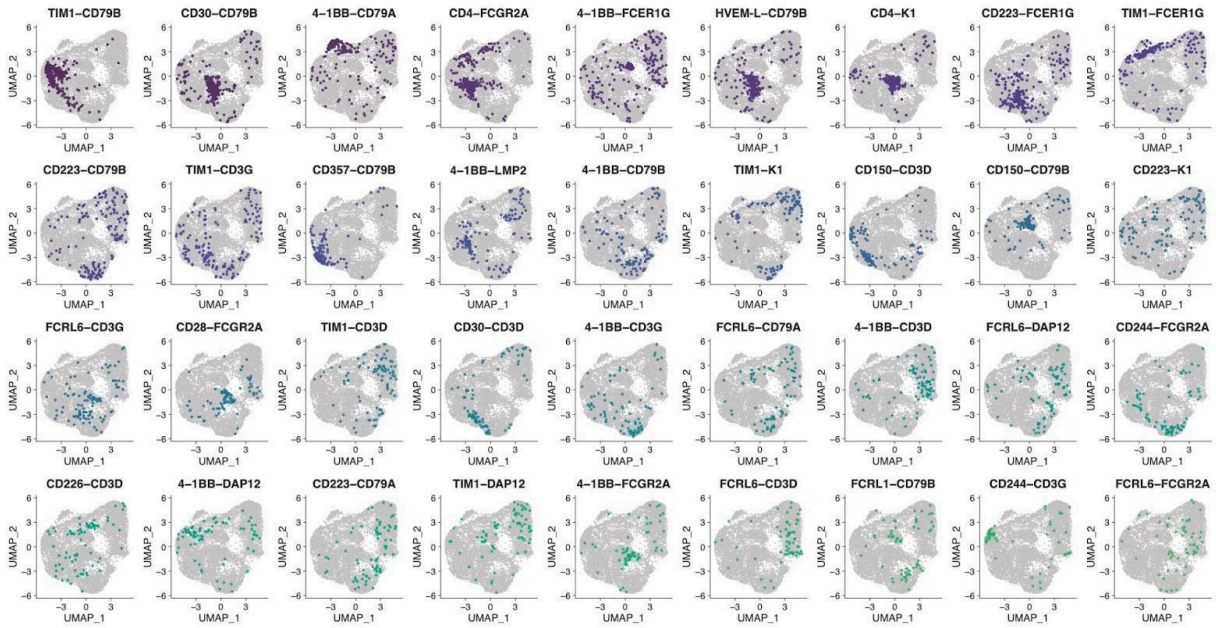

Supplementary Figure 8: After demultiplexing CAR variants map on to different regions of the T cell phenotypic landscape

Distribution of cells for the top 36 CAR variants within the UMAP embedding of Figure 3.

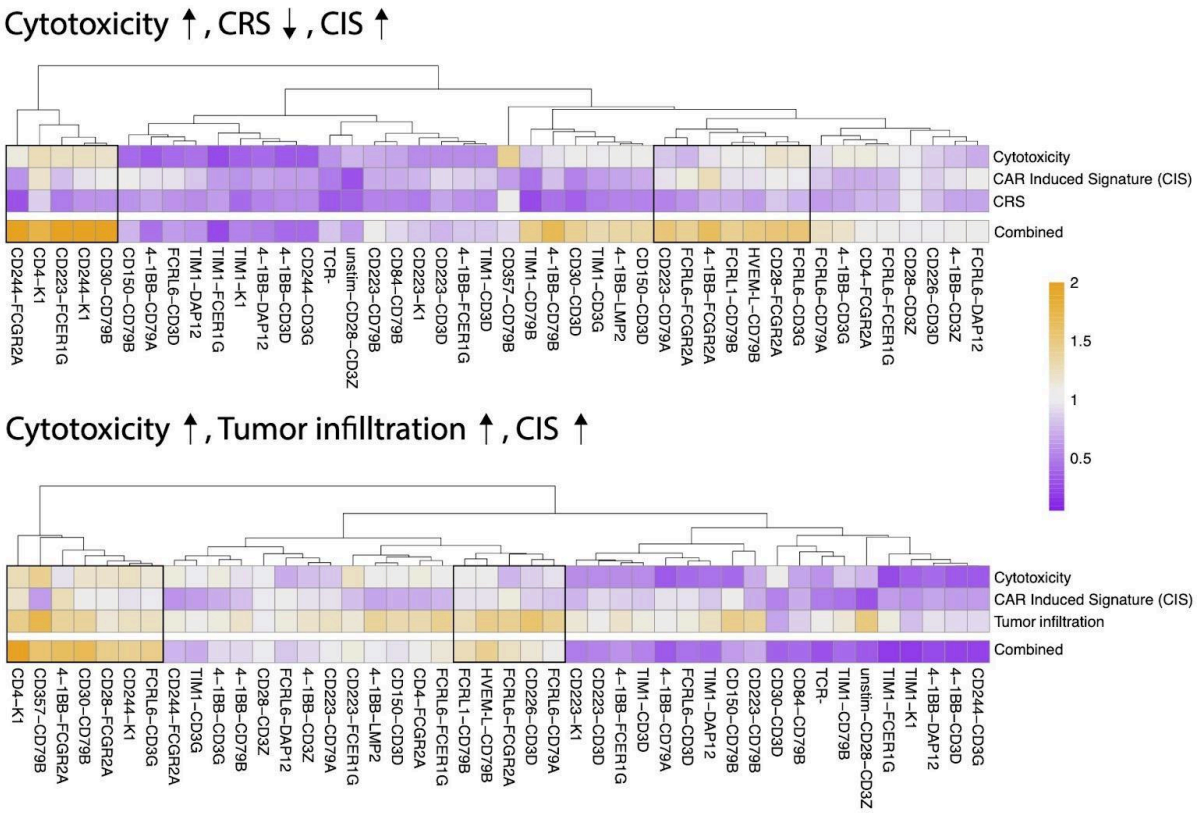

Supplementary Figure 9: Phenotypic characterization of CAR variants based on the combination of gene set expression scoring

Heatmap showing the difference in gene set scores between the 40 most represented CAR variants, stimulated and unstimulated 28z CAR, BBz CAR and TCR- T cells, for gene sets of choice. The mean score per variant is given as a fold change measurement when compared to 28z WT CAR. The mean score fold change of the different gene sets is later on combined by multiplying or dividing the fold change values according to whether the gene sets are aimed to be enriched or depleted.

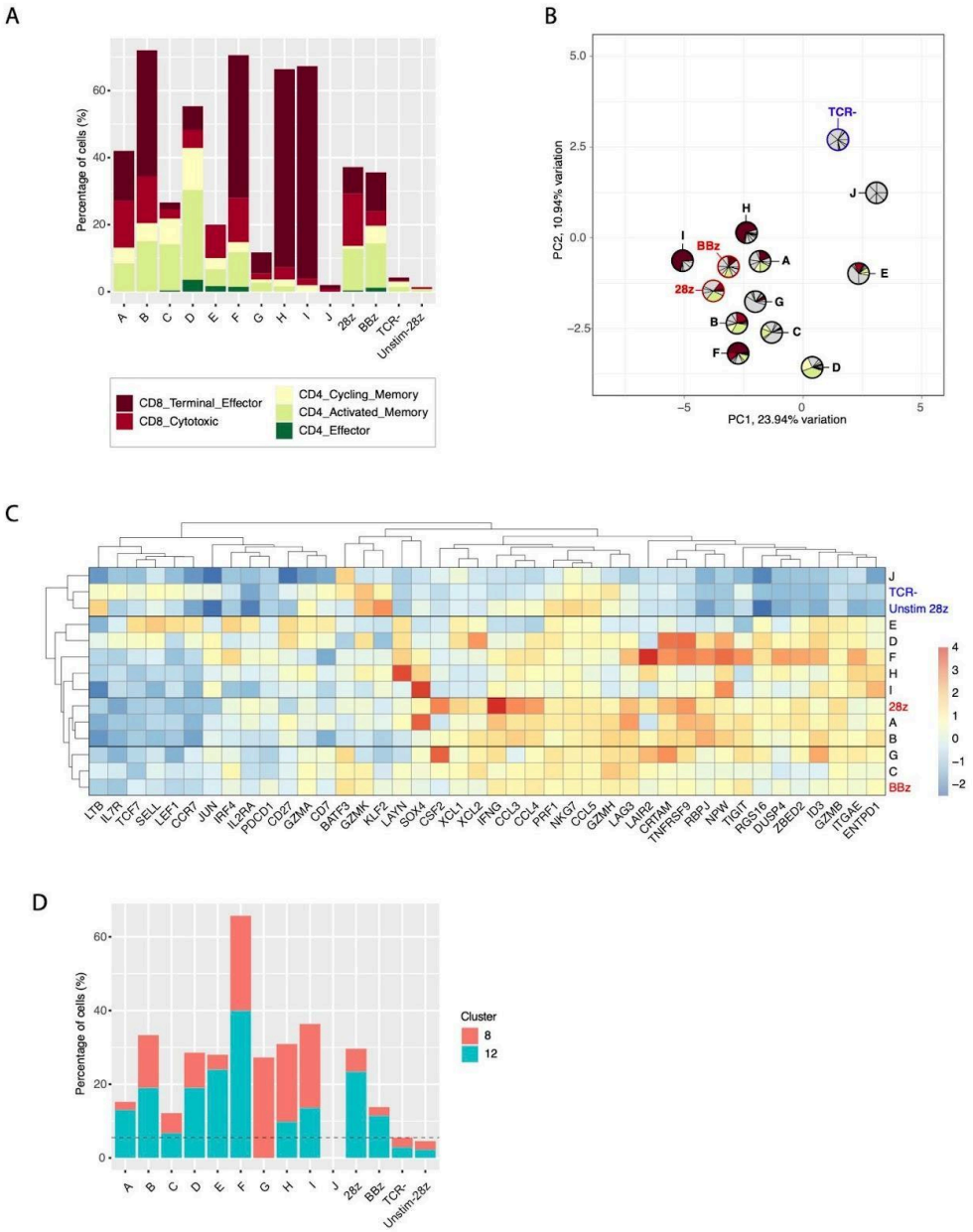

Supplementary Figure 10: Transcriptome guided selection of functional CARs

A) Bar plot depicting the percentage of cells per CAR variant that belong to the 5 different CICs described in Figure 3. **B)** Principal component analysis (PCA) of pseudo-bulked scRNA-seq data of a selection of CAR candidates, 28z and BBz CARs coloured in red and TCR- T cells coloured in blue. To avoid batch effect variation only data from Donor 3 is used. Overlayed over each data point, pie charts represent the enrichment of cells in CICs from Fig. 3f. **C)** Expression levels of a set of 42 T cell marker genes across CD8+ pseudo-bulked scRNA-seq samples of a selection of CAR variants, 28z and BBz benchmark CAR T cells, TCR- T cells and unstimulated 28z CAR T cells. **D)** Enrichment of cells in tumor reactive TIL associated clusters 8 and 12, identified in figure 5, across a selection of CAR variants.

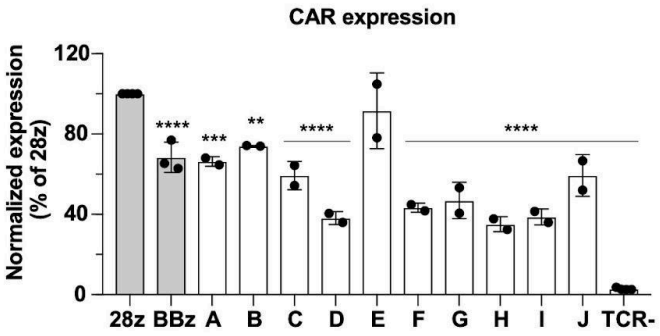

Supplementary Figure 11: The CAR signaling variants are expressed at different levels on the surface of primary T cells than 28z CAR

Bar plot showing CAR surface expression levels from genome-edited primary T cells, as assessed by flow cytometry and detection of the Strep tag II. To assess significant differences between each variant and 28z, one-way ANOVA and Dunnett's multiple comparisons test was used with the following significance indicators: * p-value < 0.05, ** p-value < 0.01, *** p-value < 0.001 and **** p-value < 0.0001. TCR- refers to T cells without a TCR and error bars represent the S.D. (n=2 independent experimental replicates for variants A-J and n=4 for control groups).

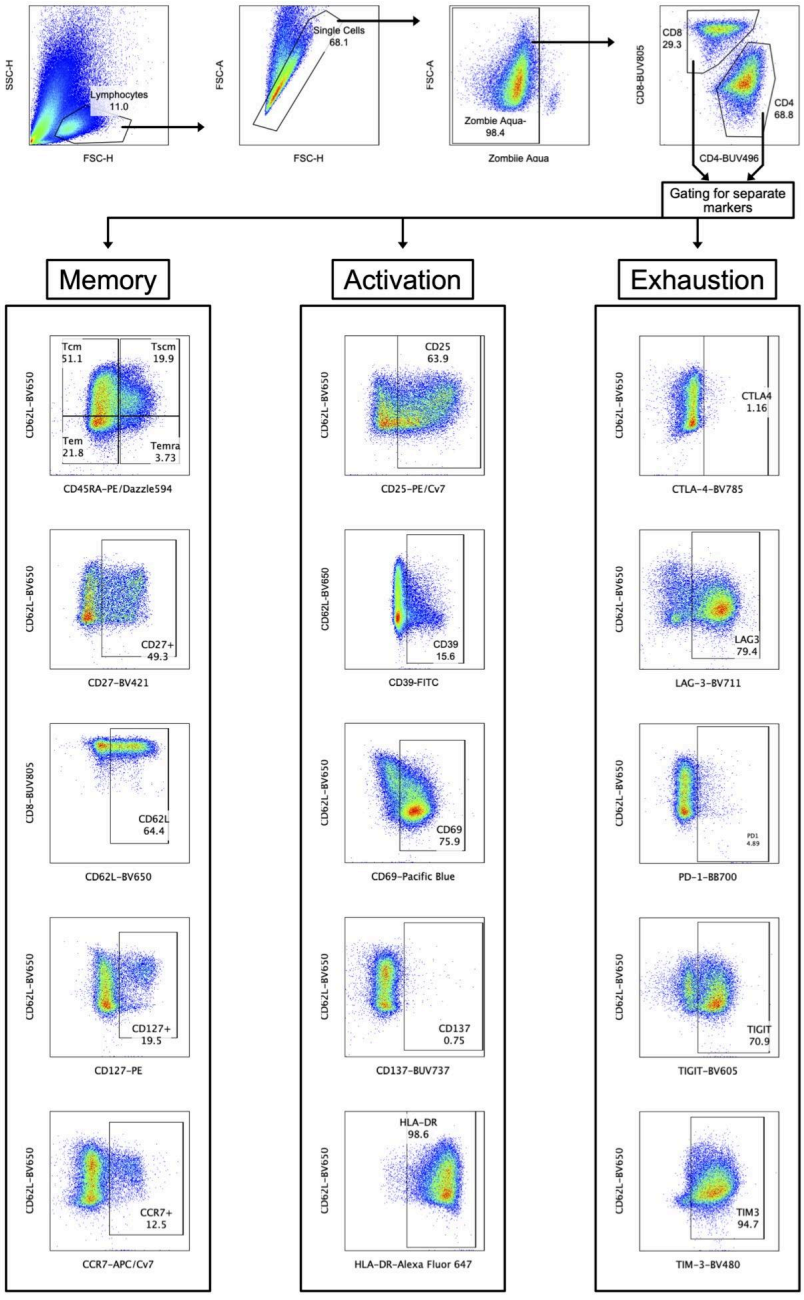

Supplementary Figure 12: Flow cytometry gating strategy used to determine the expression of a panel of T cell surface markers

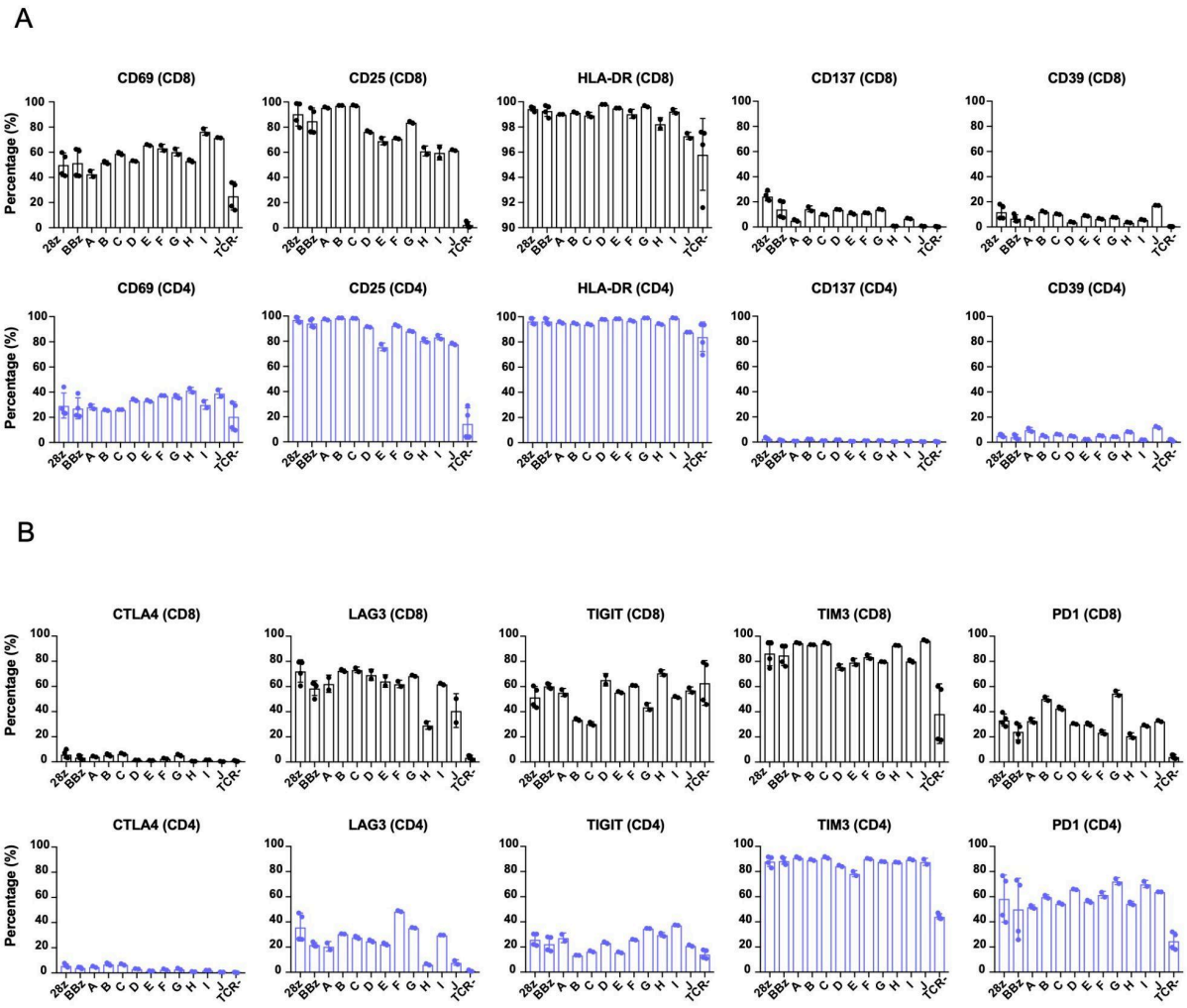

Supplementary Figure 13:Comparison of surface marker expression across CAR variants following tumor co-culture

Percentage of T cells expressing individual T cell surface markers across different CAR variants, 28z and BBz benchmark CARs and TCR-negative T cells following a 4 day co-culture with SKBR3 cells (4:1 E:T ratio). A panel of different T cell activation markers (**A)** and T cell exhaustion markers (**B**) was chosen and measured by flow cytometry. In all panels, TCR- refers to T cells without a TCR and error bars represent the S.D. (n=2 independent technical replicates for variants A-J and n=2 technical replicates from 2 independent experiments for control groups).

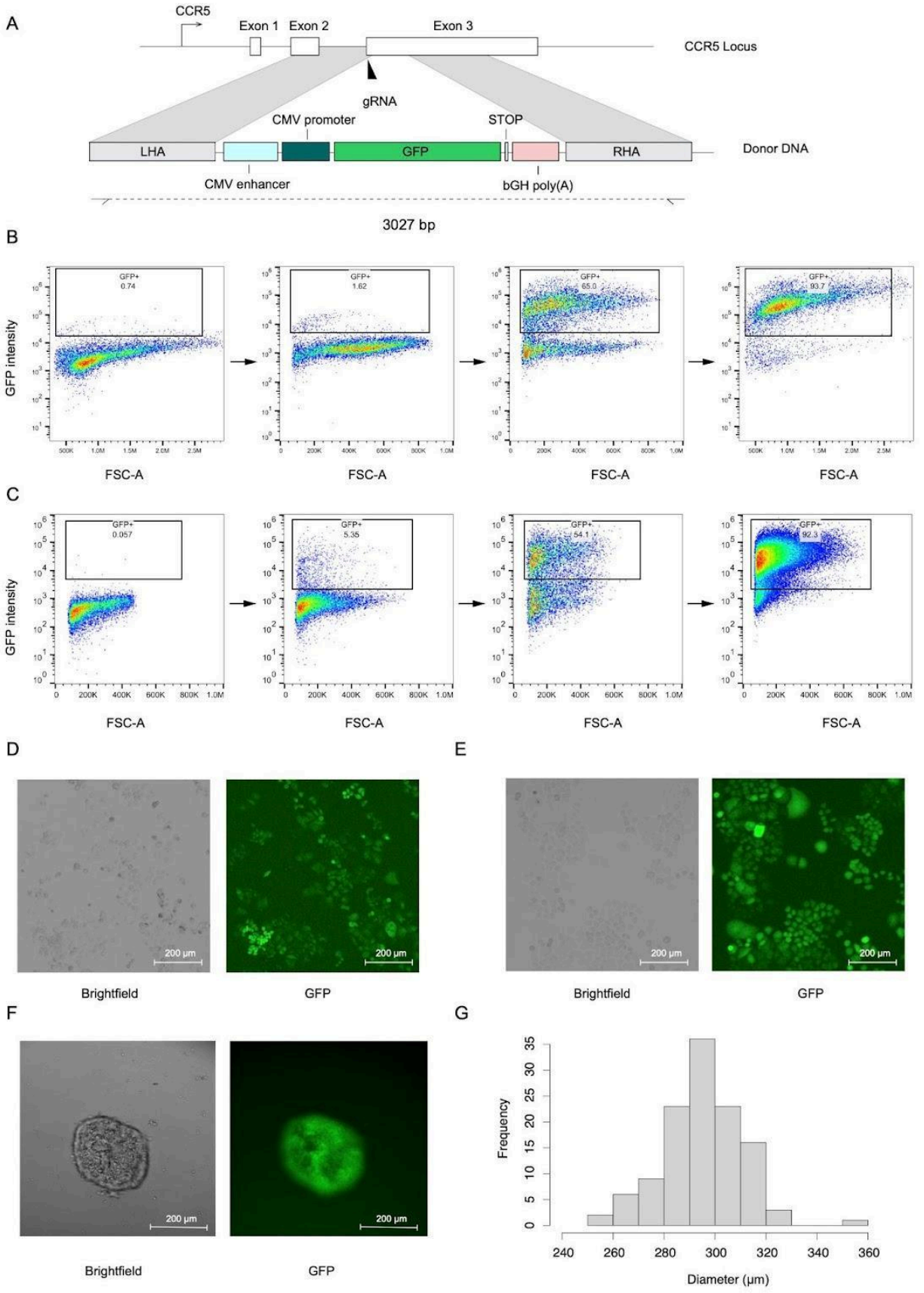
A
CCR5
Exon 1
Exon 2
Exon 3
CCR5 Locus
gRNA
CMV promoter
STOP
LHA
GFP
RHA
Donor DNA
CMV enhancer
bGH poly(A)
3027 bp
B
GFP intensity
GFP+ 0.74
GFP+ 1.62
GFP+ 65.0
GFP+ 93.7
FSC-A
C
GFP intensity
GFP+ 0.057
GFP+ 5.35
GFP+ 54.1
GFP+ 92.3
FSC-A
D
200 µm
Brightfield
GFP
E
200 µm
Brightfield
GFP
F
200 µm
Brightfield
GFP
G
Frequency
0
5
10
15
20
25
30
35
240
260
280
300
320
340
360
Diameter (µm)

Supplementary Figure 14: Genomic engineering of the cancer cell lines for imaging-based cytotoxicity assays

A) CRISPR-Cas9-based strategy for integrating a GFP expression cassette in the genome of the cell lines SKBR3 and MCF-7. A gene expression cassette was constructed harboring the two-part cytomegalovirus (CMV) promoter, the GFP ORF and a polyadenylation signal. This cassette was flanked by DNA regions homologous to the *CCR5* genomic locus and amplified by PCR to generate the repair template for HDR. A guide RNA targeting the beginning of the third exon of *CCR5* was used to generate Cas9 RNP and transfected in target cells alongside the repair template. **B) and C)** The transfected SKBR3 and MCF-7 cells respectively were sorted by FACS iteratively to select GFP-expressing cells and obtain a mostly pure (>90%) population. **D) and E)** Fluorescence microscopy confirmed the clear visibility of SKBR3 and MCF-7 cells respectively. **F)** Fluorescence image of MCF-7-GFP cells forming a spheroid structure. **G)** Frequency distribution histogram of the diameters in microns of 120 MCF-7 spheroids three days after seeding (the start of live imaging experiments).

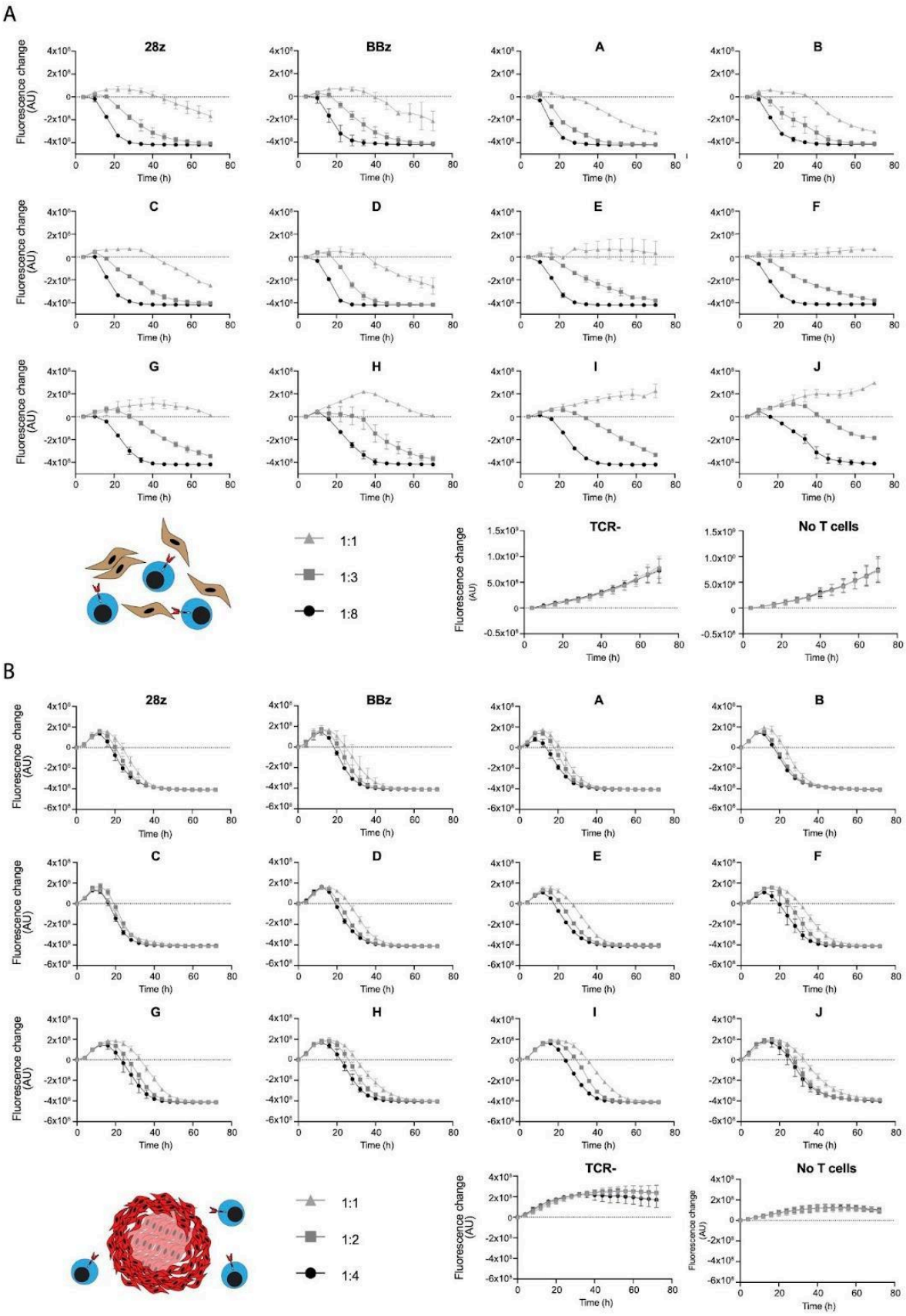
A
28z
BBz
A
B
C
D
E
F
G
H
I
J
Fluorescence change (AU)
Time (h)
1:1
1:3
1:8
TCR-
No T cells
B
1:1
1:2
1:4

Supplementary Figure 15: The CAR T cell-mediated cytotoxicity of target cells proceeds at different rates depending on the signaling domain combinations used

CAR T cell-mediated cytotoxicity of HER2+/GFP+ tumor cells quantified over time by fluorescence microscopy. The curves represent the difference in GFP intensity with regards to time point 0. CAR T cells were co-cultured at different E:T ratios with either SKBR3 adherent cells in a "sparse" 2D culture in **A** or with a single tumor spheroid of MCF-7 cells in **B**. Colors indicate different E:T ratios. In all panels, TCR- refers to T cells without a TCR and error bars represent the S.D. (n=2 independent technical replicates for variants A-J and n=2 technical replicates from 2 independent experiments for control groups).

Supplementary Table 1: crRNA sequences used in this study

Genomic target	crRNA sequence (5' to 3')
TRAC	CAGGGUUCUGGAUAUCUGU
CCR5	UGACAUCAAUUAUUAUACAU

Supplementary Table 2: Oligonucleotides used in this study

Name	Sequence (5' to 3')	Purpose
F1	gttacaggCACCTGCaacaGGTG	To amplify domains from pool A for cloning
R1	ggaactccCACCTGCcttgTGCTga	
F2	ttagcccaCACCTGCgggcAGCA	To amplify domains from pool B for cloning
R2	ccgagggcCACCTGCtcatGCGG	
F3	CGGGACTAGTGGCgtcGGTTCTGGATATCTGTGGGCTGCCAGAGTTATATTGCTGGGGTT	To amplify HDR repair template with tCTS for CRISPR-Cas9 genome editing.
R3	CACTTCCAGCACCgtcGGTTCTGGATATCTGTGGGCGAGACCACCAATCAGAGGAGTTT	
F4	GCTTGCTAGTAACAGTGGCCTTTAT	To amplify the recombined A and B domains within the CAR gene for sequencing
R4	TACAGGCCTTCCTGAGGGTTCTT	
F5	GGTCAGACAAGCTCCCGGAAAAGGA	To amplify the cytoplasmic region of the CAR gene in the *TRAC*locus for sequencing
R5	AGGTGTCCCTTCCCTGCTT	
F6	AATGATACGGCGACCACCGAGATCTACACTCTTTCCCTACACGACGCTC	scCARseq PCR1
R6	GTGACTGGAGTTCAGACGTGTGCTCTTCCGATCTCACACCCTCAGTTCGAAAAGAGTGC	
F7	AATGATACGGCGACCACCGAGATCT	scCARseq PCR2
i7-Read2	CAAGCAGAAGACGGCATACGAGAT(8N)GTGACTGGAGTTCAGACGTGTGCTCTTCCGATC	

Supplementary Table 3: Dilutions and catalog numbers of used antibodies

Target	Fluorochrome	Clone	Dilution	Source	Cat. Nr
Viability	Zombie Aqua	-	1/1000	Biolegend	423102
CD3	BUV395	UCHT1	1/500	BD Biosciences	563546
CD3	APC	UCHT1	1/200	BD Biosciences	300458
CD4	BUV496	SK3	1/500	BD Biosciences	612936
CD8	BUV805	SK1	1/500	BD Biosciences	612889
CD25	PE/Cy7	M-A251	1/50	BioLegend	356108
CD27	Brilliant Violet 421	M-T271	1/33	BioLegend	356418
CD39	FITC	A1	1/50	BioLegend	328206
CD45RA	PE/Dazzle 594	HI100	1/50	Biolegend	304146
CD62L	BV650	DREG-56	1/33	BioLegend	304832
CD69	Pacific Blue	FN50	1/50	BioLegend	310920
CD127	PE	A019D5	1/33	BioLegend	351304
CD137	BUV737	4B4-1	1/250	BD Biosciences	741861
CD152 (CTLA-4)	Brilliant Violet 785	BNI3	1/50	Biolegend	369624
CD197 (CCR7)	APC/Cyanine7	G043H7	1/50	BioLegend	353212
CD223 (LAG-3)	BV711	11C3C65	1/50	BioLegend	369320
CD279 (PD-1)	BB700	EH12.1	1/250	BD Biosciences	566460
CD366 (TIM-3)	BV480	7D3	1/250	BD Biosciences	746771
HLA-DR	Alexa Fluor 647	L243	1/50	BioLegend	307622
TIGIT	Brilliant Violet 605	A15153G	1/50	BioLegend	372712
StrepTag	Biotin	5A9F9	1/400	GenScript	A01737
SAv	BV421	-	1/200	BD Biosciences	405225
HER2	APC	24D2	1/200	BioLegend	324408

Chapter 3: Dissecting the role of CAR signaling architectures in T cell activation and persistence using pooled screens and single cell sequencing

This chapter is an author-produced adaptation of a research article "Dissecting the role of CAR signaling architectures in T cell activation and persistence using pooled screens and single cell sequencing", published as a preprint on bioRxiv (https://doi.org/10.1101/2024.02.26.582129).

Authors: Rocío Castellanos-Rueda, Kai-Ling K. Wang, Juliette L. Forster, Alice Driessen, Jessica A. Frank, María Rodríguez Martínez, Sai T. Reddy

Author's contribution: R.C.R. and S.T.R. designed the study; R.C.R., K.K.W., J.L.F. and J.A.F. performed experiments; R.C.R., K.K.W. and A.D. performed and interpreted bioinformatic analyses; M.R.M provided bioinformatics expertise; R.C.R. and S.T.R. discussed results and R.C.R. and S.T.R. wrote the manuscript with input and commentaries from all authors.

Abstract

Chimeric antigen receptor (CAR) T cells represent a promising approach for cancer treatment, yet challenges remain such as limited efficacy due to a lack of T cell persistence. Given its critical role in promoting and modulating T cell responses, it is crucial to understand how alterations in the CAR signaling architecture influence T cell function. Here, we designed a combinatorial CAR signaling domain library and performed repeated antigen stimulation assays, pooled screening and single-cell sequencing to investigate T-cell responses triggered by different CAR architectures. Parallel comparisons of CAR variants, at early, middle and late timepoints during chronic antigen stimulation systematically assessed the impact of modifying signaling domains on T cell activation and persistence. Our data reveal the predominant influence of membrane-proximal domains in driving T cell phenotype. Additionally, we highlight the critical role of CD40 costimulation in promoting potent and persistent T cell responses, followed by CTLA4, which induces a long-term cytotoxic phenotype. This work deepens the understanding of CAR T cell biology and may be used to guide the future engineering of CAR T cell therapies.

3.1 Introduction

Chimeric antigen receptor (CAR) T cells are an emerging therapeutic strategy for cancer treatment. CARs are synthetic receptors consisting of an extracellular antigen binding domain fused to intracellular signaling domains that trigger and modulate T cell responses upon activation. The infusion of genetically engineered CAR T cells in patients guides the recognition of a target tumor antigen and promotes tumor clearance while inducing long-lasting memory immunity (*1*, *2*). To date, six CAR T cell therapies have been approved by the FDA for the treatment of hematological malignancies, and there are over a thousand ongoing clinical trials for a broad range of cancer types (*3*). Despite the potential of these therapies, they still face several challenges, including associated toxicities, poor tumor infiltration, exhaustion and lack of T cell persistence, which have limited their clinical success in many indications (*4*).

In recent years, the search for solutions has motivated the engineering of different CAR designs that enable novel recognition and activation properties (*5*). In particular, the essential role of intracellular signaling elements in orchestrating cellular responses and the large diversity of existing immune signaling proteins have been harnessed to expand the repertoire of CAR signaling architectures. The architecture can be defined as the choice, number and specific arrangement (membrane proximal or distal) of signaling elements within the CAR construct. Moving beyond clinically approved CARs, which combine the signaling domains of the CD3ζ chain of the T cell receptor (TCR)/CD3 co-receptor complex and costimulatory receptors CD28 or 4-1BB, several studies have investigated the impact of making precise changes in the choice, number and order of signaling domains (*6–10*) or motifs (*11*, *12*). Despite technical limitations of functional assays, which restrict the number of constructs that can be individually produced and tested, pre-clinical studies have identified new CAR designs with distinct antitumor properties. For instance, combining CD79A and CD40 signaling domains resulted in CARs exhibiting improved proliferation and superior in vivo antitumor activity compared to clinically approved designs (*6*). Furthermore, incorporation of CTLA4 cytoplasmic tails into a CD28-CD3ζ CAR increased its cytotoxic potential while delaying T cell activation and proinflammatory cytokine production, ultimately enhancing CAR-T efficacy in a murine model of leukemia (*7*).

To further explore the vast CAR signaling domain combination space, several recent studies have designed high-throughput screening approaches to engineer CARs with distinct or enhanced functional properties. These strategies combine the use of signaling domain libraries, pooled screening, deep or single-cell sequencing and computational tools to address challenges in CAR T cell engineering. The choice of the optimal methodology, however, poses a non-trivial task. Employing different library designs and T cell platforms (primary cells or cell lines), Goodman et al. and Gordon et al. conducted pooled

phenotypic screens through fluorescence-activated cell sorting (FACS) and deep sequencing to assess the enrichment of functional variants (*13*, *14*). Daniels et al. performed arrayed screening on a subset of a CAR library, recording flow cytometry-based phenotypic information, which was followed by machine learning to predict the cytotoxicity and memory potential of a larger library of signaling architectures (*15*). Notably, our group has performed pooled functional screening of a large CAR signaling domain library and used single-cell RNA sequencing (scRNAseq) for high-throughput assessment of T cell transcriptional phenotypes (*16*).

Currently, there is still limited understanding of how the architecture of a CAR translates to the functional or transcriptional phenotype of T cells. In addition, the dynamics of how such cellular phenotypes evolve over time requires further investigation, especially in a clinically-relevant context such as chronic antigen stimulation, which is known to drive T cell exhaustion, a main cause of therapy failure (*17*, *18*). Here, we systematically study the role of CAR signaling architectures on T cell activation and persistence by combining pooled functional screening of a combinatorial signaling domain library with scRNAseq. This enables the characterization of CAR T cell responses in a high-throughput manner, while mimicking the early and late stages of chronic tumor stimulation through an in vitro model of CAR T cell dysfunction. Capturing different single-cell transcriptomic snapshots across time, our data reveal intriguing patterns, such as the prominent influence of domains proximal to the cell membrane in modulating T cell phenotype and the pivotal role of CD40 costimulation in driving a potent yet persistent T cell response. Thus our study synergizes signaling domain engineering, pooled functional screening and scRNAseq to enhance the mechanistic understanding of CAR T cell signaling.

3.2 Results

3.2.1 Design of a combinatorial signaling domain library of CAR variants

In order to systematically investigate the impact of modifying the intracellular architecture of CARs on T cell function, we generated a combinatorial signaling domain library based on 1st, 2nd or 3rd generation CAR designs; a classification based on the number of costimulatory domains (Fig. 1a). All CAR designs possessed the same extracellular domain consisting of a single-chain variable fragment (scFv) with binding specificity for the human epidermal growth factor receptor 2 (HER2), which is a tumor-associated antigen present on several solid cancers (*19*). The CD3ζ activation domain was combined with costimulatory signaling domains of five different immune receptors, which cover different receptor

families that are known to trigger distinct signaling pathways for modulating T cell activity. CD28 and 4-1BB (tumor necrosis factor receptor superfamily 9; TNFRSF9) were selected as they are the most commonly used costimulatory domains and are present in clinically approved CAR T cell therapies. In addition, we included the signaling domains of CD40 (TNFRSF5) and the cytokine receptor chain IL15RA, which in preclinical studies have demonstrated the ability to enhance the anti-tumor properties of CARs (*6*, *20*, *21*). Lastly, CTLA4 was chosen as an example of an inhibitory receptor on T cells that still may enhance anti-tumor responses when incorporated into CARs (*7*). As a negative control, a non-signaling CAR (NS-CAR) was designed that lacks any intracellular signaling domains and is therefore unable to initiate CAR-dependent T cell activation. This results in a library with 32 different designs: one 1st generation, five 2nd generation, 25 3rd generation CARs and the NS-CAR as negative control (Fig. 1a).

Next, we used CRISPR-Cas9 and homology-directed repair (HDR) to genomically integrate the CAR library into the TCR alpha chain (*TRAC*) locus of primary human T cells (Fig. 1b). Precise integration of the CAR gene into the *TRAC* locus ensures that every variant is expressed under the same transcriptional regulation while simultaneously knocking out the TCR (*22*), an appropriate setting to compare library candidates in a pooled manner. Following genome editing, engineered T cells were selected based on positive surface expression of a CAR (StrepTag) and negative expression of the TCR (CD3ε co-receptor) using FACS (Fig. 1c). To verify the quality of the engineered CAR-T cell product and validity of the library controls, we first examined the CAR surface expression and cytotoxic potential of T cells engineered with the CD28 2nd generation CAR (28z) or the negative control NS-CAR. Both CAR-T cell products displayed similar levels of CAR surface expression after enrichment (Sup. Fig 1a). Subsequently, T cell killing potential was measured by monitoring the growth curves of SKBR3 cells, a HER2-positive breast cancer cell line, following a 48h co-culture. As expected, 28z CAR T cells were able to efficiently eliminate all tumor cells, while NS-CAR T cells were unresponsive (Supp. Fig. 1b).

We next proceeded to produce a pooled library of CAR T cells including all 32 CAR variants. Surface expression of the CAR library in sorted T cells appeared to be more heterogeneous compared to the 28z CAR (Fig. 1d), indicating CAR variant-specific differences in cell surface expression. This is in particular expected for CARs containing a CTLA4 domain, where the presence of an endocytosis motif has been previously described to drive receptor recycling and degradation (*23*). Targeted deep sequencing of the CAR library confirmed that all variants were expressed and could be enriched by FACS. Except for a few variants that showed a lower enrichment, most of which indeed contained the signaling domain of

CTLA4, the library variants were distributed at similar levels (Fig. 1e; CAR nomenclature is described in Supp. Table 1).

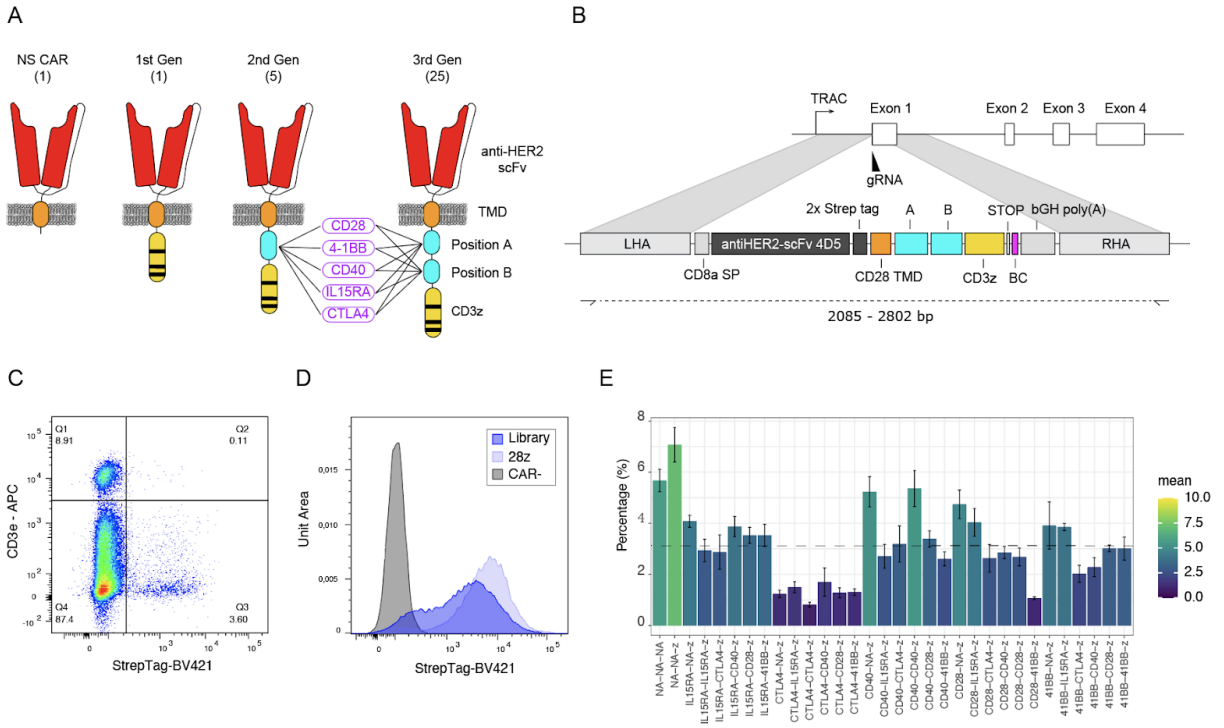

Figure 1: Design and production of a combinatorial signaling domain library of CAR variants

A) Schematic representation of the CAR library design. The library consists of 2nd and 3rd generation CAR designs that incorporate five selected costimulatory domains, which are shuffled in all possible combinations. The library also includes a 1st generation CAR and a non-signaling (NS) CAR that lacks signaling domains. When referring to domain positioning within the CAR, positions A and B denote domains located proximal or distal to the cell membrane, respectively. All variants contain an anti-HER2 single-chain variable fragment (scFv) and a CD28 transmembrane domain (TMD). **B**) Schematic shows the targeted genomic integration of the CAR library into the *TRAC* locus of T cells. Following a CRISPR-Cas9 guide RNA (gRNA)-directed double-stranded break at the start of exon 1 of the *TRAC* locus, a dsDNA repair template possessing left and right homology arms (LHA, RHA) and a full CAR gene (signal peptide (SP), scFv, TMD, signaling domains and poly-A signal) is used to induce homology-directed repair (HDR) and CAR gene insertion. **C**) Flow cytometry plot illustrating the T cell product obtained six days after the engineering of the CAR library into primary human T cells. Positive surface expression of a CAR (StrepTag) and negative expression of the TCR (CD3ε co-receptor) identifies correctly engineered CAR T cells. **D**) Flow cytometry histograms display CAR surface expression profiles of 28z and the pooled library of CAR T cells after enrichment compared to unedited T cells. **E**) Library diversity of the CAR T cell final product following enrichment and a 12-day expansion, assessed by deep sequencing. The dashed line represents the theoretically balanced distribution of the library. Barplot shows the mean of five biological replicates (CAR T cell products engineered from different healthy donors) and error bars represent SEM.

3.2.2 Assessment of library persistence following repeated antigen stimulation

Next, we characterized CAR signaling domain variants using in vitro repeated antigen stimulation (RAS), an experimental workflow that aims to mimic chronic antigen stimulation from tumor cells (*24*, *25*), which is associated with CAR T cell exhaustion during clinical treatment. The pooled library of CAR T cells was repeatedly challenged with HER2-expressing SKBR3 cells for 12 days. Every third day, a sample of the co-cultured cells was restimulated with fresh SKBR3 cells and their effector potential was assessed by flow cytometry based on surface expression of the degranulation marker CD107a and intracellular expression of pro-inflammatory cytokines IFNγ and TNFα (Fig. 2a and Supp. Fig 2). At an early stage of the RAS assay (day 3), the CAR T cell library showed robust effector potential as evidenced by high degranulation and cytokine production (Fig. 2b). A consistent and gradual decline of this effector phenotype was observed towards later time points, indicating that the RAS assay could effectively recapitulate the progressive exhaustion of CAR T cells. Throughout the assay, CD8 T cells seemed to lose effector potency faster than CD4 T cells. In line with this observation, the fraction of CD8 T cells consistently dropped in time in favor of CD4 T cells, which seemed to have a longer lifespan in the context of an in vitro RAS co-culture (Fig. 2c).

Based on the RAS functional characterization, we observed that the library of CAR T cells reached a pre-dysfunctional state by day 9. The anti-tumor potential at this stage was evidently reduced; however, T cells were still able to control tumor cell growth. To assess the persistence of the different CARs, we aimed to resolve the library diversity following a FACS-based selection of cells that remained positive for effector markers (CD107a or IFNγ) by day 9 of the RAS assay (Fig. 2d). Targeted deep sequencing of the CAR transgenes was performed and enrichment scores were computed using post-enrichment library frequencies normalized to baseline (library frequencies on day 9 before selection) for the CD8 and CD4 T cell populations. As expected, the NS-CAR was consistently depleted for every marker (Fig. 2e). Notably, the CD40 signaling domain in position A (proximal to the cell membrane) was a key driver of T cell persistence, resulting in high enrichment scores for all groups (Fig. 2e and Supp. Fig 3). However, CD40 in position B (distal from the cell membrane) showed lower enrichment scores, but still promoted a proinflammatory phenotype in CD8 cells. In addition, CTLA4 in position B was enriched in CD107a+ cells and thus appears to drive a more persistent cytotoxic phenotype. CD28 and 4-1BB signaling domains induced a moderate or reduced persistence.

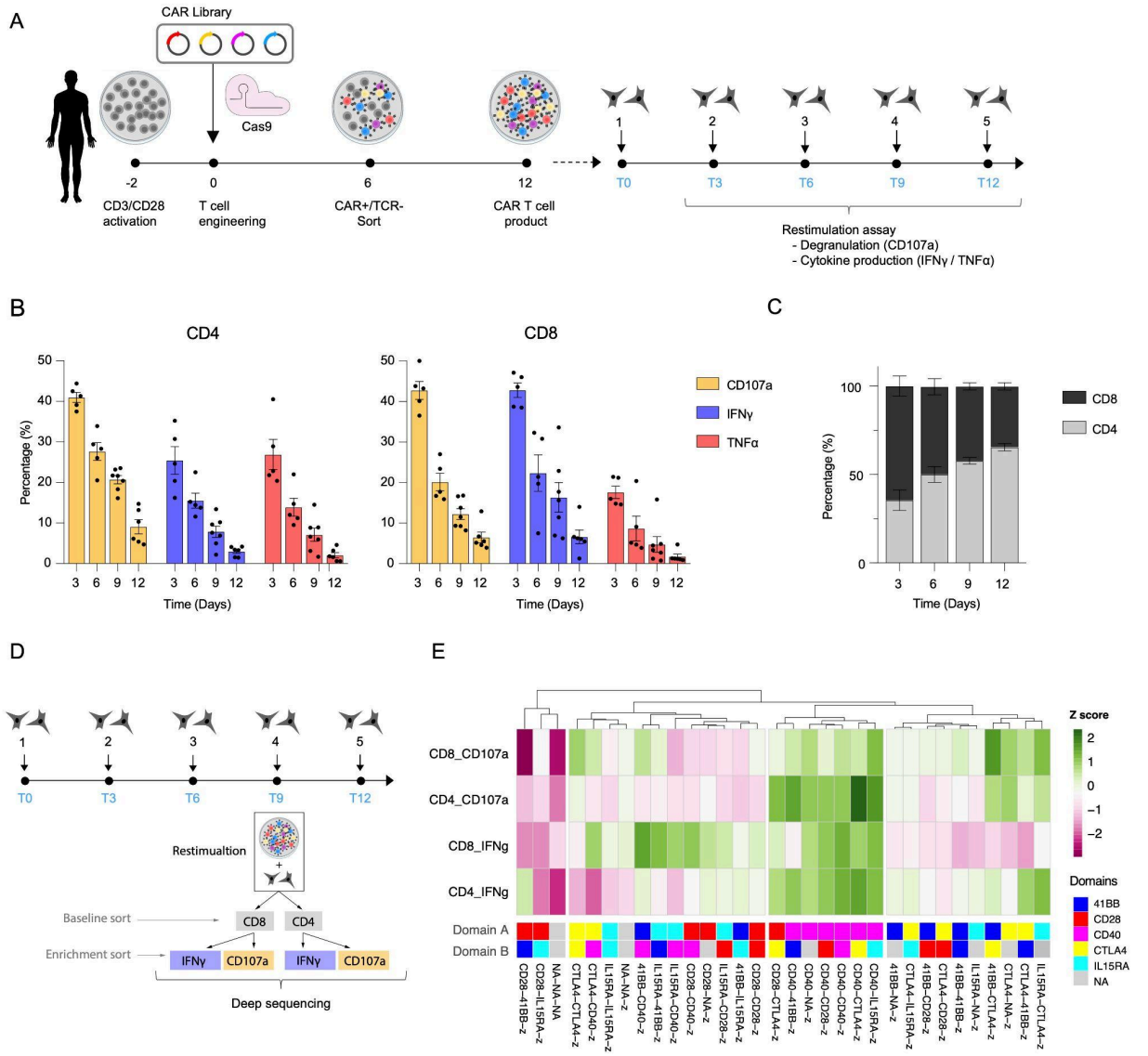

Figure 2: Assessment of T cell dysfunction using a repeated tumor rechallenge assay

A) Schematic representing the CAR library T cell production protocol followed by a repeated antigen stimulation (RAS) assay. 12 days after T cell engineering, a purified population of library CAR T cells was co-cultured with HER2+ SKBR3 target tumor cells at a 1:1 effector to target (E:T) ratio. Every three days, the co-culture was reset and a fraction of the cultured cells was used to assess the T cell anti-tumor potential through the RAS assay. **B**) Percentage of CD4 and CD8 cells presenting surface expression of CD107a or intracellular production of IFNγ and TNFα at different stages of the RAS assay. **C**) Percentage of CD4 and CD8 cells observed at different stages of the RAS assay. (**B** and **C**: n=7, technical replicates including 4 different donors. Error bars represent SEM). **D**) Schematic describing the sorting strategy used to assess the enrichment of the CAR library in degranulating (CD107a) and proinflammatory (IFNγ) T cells at a pre-exhausted stage of the RAS assay. **E**) Hierarchical clustering of the CAR library according to the enrichment or depletion of variants following a CD107a or IFNγ positive selection after 9 days of RAS assay. Variants are clustered according to Z-scores, which are calculated based on the log2 fold change in the relative library frequencies before and after enrichment for effector markers shown in panel (D). CD8 and CD4 T cell compartments were analyzed separately (n=3, independent biological replicates). Panels A and D were partially created with BioRender.

3.2.3 Single-cell transcriptional profiling resolves CAR-induced phenotypes

We next sought to further resolve the CAR-induced T cell phenotypes of the library across RAS using the multidimensional readout of scRNAseq. CAR T cell library cells were produced from two healthy donors and transcriptomic data was generated at early, middle and late stages of the RAS assay (days 0, 6 and 12). At each of these time points, CAR T cells were stimulated with HER2-expressing SKBR3 cells for 6h and then sequenced (Fig. 3a). In addition to the scRNAseq data, we performed single-cell cellular indexing of transcriptomes and epitopes (scCITEseq), to detect a panel of T cell surface marker proteins. Finally, we also performed scCARseq using an adapted protocol from our previous work (*16*), which enables de-multiplexing of the pooled CAR library by identifying the CAR variant of each cell. (Supp. Fig. 4).

Single-cell sequencing and data processing resulted in a total of 62,934 annotated CAR T cells across the three different time points, with full coverage of the CAR library across every time point and donor. An additional random subsampling of abundant variants was performed to correct for arbitrary clonal expansion, resulting in 58,949 cells, which were used for downstream phenotypic analysis. The lack of correlation between the expression of TCR variable genes across CAR variants, time points or donors validated the presence of sufficient clonal diversity in our library (Supp. Fig. 5). Dimensionality reduction by uniform manifold approximation and projection (UMAP) and unsupervised cell clustering separated cells into 16 different clusters (Fig. 3b). Annotation of the clusters was based on CD4 and CD8 expression, cell cycle phase prediction and differential gene and surface expression of key T cell marker genes (Fig. 3c and Supp. Fig. 6); both CD4 and CD8 T cell subsets presented a resting memory cluster characterized by the expression of TCF7, CCR7, LEF1 and SELL genes and protein surface expression of CD45RA and CD62L. The CD8 memory cluster then progressively transitioned into activated and effector phenotypes characterized by the increased expression of activated (TNFRSF9, TBX21, ZBED2), cytotoxic (GZMB, PRF1, FASLG) and proinflammatory (CRTAM, IFNG, TNF, CSF2, XCL1, XCL2) genes and eventually into a late cytotoxic phenotype characterized by the expression of late effector differentiation genes such as HOPX, ENTPD1, LAG3, HAVCR3 and GNLY. Cytotoxicity was also evidenced by the increased surface detection of HER2 on CAR T cells as a result of trogocytosis, a process by which there is a unidirectional transfer of plasma membrane and associated surface proteins from target cells to effector lymphocytes (*26*) (Supp. Fig. 6c). Lastly, a CD8 cluster was observed that presented a CAR-independent, bystander T cell signature (GZMK, GZMH and several KLR genes), which could be attributed to the effect of the cytokine storms and the cell killing environment on unstimulated T cells. Likewise, the CD4 memory cluster also transitioned into activated and more

differentiated phenotypes evidenced by the expression of activation genes such as CD40LG, IL2RA, ICOS, TNFSF14, TNFSF and IL17RB and a broad range of cytokines. This activated phenotype later transitioned into a rather dysfunctional phenotype and a Treg-like cluster characterized by the expression of FOXP3 and CTLA4. Lastly, a mixed CD4 and CD8 cluster, high in mitochondrial gene expression, was annotated as a terminal phenotype.

The progression of T cell phenotypes from a memory and early activation state, through a potent effector phenotype, to a late, less functional state correlated with the scCITEseq data for surface expression of early, middle and late T cell activation markers (Supp. Fig. 6b), as well as the time points at which the samples were collected (Fig. 3d and Supp. Fig. 7a). As previously observed, the CD8 compartment was drastically reduced through RAS progression in favor of a growing ratio of dysfunctional CD4 CAR T cells. The absence of CD8 cells presenting a terminally exhausted phenotype and the drop in the overall number of T cells in late co-cultures suggest the death of CD8 cells following their terminal effector differentiation.

Having resolved the recorded T cell phenotypes, scCARseq enabled us to de-multiplex the CAR library identity and investigate how different CAR signaling architectures can drive distinct T cell responses upon both initial and repeated antigen stimulation. First, we examined the T cell phenotypes of the NS-CAR through time (Fig. 3e). As expected, the lack of CAR signaling domains resulted in non-activated T cells that remained in a resting memory phenotype at early and even late time points, with only a small fraction of cells presenting a bystander T cell activation phenotype. Cluster enrichment of CD4 and CD8 cells across time points for the rest of the library variants indicated that every other CAR was able to trigger T cell activation, as evidenced by the lack of cells presenting a resting memory phenotype (Supp. Fig. 7b).

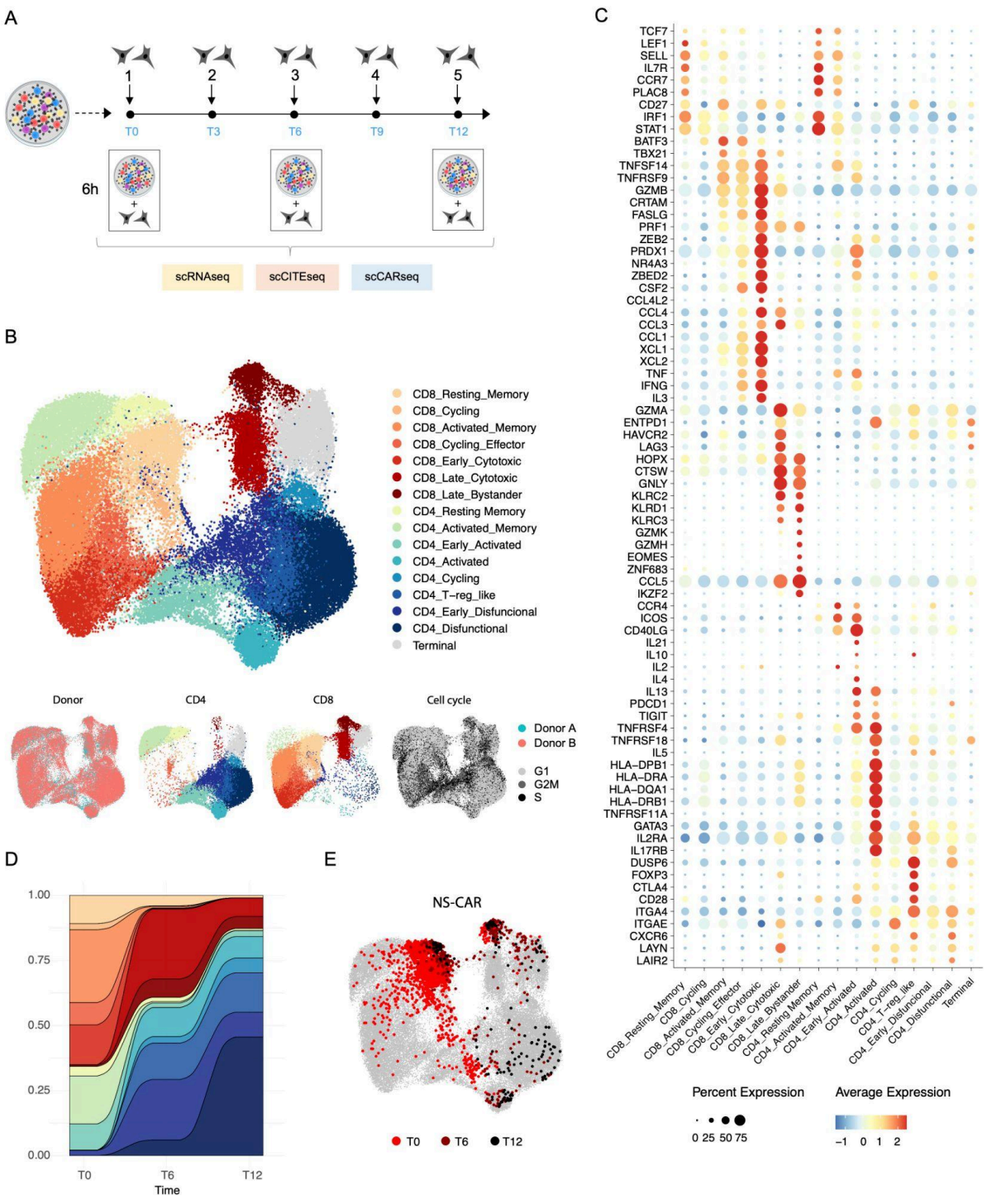

Figure 3: CAR-induced transcriptional phenotypes at single-cell resolution

A) Schematic describing the generation of single-cell data. The pooled library of CAR T cells from early, middle and late time points in the repeated antigen stimulation assay (RAS) was stimulated for 6h in the presence of SKBR3 target tumor cells and then processed using scRNAseq, scCARseq and scCITEseq. **B**) UMAP embedding and unsupervised cell clustering of the scRNAseq data generated as described in (**A**). 58,949 cells from 2 healthy donors and three time points are shown. At the bottom, UMAP embeddings are colored based on Donor, CD4 or CD8 annotation and cell cycle phase. **C**) Dot plot shows the expression of a selection of differentially expressed T cell marker genes that are used to annotate the clusters described in (**B**). **D**) Change in

cluster representation across time points. **E**) Distribution of cells annotated to display a non-signaling CAR (NS CAR) within the UMAP embedding of (**B**). Panel (**A**) was partially created with BioRender.

3.2.4 Role of signaling domain combinations in early activation of CAR T cells

To understand how signaling domain combinations shape the early activation of T cells, we examined transcriptional phenotypes after 6h of tumor co-culture. For both CD8 and CD4 subsets, we could observe the separation of cells across a T cell differentiation axis. When ordering cells according to a predicted pseudotime, the annotated clusters indeed followed such a trajectory, evolving from a resting memory to a potent effector phenotype (Supp. Fig. 8). The enrichment of CAR variants across these clusters can therefore reveal differences in early activation signatures triggered by the different CARs. For the CD8 cell compartment, the presence of the CD40 domain in position A appeared to be the main driver of a fast and potent effector phenotype, as all CD40 variants (except CD40–41BB) presented the highest percentage of cells within the effector and cytotoxic clusters (Fig. 4a). On the other hand, 4-1BB containing CARs, while still activated, appeared to trigger a less potent but stronger effector memory-like phenotype. Notably, CD4 cells showed a different trend; for example, CTLA4-containing CARs appeared to drive the strongest CD4 activation and differentiation, while CD40, CD28 and 4-1BB retained an overall CD4 effector memory phenotype.

In addition to cluster enrichment, we used single-cell gene set scoring to further resolve the activation signatures based on the simultaneous expression of several marker genes. The CD8 effector phenotype was assessed for its cytotoxic and proinflammatory potential and a memory phenotype score was computed for all cells (Fig. 4b). Based on these scores, in silico sorting of cells was performed to assess the different CAR library variants by their enrichment in such phenotypes. Using the NS-CAR to set a baseline threshold, we then investigated the impact of CAR signaling domain composition on the appearance of each of these phenotypes (Fig. 4c). As described previously, all CAR constructs were able to trigger a strong cytotoxic phenotype (40-70% of CD8 cells); however, once again, the CD40 domain in position A appeared to drive a particularly high cytotoxicity that was enhanced when the CD40 domain is repeated. This pattern is even more striking when examining the proinflammatory signature. CD40 in position A also resulted in the most powerful proinflammatory phenotype that appears to be slightly restrained when incorporating 4-1BB or CTLA-4. The second generation 28z CAR, as expected, induced several of the most potent cytotoxic and proinflammatory signatures, serving as validation of our results. Lastly, the memory phenotype signature seemed to be highly enriched in 41BB-containing CARs, once again aligning with previous studies (*27*, *28*).

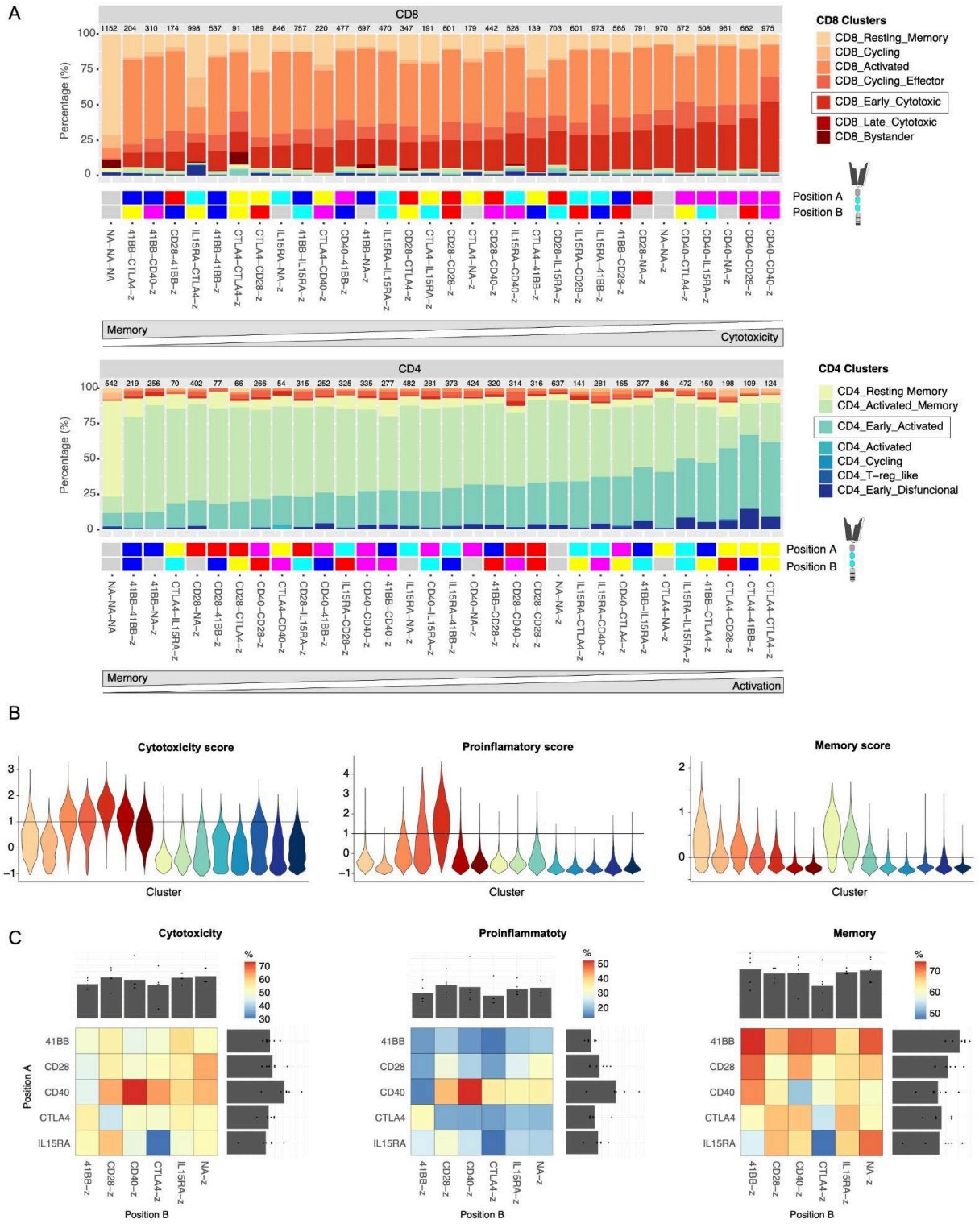

Figure 4: CAR-specific signatures following initial CAR T cell activation

A) Cluster enrichment observed for the different CAR T cell variants following 6h of tumor co-culture. CD8 and CD4 annotated cells are shown in different plots and variants are ordered (right to left) by the enrichment in the cluster highlighted with a black

box. Under each bar plot, a heatmap describes the intracellular domain combination of the library candidates. The number of cells used to define the cluster distribution is reported at the top of each bar. **B**) Distribution of single-cell gene-set scores across the different clusters described in Figure 3. A horizontal line determines a threshold at which cells are considered to be positive for each given score. **C**) Heatmaps show the percentage of cells with a positive score based on the thresholds described in (**B**) following 6h of tumor co-culture. Each heatmap separates variants based on the CAR signaling domains in position A (proximal to the cell membrane) or position B (distal from cell membrane). In addition, bar plots at the top and right-hand side of the heatmap compile the frequencies for all variants presenting a given domain in the different positions. Heatmaps for cytotoxicity and proinflammatory scores only include CD8 cells, while the memory score includes both CD4 and CD8 cells.

3.2.5 CAR co-stimulation can modulate long-term T cell persistence

A common limitation often faced by CAR T cell therapies is the transient persistence of T cells, ultimately resulting in their inability to control tumor growth and disease progression (*4*, *29*). Identifying CAR design features that promote a more persistent phenotype is of substantial value. To address this, we next leveraged the RAS assay to study the progression of T cell phenotypes across the CAR library. The scRNAseq data of CAR T cells from middle and late time points in the RAS assay were separated by CD4 and CD8 annotation and re-clustered to further resolve the RAS late-stage phenotypes.

Amongst the CD8 compartment, we observed two clusters, annotated as proinflammatory (CRTAM, IFNG, CSF2) and cytotoxic (PRF1, GZMB, GNLY, IL2RA) that still present effector potential (Fig. 5 a-c). Excluding a resting memory-associated cluster, the remainder of the clusters start to lose the expression of key effector marker genes, reaching a dysfunctional and subsequent terminal phenotype that ultimately leads to cell death. Using the enrichment of proinflammatory and cytotoxic clusters at a RAS late time point (12 days) as a marker for persistence, we observed that CD40, mainly in position A, appeared to be a key domain for long-term persistence (for both proinflammatory and cytotoxicity phenotypes). 4-1BB and CTLA4 promoted a late-stage cytotoxic, but not a proinflammatory, phenotype. IL15RA and CD28, on the other hand, had the largest percentage of cells already transitioning into a dysfunctional phenotype (Supp. Fig. 9).

Another feature to take into consideration within the CD8 T cell compartment is the decline in CD8 cell numbers over time. As previously mentioned, this reduction in the CD8/CD4 ratio appears to correlate with terminal effector differentiation, ultimately leading to cell death of only CD8 cells. A faster drop in CD8/CD4 ratio can therefore be associated with a lack of persistence. By combining CD8/CD4 fold change (Supp. Fig. 10) with the enrichment in the late effector clusters, we can obtain a more comprehensive persistence score (Fig. 5d). Based on this, CD40 once again proves to be the signaling domain that induces the most persistent phenotype, followed by CTLA-4.

Amongst the CD4 subset, another two main functional clusters, a proinflammatory Th1 (TBX21, CRTAM, IFNG, GZMB) and a polyfunctional Th2 cluster (GATA3, IL4, IL5, IL13), were identified in addition to other cycling, T-reg-like and dysfunctional clusters (Fig. 5e and f). The Th1 and Th2 signature was also confirmed by gene set scoring (Fig. 5g). Cluster enrichment was then used to evaluate the persistence of CD4 CAR T cell variants. CD40 consistently drove the most persistent proinflammatory signature by being the most enriched in the Th1 cluster, while CTLA4 and 4-1BB promoted a Th2-enriched persistent phenotype (Fig. 5h). On the other hand, CD28-containing CARs were consistently the most enriched variants in the dysfunctional cluster, suggesting once again that CD28-containing CARs are prone to induce poor persistence (Supp. Fig. 9).

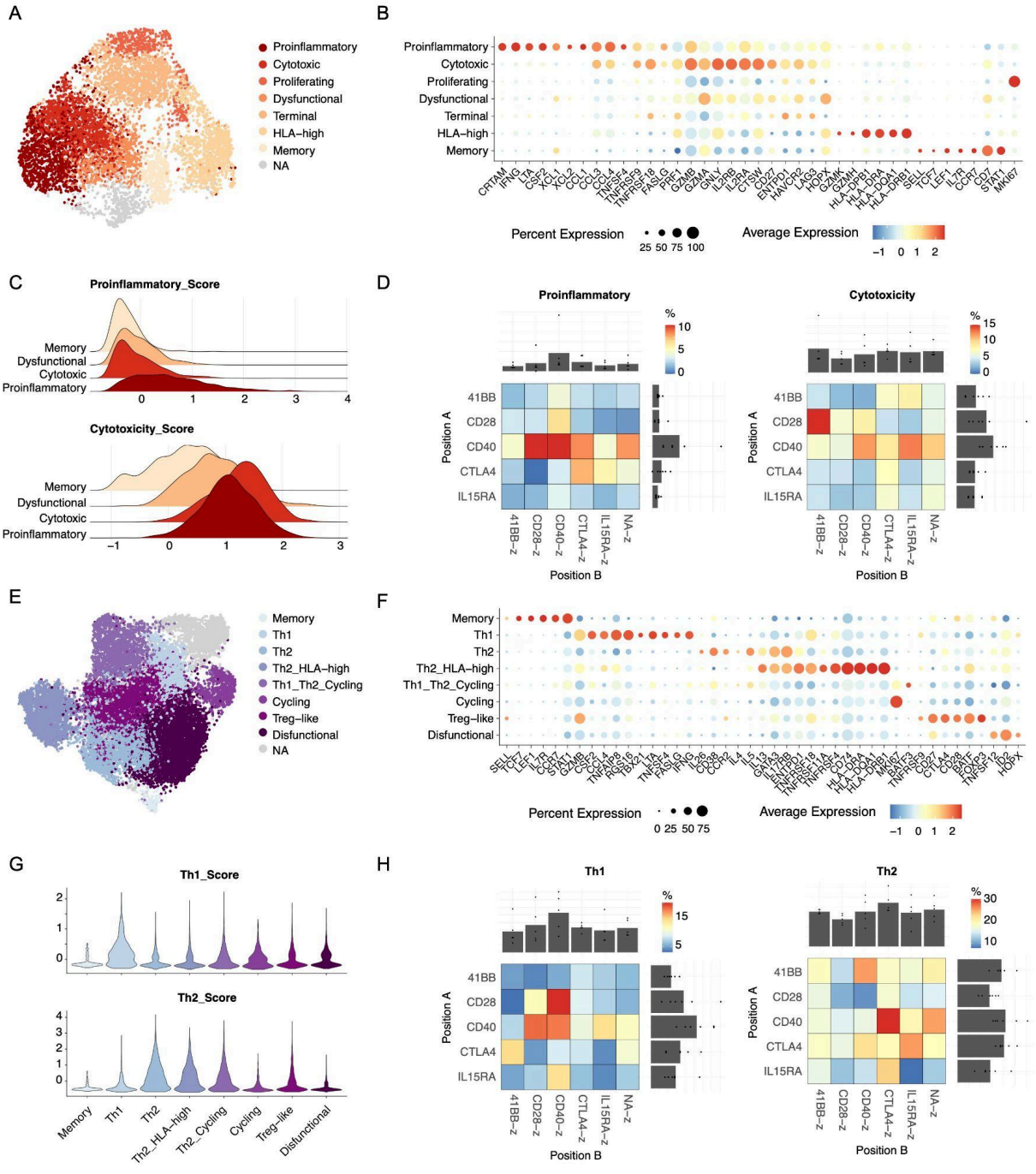

Figure 5: CAR-specific signatures following repeated antigen stimulation

A) UMAP embedding and unsupervised cell clustering of CD8 annotated cells at middle and late time points in the RAS assay (6 and 12 days). Cluster annotated as NA includes misannotated cells presenting a CD4-specific phenotype. **B**) Dot plot shows the expression of a selection of differentially expressed T cell marker genes, used to annotate the clusters described in (**A**). **C**) Distribution of single-cell gene-set scores across relevant clusters described in (**A**). **D**) Heatmaps show the enrichment of CD8 cells in the proinflammatory or cytotoxic clusters at a late time point in the RAS assay (12 days). The enrichment is corrected by the CD8/CD4 ratio fold change from day 0. Each heatmap separates variants based on the CAR signaling domains in position A (proximal to the cell membrane) or position B (distal from the cell membrane). In addition, bar plots at the top and right-hand

side of the heatmap compile the frequencies for all variants presenting a given domain in the different positions. **E**) UMAP embedding and unsupervised cell clustering of CD4 annotated cells at middle and late time points in the RAS assay (6 and 12 days). Cluster annotated as NA includes misannotated cells presenting a CD8-specific phenotype and dying cells with high mitochondrial gene expression. **F**) Dot plot shows the expression of a selection of differentially expressed T cell marker genes that are used to annotate the clusters described in (**E**). **G**) Distribution of single-cell gene-set scores across different clusters described in (**E**). **H**) Heatmaps show the enrichment of CD4 cells in the Th1 or Th2 clusters at a late time point in the RAS assay (12 days). Each heatmap separates variants based on the presence of CAR signaling domains in position A or position B . In addition, bar plots at the top and right-hand side of the heatmap compile the frequencies for all variants presenting a given domain in the different positions.

3.3 Discussion

Domain recombination has been pivotal in the evolution of signaling networks, operating on the principle that the function of a protein domain is modular and can promote new functions when embedded differently within a cellular network (*30*). As a product of rational domain recombination, CARs can be further optimized through additional signaling domain rearrangements. Despite the remarkable progress in the field of CAR T cell engineering (*5*, *31*), significant gaps persist in understanding how changes in the CAR signaling architecture impact resulting T cell phenotypes and their therapeutic potential. In particular, costimulatory domains have proven to be key in providing CAR T cells with essential properties for clinical efficacy, but the impact of changing the type, number and order of costimulatory domains has yet to be systematically characterized. In this study, we bridge these gaps by combining the use of a combinatorial CAR signaling domain library, pooled screening assays and scRNAseq to systematically study the dynamics governing CAR-induced phenotypes at high resolution.

We evaluated the impact of recombining five immune-receptor signaling domains, resulting in a 32-candidate CAR library that revealed architecture-specific patterns. While all CAR designs were capable of eliciting a T cell activation response, the incorporation of CD28 or 4-1BB domains replicated known phenotypic features associated with these domains (*27*, *28*, *32*); CD28 induced a potent but less persistent T cell activation, while 4-1BB promoted an effector memory phenotype. In parallel comparisons with benchmark CARs, insights into three additional domains were observed. CD40 consistently distinguished itself by triggering the most potent and persistent T cell responses. This aligns with previous findings indicating that CARs combining the signaling domains of MyD88 or CD79A with CD40 exhibit superior proliferation and antitumor activities in preclinical tumor xenograft mouse models (*6*, *20*). Moreover, CD40-containing CARs were selected amongst the top candidates when performing pooled screens of two CAR libraries (*13*, *14*), further highlighting the role of this domain in enhancing CAR signaling.

CTLA4, recognized as an inhibitory receptor on T cells, when embedded in the CAR signaling architecture resulted in potent CARs capable of promoting a robust T cell response, particularly amongst the CD4 compartment, with a persistent cytotoxic phenotype. Despite the inhibitory effect of CTLA4 signaling (*23*), our findings align with recent research reporting that the addition of CTLA4 cytoplasmic tails to a 28z CAR led to increased cytotoxicity and reduced production of pro-inflammatory cytokines (*7*). Despite its previous association with enhancing T cell anti-tumor potential (*21*), the IL15RA cytoplasmic domain did not seem to provide impactful T cell co-stimulation amongst the variants. The reduced size of its intracellular domain, coupled with the central role of its extracellular portion in carrying out its molecular function (*33*), suggests that the IL15RA domain may act as a molecular spacer within the CAR architecture.

With regard to domain positioning, our study also revealed distinctive patterns. In agreement with prior research that addressed the impact of altering the positioning of domains within the CAR (*34–36*), we observed that domains located closer to the cell membrane exhibited a dominant effect on phenotype. For instance, CD40 and 4-1BB respectively induced a distinct polarization towards effector or memory phenotype mainly when present in a membrane-proximal position. Nevertheless, domains in a more distal position continued to exert influence on phenotype, seemingly producing an additive effect. For example, CD40-z demonstrated a potent cytotoxic and proinflammatory phenotype, further potentiated in CD40-CD40-z but moderated in CD40-4-1BB-z, favoring a more memory-like phenotype. Despite these general observations, the mechanistic complexity associated with the introduction of domain rearrangements within a signaling network is far more sophisticated and highly dependent on the nature of the domains used. For example, CTLA4 displayed a more prominent role in promoting cytotoxicity when situated in a membrane-distal position. This observation, also suggested by Zhou et al. (*7*), may be linked to the role of its endocytosis motif in receptor recycling. This mechanistic feature could benefit from distal positioning, while distancing CTLA4 inhibitory signaling from the dominating membrane-proximal position.

The enormous complexity associated with rewiring signaling networks highlights the value of conducting systematic studies of CAR signaling domain rearrangements. In addition, the diversity of the CAR signaling domain combination space requires high-throughput approaches that enable parallel comparisons of multiple architectures. Pooled screening of CAR libraries combined with scRNAseq provides such a high-throughput approach (*13*, *14*, *16*, *37*). An exciting frontier of this field is the integration of CAR libraries with machine learning, as previously demonstrated by Daniels et al. (*15*). Machine learning-guided CAR T cell engineering may further elucidate mechanistic nuances of signaling

domains and enable novel CAR designs. The compact yet systematic design of our library, combined with the comprehensive and high-resolution data generated in this study, may provide training data for machine learning models that are able to decipher the rules of CAR signaling.

While our study provides valuable insights into the intricate landscape of CAR signaling and its impact on T cell phenotypes, we acknowledge certain limitations and outline future perspectives. In the context of pooled screens, the unavoidable bystander effect resulting from paracrine signaling poses logical concerns. Despite this limitation, the inclusion of a NS CAR as a negative control validated the minimal impact of this paracrine effect in overall T cell phenotype and stresses the importance of incorporating such controls in pooled library assays. Secondly, reproducing a clinically relevant T cell activation context poses a significant challenge. In vitro co-culture lacks the cellular heterogeneity, tumor microenvironment and anatomical barriers encountered in real clinical scenarios. While in vivo settings attempt to address some of these challenges, human tumor xenograft mouse models in immunocompromised mice often also fall short in replicating clinical conditions. Our choice of using ex vivo RAS provided extensive phenotypic characterization of CAR signaling in a simplified setup mimicking the clinical challenge of CAR T cell dysfunction following chronic antigen exposure. Despite this, the limited understanding of the correlation of CAR T cell phenotypes with clinical outcomes still makes it difficult to speculate which variant could exhibit better clinical performance, necessitating further functional validation (*38*). Lastly, while this study provides a systematic and in-depth analysis of such a large number of CARs, such an approach can be adapted to larger libraries or can include other CAR modules, such as antigen binding domains of varying affinities (*39*), hinges and transmembrane domains (*40*).

3.4 Materials and methods

Library cloning

The CAR library was cloned using a Type II restriction enzyme cloning strategy as previously described (*41*). A backbone plasmid containing an anti-HER2 first generation CAR gene (composed of a CD8α secretion peptide, a Herceptin-derived scFv (4D5), two Strep tags, CD28 hinge and transmembrane domains, the CD3ζ cytoplasmic region and a bGH polyA sequence) flanked by *TRAC* locus-specific homology arms was generated. In addition, a cloning cassette with inverted AarI sites was introduced between the TMD and the CD3ζ sequence. Lastly, a 3’ UTR barcode sequence was added using an overhang PCR and recircularization strategy. Synthetic gene fragments containing the cytoplasmic sequence of CD28, 4-1BB, CD40, IL15RA and CTLA4 genes were generated (Twist Bioscience) with

different sets of flanking sequences containing an AarI recognition site that allows for the ligation of a defined number and order of domains within the CAR backbone. Domain sequences were individually amplified, digested with AarI (Thermo Fisher; 4 h, 37 °C) and ligated into the previously digested backbone plasmid using a T4 ligase (NEB; 30 min, 37 °C). For each library candidate, the ligated plasmids were transformed into E. coli DH5α cells, purified and sequence verified using Sanger sequencing. The NS-CAR and the 1st generation CAR were independently cloned using deletion Q5 mutagenesis. Finally, all library candidate plasmids were pooled at a 1:1 ratio.

Primary human T cell isolation and culture

Buffy coats from healthy donors were acquired through the Blutspendezentrum Basel (University of Basel). All participating volunteers provided written informed consent in accordance with the general guidelines approved by Swissethics (Swiss Association of Research Ethics Committees). Peripheral blood mononuclear cells (PBMCs) were isolated using a Ficoll-based density gradient and stored in liquid nitrogen until needed. Immediately after thawing, negative selection of T cells was performed using the EasySep human T cell isolation kit (Stemcell) and cultured in X-VIVO 15 medium (Lonza) supplemented with 5% fetal bovine serum (FBS), 50 µM β-mercaptoethanol, 100 µg/mL Normocin (Invivogen) and 100 U/mL IL-2 (Peprotech), referred to as T cell growth medium.

Primary human T cell genome editing

Primary human T cells were engineered to integrate a CAR gene into the *TRAC* genomic locus using CRISPR-Cas9 genome editing. Double-stranded DNA HDR template and Cas9 ribonucleoprotein (RNP) were prepared as previously described (*16*). T cells were activated using Human T-Activator CD3/CD28 Dynabeads (Thermo Fisher) at a 1:1 cell:bead ratio in T cell growth medium. After 48 h, beads were magnetically removed and cells were electroporated using the Lonza 4D electroporation system. To do this, $1x10^6$ cells were washed once in PBS, resuspended in 20 uL of P3 nucleofection buffer (Lonza) containing 1.2 uL of Cas9 RNP mix and 0.4 ug double-stranded DNA HDR template and electroporated using the EH-115 program. After electroporation, cells were immediately recovered in 150 uL of T cell growth medium. For each batch of CAR library T cells, at least $1x10^7$ T cells were engineered to achieve sufficient clonal diversity across all candidates.

Cell line culture

SKBR3-GFP cell line was cultured in Dulbecco's Modified Eagle Medium (DMEM; Gibco) supplemented with 10% FBS, 1% penicillin-streptomycin (Gibco) and 100 µg/mL Normocin (Invivogen).

CAR T cell staining and cell sorting

Flow cytometry was used to analyze and select correctly engineered CAR T cells based on the positive staining of a StrepTag located in the extracellular portion of the CAR and the lack of expression of the TCR complex. A two-step staining strategy was employed, initially using a biotinylated anti-Strep tag antibody (Supp. Table 3), followed by a combination of streptavidin-BV421 conjugate and CD3ε-APC antibody (Supp. Table 3). T cells were washed in FACS buffer (PBS, 2 % FBS, 1 mM EDTA) and then incubated in FACS buffer containing the antibody mix for 20 minutes. Cells were then washed again and analyzed using a Fortessa LSR flow cytometer (BD) or sorted using a FACS Aria Fusion (BD).

Deep sequencing of CAR libraries

The diversity of library CAR T cells was determined using deep sequencing. Genomic DNA from 5,000 - 50,000 CAR-expressing T cells was extracted using Quick Extract (Lucigen) and used as the template for a 2-step PCR strategy. In a first PCR reaction, primers F1 and R1 (Supp. Table 2) were used to amplify a region of the CAR gene (2000 - 2500 bp), which confirmed the CAR integration into the *TRAC* locus. Following a 0.6X SPRIselect bead DNA cleanup (Beckman Coulter) the DNA product was used as a template for a second PCR reaction using primer mix F2 and R2 (Supp. Table 2). This amplified a 261 bp sequence in the CAR 3'UTR region that contained the barcode sequence, which determines its library identity. The resulting amplicons were purified using a 1.2X-0.6X double-sided SPRIselect bead DNA cleanup (Beckman Coulter), prepared for sequencing using a KAPA HyperPrep kit (Roche) and sequenced on an Illumina MiSeq system. Sequencing data analysis was performed using the Biostrings package in R.

In vitro repeated antigen stimulation (RAS)

To simulate a chronic antigen stimulation, CAR-T cells were repeatedly co-cultured with the HER2-expressing tumor cell line SKBR3. On day 14 (12 days after bead removal and T cell engineering) T cells were co-cultured with SKBR3-GFP cells at a 1:1 E:T ratio in CAR media supplemented with 30 IU/mL of IL-2. Every 3 days cells were counted using a hemocytometer and new SKBR3-GFP cells were added to re-adjust the co-culture to a 1:1 E:T ratio.

Degranulation and cytokine production assay

To assess the effector potential of co-cultured CAR-T cells, we measured degranulation and the production of cytokines following the restimulation of CAR-T cells with SKBR3-GFP cells. 50,000 CAR-T cells were co-cultured with 100,000 target cells for 5h in the presence of CD107a antibody (Supp. Table 3) and 1x Brefeldin A (Biolegend). Following co-culture, cells were stained for dead cells (Zombie

NIR; Biolegend) and surface markers (CD4 and CD8; Supp. Table 3), fixed using Fixation Buffer (Biolegend) and stained for the intracellular accumulation of IFNγ and TNFα (Supp. Table 3) in 1x Permeabilization Buffer (Biolegend). Samples were analyzed using a Fortessa LSR flow cytometer (BD) or sorted using a FACS Aria Fusion (BD).

Single-cell sequencing (scRNAseq)

Library CAR T cells derived from two healthy donors were subjected to a RAS assay, as previously described. At days 0, 6 and 12 of the RAS assay, CAR library T cells were co-cultured with SKBR3-GFP cells for 6h in 30 IU/mL of IL-2. Following this time, the co-cultures were washed with FACS buffer, stained using DRAQ7, and the live GFP-negative population was sorted using a FACS Aria Fusion (BD). Cells were then stained using 20 Totalseq B antibodies (Supp. Table 4) and introduced into the Chromium Single Cell 3' scRNAseq pipeline v3.1 (10x genomics) following the manufacturer's guidelines (User guide CG000317 Rev D). In short, 20,000 cells were loaded into each Chromium chip lane to generate single-cell emulsions containing barcoded oligonucleotides that allow the generation of barcoded cDNA from mRNA and oligo-tagged antibodies. Using the amplified cDNA as a template, scRNAseq and scCITEseq libraries were generated and sequenced using the Illumina Novaseq platform.

Single-cell CAR sequencing (scCARseq)

Demultiplexing of the CAR library to define the CAR identity for each cell in scRNAseq data was achieved using an adapted version of a previously described scCARseq methodology (*16*) (Supp. Fig 3). Using 10 uL of the cDNA product resulting from the single-cell sequencing pipeline, the 3' UTR region of the CAR transcripts, containing a CAR variant specific barcode (CAR-BC), was amplified using F3 and R3 primers (Supp. Table 2) and KAPA-Hifi polymerase (Roche). Following a 1X SPRIselect bead DNA cleanup (Beckman Coulter), the DNA product containing partial Illumina-specific adaptors was further amplified and indexed using Dual Index Kit TT, Set A primers (10x Genomics, PN-1000215). The final scCARseq library was then purified using a 1X-0.6X double-sided SPRIselect bead DNA cleanup (Beckman Coulter) and sequenced with the Illumina platform using the same cycle scheme as the scRNAseq and scCITEseq libraries. scCARseq data analysis was conducted using the Biostrings package in R. Only cells with at least 2 different unique molecular identifiers (UMIs) defining the same CAR annotation were accepted.

Single-cell sequencing data analysis

The raw sequencing data was aligned to the GRCh38 human reference genome using Cell Ranger (10x Genomics, version 6.0.0) and imported into R (version 4.2.3) to perform downstream analysis using the

Seurat package (version 4.3.0.1). In the first place, only cells assigned to a single CAR variant were selected. Low-quality cells were removed based on the detection of a low number of genes (*nFeature_RNA > 300*), high number of gene expression UMIs (*nFeature_RNA < 50,000*), high number of Antibody-Derived Tags (ADT) UMIs (*nCount_ADT < 30,000*), or a high percentage of mitochondrial genes (*percent.mt < 20*). Lastly, in order to correct for arbitrary clonal expansion that may occur through RAS, a subsampling step was performed; for each sample (different time point or donor), CAR variants exceeding two times the theoretical balanced library distribution (maximum 6.25% of cells per CAR variant) were randomly subsampled to meet this criteria.

The resulting 58,949 single-cell transcriptomes were then normalized, scaled while regressing out the effect of cell cycle phase and percent of mitochondrial genes and finally integrated using Harmony (*42*) (applying a lambda of 1 and 200 for sample variables 'Donor' and 'Time' respectively). Dimensionality reduction using UMAP and unsupervised cell clustering was then used to visualize and analyze the resulting T cell phenotypes. ADT data was normalized using dsb (*43*) in *Python*, using the parameters 'pseudocount=10' and 'denoise counts=True'. Empty droplets were estimated by dsb from the raw output of Cell Ranger after the exclusion of the cell-containing barcodes found in the filtered output. RNA and ADT data were combined in the annotation of cells as CD4 or CD8. The Seurat object was then further split by CD4/CD8 subsets and time point to perform a more resolved transcriptomic analysis. This analysis included the use of a single-cell gene set scoring function from the Seurat package (AddModuleScore) using the gene sets in Supp. Table 5 and pseudotime and trajectory analysis using the Monocle3 package (*44*).

References for Chapter 3

1. J. J. Melenhorst, G. M. Chen, M. Wang, D. L. Porter, C. Chen, M. A. Collins, P. Gao, S. Bandyopadhyay, H. Sun, Z. Zhao, S. Lundh, I. Pruteanu-Malinici, C. L. Nobles, S. Maji, N. V. Frey, S. I. Gill, A. W. Loren, L. Tian, I. Kulikovskaya, M. Gupta, D. E. Ambrose, M. M. Davis, J. A. Fraietta, J. L. Brogdon, R. M. Young, A. Chew, B. L. Levine, D. L. Siegel, C. Alanio, E. J. Wherry, F. D. Bushman, S. F. Lacey, K. Tan, C. H. June, Decade-long leukaemia remissions with persistence of CD4+ CAR T cells. *Nature*. **602**, 503–509 (2022).

2. K. M. Cappell, J. N. Kochenderfer, Long-term outcomes following CAR T cell therapy: what we know so far. *Nat. Rev. Clin. Oncol.* **20**, 359–371 (2023).

3. V. Wang, M. Gauthier, V. Decot, L. Reppel, D. Bensoussan, Systematic Review on CAR-T Cell Clinical Trials Up to 2022: Academic Center Input. *Cancers* . **15** (2023), doi:10.3390/cancers15041003.

4. N. N. Shah, T. J. Fry, Mechanisms of resistance to CAR T cell therapy. *Nat. Rev. Clin. Oncol.* **16**, 372–385 (2019).

5. N. Singh, M. V. Maus, Synthetic manipulation of the cancer-immunity cycle: CAR-T cell therapy. *Immunity*. **56**, 2296–2310

(2023).

6. J. Julamanee, S. Terakura, K. Umemura, Y. Adachi, K. Miyao, S. Okuno, E. Takagi, T. Sakai, D. Koyama, T. Goto, R. Hanajiri, M. Hudecek, P. Steinberger, J. Leitner, T. Nishida, M. Murata, H. Kiyoi, Composite CD79A/CD40 co-stimulatory endodomain enhances CD19CAR-T cell proliferation and survival. *Mol. Ther.* **29**, 2677–2690 (2021).

7. X. Zhou, H. Cao, S.-Y. Fang, R. D. Chow, K. Tang, M. Majety, M. Bai, M. B. Dong, P. A. Renauer, X. Shang, K. Suzuki, A. Levchenko, S. Chen, CTLA-4 tail fusion enhances CAR-T antitumor immunity. *Nat. Immunol.* **24**, 1499–1510 (2023).

8. H. Kintz, E. Nylen, A. Barber, Inclusion of Dap10 or 4-1BB costimulation domains in the chPD1 receptor enhances anti-tumor efficacy of T cells in murine models of lymphoma and melanoma. *Cell. Immunol.* **351**, 104069 (2020).

9. R. M.-H. Velasco Cárdenas, S. M. Brandl, A. V. Meléndez, A. E. Schlaak, A. Buschky, T. Peters, F. Beier, B. Serrels, S. Taromi, K. Raute, S. Hauri, M. Gstaiger, S. Lassmann, J. B. Huppa, M. Boerries, G. Andrieux, B. Bengsch, W. W. Schamel, S. Minguet, Harnessing CD3 diversity to optimize CAR T cells. *Nat. Immunol.* **24**, 2135–2149 (2023).

10. A. M. Tousley, M. C. Rotiroti, L. Labanieh, L. W. Rysavy, W.-J. Kim, C. Lareau, E. Sotillo, E. W. Weber, S. P. Rietberg, G. N. Dalton, Y. Yin, D. Klysz, P. Xu, E. L. de la Serna, A. R. Dunn, A. T. Satpathy, C. L. Mackall, R. G. Majzner, Co-opting signalling molecules enables logic-gated control of CAR T cells. *Nature*. **615**, 507–516 (2023).

11. S. Guedan, A. Madar, V. Casado-Medrano, C. Shaw, A. Wing, F. Liu, R. M. Young, C. H. June, A. D. Posey Jr, Single residue in CD28-costimulated CAR-T cells limits long-term persistence and antitumor durability. *J. Clin. Invest.* **130**, 3087–3097 (2020).

12. J. Feucht, J. Sun, J. Eyquem, Y.-J. Ho, Z. Zhao, J. Leibold, A. Dobrin, A. Cabriolu, M. Hamieh, M. Sadelain, Calibration of CAR activation potential directs alternative T cell fates and therapeutic potency. *Nat. Med.* **25**, 82–88 (2019).

13. K. S. Gordon, T. Kyung, C. R. Perez, P. V. Holec, A. Ramos, A. Q. Zhang, Y. Agarwal, Y. Liu, C. E. Koch, A. Starchenko, B. A. Joughin, D. A. Lauffenburger, D. J. Irvine, M. T. Hemann, M. E. Birnbaum, Screening for CD19-specific chimaeric antigen receptors with enhanced signalling via a barcoded library of intracellular domains. *Nat Biomed Eng*. **6**, 855–866 (2022).

14. D. B. Goodman, C. S. Azimi, K. Kearns, A. Talbot, K. Garakani, J. Garcia, N. Patel, B. Hwang, D. Lee, E. Park, V. S. Vykunta, B. R. Shy, C. J. Ye, J. Eyquem, A. Marson, J. A. Bluestone, K. T. Roybal, Pooled screening of CAR T cells identifies diverse immune signaling domains for next-generation immunotherapies. *Sci. Transl. Med.* **14**, eabm1463 (2022).

15. K. G. Daniels, S. Wang, M. S. Simic, H. K. Bhargava, S. Capponi, Y. Tonai, W. Yu, S. Bianco, W. A. Lim, Decoding CAR T cell phenotype using combinatorial signaling motif libraries and machine learning. *Science*. **378**, 1194–1200 (2022).

16. R. Castellanos-Rueda, R. B. Di Roberto, F. Bieberich, F. S. Schlatter, D. Palianina, O. T. P. Nguyen, E. Kapetanovic, H. Läubli, A. Hierlemann, N. Khanna, S. T. Reddy, speedingCARs: accelerating the engineering of CAR T cells by signaling domain shuffling and single-cell sequencing. *Nat. Commun.* **13**, 6555 (2022).

17. C. M. Bucks, J. A. Norton, A. C. Boesteanu, Y. M. Mueller, P. D. Katsikis, Chronic antigen stimulation alone is sufficient to drive CD8+ T cell exhaustion. *J. Immunol.* **182**, 6697–6708 (2009).

18. J. A. Fraietta, S. F. Lacey, E. J. Orlando, I. Pruteanu-Malinici, M. Gohil, S. Lundh, A. C. Boesteanu, Y. Wang, R. S. O'Connor, W.-T. Hwang, E. Pequignot, D. E. Ambrose, C. Zhang, N. Wilcox, F. Bedoya, C. Dorfmeier, F. Chen, L. Tian, H. Parakandi, M. Gupta, R. M. Young, F. B. Johnson, I. Kulikovskaya, L. Liu, J. Xu, S. H. Kassim, M. M. Davis, B. L. Levine, N. V. Frey, D. L. Siegel, A. C. Huang, E. J. Wherry, H. Bitter, J. L. Brogdon, D. L. Porter, C. H. June, J. J. Melenhorst, Determinants of response and resistance to CD19 chimeric antigen receptor (CAR) T cell therapy of chronic lymphocytic leukemia. *Nat. Med.* **24**, 563–571 (2018).

19. D. Yu, M.-C. Hung, Overexpression of ErbB2 in cancer and ErbB2-targeting strategies. *Oncogene*. **19**, 6115–6121 (2000).

20. B. Prinzing, P. Schreiner, M. Bell, Y. Fan, G. Krenciute, S. Gottschalk, MyD88/CD40 signaling retains CAR T cells in a less differentiated state. *JCI Insight*. **5** (2020), doi:10.1172/jci.insight.136093.

21. S. Nair, J.-B. Wang, S.-T. Tsao, Y. Liu, W. Zhu, W. B. Slayton, J. S. Moreb, L. Dong, L.-J. Chang, Functional Improvement of Chimeric Antigen Receptor Through Intrinsic Interleukin-15Rα Signaling. *Curr. Gene Ther.* **19**, 40–53 (2019).

22. J. Eyquem, J. Mansilla-Soto, T. Giavridis, S. J. C. van der Stegen, M. Hamieh, K. M. Cunanan, A. Odak, M. Gönen, M. Sadelain, Targeting a CAR to the TRAC locus with CRISPR/Cas9 enhances tumour rejection. *Nature*. **543**, 113–117 (2017).

23. V. D. Fedorov, M. Themeli, M. Sadelain, PD-1- and CTLA-4-based inhibitory chimeric antigen receptors (iCARs) divert off-target immunotherapy responses. *Sci. Transl. Med.* **5**, 215ra172 (2013).

24. M. P. Trefny, N. Kirchhammer, P. Auf der Maur, M. Natoli, D. Schmid, M. Germann, L. Fernandez Rodriguez, P. Herzig, J. Lötscher, M. Akrami, J. C. Stinchcombe, M. A. Stanczak, A. Zingg, M. Buchi, J. Roux, R. Marone, L. Don, D. Lardinois, M. Wiese, L. T. Jeker, M. Bentires-Alj, J. Rossy, D. S. Thommen, G. M. Griffiths, H. Läubli, C. Hess, A. Zippelius, Deletion of SNX9 alleviates CD8 T cell exhaustion for effective cellular cancer immunotherapy. *Nat. Commun.* **14**, 86 (2023).

25. C. R. Good, M. A. Aznar, S. Kuramitsu, P. Samareh, S. Agarwal, G. Donahue, K. Ishiyama, N. Wellhausen, A. K. Rennels, Y. Ma, L. Tian, S. Guedan, K. A. Alexander, Z. Zhang, P. C. Rommel, N. Singh, K. M. Glastad, M. W. Richardson, K. Watanabe, J. L. Tanyi, M. H. O'Hara, M. Ruella, S. F. Lacey, E. K. Moon, S. J. Schuster, S. M. Albelda, L. L. Lanier, R. M. Young, S. L. Berger, C. H. June, An NK-like CAR T cell transition in CAR T cell dysfunction. *Cell*. **184**, 6081–6100.e26 (2021).

26. D. Hudrisier, J. Riond, H. Mazarguil, J. E. Gairin, E. Joly, Cutting edge: CTLs rapidly capture membrane fragments from target cells in a TCR signaling-dependent manner. *J. Immunol.* **166**, 3645–3649 (2001).

27. A. I. Salter, R. G. Ivey, J. J. Kennedy, V. Voillet, A. Rajan, E. J. Alderman, U. J. Voytovich, C. Lin, D. Sommermeyer, L. Liu, J. R. Whiteaker, R. Gottardo, A. G. Paulovich, S. R. Riddell, Phosphoproteomic analysis of chimeric antigen receptor signaling reveals kinetic and quantitative differences that affect cell function. *Sci. Signal.* **11** (2018), doi:10.1126/scisignal.aat6753.

28. O. U. Kawalekar, R. S. O'Connor, J. A. Fraietta, L. Guo, S. E. McGettigan, A. D. Posey Jr, P. R. Patel, S. Guedan, J. Scholler, B. Keith, N. W. Snyder, I. A. Blair, M. C. Milone, C. H. June, Distinct Signaling of Coreceptors Regulates Specific Metabolism Pathways and Impacts Memory Development in CAR T Cells. *Immunity*. **44**, 380–390 (2016).

29. V. Wittibschlager, U. Bacher, K. Seipel, N. Porret, G. Wiedemann, C. Haslebacher, M. Hoffmann, M. Daskalakis, D. Akhoundova, T. Pabst, CAR T-Cell Persistence Correlates with Improved Outcome in Patients with B-Cell Lymphoma. *Int. J. Mol. Sci.* **24** (2023), doi:10.3390/ijms24065688.

30. R. B. Di Roberto, S. G. Peisajovich, The role of domain shuffling in the evolution of signaling networks. *J. Exp. Zool. B Mol. Dev. Evol.* **322**, 65–72 (2014).

31. L. Labanieh, C. L. Mackall, CAR immune cells: design principles, resistance and the next generation. *Nature*. **614**, 635–648 (2023).

32. S. J. Priceman, E. A. Gerdts, D. Tilakawardane, K. T. Kennewick, J. P. Murad, A. K. Park, B. Jeang, Y. Yamaguchi, X. Yang, R. Urak, L. Weng, W.-C. Chang, S. Wright, S. Pal, R. E. Reiter, A. M. Wu, C. E. Brown, S. J. Forman, Co-stimulatory signaling determines tumor antigen sensitivity and persistence of CAR T cells targeting PSCA+ metastatic prostate cancer. *Oncoimmunology*. **7**, e1380764 (2018).

33. K. S. Schluns, T. Stoklasek, L. Lefrançois, The roles of interleukin-15 receptor alpha: trans-presentation, receptor component, or both? *Int. J. Biochem. Cell Biol.* **37**, 1567–1571 (2005).

34. S. Guedan, A. D. Posey Jr, C. Shaw, A. Wing, T. Da, P. R. Patel, S. E. McGettigan, V. Casado-Medrano, O. U. Kawalekar, M. Uribe-Herranz, D. Song, J. J. Melenhorst, S. F. Lacey, J. Scholler, B. Keith, R. M. Young, C. H. June, Enhancing CAR T cell persistence through ICOS and 4-1BB costimulation. *JCI Insight*. **3** (2018), doi:10.1172/jci.insight.96976.

35. T. Muliaditan, L. Halim, L. M. Whilding, B. Draper, D. Y. Achkova, F. Kausar, M. Glover, N. Bechman, A. Arulappu, J. Sanchez, K. R. Flaherty, J. Obajdin, K. Grigoriadis, P. Antoine, D. Larcombe-Young, C. M. Hull, R. Buus, P. Gordon, A. Grigoriadis, D. M. Davies, A. Schurich, J. Maher, Synergistic T cell signaling by 41BB and CD28 is optimally achieved by membrane proximal positioning within parallel chimeric antigen receptors. *Cell Rep Med*. **2**, 100457 (2021).

36. W. Si, Y.-Y. Fan, S.-Z. Qiu, X. Li, E.-Y. Wu, J.-Q. Ju, W. Huang, H.-P. Wang, P. Wei, Design of diversified chimeric antigen receptors through rational module recombination. *iScience*. **26**, 106529 (2023).

37. R. Castellanos-Rueda, R. B. Di Roberto, F. S. Schlatter, S. T. Reddy, Leveraging Single-Cell Sequencing for Chimeric Antigen Receptor T Cell Therapies. *Trends Biotechnol.* **39**, 1308–1320 (2021).

38. N. J. Haradhvala, M. V. Maus, Understanding Mechanisms of Response to CAR T-cell Therapy through Single-Cell Sequencing: Insights and Challenges. *Blood Cancer Discov*, OF1–OF4 (2024).

39. C. He, J. Mansilla-Soto, N. Khanra, M. Hamieh, V. Bustos, A. J. Paquette, A. Garcia Angus, D. M. Shore, W. J. Rice, G. Khelashvili, M. Sadelain, J. R. Meyerson, CD19 CAR antigen engagement mechanisms and affinity tuning. *Sci Immunol*. **8**, eadf1426 (2023).

40. X. Rios, O. Pardias, M. A. Morales, P. Bhattacharya, Y. Chen, L. Guo, C. Zhang, E. J. Di Pierro, G. Tian, G. A. Barragan, P. Sumazin, L. S. Metelitsa, Refining chimeric antigen receptors via barcoded protein domain combination pooled screening. *Mol. Ther.* **31**, 3210–3224 (2023).

41. R. B. Di Roberto, B. M. Scott, S. G. Peisajovich, Directed Evolution Methods to Rewire Signaling Networks. *Methods Mol. Biol.* **1596**, 321–337 (2017).

42. I. Korsunsky, N. Millard, J. Fan, K. Slowikowski, F. Zhang, K. Wei, Y. Baglaenko, M. Brenner, P.-R. Loh, S. Raychaudhuri, Fast, sensitive and accurate integration of single-cell data with Harmony. *Nat. Methods*. **16**, 1289–1296 (2019).

43. M. P. Mulè, A. J. Martins, J. S. Tsang, Normalizing and denoising protein expression data from droplet-based single cell profiling. *Nat. Commun.* **13**, 2099 (2022).

44. C. Trapnell, D. Cacchiarelli, J. Grimsby, P. Pokharel, S. Li, M. Morse, N. J. Lennon, K. J. Livak, T. S. Mikkelsen, J. L. Rinn, The dynamics and regulators of cell fate decisions are revealed by pseudotemporal ordering of single cells. *Nat. Biotechnol.* **32**, 381–386 (2014).

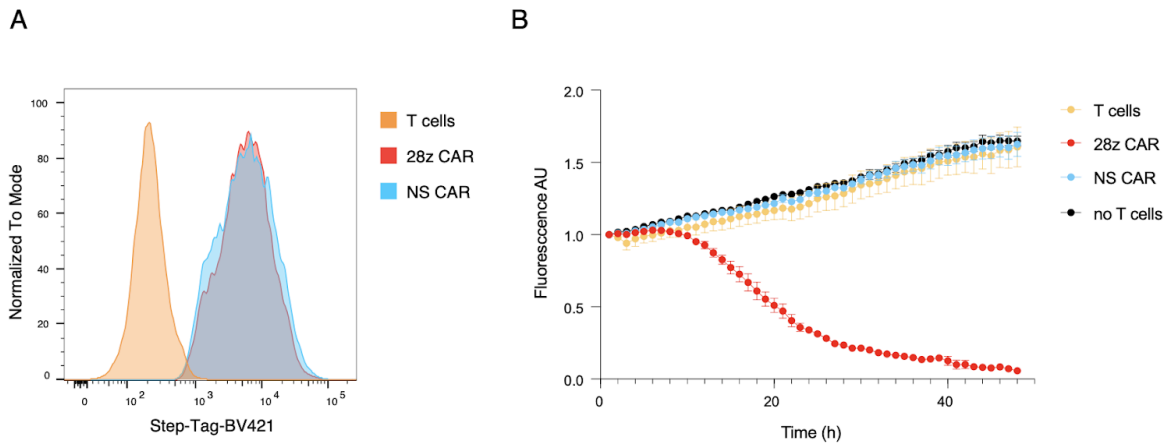

Supp. Figure 1: A non-signaling CAR serves as an internal library negative control
A) Overlaid histograms show the CAR surface expression profiles of 28z and NS CAR T cells compared to unedited T cells. An antiStrep-Tag-BV421 antibody was used to detect CARs by flow cytometry. **B**) CAR T cell mediated cytotoxicity of 28z and NS CAR T cells compared to unedited T cells. T cells and HER2+GFP+ SKBR3 cells were co-cultured at a 1:1 E:T ratio and the change in GFP fluorescence was monitored over time (n=3, technical replicates, error bars represent SEM).

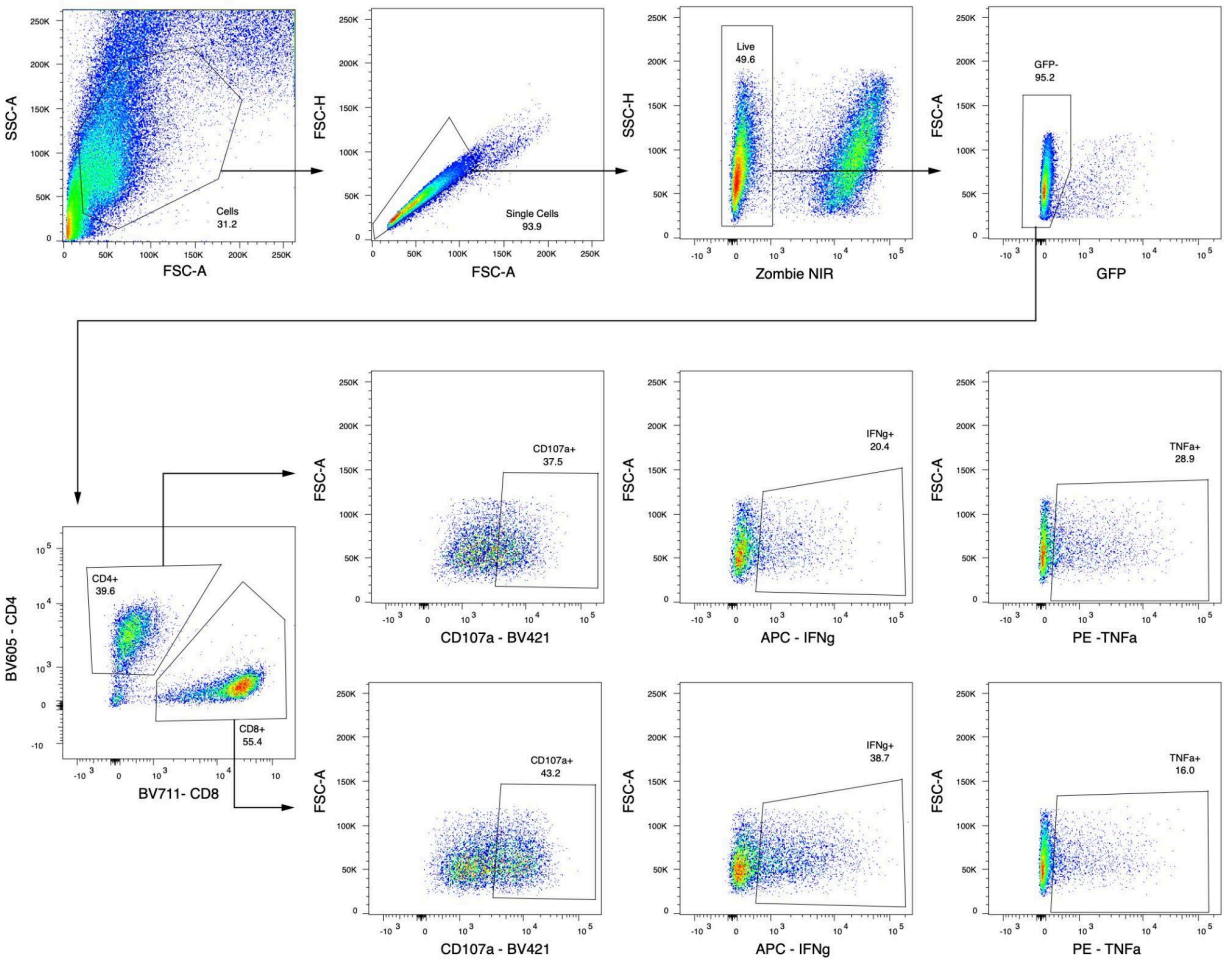

Supp. Figure 2: Flow cytometry gating strategy used to determine the expression of a panel of T cell effector markers following tumor co-culture

Following 5h of co-culture of CAR T cells and SKBR3-GFP tumor cells, cells were stained for surface markers and the intracellular accumulation of pro-inflammatory cytokines IFNγ and TNFα.

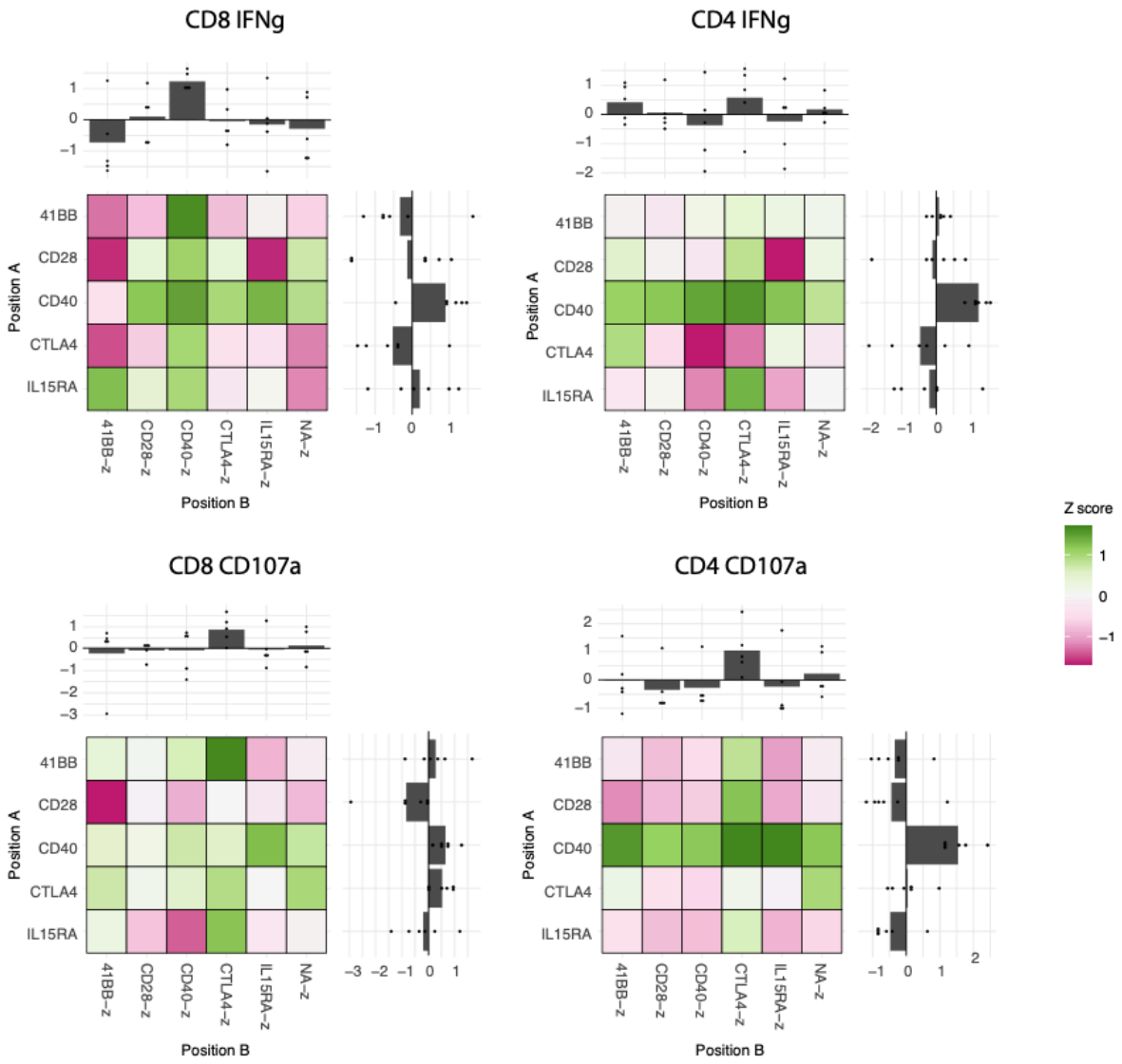

Supp. Figure 3: Domain identity and position impact CAR T cell persistence during repeated antigen stimulation
Heatmaps show the enrichment or depletion of CAR variants following a CD107a or IFNγ positive selection after 9 days of RAS. Z-scores were calculated based on the fold change in relative library frequencies before and after selection. CD8 and CD4 T cell compartments were analyzed separately. Each heatmap separates variants based on the presence of CAR signaling domains in position A (proximal to the cell membrane) or position B (distal from cell membrane). In addition, bar plots at the top and right-hand side of the heatmap compile the scores for all variants presenting a given domain in a given position.

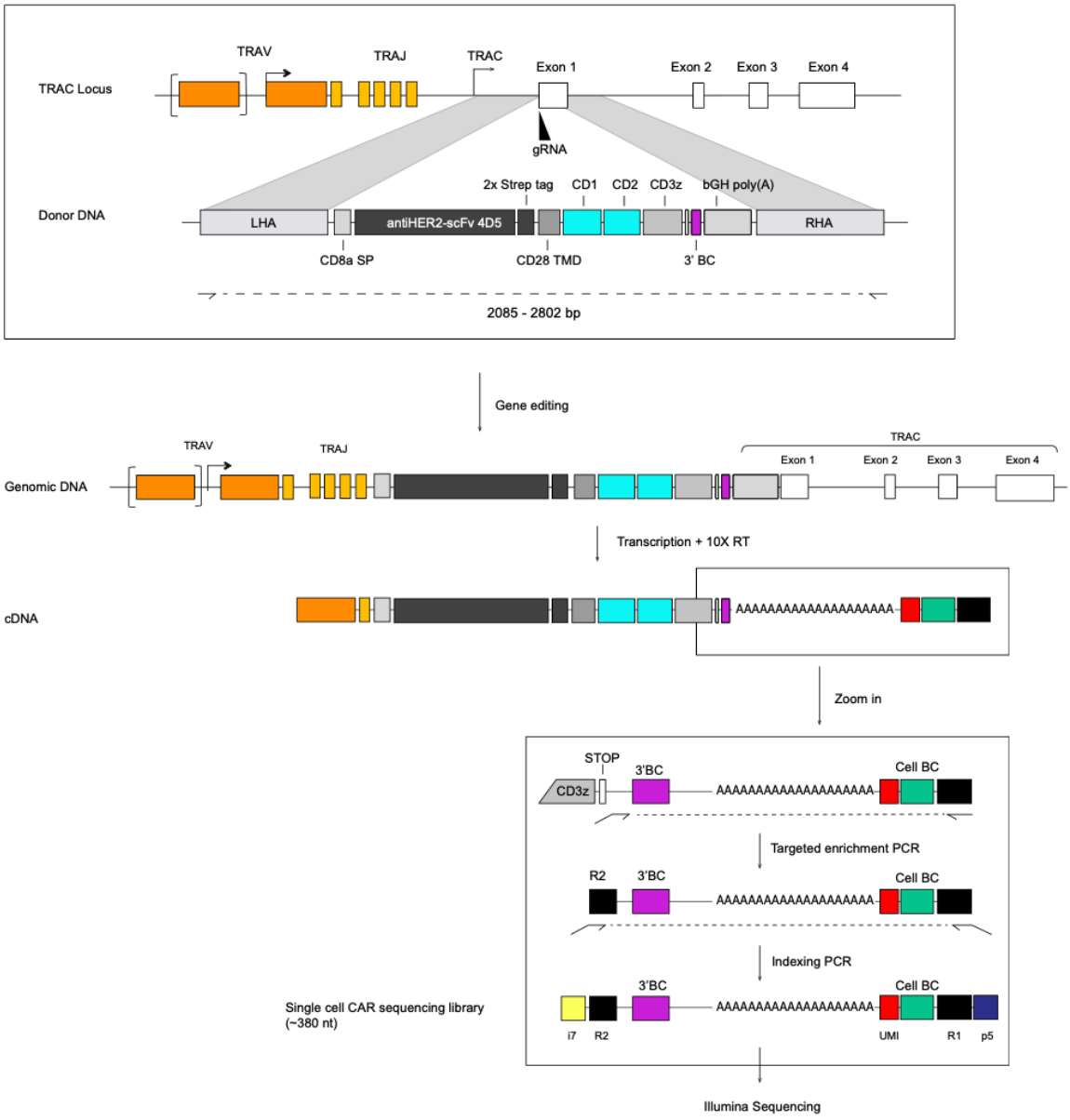

Supp. Figure 4: scCARseq strategy for library demultiplexing

Following CAR T cell engineering through CRISPR-Cas9 genome editing, a single copy of a CAR gene is integrated into the TRAC locus. In addition to the CAR components, each CAR gene contains a variant-specific barcode (purple) located in the 3' UTR region. The CAR gene is then transcribed into mRNA following *TRAC*-specific gene regulation. During the scRNAseq pipeline, mRNA is reverse transcribed to cDNA, and each transcript (including the CAR mRNA) incorporates a 3' barcode (green) specific to its cell of origin (cell-BC). In order to produce the scCARseq library, a two-step PCR amplification strategy first does a targeted amplification of the 3' UTR sequence of the CAR gene (that links the CAR-BC and the cell-BC) followed by an indexing PCR that adds the rest of the Illumina adaptors and sample index. The resulting library can then be sequenced using an Illumina platform to trace the origin of CAR transcripts and link them to the individual cells identified in the 10X gene expression pipeline.

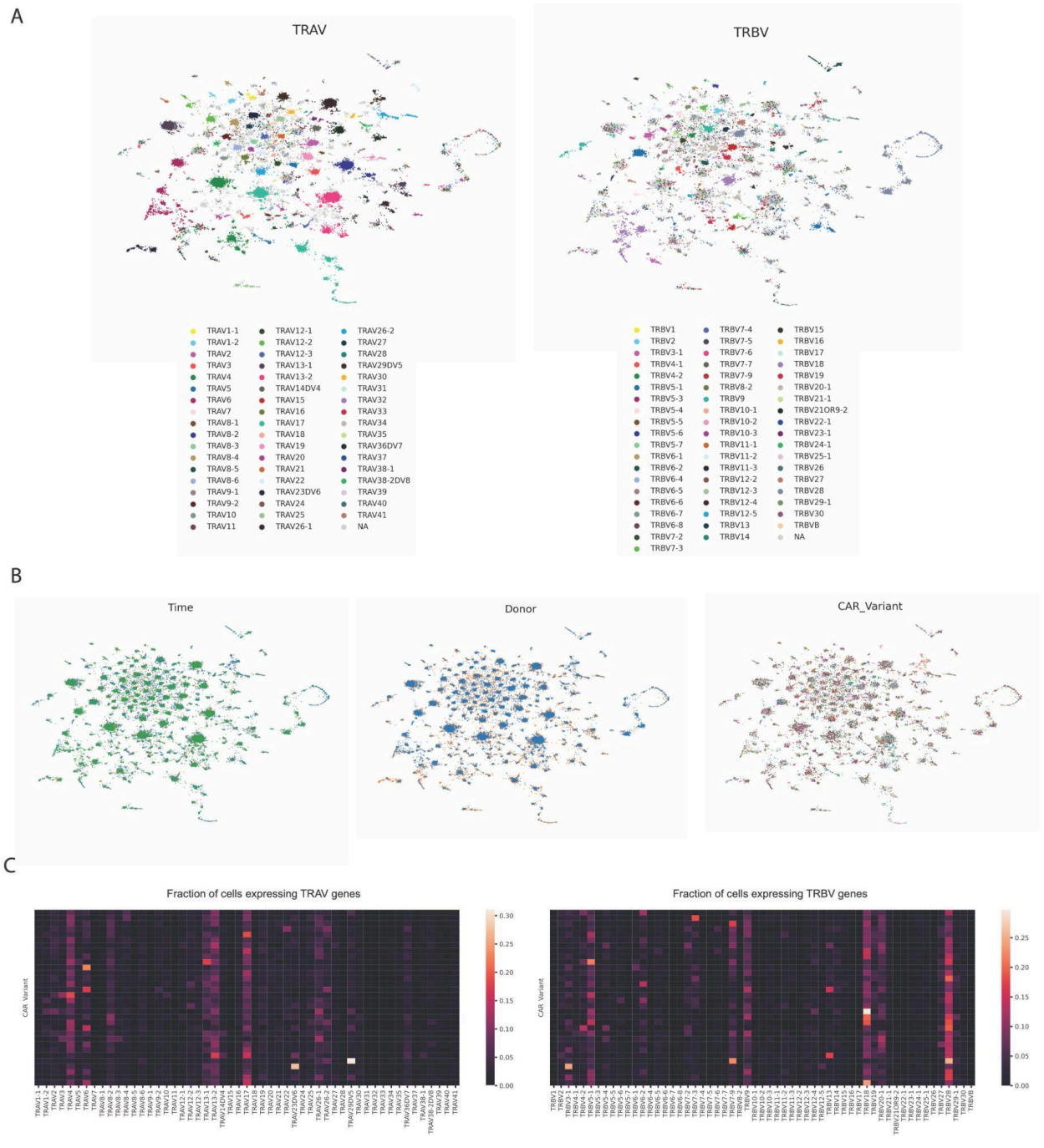

Supp. Figure 5: Distribution of TCR variable genes across the CAR library scRNAseq data

A) UMAP visualizations based on raw counts of TCR variable-alpha and variable-beta genes. Clustering in the UMAP space is driven by TRAV and TRBV germline gene segments (TRAJ and TRBJ included in UMAP learning but not shown). **B**) UMAP visualization in A, coloured by time point, donor or CAR variant identity. **C**) Heatmap illustrating the fraction of cells for each CAR variant, expressing each of the TRAV (left) or TRBV (right) genes.

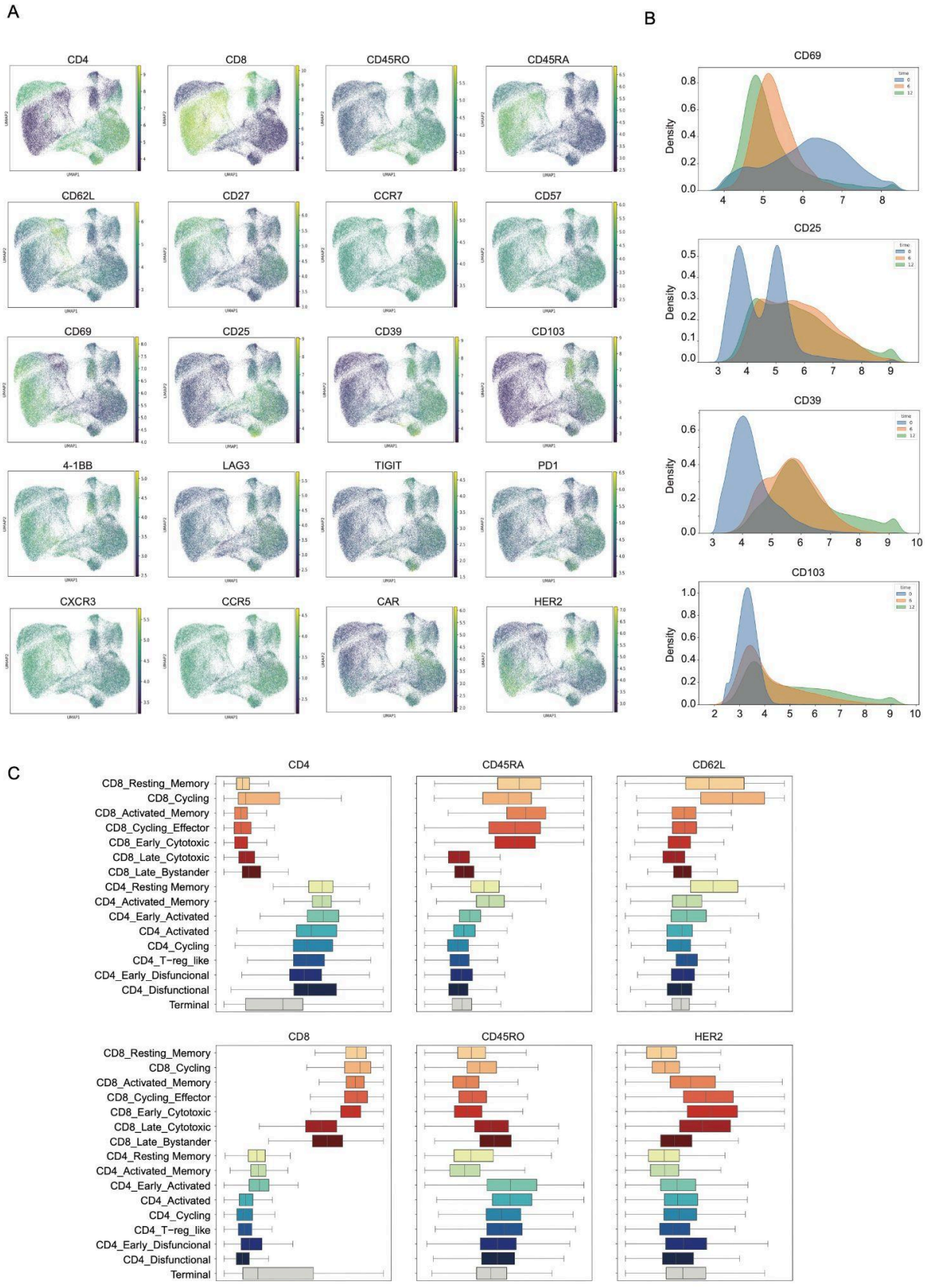
A
CD4
CD8
CD45RO
CD45RA
CD62L
CD27
CCR7
CD57
CD69
CD25
CD39
CD103
4-1BB
LAG3
TIGIT
PD1
CXCR3
CCR5
CAR
HER2
B
CD69
CD25
CD39
CD103
Density
C
CD4
CD45RA
CD62L
CD8
CD45RO
HER2
CD8_Resting_Memory
CD8_Cycling
CD8_Activated_Memory
CD8_Cycling_Effector
CD8_Early_Cytotoxic
CD8_Late_Cytotoxic
CD8_Late_Bystander
CD4_Resting Memory
CD4_Activated_Memory
CD4_Early_Activated
CD4_Activated
CD4_Cycling
CD4_T−reg_like
CD4_Early_Disfuncional
CD4_Disfunctional
Terminal

Supp. Figure 6: scCITEseq characterization of T cell phenotypes

A) UMAP embeddings from Figure 3B coloured based on the identification of different protein surface markers using scCITEseq. To increase contrast in the UMAPs, only dsb-normalized values between the 0.01 and 0.99 percentile are displayed, effectively removing the most extreme outliers that skew the color scale. **B**) Change in dsb-normalized surface expression of early (CD69), middle (CD25) and late (CD39 and CD103) T cell activation markers across time. **C**) Boxplot presenting the dsb-normalized surface display values for a selection of T cell marker genes across the different T cell clusters identified in Figure 3B.

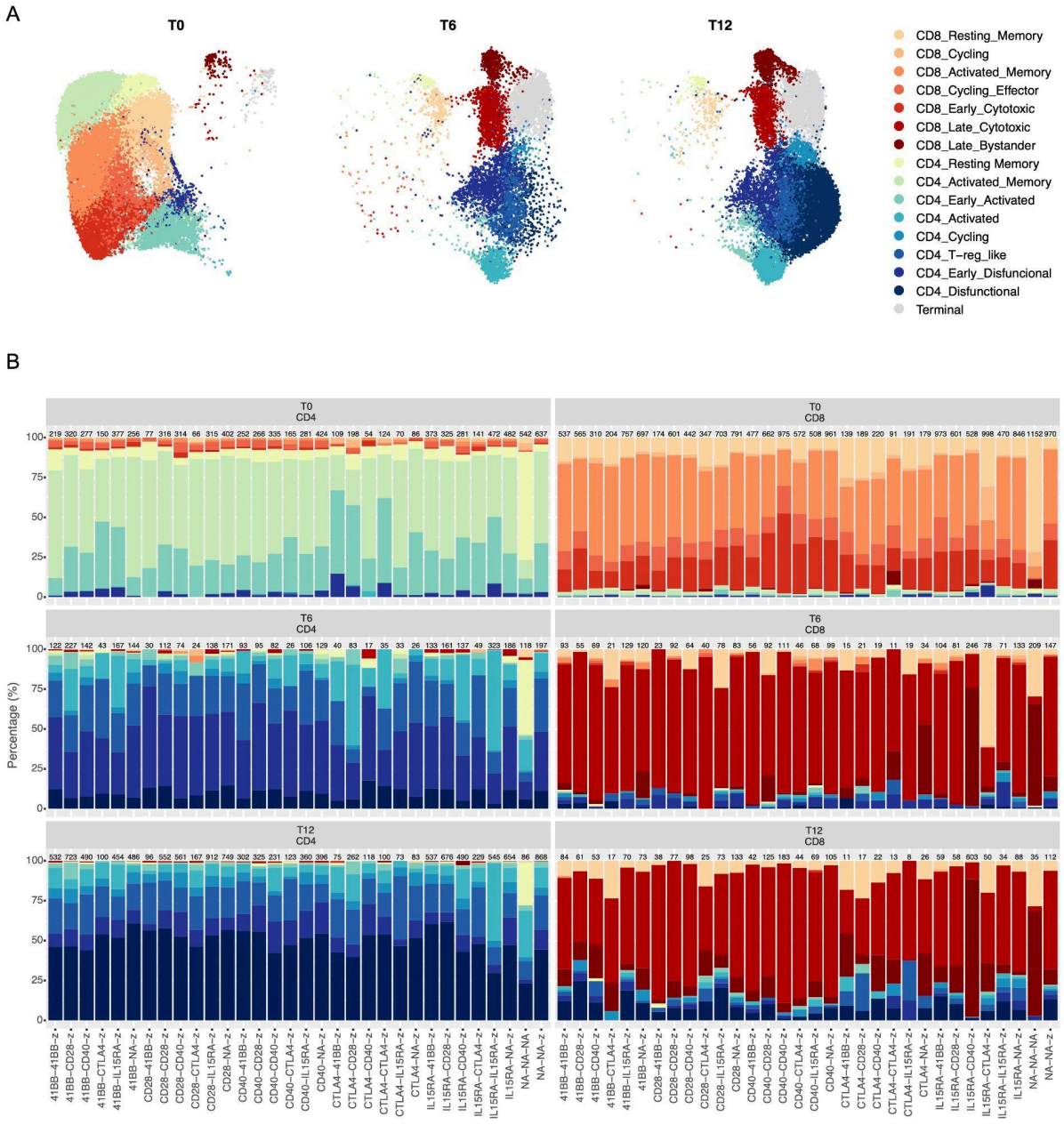

Supp. Figure 7: Cluster enrichment across CAR variants, subsets and time

A) UMAP embedding coloured by the clusters annotated in Figure 3 and split by the different time points of sample collection. **B**) Cluster enrichment observed for the different CAR variants at early, middle and late time points of repeated tumor co-culture. The different time points for each CD8 or CD4 cell compartment are shown in different plots. The number of cells used to define the cluster distribution is reported at the top of each bar.

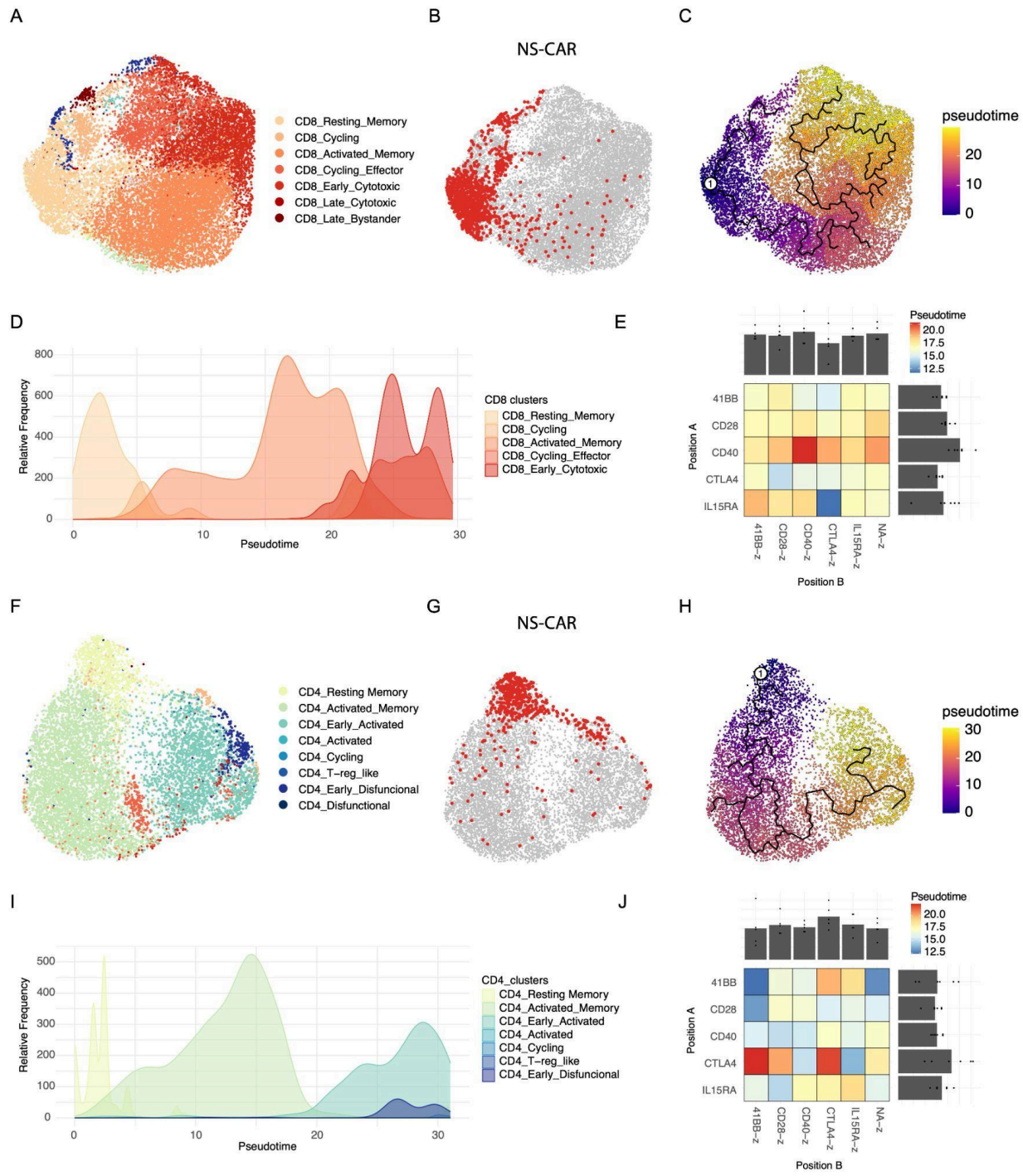

Supp. Figure 8: Trajectories and pseudotime analysis of CAR T cell scRNAseq data at early activation orders cells by a T cell differentiation axis

A) UMAP visualization of CD8 annotated cells at early time point, coloured by the cluster annotation from Figure 3. **B**) UMAP embedding from (**B**) highlighting non-signaling CAR (NS CAR) annotated cells. **C**) UMAP embedding from (**B**) showing a predicted cell trajectory depicted by a black line and coloured by predicted pseudotime. The trajectory was rooted manually by selecting the closest node to the NS-CAR population. **D**) Distribution plot describing the cluster-specific relative frequency of cells along predicted pseudotime. **E**) Heatmap showing the average pseudotime for CD8 CAR T cells during early activation across the different library variants. The heatmap separates variants based on the presence of CAR signaling domains in position

A (proximal to the cell membrane) or position B (distal from cell membrane). In addition, bar plots at the top and right-hand side of the heatmap compile the pseudotime for all variants presenting a given domain in the different positions. **F-J**- same as **(A-E)** but for CD4 cells.

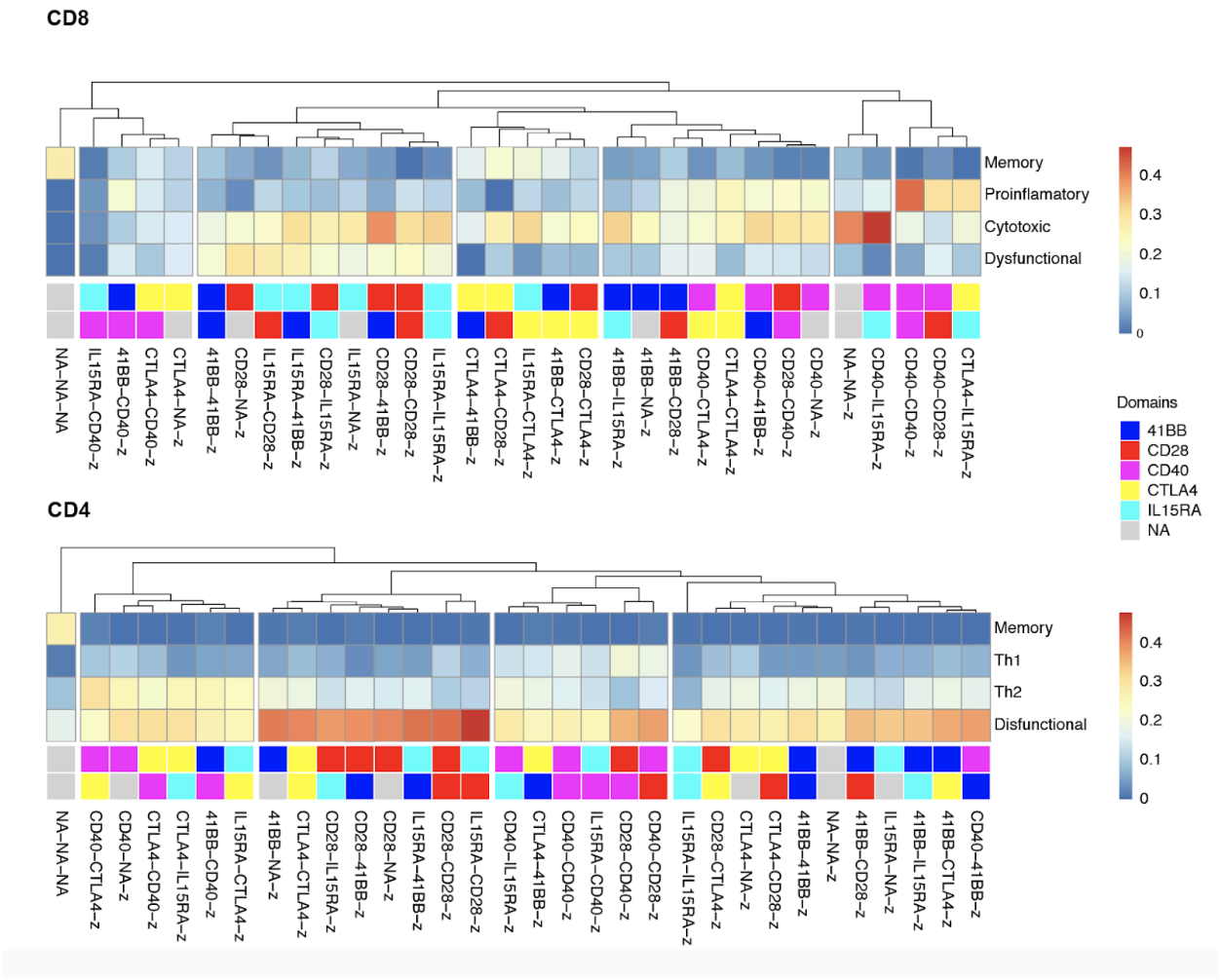

Supp. Figure 9: Clustering of CAR variants according to functional clusters at late time point
Hierarchical clustering of the CAR library according to the enrichment in late CD8 and CD4 clusters described in Figure 5 at the late time point (12 days) of the RAS assay.

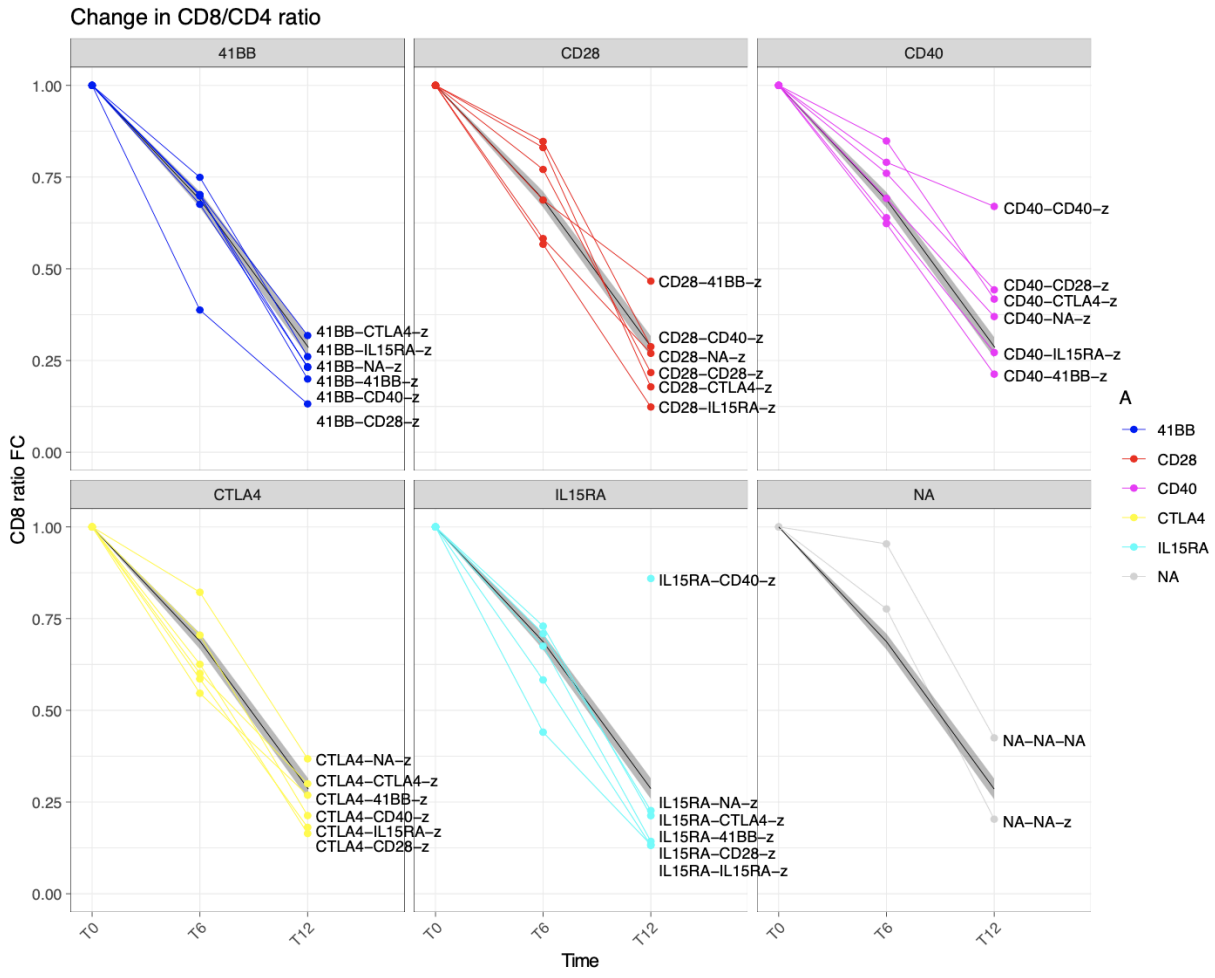

Supp. Figure 10: CD8/CD4 ratio fold change over time across variants

CD8 fold change (FC) throughout the progression of RAS based on scRNAseq data. Variants are coloured based on the domain located in a cell membrane-proximal position. A black line shows the mean FC with SEM in grey. FC was calculated by computing the difference in CD8/CD4 ratio compared to time-point 0.

Supp. Table 1: CAR library nomenclature

Comprehensive overview of the usage of intracellular signaling domains across the CAR library candidates. Positions A and B denote domains located proximal or distal to the cell membrane, respectively. NA indicates the absence of any domain in that given position. For each candidate, its associated molecular barcode is stated.

Variant	Position A	Position B	CD3z	Barcode
41BB-41BB-z	41BB	41BB	z	ACGGCGTTTCA
41BB-CD28-z	41BB	CD28	z	GCCGACCTATA
41BB-CD40-z	41BB	CD40	z	CCCGTCATCGG
41BB-CTLA4-z	41BB	CTLA4	z	ATGGTCTTAAC
41BB-IL15RA-z	41BB	IL15RA	z	ATCGCACTGTA
41BB-NA-z	41BB	NA	z	GCCGGTCTAGT
CD28-41BB-z	CD28	41BB	z	CTCGGCCTAAC
CD28-CD28-z	CD28	CD28	z	AATGATATTAC
CD28-CD40-z	CD28	CD40	z	CCCGCAATCCG
CD28-CTLA4-z	CD28	CTLA4	z	AAGGAATTCTA
CD28-IL15RA-z	CD28	IL15RA	z	GACGTTATAAA
CD28-NA-z	CD28	NA	z	CCAGCTGTACT
CD40-41BB-z	CD40	41BB	z	CAAGTCCTGAG
CD40-CD28-z	CD40	CD28	z	GCAGGTCTGAC
CD40-CD40-z	CD40	CD40	z	GCCGCCATGCC
CD40-CTLA4-z	CD40	CTLA4	z	CCAGCCGTACA
CD40-IL15RA-z	CD40	IL15RA	z	CGGGCAGTGCG
CD40-NA-z	CD40	NA	z	TACGCTATTAA
CTLA4-41BB-z	CTLA4	41BB	z	AAGGATATTAG
CTLA4-CD28-z	CTLA4	CD28	z	GACGGTGTTAG
CTLA4-CD40-z	CTLA4	CD40	z	CCTGGCGTACG
CTLA4-CTLA4-z	CTLA4	CTLA4	z	AGTGGGGTTCA
CTLA4-IL15RA-z	CTLA4	IL15RA	z	TCTGCGTTTCC
CTLA4-NA-z	CTLA4	NA	z	GACGATATACG
IL15RA-41BB-z	IL15RA	41BB	z	CTCGAAATGCA
IL15RA-CD28-z	IL15RA	CD28	z	ATAGAAATCCC
IL15RA-CD40-z	IL15RA	CD40	z	TAGGTAATGGA
IL15RA-CTLA4-z	IL15RA	CTLA4	z	GCCGCGATCCA
IL15RA-IL15RA-z	IL15RA	IL15RA	z	ATCGAATTGTT
IL15RA-NA-z	IL15RA	NA	z	ACGGGTATACG
NA-NA-z	NA	NA	z	AAAGTGTTTAA
NA-NA-NA	NA	NA	NA	CCGGCACTATC

Supp. Table 2: Primers used in this study

Name	Sequence (5' to 3')	Purpose
F1	GGTCAGACAAGCTCCCGGAAAAGGA	To amplify the cytoplasmic region of the CAR transgene integrated in the *TRAC*locus
R1	AGGTGTCCCTTCCCTGCTT	
F2-mix	GTCACCTAAATGCTAGAGCTCGC	To amplify the 3' UTR region of the CAR transgene (containing a variant-specific barcode identifier). Primer degeneration is used to avoid illumina sequencing problems due to sequence similarity.
	aGTCACCTAAATGCTAGAGCTCGC	
	tcGTCACCTAAATGCTAGAGCTCGC	
R2-mix	TACACGGCATGCCTGCTATTCT	
	aTACACGGCATGCCTGCTATTCT	
	tcTACACGGCATGCCTGCTATTCT	
F3	GTGACTGGAGTTCAGACGTGTGCTCTTCCGATCTTGTCACCTAAATGCTAGAGCTCGCTG	scCARseq PCR1
R3	ACACTCTTTCCCTACACGACGCTC	
Dual Index Kit TT, Set A (PN-1000215)	AATGATACGGCGACCACCGAGATCTACAC-N10-ACACTCTTTCCCTACACGACGCTC	scCARseq PCR2
	CAAGCAGAAGACGGCATACGAGAT-N10-GTGACTGGAGTTCAGACGTGT	

Supp. Table 3: Antibodies used in this study for flow cytometry

Target	Fluorochrome	Clone	Dilution	Source	Cat. Nr
StrepTag	Biotin	5A9F9	1/200	GenScript	A01737
SAv	BV421	-	1/80	Biolegend	405226
CD3ε	APC	UCHT1	1/200	Biolegend	300458
Viability dye	Zombie NIR	-	1/500	Biolegend	423105
Viability dye	DRAQ7	-	1/200	Biolegend	424001
CD4	BV605	OKT4	1/100	Biolegend	317437
CD8a	BV711	RPA-T8	1/100	Biolegend	301043
CD107a	BV421	H4A3	1/80	Biolegend	328626
IFNγ	APC	B27	1/50	Biolegend	506510
TNFα	PE	MAb11	1/200	Biolegend	502909

Supp. Table 4: CITE-seq antibodies used in this study

Name	Target	Clone	Dilution	Source	Cat. Nr
TotalSeq™-B0953 PE Streptavidin	SAv	-	1/400	Biolegend	405289
TotalSeq™-B0072 anti-human CD4	CD4	RPA-T4	1/50	Biolegend	300565
TotalSeq™-B0046 anti-human CD8	CD8	SK1	1/50	Biolegend	344757
TotalSeq™-B0087 anti-human CD45RO	CD45RO	UCHL1	1/50	Biolegend	304257
TotalSeq™-B0063 anti-human CD45RA	CD45RA	HI100	1/50	Biolegend	304161
TotalSeq™-B0154 anti-human CD27	CD27	O323	1/50	Biolegend	302851
TotalSeq™-B0148 anti-human CD197 (CCR7)	CCR7	G043H7	1/50	Biolegend	353249
TotalSeq™-B0085 anti-human CD25	CD25	BC96	1/50	Biolegend	302647
TotalSeq™-B0168 anti-human CD57	CD57	QA17A04	1/50	Biolegend	393323
TotalSeq™-B0146 anti-human CD69	CD69	FN50	1/50	Biolegend	310949
TotalSeq™-B0088 anti-human CD279 (PD-1)	PD1	EH12.2H7	1/50	Biolegend	329961
TotalSeq™-B0176 anti-human CD39	CD39	A1	1/50	Biolegend	328241
TotalSeq™-B0140 anti-human CD183 (CXCR3)	CXCR3	G025H7	1/50	Biolegend	353751
TotalSeq™-B0141 anti-human CD195 (CCR5) Antibody	CCR5	J418F1	1/50	Biolegend	359139
TotalSeq™-B0355 anti-human CD137 (4-1BB)	41BB	4B4-1	1/50	Biolegend	309837
TotalSeq™-B0133 anti-human CD340 (erbB2/HER-2)	HER2	24D2	1/50	Biolegend	324425
TotalSeq™-B0145 anti-human CD103 (Integrin αE)	CD103	Ber-ACT8	1/50	Biolegend	350235
TotalSeq™-B0152 anti-human CD223 (LAG-3)	LAG3	11C3C65	1/50	Biolegend	369337
TotalSeq™-B0089 anti-human TIGIT (VSTM3)	TIGIT	A15153G	1/50	Biolegend	372727
TotalSeq™-B0147 anti-human CD62L	CD62L	DREG-56	1/50	Biolegend	304849

Supp. Table 5: Gene sets used for gene set scoring

Cytotoxicity	Proinflamatory	Memory	CD4_Th1	CD4_Th2
GZMB	IFNG	TCF7	IL2	IL5
PRF1	TNF	SELL	IFNG	IL13
FASLG	CRTAM	CCR7	TNF	IL4
	CSF2	LEF1		
	XCL1	IL7R		
	XCL2			
	CCL1			
	CCL4			

Chapter 4: General Discussion and Outlook

The immune system has naturally developed immune surveillance mechanisms by which immune cells monitor the body for the presence of premalignant or malignant cells which they detect and destroy. T lymphocytes, as key players in this process, are being harnessed in the development of immunotherapies aimed at enhancing or redirecting T cell antitumor potential against cancer cells. Chimeric antigen receptors (CARs), at the forefront of immunotherapy, have demonstrated immense potential in driving durable and specific antitumor immune responses (*1*–*5*). Their rational design cleverly exploits natural protein domains, optimized through evolution, to guide a patient's own T cells to target a surface tumor-associated antigen (TAA) of choice. By linking an extracellular antigen-binding module with the signaling domains of canonical T-cell signaling proteins, CARs direct cells to initiate precise T cell activation programs in response to malignant cells, ultimately leading to their targeted elimination. Despite the unprecedented success of CAR T cell therapies in treating B-cell malignancies, numerous challenges persist, hindering both the efficacy of current treatments and their suitability for addressing a wider array of cancer types (*6*). This emphasizes the need for new tools to investigate the factors limiting the success of existing CAR T cell therapies and to drive the engineering of CAR with enhanced properties.

To address this, this thesis explores the value of combining high-throughput CAR engineering strategies and single-cell sequencing to investigate the role of CAR signaling architectures in T cell phenotype and to guide the engineering of new CAR designs with enhanced therapeutic potential. At the intersection of synthetic biology and genomics, we developed speedingCARs, an integrated method for high-throughput functional screening of pooled signaling CAR libraries using single-cell sequencing. In this method, domain recombination is employed to construct combinatorial signaling domain libraries, which are subsequently integrated into primary T cells via CRISPR-Cas9 genome editing. Following this, pooled screens, combined with single-cell RNA sequencing (scRNAseq), enable the comprehensive profiling of the gene expression signatures triggered by different CARs, facilitating the identification of variants with distinct functional characteristics. For the first time, this method allows for the simultaneous study of a large number of different CARs at high resolution, a significant advancement in the field of CAR engineering.

The speedingCARs method was applied for the screening of two libraries designed to address different challenges in the field of CAR engineering. In Chapter 2, a large library composed of 180 CAR signaling

variants was generated by recombining the natural diversity present within the immune signaling protein space. The resulting functional diversity was subsequently screened in the search for variants with distinct transcriptional phenotypes. This ultimately led to the discovery of CARs demonstrating enhanced functionality in pre-clinical assays. Notably, in this chapter, speedingCARs was utilized for candidate selection by screening a large pool of CAR candidates. Conversely, Chapter 3 focused on a more compact library of 32 CAR constructs aiming to systematically study the impact of the CAR signaling architecture on T cell phenotype. By narrowing the diversity source to a limited set of parameters (choice, number and order of 5 costimulatory domains), this study adopted a comprehensive approach to thoroughly explore patterns arising across the entire library space. Furthermore, the utilization of an in vitro model of CAR T cell dysfunction, simulating chronic tumor stimulation, provided a pertinent context for studying CAR T cell persistence, a critical limitation in CAR T cell therapies. This chapter thus demonstrates the application of the speedingCARs technology as a tool for gaining mechanistic insight into the impact of CAR design on T cell phenotype, and illustrates how the selection of a relevant screening context can tailor the speedingCARs method to address specific challenges in CAR T cell engineering.

4.1 Technical considerations for CAR T cell high-throughput engineering

Since CARs were first described, there have been significant technological developments, which have reshaped the landscape of cellular biology research and protein engineering. Notably, breakthroughs in next-generation sequencing directed evolution (*7*) and CRISPR-Cas9 genome editing (*8*) (the latter two being Nobel Prize-winning technologies) have emerged as transformative tools in the fields of synthetic immunology. These technologies have been instrumental in the development of high-throughput screening platforms to engineer proteins with immunotherapy applications (*9–12*). While traditional CAR engineering methods have relied on viral delivery of rationally designed CAR genes and functional assessments using flow cytometry, cell killing assays and cytokine secretion assays, this thesis proposes a novel streamlined pipeline for accelerating CAR engineering by integrating cutting-edge technologies from protein engineering, synthetic biology and genomics.

One of the fundamental pillars of this work is the rapid diversification of signaling proteins using domain recombination (*13*). Studies in CAR engineering have highlighted that modifications in the CAR signaling architecture can significantly impact T cell behavior, leading to enhanced therapeutic properties (*14–18*). Despite this, only a limited number of rationally designed CAR signaling architectures are currently being exploited for therapeutic use. T cells have a complex signaling network, integrated by many costimulatory and coinhibitory receptors which enable them to respond to diverse signals within

their environment (*19*). The integration of these signals influences T cell function and shapes their responses. We hypothesized that this large immune signaling protein space holds unexplored potential for engineering CARs capable of eliciting distinct T cell responses. Indeed, this was demonstrated in Chapter 2 where domain recombination of 27 domains within the CAR signaling architecture led to the identification of variants that could drive different patterns of tumor cell killing and cytokine secretion. Furthermore, in Chapter 3, we validated this hypothesis by observing significant phenotypic differences in T cells during activation and long-term stimulation, influenced by alterations in the number, order and nature of the domains used. In particular, amongst all the studied domains, the incorporation of the signaling domain of CD3G, Fc or Fc-like receptors like FCGR2A or FCRL6 and CD40 into a CAR resulted to be particularly productive in driving potent T cell responses. Concurrently, other research groups have also leveraged domain or motif recombination to introduce signaling diversity into the CAR architecture (*20–22*), underscoring the potency of this method, which we envision will continue to be exploited for engineering synthetic signaling proteins.

A primary bottleneck hindering the study of this diversity is the limited number of candidates that can be simultaneously tested, owing to the low throughput of traditional CAR T cell engineering strategies. Consequently, another fundamental principle driving this research is the need for high-throughput technologies to assess the vast array of signaling CAR architectures present in combinatorial domain libraries. High-throughput screening of CAR libraries necessitates a relevant cellular context and an efficient screening strategy. In the past, cell lines coupled with reporter systems have facilitated the screening of libraries containing up to 10^6 variants simultaneously (*11*, *23*, *24*). While this setup has proven valuable for screening simple traits like receptor affinity in the context of CARs (*25*, *26*), the complexity of T cell signaling involves an intricate network of downstream effectors that is often not fully functional in immortalized cell lines such as hybridoma cells or Jurkat cells. Therefore, we and other research groups have reasoned that primary T cells provide a more suitable context for screening signaling architectures (*27–30*). Moreover, the development of CRISPR-Cas9 genome editing tools has facilitated targeted genomic integration of CAR genes and their controlled expression via the *TRAC* promoter, resulting in the uniform and more physiologically relevant expression of CARs (*31*). CRISPR-based engineering of CAR libraries into primary T cells as performed in this thesis thus increases the translatability of the screening results.

A third technical consideration when studying and screening T cell phenotypes is the extensive heterogeneity observed within T cell populations, encompassing numerous cell subpopulations and functional states. While flow cytometry allows for the identification of T cell markers at single-cell

resolution, only a limited number of markers can be studied simultaneously. This often fails to capture the full phenotypic complexity of T cells. The emergence of scRNAseq technologies has been pivotal in enabling the comprehensive profiling of the intricate cellular heterogeneity within immune cells (*32–34*). As reviewed in Chapter 1, by providing a high-resolution view of cellular phenotypes that were previously assumed to be homogeneous based on surface marker analysis, single-cell sequencing offers an unprecedented tool to decipher CAR T cell biology in both preclinical and clinical settings. In this thesis, by coupling functional CAR T cell library screening with scRNAseq we resolve the T cell phenotypes induced by different CAR signaling architectures while using CAR genomic integration for molecular barcoding of library identity. As described in Chapter 2 and further applied in Chapter 3, scCARseq now enables high-throughput profiling of T cell states in a pooled format, facilitating efficient functional screening of CAR signaling candidates.

In contrast to other CAR library screening tools designed in parallel to our work, which rely on FACS-based screening using T cell markers such as CD69, PD-1, or the intracellular accumulation of cytokines (*20*, *28*), scRNAseq readout enables candidate selection based on a multidimensional readout. By capturing a transcriptional snapshot of existing phenotypes, it offers the possibility of conducting parallel in-silico sorts based on single marker genes, gene sets, or the full transcriptional diversity. Moreover, incorporating additional single-cell omic tools such as scCITEseq (*35*) (as demonstrated in Chapter 3) or scATACseq (*36*) can further resolve T cell phenotypes, providing more means for screening. These tools enable, for example, the examination of cytotoxicity markers such as trogocytosis or the chromatin accessibility of key transcription factors, which are often involved in the mechanisms of CAR T cell exhaustion (*17*). As more scRNAseq datasets are generated and more computational tools become available (*37*), the construction of a comprehensive atlas of CAR-induced T cell phenotypes holds promise for helping us understand the role of CAR signaling in T cell phenotype and supporting CAR engineering. Overall, despite existing limitations regarding the size of libraries scRNAseq can screen compared to unidimensional FACS-based screening, scRNAseq has proven to be highly suitable for evaluating mid-sized libraries. Whether screening for CAR libraries or studying the resulting phenotypes of individual CAR candidates, scRNAseq is positioned to become routine in analyzing CAR T cell phenotypes.

As technological advances continue to unfold, the field of synthetic biology and CAR engineering will further evolve to facilitate the engineering of enhanced therapies or treatments applicable across a broader spectrum of indications. Particularly, with the progress in machine learning and artificial intelligence, there is significant anticipation regarding the integration of these predictive tools into CAR engineering.

Pioneering work by Daniels et al., employed combinatorial signaling motif libraries and flow cytometry readouts to decode the grammar of CAR signaling and guide the optimization of CAR design (*21*). Following their example, coupling high-throughput screening data on CAR libraries with machine learning could be utilized to train models capable of predicting the most effective signaling combinations.

4.2. Future application of speedingCARs

The speedingCARs methodology demonstrated in this thesis represents a potent tool for investigating the influence of CAR signaling on T cell behavior. It establishes a framework for engineering CARs with optimized designs, tailored to deliver superior therapeutic outcomes. In the future, this high-throughput screening technology can be leveraged in the context of different library designs, cellular systems or screening contexts, holding great promise to tackle existing challenges in cancer immunotherapy.

One crucial consideration when devising a CAR screening setup is the library design. This thesis focuses primarily on the CAR signaling architecture due to its critical role in triggering T cell phenotypes. The existing immune signaling domain landscape is, however, broader than what has been addressed by the libraries in this thesis or parallel investigations (*20*, *28*). Designing larger or more exotic libraries that encompass a broader range of signaling domains, such as cytokine receptor domains (*38*) or intracellular signaling proteins (*39*), offers opportunities to further explore function in the CAR signaling combination space. Furthermore, within signaling domains, it is motifs that primarily drive the signaling function. Breaking down domains into motifs and performing motif recombination, as demonstrated by Daniels et al. (*21*) and Si et al. (*22*), represents an additional strategy for rewiring the T cell signaling network. Lastly, speedingCARs can be applied to further explore the amino acid sequence space of CAR signaling domains. As demonstrated for CD28 and CD3z domains, even single mutations in CAR signaling domains can impact CAR function (*40*, *41*). High-throughput library-based screening can therefore also be utilized to evaluate the effects of single or combinatorial mutations on CAR signaling and phenotype. Similar to the approach used by Di Roberto et al., who conducted mutagenesis on the CDR3 of the CAR scFv to adjust its binding affinity (*26*), deep mutational scanning of CAR signaling domains can serve as a strategy to fine-tune CAR activity.

As our understanding of CAR design deepens, it becomes clear that every component of the CAR contributes to T cell response, and only the synergistic effect of all components drives T cell phenotype (*42*). For instance, scFv affinity has been shown to influence signaling (*26*), and the hinge and TMD play active roles in receptor complexing and surface expression (*43*, *44*), thereby also affecting signaling. As

evidenced by Rios et al., who designed libraries of CARs combining different hinges, TMDs, and signaling domains, different scFvs may require different hinges for optimal signaling (*29*). For this reason, the design of CAR libraries that extend beyond the signaling architecture or that recombine different modules warrants further investigation.

In addition to the library design, the screening context can be tailored to provide a relevant environment for studying CAR-induced phenotypes. Similar to how in vitro chronic stimulation helped address the issue of CAR T cell dysfunction and persistence in Chapter 3, adapting this setup to study other challenges, such as in vivo tumor infiltration or survival in solid tumor microenvironments, would be valuable. For example, while current pooled screens of CAR libraries have been performed using in vitro assays, the use of xenograft mouse models could facilitate the study of tumor infiltration by evaluating the library candidates capable of migrating to the tumor and investigating their associated phenotype. Furthermore, while no method can completely replicate the intricate human TME in a mouse model, sophisticated humanized mice, generated by engrafting immunodeficient mice with human immune system, have been developed to recapitulate a larger part of human physiology (*45*). Alternatively, advances in 3D tumor organoids hold great potential for generating setups that more accurately replicate the heterogeneity and complexity of the TME (*46*).

While T cells are the most well-known and widely studied form of CAR therapy, CARs have also been explored for use with other cell types or nonconventional T cells with the aim to expand the scope and efficacy of CAR immunotherapies beyond traditional CAR T cell approaches (*47*). For instance, researchers have incorporated CARs into natural killer cells (*48–50*), macrophages (*51*) or neutrophils (*52*) to harness their intrinsic characteristics, such as tumor-killing abilities, tropism towards tumor sites, cytokine secretion profiles or lack of alloreactivity, to target cancer cells. Additionally, the immunosuppressive properties of regulatory T cells have been utilized in other contexts such as transplantation or autoimmunity (*53*, *54*). The CARs used in these alternative cellular contexts often share similar designs with conventional CARs. However, these CARs have been engineered and optimized to trigger responses in T cells, and as such, their constructs and signaling architecture may not be ideal for eliciting the desired immune response in other cell types. For this reason the adaptation of the speedingCARs method to other cell types would be valuable to enable the customization of CAR designs for different immunotherapy approaches.

Lastly, as the field of immunotherapies expands to incorporate other types of synthetic receptors, our high-throughput method for CAR engineering could be adapted to screen other types of synthetic

constructs that rewire T cell signaling. This could be applied for instance in the case of chimeric TCR receptors such as STARs (*55*) or HIT receptors (*56*). By replacing the variable region of a TCR with an scFv specific for a target surface TAA, these receptors utilize the signaling machinery of the full TCR complex to elicit T cell activation. Furthermore, the incorporation of costimulatory signaling into this architecture has been proposed to provide the necessary costimulation to fully unlock the therapeutic potential of T cells. However, the impact of incorporating such costimulatory modules in T cell phenotype remains largely unexplored. Similarly, combining CARs with chimeric co-receptors (*57*) or cytokine receptors (*58*, *59*) aims to complement CAR signaling to trigger the necessary cellular programs for driving enhanced immune responses. However, optimal signaling combinations are yet to be determined. Therefore, the speedingCARs method offers a means to investigate the role of these alternative architectures in shaping T cell phenotype.

To conclude, high-throughput CAR screening tools, such as those developed in this thesis, represent a shift in our study and engineering of CARs and other synthetic receptors. As cell therapy solutions continue to expand their reach, tools like ours will become common practice for optimizing synthetic constructs tailored to specific clinical indications. Looking ahead, integrating our high-throughput screening approach with emerging technologies in synthetic biology and systems immunology holds promise for enhancing the sensitivity and efficacy of CAR immunotherapies and paves the way for novel approaches in personalized medicine.

4.3. General considerations on CAR T cell therapy development

In order to improve CAR therapies, CAR T cell research is actively focused on trying to understand the impact of CAR signaling on T cell behavior and to identify the critical factors driving successful CAR-T cell immune responses. Preclinical research employs various in vitro and in vivo models to mimic tumor-immune cell interactions and evaluate the therapeutic potential of CAR T cells (*60*). Many of these efforts have driven CARs to clinical trials (*61*) and led to the clinical approval of several CAR T cell products (*62*). In these cases, clinical research, through the observation of the efficacy and safety of administered CAR T cells and the analysis of patient-derived samples from ongoing treatments, is crucial in identifying limitations and guiding the improvement of CAR immunotherapies. Despite the indispensable contributions of both preclinical and clinical research, there are bottlenecks that limit the translation of findings from bench to bedside. In the first place, preclinical models, while essential for CAR T cell development, often only partially fulfill the criteria necessary for comprehensive CAR T cell

evaluation. Consequently, the antitumor efficacy observed in preclinical models does not always align with clinical outcomes. Moreover, access to clinical samples is restricted by limited availability (often requiring invasive procedures to extract from patients), or their total lack of availability in contexts where CAR therapies have yet to be introduced into clinical settings. Even with access to such samples, identifying the features distinguishing superior CAR T cell products remains challenging, thereby complicating the task of engineering better therapies. Acknowledging these limitations and seeking ways to enhance preclinical CAR T cell evaluation (*45*, *46*) and maximize the utility of available clinical samples is therefore necessary.

As previously highlighted, scRNAseq offers a potent approach to resolve T cell heterogeneity, proving particularly valuable in maximizing data extraction from clinical samples. Indeed, the increasing utilization of single-cell sequencing has enabled the recording and analysis of transcriptional programs in CAR T cells from infusion products or collected at various time points post-treatment (reviewed in section 1.2). Analysis of such scRNAseq data, when annotated for clinical outcomes, has for instance revealed significant findings, indicating that shorter manufacturing protocols preserving a memory T cell phenotype and the depletion of regulatory CAR T cells from infusion products could enhance clinical efficacy in B-cell malignancies (*63*). The power of scRNAseq to digitize snapshots of CAR T cell phenotypes and identify predictive hallmarks of clinical response will likely make this tool routine in clinical research. In the future, this may also lead to the standardization of clinical procedures involving single-cell sequencing of apheresis or infusion products to inform treatment decision-making. Despite its power, the development of analysis tools is still ongoing, and challenges in data interpretation must still be addressed. As consensus in scRNAseq data analysis is established, characterizing the dynamics of CAR T cells in patient samples and their role in therapy success will become much faster.

Despite the difficulty in defining what constitutes a superior CAR, the existing knowledge on CAR T cell therapies highlights several critical factors contributing to therapy failure, including CAR T cell exhaustion, limited tumor infiltration or T cell persistence and the hostility of the tumor microenvironment. Moreover, antigen escape mechanisms and associated toxicities represent significant hurdles in achieving durable therapeutic responses (*6*). To address these challenges, innovative strategies in CAR design or manufacturing aimed at preserving a memory T cell phenotype (*64–66*), conferring persistence and resistance to T cell exhaustion (*67*, *68*) and mitigating the effects of the immunosuppressive tumor microenvironment (*69*, *70*) are currently regarded as the main general guidelines to improve CAR T cell therapies. As a result, the focus of the work presented in this thesis has been on examining T cell phenotypes in search of memory, persistence, cytotoxicity, and proinflammatory

phenotypes. However, as new specifications emerge, our method for data generation and the recorded datasets stand ready for screening in alternative ways to identify candidates that meet these new requirements.

As the field of CAR cell therapies advances, efforts are underway to expand their application beyond hematological malignancies to include solid tumors or novel treatment modalities such as autoimmune diseases. Efforts will also focus on making these therapies more accessible and affordable (*71*) and bringing them into early lines of treatment. Furthermore, there might be a shift towards more personalized therapies, where different CAR products will be tailored to individual patient needs. Additionally, the in vivo generation of CAR T cells represents a promising avenue for simplifying the technical challenges associated with CAR T cell manufacturing (*72*). Accomplishing these objectives will depend on various technological advancements, including receptor engineering platforms like the one proposed in this thesis, sophisticated in vitro models such as 3D organ-on-a-chip systems, single-cell multi-omic technologies and innovations in manufacturing techniques. Through concerted efforts in these areas, the field is poised to revolutionize immune therapy and significantly improve patient outcomes.

References for Chapter 4

1. J. N. Kochenderfer, W. H. Wilson, J. E. Janik, M. E. Dudley, M. Stetler-Stevenson, S. A. Feldman, I. Maric, M. Raffeld, D.-A. N. Nathan, B. J. Lanier, R. A. Morgan, S. A. Rosenberg, Eradication of B-lineage cells and regression of lymphoma in a patient treated with autologous T cells genetically engineered to recognize CD19. *Blood* **116**, 4099–4102 (2010).

2. D. L. Porter, B. L. Levine, M. Kalos, A. Bagg, C. H. June, Chimeric antigen receptor-modified T cells in chronic lymphoid leukemia. *N. Engl. J. Med.* **365**, 725–733 (2011).

3. S. J. Schuster, J. Svoboda, E. A. Chong, S. D. Nasta, A. R. Mato, Ö. Anak, J. L. Brogdon, I. Pruteanu-Malinici, V. Bhoj, D. Landsburg, M. Wasik, B. L. Levine, S. F. Lacey, J. J. Melenhorst, D. L. Porter, C. H. June, Chimeric Antigen Receptor T Cells in Refractory B-Cell Lymphomas. *N. Engl. J. Med.* **377**, 2545–2554 (2017).

4. C. J. Turtle, L.-A. Hanafi, C. Berger, M. Hudecek, B. Pender, E. Robinson, R. Hawkins, C. Chaney, S. Cherian, X. Chen, L. Soma, B. Wood, D. Li, S. Heimfeld, S. R. Riddell, D. G. Maloney, Immunotherapy of non-Hodgkin's lymphoma with a defined ratio of CD8+ and CD4+ CD19-specific chimeric antigen receptor-modified T cells. *Sci. Transl. Med.* **8**, 355ra116 (2016).

5. N. C. Munshi, L. D. Anderson Jr, N. Shah, D. Madduri, J. Berdeja, S. Lonial, N. Raje, Y. Lin, D. Siegel, A. Oriol, P. Moreau, I. Yakoub-Agha, M. Delforge, M. Cavo, H. Einsele, H. Goldschmidt, K. Weisel, A. Rambaldi, D. Reece, F. Petrocca, M. Massaro, J. N. Connarn, S. Kaiser, P. Patel, L. Huang, T. B. Campbell, K. Hege, J. San-Miguel, Idecabtagene Vicleucel in Relapsed and Refractory Multiple Myeloma. *N. Engl. J. Med.* **384**, 705–716 (2021).

6. R. C. Sterner, R. M. Sterner, CAR-T cell therapy: current limitations and potential strategies. *Blood Cancer J.* **11**, 69 (2021).

7. K. Chen, F. H. Arnold, Tuning the activity of an enzyme for unusual environments: sequential random mutagenesis of subtilisin E for catalysis in dimethylformamide. *Proc. Natl. Acad. Sci. U. S. A.* **90**, 5618–5622 (1993).

8. M. Jinek, K. Chylinski, I. Fonfara, M. Hauer, J. A. Doudna, E. Charpentier, A programmable dual-RNA-guided DNA endonuclease in adaptive bacterial immunity. *Science* **337**, 816–821 (2012).

9. M. Pogson, C. Parola, W. J. Kelton, P. Heuberger, S. T. Reddy, Immunogenomic engineering of a plug-and-(dis)play

hybridoma platform. *Nat. Commun.* **7**, 12535 (2016).

10. D. M. Mason, C. R. Weber, C. Parola, S. M. Meng, V. Greiff, W. J. Kelton, S. T. Reddy, High-throughput antibody engineering in mammalian cells by CRISPR/Cas9-mediated homology-directed mutagenesis. *Nucleic Acids Res.* **46**, 7436–7449 (2018).

11. R. Vazquez-Lombardi, J. S. Jung, F. S. Schlatter, A. Mei, N. R. Mantuano, F. Bieberich, K.-L. Hong, J. Kucharczyk, E. Kapetanovic, E. Aznauryan, C. R. Weber, A. Zippelius, H. Läubli, S. T. Reddy, High-throughput T cell receptor engineering by functional screening identifies candidates with enhanced potency and specificity. *Immunity* **55**, 1953–1966.e10 (2022).

12. T. L. Roth, P. J. Li, F. Blaeschke, J. F. Nies, R. Apathy, C. Mowery, R. Yu, M. L. T. Nguyen, Y. Lee, A. Truong, J. Hiatt, D. Wu, D. N. Nguyen, D. Goodman, J. A. Bluestone, C. J. Ye, K. Roybal, E. Shifrut, A. Marson, Pooled Knockin Targeting for Genome Engineering of Cellular Immunotherapies. *Cell* **181**, 728–744.e21 (2020).

13. R. B. Di Roberto, B. M. Scott, S. G. Peisajovich, Directed Evolution Methods to Rewire Signaling Networks. *Methods Mol. Biol.* **1596**, 321–337 (2017).

14. S. Guedan, A. D. Posey Jr, C. Shaw, A. Wing, T. Da, P. R. Patel, S. E. McGettigan, V. Casado-Medrano, O. U. Kawalekar, M. Uribe-Herranz, D. Song, J. J. Melenhorst, S. F. Lacey, J. Scholler, B. Keith, R. M. Young, C. H. June, Enhancing CAR T cell persistence through ICOS and 4-1BB costimulation. *JCI Insight* **3** (2018).

15. R. M.-H. Velasco Cárdenas, S. M. Brandl, A. V. Meléndez, A. E. Schlaak, A. Buschky, T. Peters, F. Beier, B. Serrels, S. Taromi, K. Raute, S. Hauri, M. Gstaiger, S. Lassmann, J. B. Huppa, M. Boerries, G. Andrieux, B. Bengsch, W. W. Schamel, S. Minguet, Harnessing CD3 diversity to optimize CAR T cells. *Nat. Immunol.* **24**, 2135–2149 (2023).

16. Y. He, M. Vlaming, T. van Meerten, E. Bremer, The Implementation of TNFRSF Co-Stimulatory Domains in CAR-T Cells for Optimal Functional Activity. *Cancers* **14** (2022).

17. P. Jiang, Z. Zhang, Y. Hu, Z. Liang, Y. Han, X. Li, X. Zeng, H. Zhang, M. Zhu, J. Dong, H. Huang, P. Qian, Single-cell ATAC-seq maps the comprehensive and dynamic chromatin accessibility landscape of CAR-T cell dysfunction. *Leukemia* **36**, 2656–2668 (2022).

18. J. Julamanee, S. Terakura, K. Umemura, Y. Adachi, K. Miyao, S. Okuno, E. Takagi, T. Sakai, D. Koyama, T. Goto, R. Hanajiri, M. Hudecek, P. Steinberger, J. Leitner, T. Nishida, M. Murata, H. Kiyoi, Composite CD79A/CD40 co-stimulatory endodomain enhances CD19CAR-T cell proliferation and survival. *Mol. Ther.* **29**, 2677–2690 (2021).

19. L. Chen, D. B. Flies, Molecular mechanisms of T cell co-stimulation and co-inhibition. *Nat. Rev. Immunol.* **13**, 227–242 (2013).

20. K. S. Gordon, T. Kyung, C. R. Perez, P. V. Holec, A. Ramos, A. Q. Zhang, Y. Agarwal, Y. Liu, C. E. Koch, A. Starchenko, B. A. Joughin, D. A. Lauffenburger, D. J. Irvine, M. T. Hemann, M. E. Birnbaum, Screening for CD19-specific chimaeric antigen receptors with enhanced signalling via a barcoded library of intracellular domains. *Nat Biomed Eng* **6**, 855–866 (2022).

21. K. G. Daniels, S. Wang, M. S. Simic, H. K. Bhargava, S. Capponi, Y. Tonai, W. Yu, S. Bianco, W. A. Lim, Decoding CAR T cell phenotype using combinatorial signaling motif libraries and machine learning. *Science* **378**, 1194–1200 (2022).

22. W. Si, Y.-Y. Fan, S.-Z. Qiu, X. Li, E.-Y. Wu, J.-Q. Ju, W. Huang, H.-P. Wang, P. Wei, Design of diversified chimeric antigen receptors through rational module recombination. *iScience* **26**, 106529 (2023).

23. P. Ma, P. Ren, C. Zhang, J. Tang, Z. Yu, X. Zhu, K. Fan, G. Li, W. Zhu, W. Sang, C. Min, W. Chen, X. Huang, G. Yang, R. A. Lerner, Avidity-Based Selection of Tissue-Specific CAR-T Cells from a Combinatorial Cellular Library of CARs. *Adv. Sci.* **8**, 2003091 (2021).

24. T. Kula, M. H. Dezfulian, C. I. Wang, N. S. Abdelfattah, Z. C. Hartman, K. W. Wucherpfennig, H. K. Lyerly, S. J. Elledge, T-Scan: A Genome-wide Method for the Systematic Discovery of T Cell Epitopes. *Cell* **178**, 1016–1028.e13 (2019).

25. J. Rydzek, T. Nerreter, H. Peng, S. Jutz, J. Leitner, P. Steinberger, H. Einsele, C. Rader, M. Hudecek, Chimeric Antigen Receptor Library Screening Using a Novel NF-κB/NFAT Reporter Cell Platform. *Mol. Ther.* **27**, 287–299 (2019).

26. R. B. Di Roberto, R. Castellanos-Rueda, S. Frey, D. Egli, R. Vazquez-Lombardi, E. Kapetanovic, J. Kucharczyk, S. T. Reddy, A Functional Screening Strategy for Engineering Chimeric Antigen Receptors with Reduced On-Target, Off-Tumor Activation. *Mol. Ther.* **28**, 2564–2576 (2020).

27. R. Castellanos-Rueda, R. B. Di Roberto, F. Bieberich, F. S. Schlatter, D. Palianina, O. T. P. Nguyen, E. Kapetanovic, H. Läubli, A. Hierlemann, N. Khanna, S. T. Reddy, speedingCARs: accelerating the engineering of CAR T cells by signaling domain shuffling and single-cell sequencing. *Nat. Commun.* **13**, 6555 (2022).

28. D. B. Goodman, C. S. Azimi, K. Kearns, A. Talbot, K. Garakani, J. Garcia, N. Patel, B. Hwang, D. Lee, E. Park, V. S. Vykunta, B. R. Shy, C. J. Ye, J. Eyquem, A. Marson, J. A. Bluestone, K. T. Roybal, Pooled screening of CAR T cells identifies diverse immune signaling domains for next-generation immunotherapies. *Sci. Transl. Med.* **14**, eabm1463 (2022).

29. X. Rios, O. Pardias, M. A. Morales, P. Bhattacharya, Y. Chen, L. Guo, C. Zhang, E. J. Di Pierro, G. Tian, G. A. Barragan, P. Sumazin, L. S. Metelitsa, Refining chimeric antigen receptors via barcoded protein domain combination pooled screening. *Mol. Ther.* **31**, 3210–3224 (2023).

30. R. Castellanos-Rueda, K.-L. K. Wang, J. L. Forster, A. Driessen, J. A. Frank, M. R. Martínez, S. T. Reddy, Dissecting the role of CAR signaling architectures on T cell activation and persistence using pooled screening and single-cell sequencing, *bioRxiv* (2024)p. 2024.02.26.582129.

31. J. Eyquem, J. Mansilla-Soto, T. Giavridis, S. J. C. van der Stegen, M. Hamieh, K. M. Cunanan, A. Odak, M. Gönen, M. Sadelain, Targeting a CAR to the TRAC locus with CRISPR/Cas9 enhances tumour rejection. *Nature* **543**, 113–117 (2017).

32. E. Azizi, A. J. Carr, G. Plitas, A. E. Cornish, C. Konopacki, S. Prabhakaran, J. Nainys, K. Wu, V. Kiseliovas, M. Setty, K. Choi, R. M. Fromme, P. Dao, P. T. McKenney, R. C. Wasti, K. Kadaveru, L. Mazutis, A. Y. Rudensky, D. Pe'er, Single-Cell Map of Diverse Immune Phenotypes in the Breast Tumor Microenvironment. *Cell* **174**, 1293–1308.e36 (2018).

33. M. Sade-Feldman, K. Yizhak, S. L. Bjorgaard, J. P. Ray, C. G. de Boer, R. W. Jenkins, D. J. Lieb, J. H. Chen, D. T. Frederick, M. Barzily-Rokni, S. S. Freeman, A. Reuben, P. J. Hoover, A.-C. Villani, E. Ivanova, A. Portell, P. H. Lizotte, A. R. Aref, J.-P. Eliane, M. R. Hammond, H. Vitzthum, S. M. Blackmon, B. Li, V. Gopalakrishnan, S. M. Reddy, Z. A. Cooper, C. P. Paweletz, D. A. Barbie, A. Stemmer-Rachamimov, K. T. Flaherty, J. A. Wargo, G. M. Boland, R. J. Sullivan, G. Getz, N. Hacohen, Defining T Cell States Associated with Response to Checkpoint Immunotherapy in Melanoma. *Cell* **175**, 998–1013.e20 (2018).

34. P. A. Szabo, H. M. Levitin, M. Miron, M. E. Snyder, T. Senda, J. Yuan, Y. L. Cheng, E. C. Bush, P. Dogra, P. Thapa, D. L. Farber, P. A. Sims, Single-cell transcriptomics of human T cells reveals tissue and activation signatures in health and disease. *Nat. Commun.* **10**, 4706 (2019).

35. M. Stoeckius, C. Hafemeister, W. Stephenson, B. Houck-Loomis, P. K. Chattopadhyay, H. Swerdlow, R. Satija, P. Smibert, Simultaneous epitope and transcriptome measurement in single cells. *Nat. Methods* **14**, 865–868 (2017).

36. A. T. Satpathy, J. M. Granja, K. E. Yost, Y. Qi, F. Meschi, G. P. McDermott, B. N. Olsen, M. R. Mumbach, S. E. Pierce, M. R. Corces, P. Shah, J. C. Bell, D. Jhutty, C. M. Nemec, J. Wang, L. Wang, Y. Yin, P. G. Giresi, A. L. S. Chang, G. X. Y. Zheng, W. J. Greenleaf, H. Y. Chang, Massively parallel single-cell chromatin landscapes of human immune cell development and intratumoral T cell exhaustion. *Nat. Biotechnol.* **37**, 925–936 (2019).

37. M. Lotfollahi, M. Naghipourfar, M. D. Luecken, M. Khajavi, M. Büttner, M. Wagenstetter, Ž. Avsec, A. Gayoso, N. Yosef, M. Interlandi, S. Rybakov, A. V. Misharin, F. J. Theis, Mapping single-cell data to reference atlases by transfer learning. *Nat. Biotechnol.* **40**, 121–130 (2022).

38. A. J. Brooks, F. Dehkhoda, B. B. Kragelund, "Cytokine Receptors" in *Principles of Endocrinology and Hormone Action*, A. Belfiore, D. LeRoith, Eds. (Springer International Publishing, Cham, 2016), pp. 1–29.

39. A. M. Tousley, M. C. Rotiroti, L. Labanieh, L. W. Rysavy, W.-J. Kim, C. Lareau, E. Sotillo, E. W. Weber, S. P. Rietberg, G. N. Dalton, Y. Yin, D. Klysz, P. Xu, E. L. de la Serna, A. R. Dunn, A. T. Satpathy, C. L. Mackall, R. G. Majzner, Co-opting signalling molecules enables logic-gated control of CAR T cells. *Nature* **615**, 507–516 (2023).

40. S. Guedan, A. Madar, V. Casado-Medrano, C. Shaw, A. Wing, F. Liu, R. M. Young, C. H. June, A. D. Posey Jr, Single residue in CD28-costimulated CAR-T cells limits long-term persistence and antitumor durability. *J. Clin. Invest.* **130**, 3087–3097 (2020).

41. J. Feucht, J. Sun, J. Eyquem, Y.-J. Ho, Z. Zhao, J. Leibold, A. Dobrin, A. Cabriolu, M. Hamieh, M. Sadelain, Calibration of CAR activation potential directs alternative T cell fates and therapeutic potency. *Nat. Med.* **25**, 82–88 (2019).

42. S. E. Lindner, S. M. Johnson, C. E. Brown, L. D. Wang, Chimeric antigen receptor signaling: Functional consequences and design implications. *Sci Adv* **6**, eaaz3223 (2020).

43. K. Fujiwara, A. Tsunei, H. Kusabuka, E. Ogaki, M. Tachibana, N. Okada, Hinge and Transmembrane Domains of Chimeric

Antigen Receptor Regulate Receptor Expression and Signaling Threshold. *Cells* **9** (2020).

44. Y. D. Muller, D. P. Nguyen, L. M. R. Ferreira, P. Ho, C. Raffin, R. V. B. Valencia, Z. Congrave-Wilson, T. L. Roth, J. Eyquem, F. Van Gool, A. Marson, L. Perez, J. A. Wells, J. A. Bluestone, Q. Tang, The CD28-Transmembrane Domain Mediates Chimeric Antigen Receptor Heterodimerization With CD28. *Front. Immunol.* **12**, 639818 (2021).

45. R. Kumari, G. Feuer, L. Bourré, Humanized Mouse Models for Immuno-oncology Drug Discovery. *Curr Protoc* **3**, e852 (2023).

46. C.-P. Sun, H.-R. Lan, X.-L. Fang, X.-Y. Yang, K.-T. Jin, Organoid Models for Precision Cancer Immunotherapy. *Front. Immunol.* **13**, 770465 (2022).

47. A. K. M. N. Hossian, C. S. Hackett, R. J. Brentjens, S. Rafiq, Multipurposing CARs: Same engine, different vehicles. *Mol. Ther.* **30**, 1381–1395 (2022).

48. A. Kruschinski, A. Moosmann, I. Poschke, H. Norell, M. Chmielewski, B. Seliger, R. Kiessling, T. Blankenstein, H. Abken, J. Charo, Engineering antigen-specific primary human NK cells against HER-2 positive carcinomas. *Proc. Natl. Acad. Sci. U. S. A.* **105**, 17481–17486 (2008).

49. Y. Li, D. L. Hermanson, B. S. Moriarity, D. S. Kaufman, Human iPSC-Derived Natural Killer Cells Engineered with Chimeric Antigen Receptors Enhance Anti-tumor Activity. *Cell Stem Cell* **23**, 181–192.e5 (2018).

50. E. Liu, D. Marin, P. Banerjee, H. A. Macapinlac, P. Thompson, R. Basar, L. Nassif Kerbauy, B. Overman, P. Thall, M. Kaplan, V. Nandivada, I. Kaur, A. Nunez Cortes, K. Cao, M. Daher, C. Hosing, E. N. Cohen, P. Kebriaei, R. Mehta, S. Neelapu, Y. Nieto, M. Wang, W. Wierda, M. Keating, R. Champlin, E. J. Shpall, K. Rezvani, Use of CAR-Transduced Natural Killer Cells in CD19-Positive Lymphoid Tumors. *N. Engl. J. Med.* **382**, 545–553 (2020).

51. M. Klichinsky, M. Ruella, O. Shestova, X. M. Lu, A. Best, M. Zeeman, M. Schmierer, K. Gabrusiewicz, N. R. Anderson, N. E. Petty, K. D. Cummins, F. Shen, X. Shan, K. Veliz, K. Blouch, Y. Yashiro-Ohtani, S. S. Kenderian, M. Y. Kim, R. S. O'Connor, S. R. Wallace, M. S. Kozlowski, D. M. Marchione, M. Shestov, B. A. Garcia, C. H. June, S. Gill, Human chimeric antigen receptor macrophages for cancer immunotherapy. *Nat. Biotechnol.* **38**, 947–953 (2020).

52. Y. Chang, R. Syahirah, X. Wang, G. Jin, S. Torregrosa-Allen, B. D. Elzey, S. N. Hummel, T. Wang, C. Li, X. Lian, Q. Deng, H. E. Broxmeyer, X. Bao, Engineering chimeric antigen receptor neutrophils from human pluripotent stem cells for targeted cancer immunotherapy. *Cell Rep.* **40**, 111128 (2022).

53. D. Blat, E. Zigmond, Z. Alteber, T. Waks, Z. Eshhar, Suppression of Murine Colitis and its Associated Cancer by Carcinoembryonic Antigen-Specific Regulatory T Cells. *Mol. Ther.* **22**, 1018–1028 (2014).

54. S. K. Eskandari, A. Daccache, J. R. Azzi, Chimeric antigen receptor Treg therapy in transplantation. *Trends Immunol.* **45**, 48–61 (2024).

55. Y. Liu, G. Liu, J. Wang, Z.-Y. Zheng, L. Jia, W. Rui, D. Huang, Z.-X. Zhou, L. Zhou, X. Wu, S. Lin, X. Zhao, X. Lin, Chimeric STAR receptors using TCR machinery mediate robust responses against solid tumors. *Sci. Transl. Med.* **13** (2021).

56. J. Mansilla-Soto, J. Eyquem, S. Haubner, M. Hamieh, J. Feucht, N. Paillon, A. E. Zucchetti, Z. Li, M. Sjöstrand, P. L. Lindenbergh, M. Saetersmoen, A. Dobrin, M. Maurin, A. Iyer, A. Garcia Angus, M. M. Miele, Z. Zhao, T. Giavridis, S. J. C. van der Stegen, F. Tamzalit, I. Rivière, M. Huse, R. C. Hendrickson, C. Hivroz, M. Sadelain, HLA-independent T cell receptors for targeting tumors with low antigen density. *Nat. Med.* **28**, 345–352 (2022).

57. A. Katsarou, M. Sjöstrand, J. Naik, J. Mansilla-Soto, D. Kefala, G. Kladis, A. Nianias, R. Ruiter, R. Poels, I. Sarkar, Y. R. Patankar, E. Merino, R. M. Reijmers, K. A. Frerichs, H. Yuan, J. de Bruijn, D. Stroopinsky, D. Avigan, N. W. C. J. van de Donk, S. Zweegman, T. Mutis, M. Sadelain, R. W. J. Groen, M. Themeli, Combining a CAR and a chimeric costimulatory receptor enhances T cell sensitivity to low antigen density and promotes persistence. *Sci. Transl. Med.* **13**, eabh1962 (2021).

58. Y. Wang, H. Jiang, H. Luo, Y. Sun, B. Shi, R. Sun, Z. Li, An IL-4/21 Inverted Cytokine Receptor Improving CAR-T Cell Potency in Immunosuppressive Solid-Tumor Microenvironment. *Front. Immunol.* **10**, 1691 (2019).

59. A. Kalbasi, M. Siurala, L. L. Su, M. Tariveranmoshabad, L. K. Picton, P. Ravikumar, P. Li, J.-X. Lin, H. Escuin-Ordinas, T. Da, S. V. Kremer, A. L. Sun, S. Castelli, S. Agarwal, J. Scholler, D. Song, P. C. Rommel, E. Radaelli, R. M. Young, W. J. Leonard, A. Ribas, C. H. June, K. C. Garcia, Potentiating adoptive cell therapy using synthetic IL-9 receptors. *Nature* **607**, 360–365 (2022).

60. X. Si, L. Xiao, C. E. Brown, D. Wang, Preclinical Evaluation of CAR T Cell Function: In Vitro and In Vivo Models. *Int. J.*

Mol. Sci. **23** (2022).

61. V. Wang, M. Gauthier, V. Decot, L. Reppel, D. Bensoussan, Systematic Review on CAR-T Cell Clinical Trials Up to 2022: Academic Center Input. *Cancers* **15** (2023).

62. A. Mitra, A. Barua, L. Huang, S. Ganguly, Q. Feng, B. He, From bench to bedside: the history and progress of CAR T cell therapy. *Front. Immunol.* **14**, 1188049 (2023).

63. N. J. Haradhvala, M. V. Maus, Understanding Mechanisms of Response to CAR T-cell Therapy through Single-Cell Sequencing: Insights and Challenges. *Blood Cancer Discov* **5**, 86–89 (2024).

64. B. Prinzing, P. Schreiner, M. Bell, Y. Fan, G. Krenciute, S. Gottschalk, MyD88/CD40 signaling retains CAR T cells in a less differentiated state. *JCI Insight* **5** (2020).

65. D. D. Klysz, C. Fowler, M. Malipatlolla, L. Stuani, K. A. Freitas, Y. Chen, S. Meier, B. Daniel, K. Sandor, P. Xu, J. Huang, L. Labanieh, V. Keerthi, A. Leruste, M. Bashti, J. Mata-Alcazar, N. Gkitsas, J. A. Guerrero, C. Fisher, S. Patel, K. Asano, S. Patel, K. L. Davis, A. T. Satpathy, S. A. Feldman, E. Sotillo, C. L. Mackall, Inosine induces stemness features in CAR-T cells and enhances potency. *Cancer Cell* **42**, 266–282.e8 (2024).

66. S. M. Collins, K. A. Alexander, S. Lundh, A. J. Dimitri, Z. Zhang, C. R. Good, J. A. Fraietta, S. L. Berger, TOX2 coordinates with TET2 to positively regulate central memory differentiation in human CAR T cells. *Sci Adv* **9**, eadh2605 (2023).

67. R. C. Lynn, E. W. Weber, E. Sotillo, D. Gennert, P. Xu, Z. Good, H. Anbunathan, J. Lattin, R. Jones, V. Tieu, S. Nagaraja, J. Granja, C. F. A. de Bourcy, R. Majzner, A. T. Satpathy, S. R. Quake, M. Monje, H. Y. Chang, C. L. Mackall, c-Jun overexpression in CAR T cells induces exhaustion resistance. *Nature* **576**, 293–300 (2019).

68. H. Seo, E. González-Avalos, W. Zhang, P. Ramchandani, C. Yang, C.-W. J. Lio, A. Rao, P. G. Hogan, BATF and IRF4 cooperate to counter exhaustion in tumor-infiltrating CAR T cells. *Nat. Immunol.* **22**, 983–995 (2021).

69. L. Liu, Y. Qu, L. Cheng, C. W. Yoon, P. He, A. Monther, T. Guo, S. Chittle, Y. Wang, Engineering chimeric antigen receptor T cells for solid tumour therapy. *Clin. Transl. Med.* **12**, e1141 (2022).

70. F. Navarro, N. Casares, C. Martín-Otal, A. Lasarte-Cía, M. Gorraiz, P. Sarrión, D. Llopiz, D. Reparaz, N. Varo, J. R. Rodriguez-Madoz, F. Prosper, S. Hervás-Stubbs, T. Lozano, J. J. Lasarte, Overcoming T cell dysfunction in acidic pH to enhance adoptive T cell transfer immunotherapy. *Oncoimmunology* **11**, 2070337 (2022).

71. S. Mallapaty, Cutting-edge CAR-T cancer therapy is now made in India - at one-tenth the cost. *Nature*, doi: 10.1038/d41586-024-00809-y (2024).

72. W. Nawaz, B. Huang, S. Xu, Y. Li, L. Zhu, H. Yiqiao, Z. Wu, X. Wu, AAV-mediated in vivo CAR gene therapy for targeting human T-cell leukemia. *Blood Cancer J.* **11**, 119 (2021).